THE UNIVERSITY OF ALBERTA

AN EXPERIMENTAL INVESTIGATION OF STATE ESTIMATION IN MULTIVARIABLE CONTROL SYSTEMS

BY

JAMES C. HAMILTON

A THESIS

SUBMITTED TO THE FACULTY OF GRADUATE STUDIES AND RESEARCH

IN PARTIAL FULFILMENT OF THE REQUIREMENTS FOR THE DEGREE

OF MASTER OF SCIENCE

DEPARTMENT OF CHEMICAL AND PETROLEUM ENGINEERING

EDMONTON, ALBERTA

FALL, 1972

ABSTRACT

This thesis presents an experimental evaluation of two state estimation techniques, the Kalman filter and the Luenberger observer. In both cases the estimated states were used in an optimal multivariable control system designed for a pilot scale double effect evaporator.

A literature survey of the theory and applications of Kalman filtering is presented along with the basic design equations. Open and closed loop simulation studies showed that the stationary Kalman filter can effectively reduce the effects of noisy measurements and accurately estimate an unmeasured state variable. This study also evaluated the effects of changing the design parameters for the Kalman filter and relates design considerations to non-ideal situations such as unmeasured process disturbances and incorrect initial state estimates. The experimental study verified the simulation results and demonstrated that the evaporator was controlled satisfactorily when the filter estimates were used in the optimal feedback control law.

A literature survey is also presented for the Luenberger observer together with the relevant theory. Simulation studies illustrated that for non-ideal situations (i.e. unmeasured disturbances, incorrect initial state estimates and process and measurement noise) some observer designs were not satisfactory and hence, "tuning" of the design parameters was required. The simulation results also revealed that "marginally" observable systems give rise to numerical problems which make it difficult to design a satisfactory observer even for ideal conditions. These results were verified experimentally where both a first and a second order observer were implemented for the evaporator.

ACKNOWLEDGEMENTS

The author gratefully acknowledges the guidance and assistance of his thesis supervisor, Dr. D.E. Seborg.

Thanks go to Dr. D.G. Fisher for his helpful suggestions and to the Data Acquisition, Control and Simulation Centre Staff for their assistance and for the use of their computing facilities.

The author would also like to thank his fellow control students for their advice and helpful comments throughout this study.

Financial support was generously given by the National Research Council.

TABLE OF CONTENTS

TABLE OF CONTENTS (continued)

TABLE OF CONTENTS (continued)

TABLE OF CONTENTS (continued)

TABLE OF CONTENTS (continued)

LIST OF TABLES

LIST OF TABLES (continued)

LIST OF FIGURES

LIST OF FIGURES (continued)

LIST OF FIGURES (continued)

LIST OF FIGURES (continued)

LIST OF FIGURES (continued)

LIST OF FIGURES (continued)

LIST OF FIGURES (continued)

LIST OF FIGURES (continued)

LIST OF FIGURES (continued)

LIST OF FIGURES (continued)

CHAPTER ONE

INTRODUCTION

Control systems designed using state space models usually require a knowledge of the state of the system, but often in practice some of the state variables cannot be determined by direct measurement. Physical variables available for measurement are usually functions of the states, referred to as outputs, and in many instances these measured outputs contain random noise which makes it difficult to get a good estimate of the state variables.

The literature reports many methods of state estimation but of these the Kalman filter [1,2] has received the most attention. Since the classic work by Kalman [1] in 1960, many theoretical studies have been reported including extensions to nonlinear systems [3-5]. The theory was originally applied in the aerospace industries and it was only later recognized to be applicable to the process industries. However, although several simulation studies have been reported, there has been very little work done on implementing the Kalman filter in the process industries.

Luenberger [6] developed an alternative method of state estimation for deterministic linear, time-invariant systems. The estimator is known as the Luenberger observer and has the advantage of being a minimal order observer. That is, the order of the observer need only be equal to the number of unmeasured states rather than the order of the process as is the case for the Kalman filter. Luenberger's work has also been extended to stochastic processes [7] and time varying systems [8]. Unfortunately, there have been only a few reports of simulation studies using the Luenberger observer and apparently no

practical applications have been reported.

1.1 OBJECTIVES OF THE STUDY

The objectives of this study can be described in two parts. Firstly, it was intended to evaluate the effectiveness of the stationary form of the Kalman filter by simulation studies and experimental application to a pilot plant double effect evaporator. For this investigation it was assumed that the observation time was long compared with the transient response of the system and that the prior noise statistics were wide sense stationary so that the use of the stationary form of the Kalman filter could be justified. It was also desired to develop some practical guidelines for the effects of the design parameters on the effectiveness of the filter.

The second part of the study involves a similar investigation of the Luenberger observer. The practical problems involved with the implementation of the observer are pointed out and the effects of noise, unmeasured disturbances and poor initial state estimates are investigated for different observer designs.

In both studies, the closed loop runs used optimal feedback control based on the state estimates. The design of the optimal controller was carried out previously by Newell [9] and his results were used in this work.

1.2 STRUCTURE OF THE THESIS

The thesis consists of five chapters including this introduction. Chapters Two and Three present the Kalman filter study and Chapters Four and Five the Luenberger observer study.

In Chapter Two a literature survey of the theory and

applications of Kalman filtering is presented together with the basic equations. Chapter Three briefly describes the double effect evaporator and presents the results of the simulation and experimental studies for the Kalman filter.

Chapter Four presents a literature survey for the Luenberger observer and the relevant theory required for the subsequent investigation, the results of which are detailed in Chapter Five.

The general conclusions from both investigations are summarized in Chapter Six.

CHAPTER TWO

LITERATURE SURVEY AND BASIC EQUATIONS FOR THE KALMAN FILTER

2.1 INTRODUCTION

In this study a literature survey is presented to summarize the theoretical and practical work which has been reported on Kalman filtering, particularly applications in the process industries. The basic equations for the Kalman filter and other relevant theory required for the evaporator application are also presented.

2.2 LITERATURE SURVEY

Since Kalman's classical analysis of linear filtering in 1960 [1], there have been numerous papers on this subject published in the literature. Several authors have modified the theory to extend the results to nonlinear systems while others have derived sub-optimal equations which have the advantages of computational efficiency.

Although there have been many simulation studies involving the application of the Kalman filter in the field of process control for both linear and (more frequently) nonlinear systems, there have been very few experimental studies reported.

It is intended that this survey give a brief outline of the work that has been done in this field and, though by no means complete, it is a representative review of the literature.

2.2.1 Basic Theory

Kalman [1] first presented the optimal linear filtering theory for continuous systems in a rigorous manner in 1960. In this paper he also introduced the Duality Principle which states that the solution to the optimal estimation problem for a stochastic process

is equivalent to the solution to an optimal deterministic regulatory control problem. One year later Kalman and Bucy [2] reported the corresponding results in discrete form. These two papers are now considered classical and are the basis for much of the recent work in the field of state and parameter estimation.

In a later paper Cox [3] gave a concise account of the solution to the problem of estimating state variables and parameters for a linear system and developed an approximation technique for nonlinear systems. Sorenson [4] presented a comprehensive review of the use of Kalman filtering techniques for both linear and nonlinear systems. In a more recent publication Bucy [5] also reviewed the theory of filtering for stochastic processes and included the historical development in this field.

Gura and Bierman [6] analyzed the question of computer requirements for various linear filters including the standard Kalman filter. Each algorithm was evaluated in terms of computer time required and storage necessary when applied to a general filtering problem. The study included as parameters, the size of the state vector, the frequency and number of observations and the frequency of state updates. The authors recommended different filters depending on the parametric values but, in general, the standard Kalman filter was found to be one of the better algorithms from a computational viewpoint. It should be noted that no attempt was made to include the accuracy and numerical stability of the filters in the evaluation. These are obviously important considerations.

Several texts [7-10] provide a basic introduction to Kalman filtering. Sage and Melsa [10] give a very clear treatment of the

pertinent equations for both the continuous and the discrete case.

2.2.2 Some Extensions and Modifications to the Theory

Aoki and Huddle [11] considered the same problem as Kalman but imposed constraints on the permissible complexity of the estimator with a view to reducing the computations required. The result was a sub-optimal filter which, it was claimed, could be comparable in performance to the optimal filter. The theory was developed for discrete, linear, time-invariant systems but Newmann [12] later proposed a similar estimation technique for the continuous case. It is interesting to note that for deterministic systems, this filter reduces to the Luenberger observer (see Chapter 4).

Wells [13] proposed an approximation to the Kalman filter for a linear system which eliminated the matrix inversion required in the filter equations and was therefore computationally more efficient.

Another example of a recent modification to the standard theory is Friedland's [14] treatment of bias or modelling errors. Friedland developed a technique for estimating the bias which is then used to correct the Kalman filter estimates. This procedure is similar to the accepted practice of augmenting the state vector of the original problem by adding additional components to represent the uncertain parameter or bias. However, Friedland claimed that, by reducing a single calculation involving large matrices, to a sequence of calculations involving smaller matrices, accuracy as well as computational speed can be increased.

The application of Kalman filtering to nonlinear systems has received a great deal of attention in recent years. Nonlinear

estimation theory was presented by Seinfeld [15] and Coggan and Noton [16]. The review by Bucy [5] also includes an account of nonlinear filtering.

Singer [17] proposed a technique to determine when a significant improvement in estimation accuracy can be achieved by using a Kalman filter rather than a Wiener filter (which in this context refers to the stationary form of the Kalman filter) to estimate the state of a time-invariant system. He concluded from this research that there are relatively few instances where the Kalman filter, with a time-varying gain matrix, provides a significant improvement over the corresponding stationary form. This conclusion lends support to the decision to use the stationary version of the Kalman filter in the present work.

2.2.3 Applications

Most of the applications of estimation theory have been in the field of aerospace and missile guidance and navigation [18], including such well known missions as Ranger, Mariner and Apollo Other applications cited by Bucy and Joseph [18] include numerical integration, submarine navigation, fire control and aircraft navigation.

In the field of chemical process control, which is the area of interest in this study, the general trend in the literature has been to emphasize the theoretical and computational aspects of filtering rather than to present actual applications. There have been several simulation studies presented but it is only in recent years that a few experimental or industrial applications have been reported.

Wells and Larson [19] presented a simulation example

combining optimal control and estimation theory to two systems in series with a time delay. The discrete form of the Kalman filter showed that a significant improvement in control could be achieved by using the combined optimal control and estimation policy.

In one of the earlier investigations of nonlinear systems, Detchmendy and Sridhar [20] considered the problem of estimating states and parameters using a sequential least squares estimator. They demonstrated the feasibility of this technique with two simple mechanical examples.

In the process control field several authors have very recently applied Kalman filtering to nonlinear systems. Coggan and Noton [16] used an extended Kalman filter for state and parameter estimation for nonlinear systems with intermittent, irregular and inaccurate measurements and large unmeasured disturbances. A blending system and a thermal system were simulated and the estimates were shown to be accurate.

Seinfeld [21] proposed feedback control of nonlinear systems using a nonlinear Kalman filter for estimating the states and unknown parameters. The scheme was applied to the control of a CSTR in a simulation study and the results proved the technique to be very successful. Gavalas and Seinfeld [22] presented a method for the online sequential estimation of state variables and kinetic parameters in plug flow reactors with slow catalyst decay. The resulting algorithms were computationally simple, especially the discrete filters. A plug flow reactor with a first order irreversible reaction and catalyst decay was simulated and two alternative discrete filters were successfully used to estimate the state variables and parameters.

Wells [23] also presented a form of the extended Kalman filter and discussed its application to nonlinear systems. In particular, a six dimensional model of a CSTR was simulated and the filter gave state estimates which were very close to the actual values. In a later paper, Wells [24] applied this algorithm to a simulated basic oxygen furnace. A reduced, inaccurate, model was used in the Kalman filter algorithm and only one measurement was used to obtain optimal estimates of four states. The model was so poor that good results were not obtained unless more measurements were made available.

Sastry and Wood [25] considered the state estimation problem where some of the parameters are unknown or known inaccurately in a discrete linear model. An iterative algorithm was developed to update or correct these parameters.

Goldmann and Sargent [26] have recently reported a significant study of the factors affecting the performance of the Kalman filter as applied to two simulated chemical processes. The authors considered measurement noise, but not process noise, in their simulations and investigated the sensitivity of the technique to errors in the design matrices, $\underline{\underline{R}}$ and $\underline{\underline{P}}(0)$ (see Section 2.3), plant modelling errors, and autocorrelated measurement noise.

As stated previously, there have been very few industrial or experimental applications of Kalman filtering (in the process industries) reported in the literature; the following are the only three cases which have been uncovered in this brief survey.

Astrom [7] reported an application of linear stochastic control theory to regulate the basis weight of paper at the dry-end

of a papermaking machine. Control of the dry basis weight was considered as a system with one input, thick stock flow, and one output, the estimate of the dry basis weight. A minimal variance control strategy was implemented and a significant reduction of the variance of the basis weight was obtained.

In a more complex application to a papermaking process, Sastry et al [27,28] used an adaptation of Kalman filtering for the identification of parameters in a nonlinear model. Simulation results showed reasonable agreement with the actual operating data and the model parameters obtained in the off-line study were used in tuning DDC loops. The simulation studies were so encouraging that the company recommended that on-line experiments should be conducted in order to optimize plant operation.

Noton et al [29,30] reported the use of an extended Kalman filter in parameter and state estimation for an industrial multi-reactor system. A nonlinear dynamic stochastic model was developed and the filter was used to determine five unknown parameters off-line. The Kalman filter was also implemented in a supervisory control scheme where the computer communicated control actions to the operator. The results were good enough to justify closed loop computer control.

2.3 THEORY

The mathematical formulation of both the optimal control problem and the optimal estimation problem is briefly outlined in this section. This theory is well known and more details can be found in several texts [8-10].

The process plant is assumed to be of the form:

$$\dot{\underline{x}}(t) = \underline{\underline{A}}\,\underline{x}(t) + \underline{\underline{B}}\,\underline{u}(t) + \underline{\underline{D}}\,\underline{d}(t) \tag{2.1}$$

with output equation:

$$\underline{y}(t) = \underline{\underline{H}}\,\underline{x}(t) \tag{2.2}$$

where $\underline{x}$, $\underline{u}$, $\underline{d}$ and $\underline{y}$ are the state (dimension n), control (dimension m), disturbance (dimension p) and output or measurement (dimension q) vectors respectively. All the variables are in normalized perturbation form and $\underline{\underline{A}}$, $\underline{\underline{B}}$, $\underline{\underline{D}}$ and $\underline{\underline{H}}$ are constant coefficient matrices.

The analytical solution to Equation (2.1) can be used to derive the following discrete model [8]:

$$\underline{x}(k+1) = \underline{\underline{\phi}}\,\underline{x}(k) + \underline{\underline{\Delta}}\,\underline{u}(k) + \underline{\underline{\theta}}\,\underline{d}(k) \quad k = 0,1,2,\ldots \tag{2.3}$$

where $\underline{\underline{\phi}}$, $\underline{\underline{\Delta}}$ and $\underline{\underline{\theta}}$ are the constant coefficient matrices for the discrete model and are derived in the usual manner [31, p. 339]:

$$\underline{\underline{\phi}} = \int_0^T e^{\underline{\underline{A}}t}\,dt \tag{2.4}$$

$$\underline{\underline{\Delta}} = \int_0^T e^{\underline{\underline{A}}(T-t)}\,\underline{\underline{B}}\,dt \tag{2.5}$$

$$\underline{\underline{\theta}} = \int_0^T e^{\underline{\underline{A}}(T-t)}\,\underline{\underline{D}}\,dt \tag{2.6}$$

where T is the sampling period.

The quadratic performance index for the regulatory control problem can be expressed as follows

$$J = \underline{x}^T(N)\,\underline{\underline{S}}\,\underline{x}(N) + \sum_{k=1}^{N} [\underline{x}^T(k)\underline{\underline{Q}}_1\underline{x}(k) + \underline{u}^T(k-1)\underline{\underline{R}}_1\underline{u}(k-1)] \tag{2.7}$$

where, $\underline{x}(N)$ is the final state vector,

$\underline{\underline{S}}$ is the final state weighting matrix (nxn),

$\underline{\underline{Q}}_1$ is the state weighting matrix (nxn),

$\underline{\underline{R}}_1$ is the (mxm) weighting matrix on the controls,

and superscript T denotes the vector transpose.

The optimal control policy, $\underline{u}^*(k)$, which minimizes J can be found using discrete dynamic programming [9]. From the performance index it can be seen that the optimal control takes the state, $\underline{x}$, from an initial state, $\underline{x}(0)$, to a final state, $\underline{x}(N)$, which is as close as possible to the origin. The first term in the performance index ensures that a nonzero final state vector, $\underline{x}(N)$, is penalized. The second term indicates that all state vectors, $\underline{x}(k)$, k = 0,1,2,..., must also be close to zero, with the constraint, due to the last term, that there is not an excessive expenditure of control "energy" in doing so.

The well known optimal control law which results for $N = \infty$ is given by:

$$\underline{u}^*(k) = \underline{\underline{K}}_{FB}\, \underline{x}(k) \tag{2.8}$$

where $\underline{\underline{K}}_{FB}$, the optimal feedback control matrix, is time invariant and the asterisk (*) denotes the optimal control policy.

Now consider the process to be a stochastic one with both process and measurement noise; the deterministic model in Equations (2.3) and (2.2) then becomes:

$$\underline{x}(k+1) = \underline{\underline{\Phi}}\, \underline{x}(k) + \underline{\underline{\Delta}}\, \underline{u}(k) + \underline{\underline{\theta}}\, \underline{d}(k) + \underline{\underline{\Gamma}}\, w(k) \tag{2.9}$$

and

$$\underline{y}(k) = \underline{\underline{H}}\,\underline{x}(k) + \underline{v}(k) \tag{2.10}$$

where

$\underline{w}(k)$ is the process noise vector (dimension r),

$\underline{v}(k)$ is the measurement noise vector (dimension q),

and $\underline{\underline{\Gamma}}$ is the coefficient matrix of the measurement noise.

If it is assumed that the probability distributions of the several variables are independent and each is uncorrelated with respect to time, then:

$$\begin{aligned} \text{cov}\,[\underline{w}(k),\underline{w}(j)] = E[\underline{w}(k)\underline{w}^T(j)] &= \underline{\underline{0}} \text{ for } k\neq j \\ &= \underline{\underline{Q}}(k) \text{ for } k=j \end{aligned} \tag{2.11}$$

$$\begin{aligned} \text{cov}\,[\underline{v}(k),\underline{v}(j)] = E[\underline{v}(k)\underline{v}^T(j)] &= \underline{\underline{0}} \text{ for } k\neq j \\ &= \underline{\underline{R}}(k) \text{ for } k=j \end{aligned} \tag{2.12}$$

$$\text{cov}\,[\underline{w}(k),\underline{v}(j)] = \text{cov}\,[\underline{v}(k),\underline{w}(j)] = \underline{\underline{0}} \text{ for all } k,j \tag{2.13}$$

where $\underline{\underline{Q}}(k)$ and $\underline{\underline{R}}(k)$ are the known (or assumed) covariance matrices for the process and measurement noise, respectively, cov denotes the covariance and E the expected value.

An unbiased estimate of the states, $\hat{\underline{x}}(k)$, is desired such that:

$$E[\hat{\underline{x}}(k)] = E[\underline{x}(k)] \tag{2.14}$$

The minimum error variance estimator provides such an estimate and minimizes the error covariance matrix, $\underline{\underline{P}}(k)$:

$$\underline{\underline{P}}(k) = E\{[\underline{x}(k) - \hat{\underline{x}}(k)][\underline{x}(k) - \hat{\underline{x}}(k)]^T\} \tag{2.15}$$

By minimizing the elements of this error variance matrix [10], the best linear estimator (i.e. filter) is obtained and is known as the

Kalman filter.

It has not been necessary to make the assumption that the noise is Gaussian. The Kalman filter is the best linear filter for any distribution; if, however, the noise is Gaussian then it is the best of all possible linear and nonlinear filters [10].

The optimal estimation problem can be solved directly (as described in Section 2.3.1) or by using Kalman's Duality Principle [1,8]. The latter method relates the optimal filtering problem to the optimal regulatory control problem. Since the optimal control problem has been fully developed from a theoretical and computational viewpoint in recent years, the optimal filter can be readily obtained by applying the Duality Principle. The rigorous derivations for both methods are well known and rather lengthy hence only the results are presented here. It should be noted that in this study both methods were successfully employed in deriving the gain matrix for the Kalman filter as a check on the calculations and the computer programming.

Since much of the present investigation is concerned with the significance of the $\underline{\underline{R}}$ and $\underline{\underline{Q}}$ matrices, it is informative to examine an alternative formulation of the problem. The Duality Principle [9] states that the foregoing estimation problem has an interpretation as the solution of a linear quadratic optimization problem. It has been shown [8] that the specific form of this performance index is:

$$\begin{aligned} J = {} & 1/2[\underline{x}(0) - \hat{\underline{x}}(0)]^T \underline{\underline{P}}^{-1}(0) [\underline{x}(0) - \hat{\underline{x}}(0)] \\ & + 1/2 \sum_{k=0}^{N} \{[\underline{y}(k) - \underline{\underline{H}} \hat{\underline{x}}(k)]^T \underline{\underline{R}}^{-1}(k) [\underline{y}(k) - \underline{\underline{H}} \hat{\underline{x}}(k)] \\ & + \hat{\underline{w}}^T(k) \underline{\underline{Q}}^{-1}(k) \hat{\underline{w}}(k)\} \end{aligned} \tag{2.16}$$

where $\underline{\underline{P}}(0)$, $\underline{\underline{Q}}(k)$ and $\underline{\underline{R}}(k)$ are defined in Equations (2.11) - (2.13) and $\hat{\underline{w}}(k)$ is the estimate of the process noise, $\underline{w}(k)$.

The problem is to find $\hat{\underline{x}}(k)$ and $\hat{\underline{w}}(k)$ such that the above performance index is a minimum. The solution is not given here but the form of Equation (2.16) should give some qualitative insight into the significance of the matrices $\underline{\underline{P}}(0)$, $\underline{\underline{R}}$ and $\underline{\underline{Q}}$ which might be helpful in understanding the results presented later.

2.3.1 Kalman Filter Equations

The solution of the optimal estimation problem yields the Kalman filter equation:

$$\hat{\underline{x}}(k) = \bar{\underline{x}}(k) + \underline{\underline{K}}(k) [\underline{y}(k) - \underline{\underline{H}}\, \bar{\underline{x}}(k)] \tag{2.17}$$

where $\underline{\underline{K}}(k)$ is the gain matrix for the Kalman filter, and

$\bar{\underline{x}}(k)$ is the value of the state vector calculated from the deterministic model:

$$\bar{\underline{x}}(k) = \underline{\underline{\phi}}\, \hat{\underline{x}}(k-1) + \underline{\underline{\Delta}}\, \underline{u}(k-1) + \underline{\underline{\theta}}\, \underline{d}(k-1) \tag{2.18}$$

Assuming that the process is statistically stationary (i.e. $\underline{\underline{Q}}$ and $\underline{\underline{R}}$ are constant), the gain matrix can be calculated off-line from the following recursive relations:

$$\underline{\underline{K}}(k) = \underline{\underline{M}}(k)\, \underline{\underline{H}}^T (\underline{\underline{H}}\, \underline{\underline{M}}(k)\, \underline{\underline{H}}^T + \underline{\underline{R}})^{-1} \tag{2.19}$$

$$\underline{\underline{M}}(k+1) = \underline{\underline{\phi}}\, \underline{\underline{P}}(k)\, \underline{\underline{\phi}}^T + \underline{\underline{\Gamma}}\, \underline{\underline{Q}}\, \underline{\underline{\Gamma}}^T \tag{2.20}$$

$$\underline{\underline{P}}(k) = (\underline{\underline{I}} - \underline{\underline{K}}(k)\, \underline{\underline{H}})\, \underline{\underline{M}}(k) \tag{2.21}$$

and the initial conditions:

$$\underline{\underline{M}}(0) = \underline{\underline{P}}(0) = E\{[\underline{x}(0) - \hat{\underline{x}}(0)][\underline{x}(0) - \hat{\underline{x}}(0)]^T\} \tag{2.22}$$

Starting with the initial conditions, Equations (2.19) - (2.21) are evaluated in an iterative manner until $\underline{\underline{K}}(k)$ converges to a constant value, $\underline{\underline{K}}$. If it is assumed that the observation interval is long compared to the system dynamics then the stationary form of Equation (2.17) can be used:

$$\hat{\underline{x}}(k) = \bar{\underline{x}}(k) + \underline{\underline{K}}[\underline{y}(k) - \underline{\underline{H}}\,\bar{\underline{x}}(k)] \tag{2.23}$$

where $\underline{\underline{K}}$ is the limiting solution of Equations (2.19) - (2.21) as $k \to \infty$.

There is a significant advantage in using this equation for implementing the Kalman filter since only one matrix, $\underline{\underline{K}}$, need be stored in the computer instead of a large set of matrices, $\underline{\underline{K}}(k)$. A further consequence of the stationary filter is that the variance of the initial error in the state estimate, $\underline{\underline{P}}(0)$, has no effect on the final gain matrix, $\underline{\underline{K}}$.

In deriving the gain matrix for the stationary Kalman filter, the critical design parameters are the matrices $\underline{\underline{R}}$ and $\underline{\underline{Q}}$ since the choice of these matrices strongly influences the elements of $\underline{\underline{K}}$ and hence the performance of the filter. Given accurate information about the noise statistics, the $\underline{\underline{Q}}$ and $\underline{\underline{R}}$ matrices can be specified exactly. However, this is not the case in practice and, since it is necessary to assume values for the elements of these matrices, it is very useful to know how incorrect guesses of $\underline{\underline{Q}}$ and $\underline{\underline{R}}$ affect the behaviour of the filter. It should be noted that although a $\underline{\underline{Q}}$ matrix with relatively large elements strictly implies a high level of process noise, it can also be loosely interpreted as a lack of confidence in the mathematical

model. Therefore, where unmeasured disturbances are anticipated or where the model is not accurate, better filter performance would be expected if the elements of $\underline{\underline{Q}}$ were chosen to be artificially large.

The specific values of the elements of matrices $\underline{\underline{R}}$ and $\underline{\underline{Q}}$ are of little consequence, but the relative magnitudes are important. In the present discussion and also in the subsequent studies, the actual noise levels remain unchanged and it is the significance of the estimates of these noise levels which is being investigated. If the elements of $\underline{\underline{R}}$ are large compared to those of $\underline{\underline{Q}}$, then, the physical implication is that there is little confidence in the noisy measurements and more confidence in the process model. By referring back to Equation (2.16) it can be seen that, due to the weighting matrices, $\underline{\underline{R}}^{-1}$ and $\underline{\underline{Q}}^{-1}$, this situation corresponds to the third term in the performance index dominating the second term. Thus, theoretically it can also be seen that the estimate of the process noise is minimized which in turn means that the estimated state vector tends towards the model state vector and thus the model response is favoured more than the measurement.

Conversely, if $\underline{\underline{Q}}$ has large elements compared to $\underline{\underline{R}}$, then there is more confidence in the measurements and more weight is placed on the measurements and less on the model when estimating the states. Again by referring to Equation (2.16), the same conclusions can be drawn, from a theoretical viewpoint. In this case the second term dominates due to the small elements of $\underline{\underline{R}}$ (relatively large elements of $\underline{\underline{R}}^{-1}$) and in minimizing the performance index, the difference between the measurements and the estimated states is also minimized.

2.3.2 Combined Estimation and Control

The optimal control law (for linear systems) based on a quadratic performance index was given earlier in Equation (2.8) and it was indicated that this scheme requires a knowledge of all the state variables. In the previous section it was also demonstrated that optimal estimates of the state variables could be made from noisy measurements of the output variables by using the Kalman filter.

If the further assumption, that both the process noise and the measurement noise are Gaussian is introduced, then according to the Separation Theorem [9] the combination of the optimal filter followed by the optimal deterministic controller is the optimal feedback control for the overall system.

The simplified block diagram in Figure 2.1 illustrates the closed loop system where the optimal estimate of the states is used in the feedback control algorithm.

The relevant equations for the overall closed loop system are thus:

Kalman filter

$$\underline{\hat{x}}(k) = \underline{\bar{x}}(k) + \underline{\underline{K}}[\underline{y}(k) - \underline{\underline{H}}\,\underline{\bar{x}}(k)] \tag{2.23}$$

where

$$\underline{\bar{x}}(k) = \underline{\underline{\phi}}\,\underline{\hat{x}}(k-1) + \underline{\underline{\Delta}}\,\underline{u}(k-1) + \underline{\underline{\theta}}\,\underline{d}(k-1) \tag{2.18}$$

Optimal controller

$$\underline{u}(k) = \underline{u}^{*}(k) = \underline{\underline{K}}_{FB}\,\underline{\hat{x}}(k) \tag{2.8}$$

2.3.3 Sub-Optimal Filters

Sub-optimal filters were also used in this study as a basis for comparison with the Kalman filter. The filter equation is

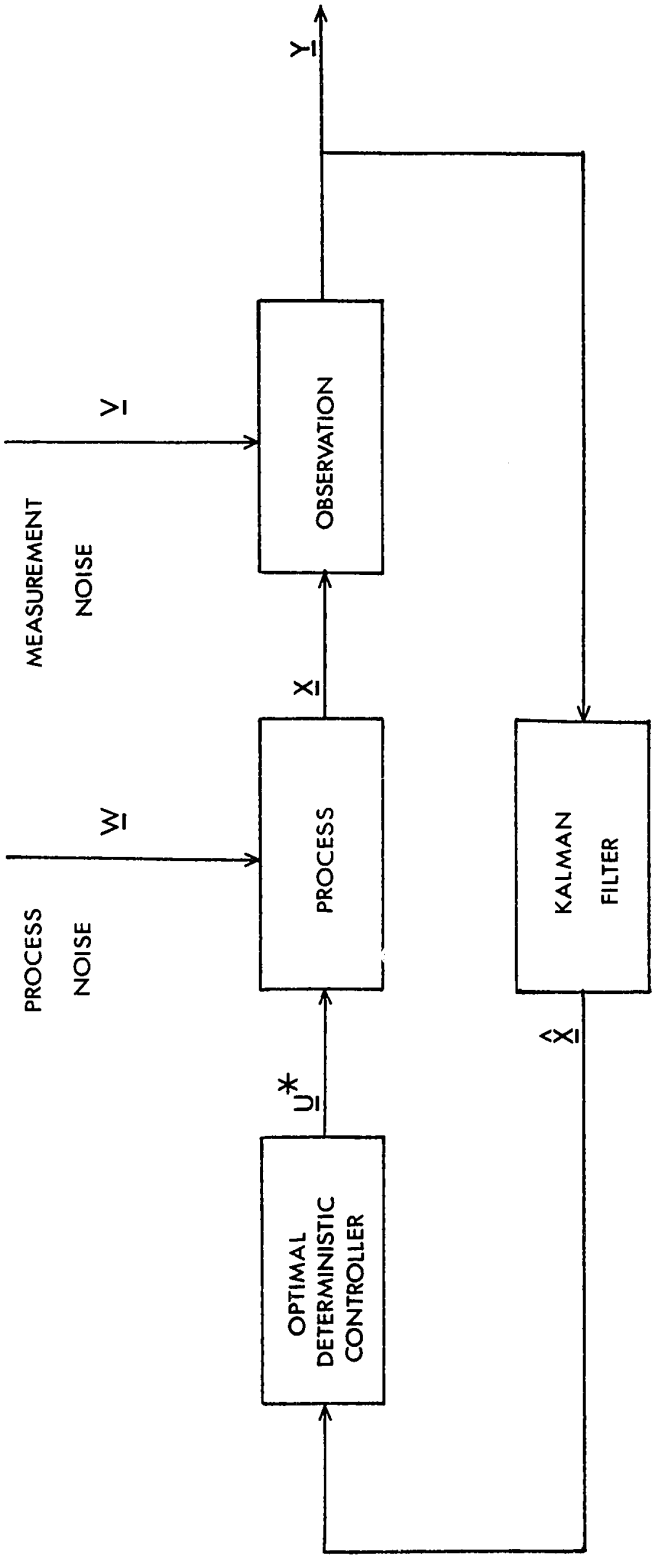

FIGURE 2.1 BLOCK DIAGRAM REPRESENTATION OF COMBINED ESTIMATION AND CONTROL

identical to that used in the optimal filter:

$$\underline{\hat{x}}(k) = \underline{\bar{x}}(k) + \underline{\underline{C}}[\underline{y}(k) - \underline{\underline{H}}\,\underline{\bar{x}}(k)] \tag{2.23}$$

However, the gain matrix, $\underline{\underline{C}}$, is no longer the optimal one found from the Kalman filter theory. Instead the elements are chosen from experience and in this study the $\underline{\underline{C}}$ matrices chosen were very sparse so that the estimates of each state variable were simply combinations of the measured value of the variable (where available) and the calculated value from the model response (Equation (2.18)). This type of filter has been used in previous evaporator studies [32,33].

2.3.4 Exponential Filter

In many DDC applications an exponential filter [34] is used to smooth noisy measurements. Since the experimental and simulation results obtained with the Kalman filter will also be compared with those from the exponential filter (see Chapter 3), the theory for the latter is presented here.

An exponential filter reduces noise in a set of measurements by combining the present measurement and the previous estimate in a fixed proportion which is specified by the user. The scalar filter equation is:

$$\hat{y}_i(k+1) = \hat{y}_i(k) + \alpha_i(y_i(k+1) - \hat{y}_i(k)) \tag{2.24}$$

where i denotes the i^{th} output variable, and α_i is the filter constant.

This equation can be used to estimate each measured state variable. Equation (2.24) indicates that the amount of filtering increases as the filter constant, α_i, decreases. At first glance it may seem that a very small value of α_i would give the best filtering,

but as α_i becomes smaller, a time lag is introduced in the filter so that it is necessary to achieve a balance between the degree of filtering and this time lag when choosing α_i. In the extreme case when $\alpha_i = 0$, the time lag is infinitely long and a constant output equal to the initial state estimate results.

It is important to realize that the exponential filter merely provides signal conditioning and gives no information about unmeasured states. For the purpose of state feedback control, where it is necessary to know all the states, the unmeasured states can be estimated by driving the deterministic model with the estimates from the exponential filters. This procedure was later carried out in estimating an unknown state variable in the simulation and experimental studies.

CHAPTER THREE

EVALUATION OF THE KALMAN FILTER

3.1 INTRODUCTION

This chapter presents the simulation and experimental studies which were carried out on a pilot plant double effect evaporator in order to evaluate the effectiveness of the stationary Kalman filter. Following a description of the process, the computer programs for the simulation study are briefly described. The simulation results are presented and discussed in two main sections: open loop studies and closed loop studies. The results of the experimental study are presented in the same format. Finally the conclusions from these studies are presented in Section 3.10.

3.2 PROCESS DESCRIPTION

A schematic flow diagram of the evaporator in a double effect "forward feed" mode of operation is shown in Figure 3.1. The first effect is a calandria type unit with an eight inch diameter tube bundle. It operates with a nominal feed rate of 5 lb/min of 3 percent aqueous triethylene glycol. The second effect is a long-tube vertical unit with three 1" x 6' tubes and is operated with externally forced circulation. The second effect is operated under vacuum and utilizes the vapour from the first effect as the heating medium. The product is about 10 percent glycol when the steam to the first effect is at its nominal flowrate of 2 lb/min.

A fifth order state-space model of the evaporator was derived by Newell [1] based on linearized material and energy balances. The model equations are of the form given in Chapter Two and are

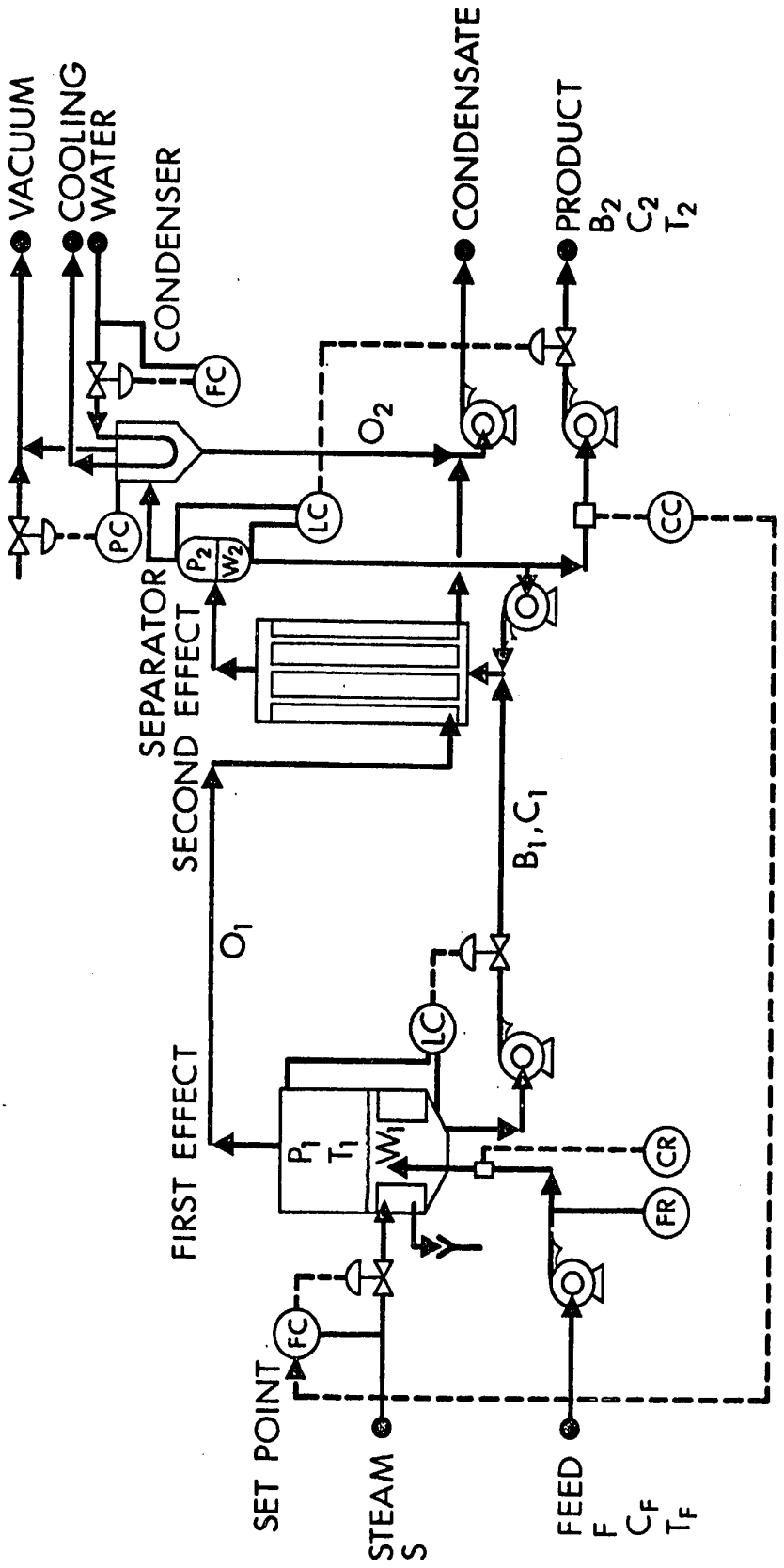

FIGURE 3.1 Schematic Diagram of the Double Effect Evaporator

presented in the appendix. The reader is referred to the notation section for definitions of the variables and normal steady state values. The process variables in the model are expressed in normalized perturbation form.

For this process, one of the five state variables, C1 (the first effect concentration), cannot be measured and in previous multivariable control studies [1] C1 was estimated by a sub-optimal combination of the deterministic model states and the measurements of the other four state variables, W1, H1, W2 and C2. T1 was in fact measured rather than H1, but this measurement together with the steady state value for C1 allowed H1 to be calculated very accurately since the dependence of this variable on C1 is very slight [1].

In the simulation study the fourth order measurement noise vector, $\underline{y}$, was generated by the IBM 1130 SSP subroutine, GAUSS, which produced Gaussian, zero mean noise for each of the four output variables. The process noise vector, $\underline{w}$, was assumed to consist of six elements associated with the three disturbances and the three manipulated variables. Thus, in addition to the deterministic contribution of these variables (accounted for in the model) it was assumed that there was also a noise component for each input. The dimension of the process noise vector is therefore six and the coefficient matrix, $\underline{\underline{\Gamma}}$, is a 5 x 6 matrix, with matrices $\underline{\underline{\theta}}$ and $\underline{\underline{\Delta}}$ as its partitions. The subroutine GAUSS was again used to generate the noise sequences.

Throughout the simulation studies the noise sequence for all ten elements (process and measurement) had a standard deviation of 0.1.

3.3 COMPUTER PROGRAMS FOR THE SIMULATION STUDY

The fifth order linear evaporator model was simulated on the Department's IBM 1800 computer. A program, called SPECS, was written to simulate both open and closed loop evaporator operation with and without disturbances. For each run it was also possible, by means of a random number generator, to include process noise or process and measurement noise. In the latter case by entering the appropriate options via the teletype, the program could punch out on cards one of the following:

1) the unfiltered measurements,

or

2) the estimated states obtained using either a Kalman, suboptimal or exponential filter.

Prior to each run, it was necessary to supply the initial states, the estimate of the initial states and whether or not the filter was to have knowledge of any step disturbances to the process.

For the closed loop runs there were additional program options. The manipulated variables could be constrained within certain physical limits to simulate the physical process more accurately. Another basic option was the type of output to be punched on cards. As in the open loop runs, the noisy measurements or the estimated states (when a filter was used) could be recorded. It was also thought desirable to be able to punch out the actual state variables to provide a better idea of what the process was really doing. Hence it was possible for all these runs to record and punch out the states before measurement noise was added.

The gain matrix for the Kalman filter was calculated off-line

by programming the recursive relations described in Chapter 2. The results from this direct method, using program GAINM, were in good agreement with those achieved by using Kalman's Duality Principle and solving the equivalent optimal regulatory control problem.

The data recorded for both the simulation and experimental runs were displayed by plotting various combinations of the states, manipulated variables and disturbances for each run. The digital plotting program, developed by Newell [2] was used and comprised two coreloads, RBNO2 (for storing the data on files) and RBNO1 (for plotting the stored data).

3.4 OPEN LOOP SIMULATION STUDY

Open loop studies were conducted to establish the significance of the weighting matrices ($\underline{\underline{Q}}$ and $\underline{\underline{R}}$), the initial state estimates, and knowledge of step disturbances on the effectiveness of the Kalman filter. One run was also made to show the performance of a sub-optimal filter for which the gain matrix was chosen arbitrarily instead of being computed from the Kalman filter equations. As a further comparison, the exponential filter was evaluated for three different values of α, the filter constant.

In order to see significant improvements over the unfiltered runs, noise levels were chosen to be reasonably high (0.1 standard deviations for both process and measurement noise in all runs).

The base case for Figures 3.2 - 3.5 was the open loop response of the deterministic model in Equation (2.3) with all the state variables initially at steady state except the product concentration, C2, which was initially 30% below the normal steady state value. In this situation, with no control and no disturbances, the product

concentration gradually increases to the steady state value without affecting the other state variables.

Figure 3.2 compares the deterministic response (i.e. the base case), the four noisy measurements and the five estimates from the Kalman filter. For the Kalman filter in this case (Kalman filter 1) the estimates ($\underline{\underline{R}}$ and $\underline{\underline{Q}}$) of the actual covariance matrices are exact and correct estimates of the initial states are also used. Thus the best possible data was supplied to the Kalman filter equations and the estimates obtained should be optimal. As can be seen from Figure 3.2, the estimated states were in fact very close to the deterministic curves and considerable improvement over the unfiltered measurements was obtained. Table 3.1 provides more information for Figures 3.2 - 3.5 and the numerical values for the parameters in this table (and the figure captions) are given in the appendix. The horizontal arrows denote the initial steady state in all the figures.

It should be emphasized that the results for the Kalman filter, such as in Figure 3.2, can look better or worse depending on the random number sequence that is used. Since the "random" numbers are generated by a computer program in a systematic fashion the number sequences are not, strictly speaking, random. For this reason, it was possible to duplicate "random" number sequences; this proved to be a useful feature in that identical noise sequences, for each variable, could be repeated for every run. It should be made clear that the number sequences of any one of the ten noise elements (six process plus four measurement) was different from all the others for any given run and not correlated in any way; but for any two runs the sequence for one noise element could be the same. This meant that any bias or

TABLE 3.1

DETAILS FOR FIGURES 3.2 - 3.5: OPEN LOOP SIMULATION

All figures show the deterministic response of the model with the second effect concentration initially 30% below the normal steady state. The other curves which appear in each figure are tabulated below (see appendix for the elements of $\underline{\underline{Q}}$, $\underline{\underline{R}}$ and $\underline{\underline{C}}$).

Figure	Filter Used	$\underline{\underline{Q}}$	$\underline{\underline{R}}$	$\underline{\underline{C}}$	Initial State Estimate
3.2	Unfiltered states	-	-	-	-
	Kalman 1	$\underline{\underline{Q1}}$	$\underline{\underline{R1}}$	-	correct
3.3	Sub-optimal	-	-	$\underline{\underline{C1}}$	correct
3.4	Kalman 1	$\underline{\underline{Q1}}$	$\underline{\underline{R1}}$	-	C2 = 0.0
3.5	Kalman 2	$\underline{\underline{Q1}}$	$\underline{\underline{R2}}$	-	correct
	Kalman 3	$\underline{\underline{Q1}}$	$\underline{\underline{R3}}$	-	correct

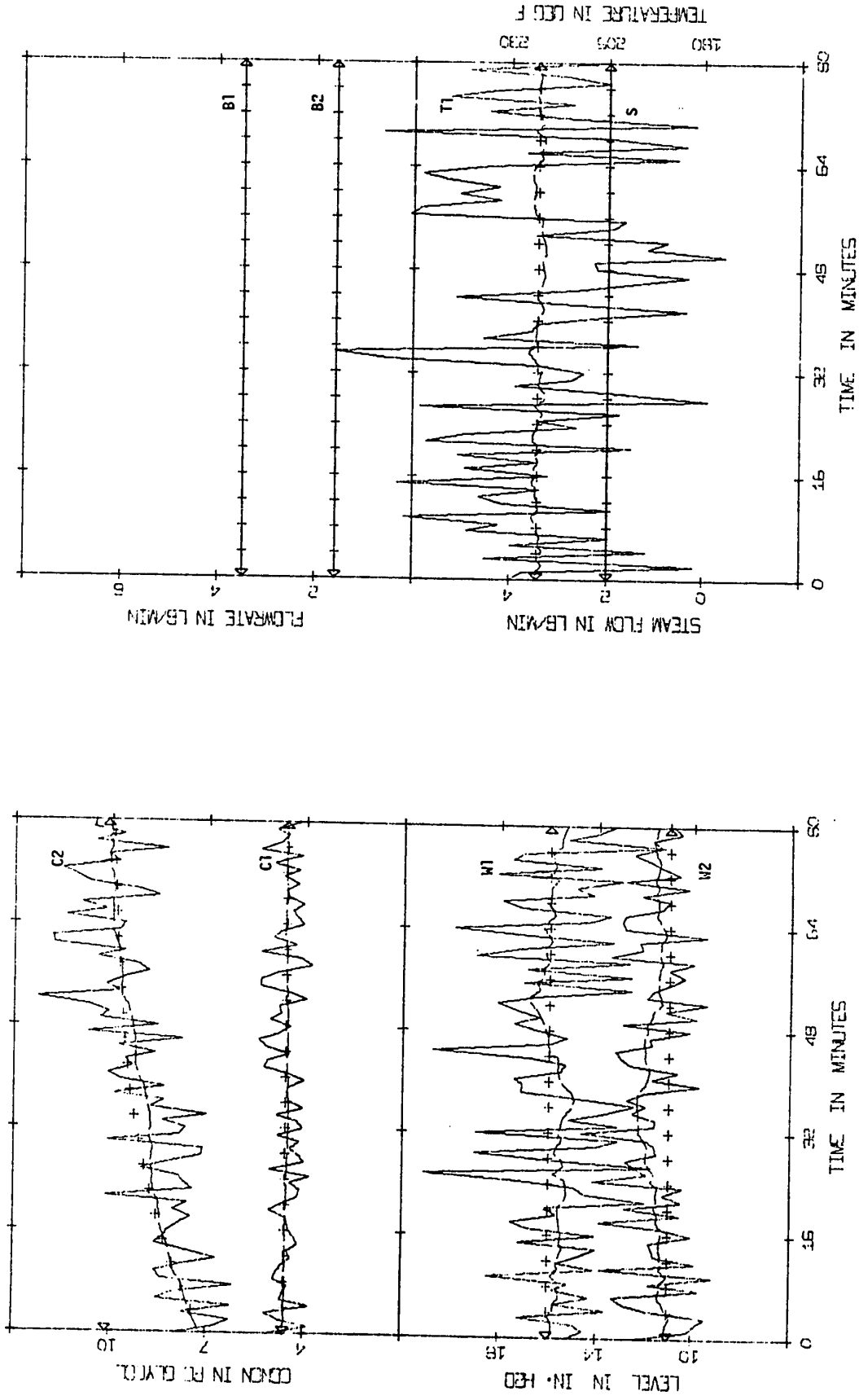

FIGURE 3.2 (SIM/OL) +++deterministic, —— unfiltered, --- Kalman filter 1

trend in the noise sequences could be repeated in every run so that a comparison between different filters was not obscured by variations in the generated noise vectors.

However, as a check on the randomness of the noise sequences and the reproducibility of the plots, five runs using the Kalman filter of Figure 3.2 were made with different random number sequences. The results (not presented) showed that short term trends in the "random" noise can result in deviations of the estimated state variables from their deterministic path but these deviations were always small. In all cases, the Kalman filter gave satisfactory state estimates comparable to those shown in Figure 3.2.

3.4.1 Comparison with a Sub-Optimal Filter

In Figure 3.3 a sub-optimal filter was used to provide estimates of the four measured states while the C1 estimate was generated by the model and is therefore much smoother. Since the degree of filtering is low here the estimates of the other four states are very noisy. This shows that the gain matrix cannot be chosen arbitrarily and on-line tuning would be required to find a satisfactory sub-optimal filter.

3.4.2 Effect of a Poor Initial State Estimate

Figure 3.4 shows the effect of a poor initial estimate of the second effect concentration on the performance of the Kalman filter. For this run, C2 was deliberately chosen to be zero instead of the true value (30% below the steady state) and it can be seen that the estimate recovers from this poor initial estimate after approximately 30 minutes.

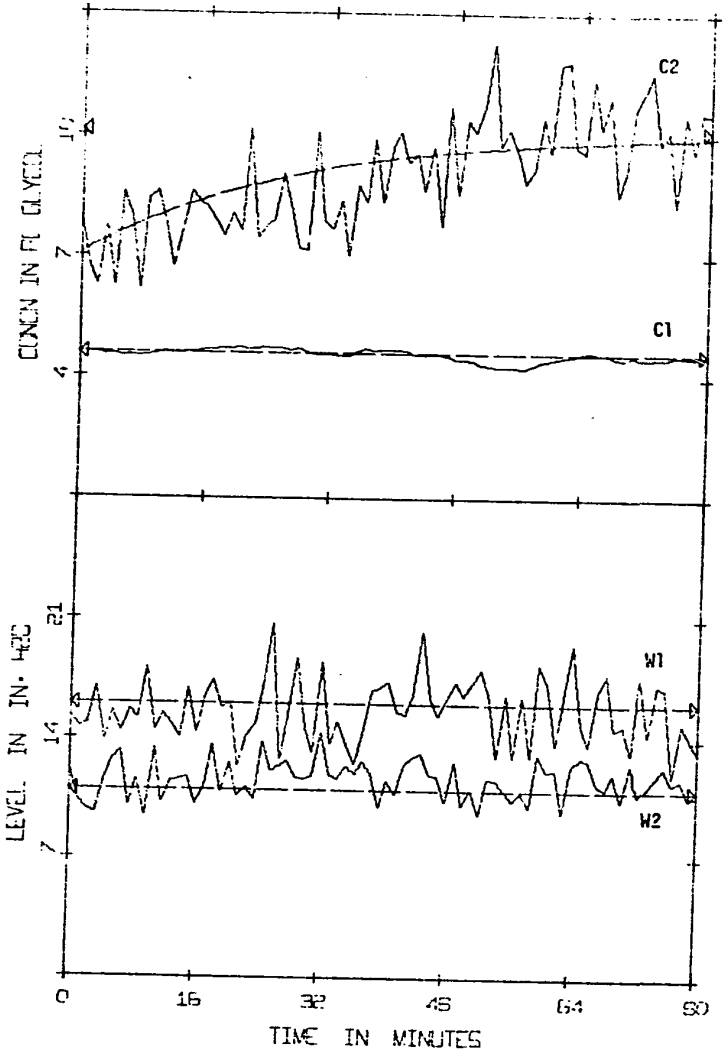

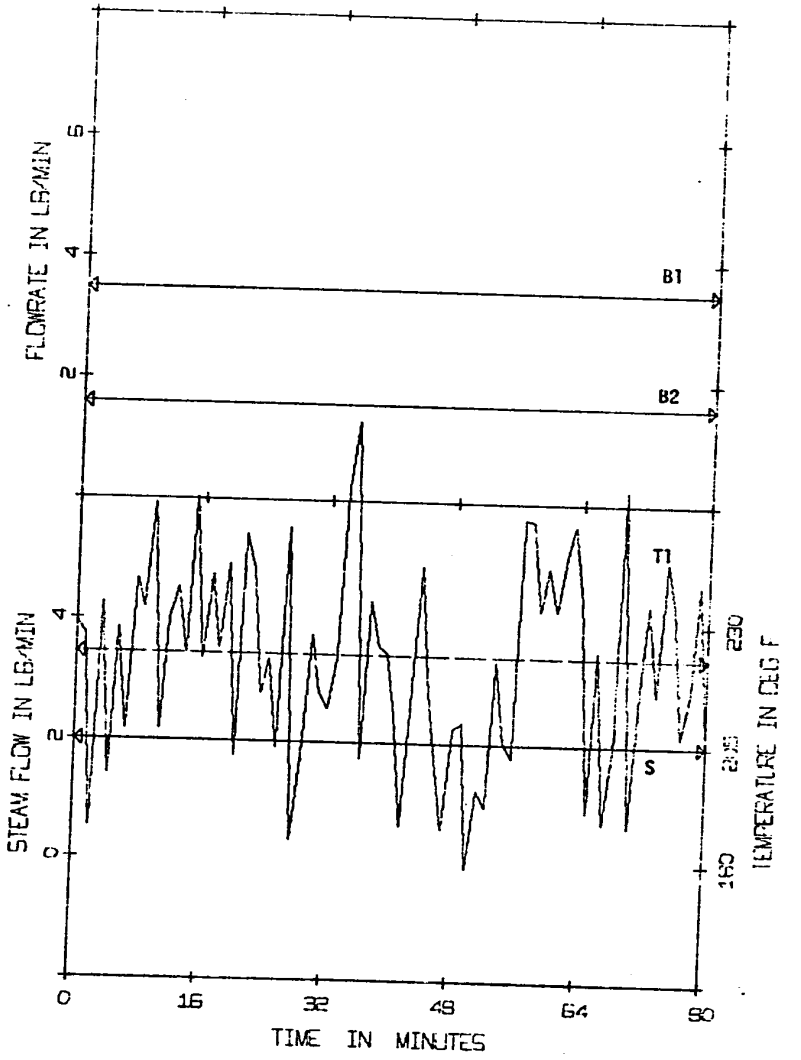

FIGURE 3.3 (SIM/OL) --- deterministic, —— sub-optimal filter 1

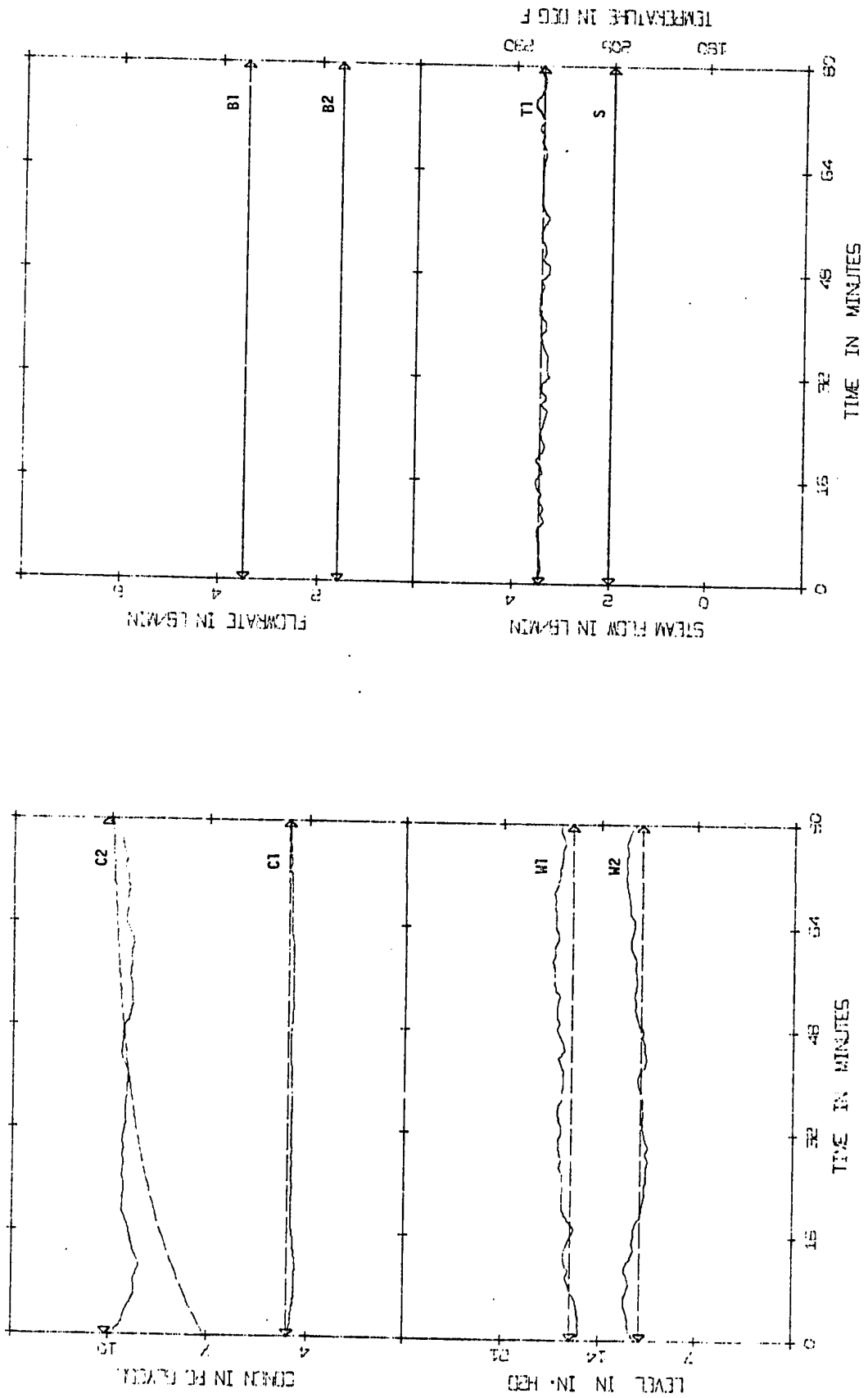

FIGURE 3.4 (SIM/OL) --- deterministic, —— Kalman filter

3.4.3 Effect of the $\underline{\underline{Q}}$ and $\underline{\underline{R}}$ Weighting Matrices

Throughout this study, the weighting matrices $\underline{\underline{R}}$ and $\underline{\underline{Q}}$ were selected to be diagonal with all the diagonal elements equal for each matrix:

$$\underline{\underline{Q}} = Q\underline{\underline{I}} \qquad \text{and} \qquad \underline{\underline{R}} = R\underline{\underline{I}}$$

Thus the scalar ratio R:Q refers to the relative magnitudes of the diagonal elements of these two design matrices. The physical implication here is that the noise levels for all of the measured variables are equal and not correlated with each other (similarly for the process noise variables).

Figure 3.5 shows the results obtained from the Kalman filter where the gain matrix, $\underline{\underline{K}}$, is computed from incorrect R:Q ratios. Kalman filter 2 uses a R:Q ratio of 1:100 which can also be interpreted as an "estimated" measurement to process noise level ratio of 1:10. This meant that there was much more confidence in the measurements than in the model and consequently little filtering took place. Thus in Figure 3.5 the estimated states are noisy but the trend is reasonably good. In the same figure the state estimates provided by Kalman filter 3 (which uses a R:Q ratio of 4:1) were also plotted. Here, there was slightly more confidence in the model than in the measurements so that the estimates tended towards the model response and hence were smoother than before. It is emphasized once more that the actual noise levels used in all the simulation runs had a standard deviation of 0.1 so that in reality the correct value of R:Q was always 1:1.

It is tempting to suggest from these results that the higher the R:Q ratio the better the filter performance and in fact, the state

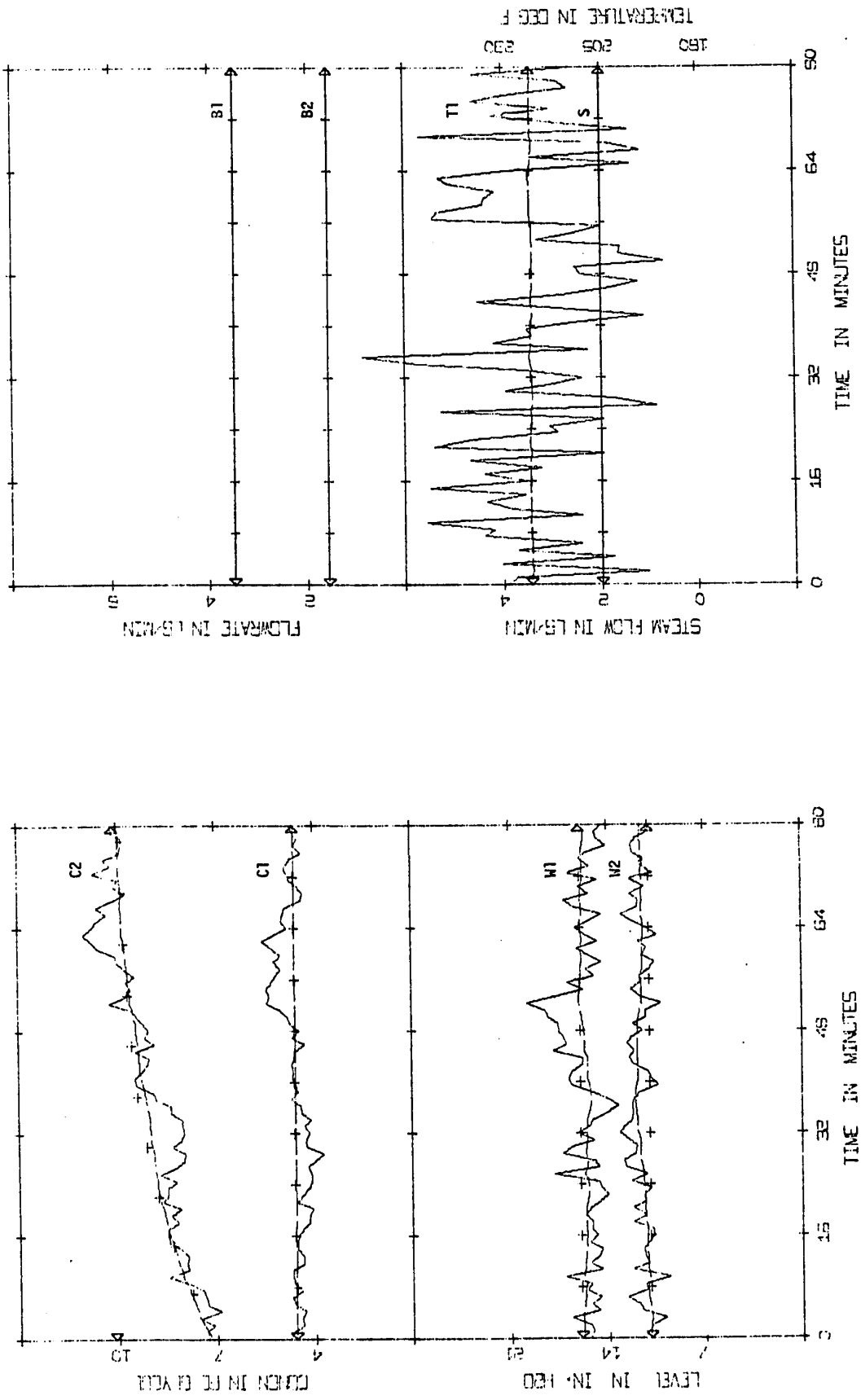

FIGURE 3.5 (SIM/OL) +++ deterministic, —— Kalman filter 2, --- Kalman filter 3

estimates become identical to the model response as R:Q tends to infinity. However, as will be shown in section 3.4.4, a large R:Q ratio is not desirable if the model is not accurate and can be disastrous if unmeasured disturbances occur (i.e. disturbances which are not measured and hence do not appear in the model calculations).

3.4.4 Effect of an Unmeasured Step Disturbance

In Figures 3.6 - 3.8 a 30% step down in feed concentration was applied to the simulated process when it was initially at the normal steady state. The details for these figures are given in Table 3.2.

Figure 3.6 compares the deterministic response, the noisy measurements and the states estimated by Kalman filter 1A. A knowledge of the step disturbance was included in the model calculations for this filter and the assumed R:Q ratio of 1:1 was exact.

The same filter was used for two runs shown in Figure 3.7 but filter 1A has knowledge of the disturbance whereas filter 1B does not. There is a significant discrepancy between the estimates and the actual states for filter 1B.

The fact that this discrepancy is exaggerated if the model is favoured more than the measurements is readily apparent from Figure 3.8 where both filters 2B and 5B were unaware of the step change in feed concentration. Kalman filter 2B, with a R:Q ratio of 1:100, favours the measurements strongly and thus the trend of the curves (though noisy) is good. Conversely Kalman filter 5B favours the model very strongly since R:Q = 100:1. Its estimates are very poor and the curves are almost straight lines since the model was not aware of the disturbance. This would obviously be an undesirable situation if

TABLE 3.2

DETAILS OF FIGURES 3.6 - 3.11: OPEN LOOP SIMULATION

All figures show the deterministic response of the model to a 30% step down in feed concentration and the estimates tabulated below.

(See appendix for the elements of $\underline{\underline{Q}}$ and $\underline{\underline{R}}$).

A - denotes a filter which has knowledge of a step disturbance
B - denotes a filter which is unaware of a step disturbance

Figure	Filter Used	$\underline{\underline{Q}}$	$\underline{\underline{R}}$	α
3.6	Unfiltered states	-	-	-
	Kalman 1A	$\underline{\underline{Q1}}$	$\underline{\underline{R1}}$	-
3.7	Kalman 1A	$\underline{\underline{Q1}}$	$\underline{\underline{R1}}$	-
	Kalman 1B	$\underline{\underline{Q1}}$	$\underline{\underline{R1}}$	-
3.8	Kalman 5B	$\underline{\underline{Q2}}$	$\underline{\underline{R1}}$	-
	Kalman 2B	$\underline{\underline{Q1}}$	$\underline{\underline{R2}}$	-
3.9	Exponential 1	-	-	$\alpha 1 = 0.7$
3.10	Exponential 3	-	-	$\alpha 3 = 0.3$
3.11	Exponential 4	-	-	$\alpha 4 = 0.1$

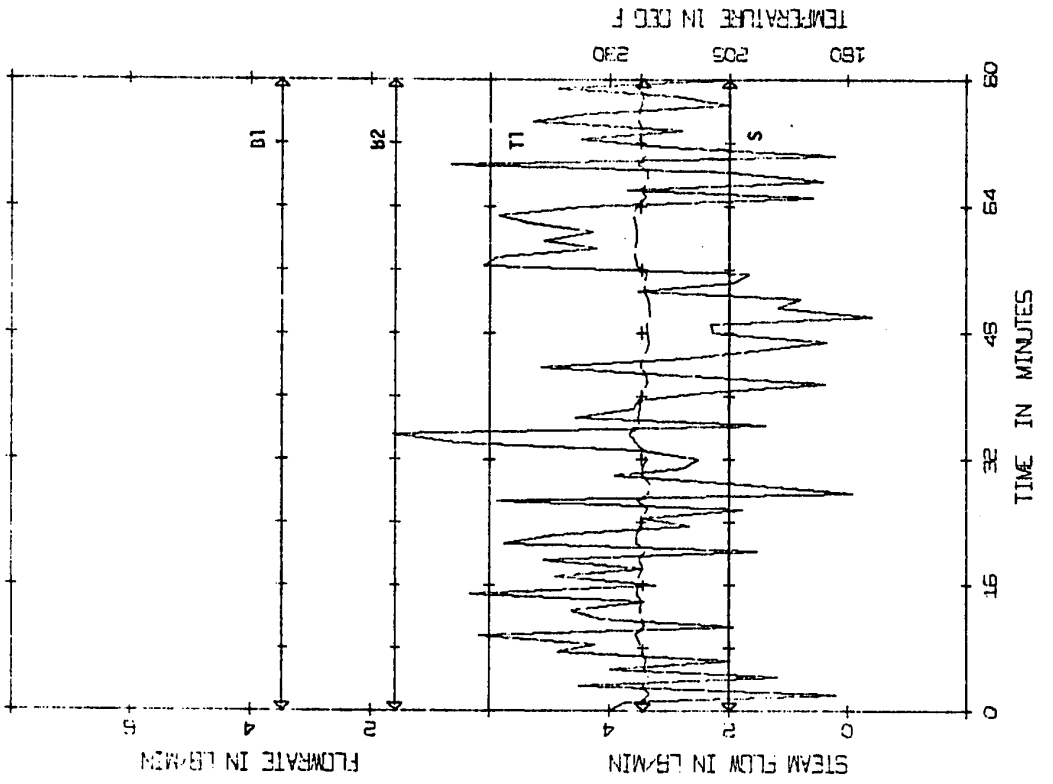

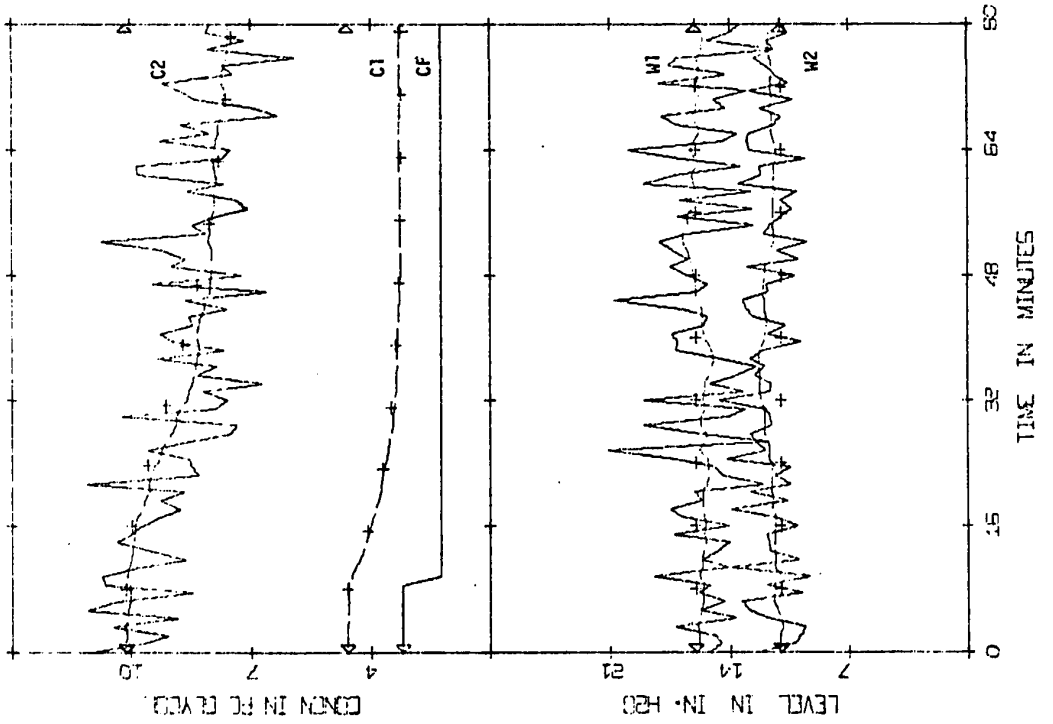

FIGURE 3.6 (SIM/-30%CF/OL) +++ deterministic, —— unfiltered, --- Kalman filter 1A

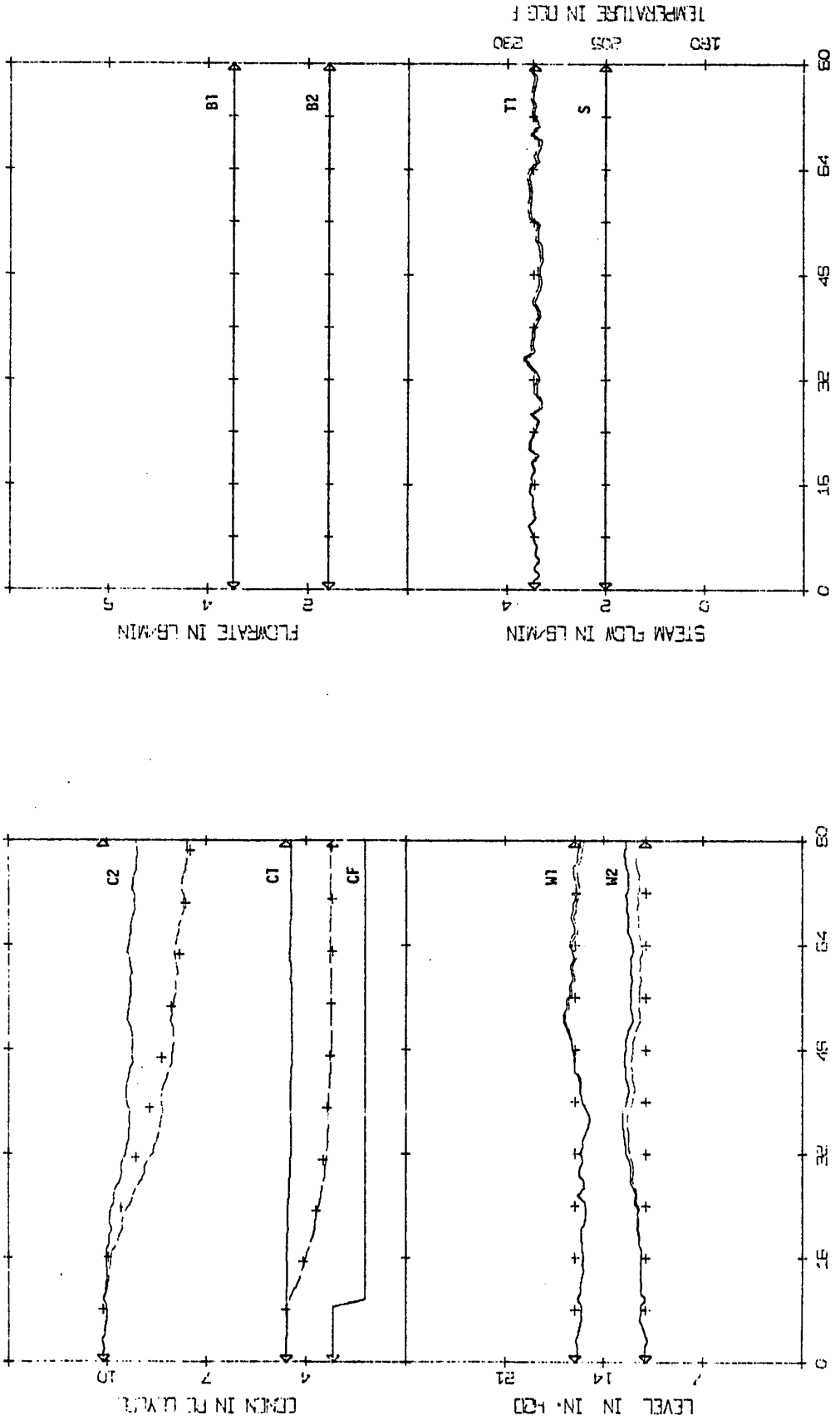

FIGURE 3.7 (SIM/-30%CF/OL) +++ deterministic, —— Kalman filter 1B, --- Kalman filter 1A

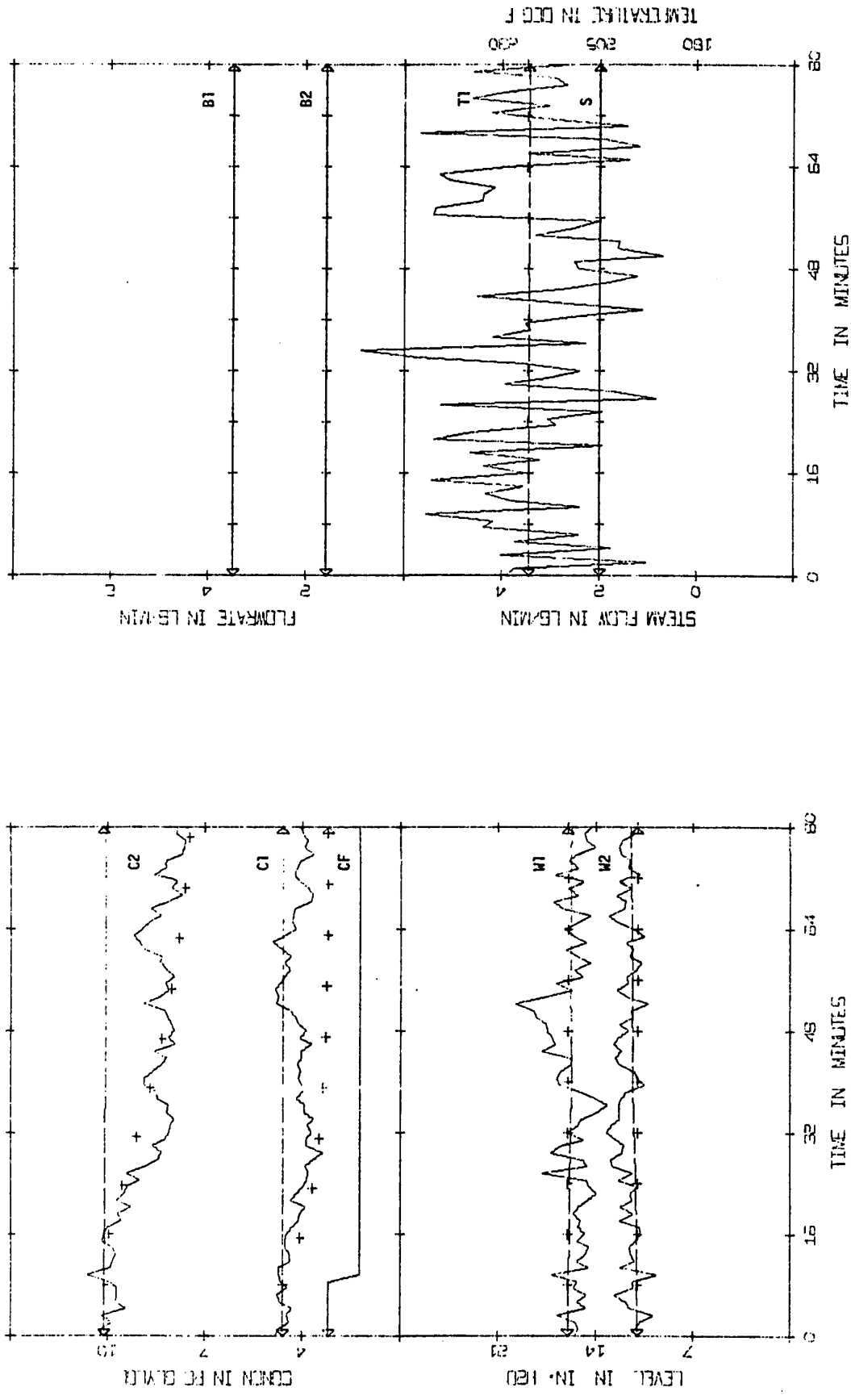

FIGURE 3.8 (SIM/-30%CF/OL) +++ deterministic, —— Kalman filter 2B, --- Kalman filter 5B

control was to be based on these estimates.

3.4.5 Comparison with the Exponential Filter

An exponential (or RC) filter was also used to estimate four of the states from the noisy measurements while the remaining state (first effect concentration) was calculated from the deterministic model. Again a 30% step down in feed concentration was applied to the steady state process and the exponential filter was used with three different values of α as shown in Figures 3.9 - 3.11. The values of α were decreased from 0.7 in Figure 3.9 to 0.3 in Figure 3.10 and finally $\alpha = 0.1$ was used in Figure 3.11. The results show that the exponential filter can only smooth out the noise effectively when a very small value of α is used. However, with the value of α used in Figure 3.11 there is a time lag introduced which later proved to be a considerable problem when implementing feedback control based on these estimates. In Figure 3.11, the time lag in the estimate of C2 is partially obscured by the fact that the particular noise sequence used tends to fall below the mean value for a period before rising again towards the end of the transient. However, by comparing this curve with the Kalman filter estimate in Figure 3.6 the time lag is more obvious.

The details for these three figures are given in Table 3.2.

3.5 CLOSED LOOP SIMULATION STUDY

Simulation studies were also carried out for combined estimation and control. The optimal feedback control for the deterministic evaporator model has been investigated previously by Newell [1] and the feedback control matrix used here (see appendix for Chapter 3) has been shown to give excellent results. The purpose of the present work was to use estimated states in the control calculations in an endeavour to

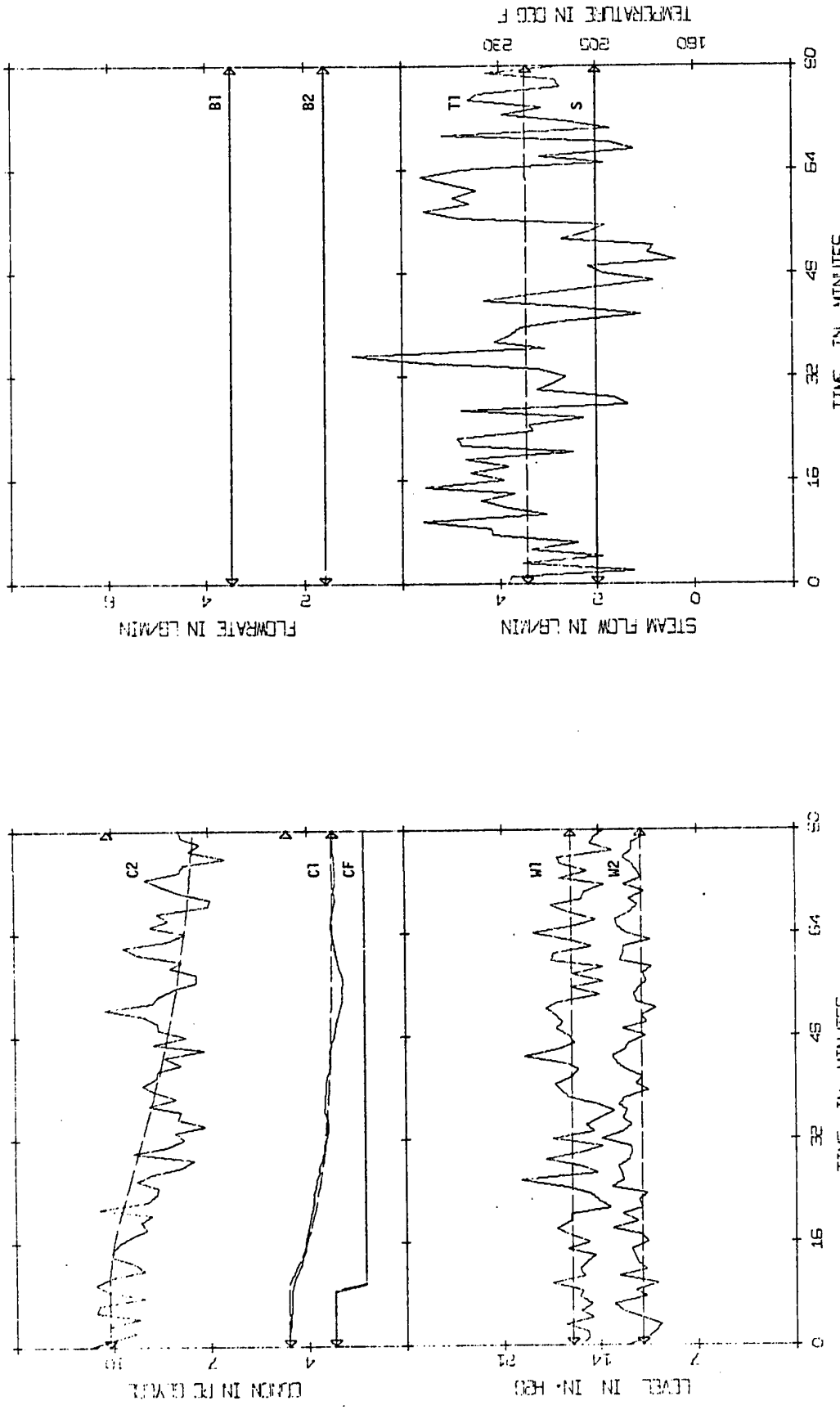

FIGURE 3.9 (SIM/OL) --- deterministic, —— exponential filter 1

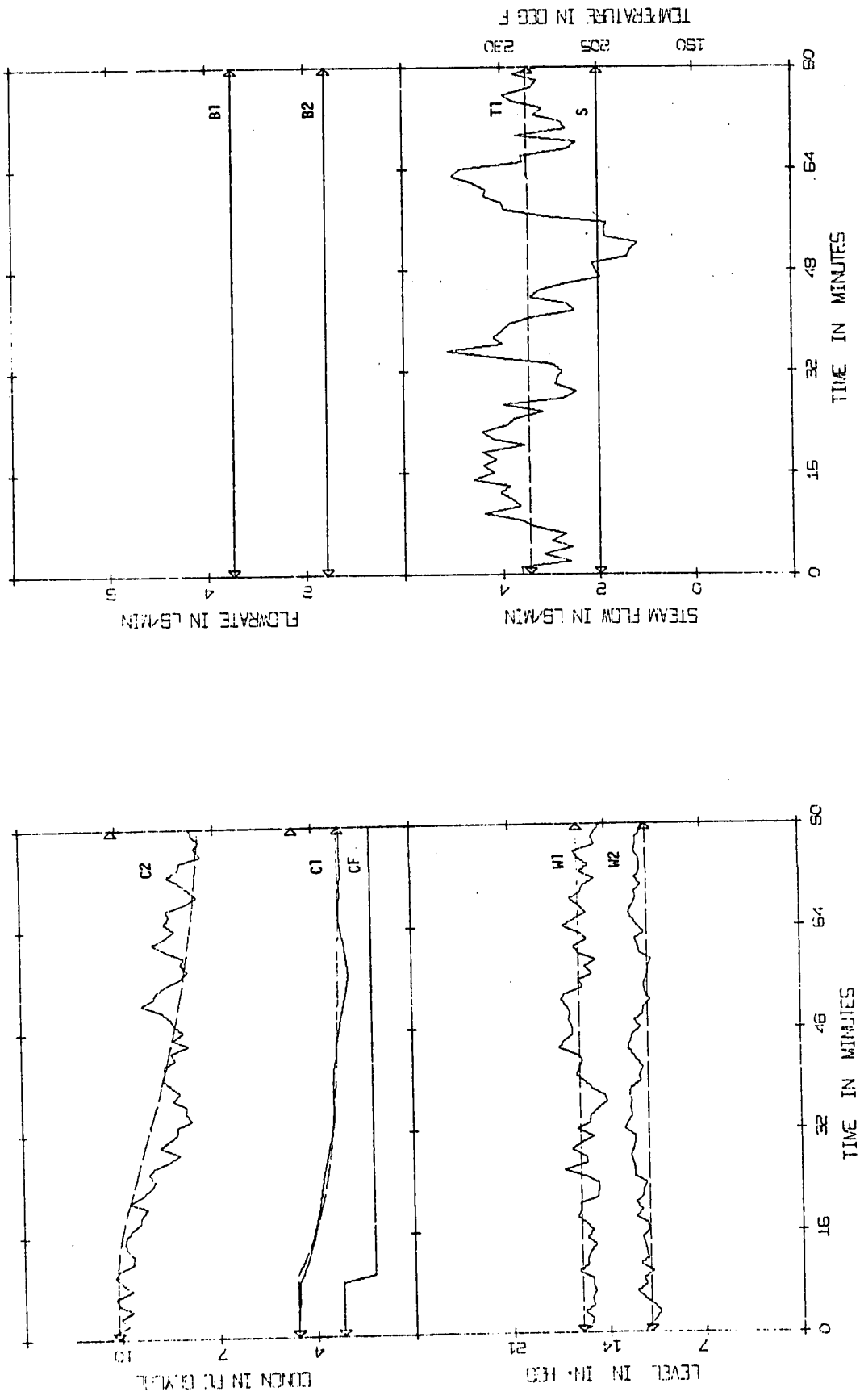

FIGURE 3.10 (SIM/OL) --- deterministic, —— exponential filter 3

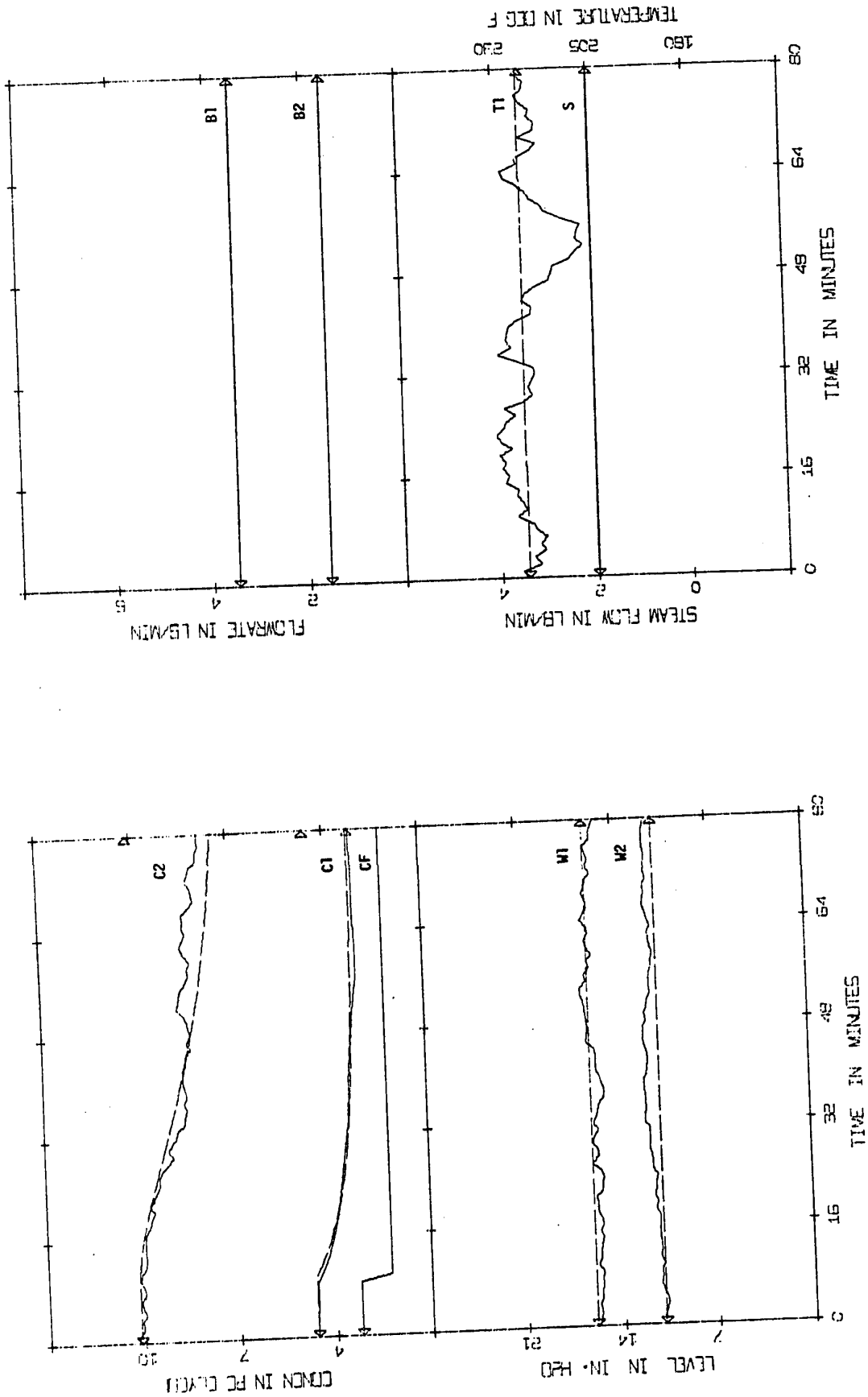

FIGURE 3.11 (SIM/OL) --- deterministic, —— exponential filter 4

improve upon the control obtained by using the unfiltered measurements.

The simulation runs show the deterministic response of the closed loop system, the response of the stochastic system without any filtering and also the response when estimated states are used in the control calculations. The details for Figures 3.12 - 3.23 are given in Table 3.3.

As indicated earlier, the states displayed in the graphs for the closed loop runs were the actual states before measurement noise was added. Although the estimated states were used in the control calculations, they were not displayed since they do not, in many instances, accurately reflect the state of the process. Again for all these runs, all noise levels were characterized by a standard deviation of 0.1.

As a base case, a deterministic closed loop run was made with a 20% step down in feed flow. Figure 3.12 shows how the simulated process responds under optimal feedback control. There was a slight offset in W1 and T1 but otherwise the states were kept very close to their original steady state values. The primary controlled variable, C2, was especially steady.

The same run was then repeated with process and measurement noise included. Figure 3.13 shows the actual states when the control was based on unfiltered measurements and a "model value" for C1. The deterministic curves also appear in the same figure as a comparison but only one of the manipulated variables (steam flow, S) is shown since the standard second page plot was almost incomprehensible due to the violent control action and overlapping of the noisy curves.

From Figure 3.13 it is evident that, although the general

TABLE 3.3

DETAILS OF FIGURES 3.12 - 3.23: CLOSED LOOP SIMULATION

Figures 3.13 - 3.23 show the deterministic closed loop response of the model to a 30% step down in feed flowrate as well as the actual closed loop responses using various filters as tabulated below (see appendix for the elements of $\underline{\underline{Q}}$, $\underline{\underline{R}}$ and $\underline{\underline{C}}$).

A - denotes a filter which has knowledge of a step disturbance

B - denotes a filter which is unaware of a step disturbance

Figure	States Displayed	Filter Used	$\underline{\underline{Q}}$	$\underline{\underline{R}}$	$\underline{\underline{C}}$	α	Remarks
3.12	Deterministic	No filter (deterministic)	-	-	-	-	
3.13	Unfiltered	No filter (noisy)	-	-	-	-	model value of C1 used in control calculations
3.14	Actual	Kalman 1A	$\underline{\underline{Q1}}$	$\underline{\underline{R1}}$	-	-	
3.15	Actual	Kalman 1B	$\underline{\underline{Q1}}$	$\underline{\underline{R1}}$	-	-	
3.16	Actual	Kalman 5A	$\underline{\underline{Q2}}$	$\underline{\underline{R1}}$	-	-	
3.17	Actual	Kalman 5B	$\underline{\underline{Q2}}$	$\underline{\underline{R1}}$	-	-	
3.18	Actual	Kalman 2A	$\underline{\underline{Q1}}$	$\underline{\underline{R2}}$	-	-	
3.19	Actual	Sub-optimal 2	-	-	$\underline{\underline{C2}}$	-	
3.20	Actual	Exponential 1	-	-	-	$\alpha 1=0.7$	model value of C1 used in control calculations
3.21	Actual	Exponential 2	-	-	-	$\alpha 2=0.5$	
3.22	Actual	Exponential 3	-	-	-	$\alpha 3=0.3$	
3.23	Actual	Exponential 4	-	-	-	$\alpha 4=0.1$	

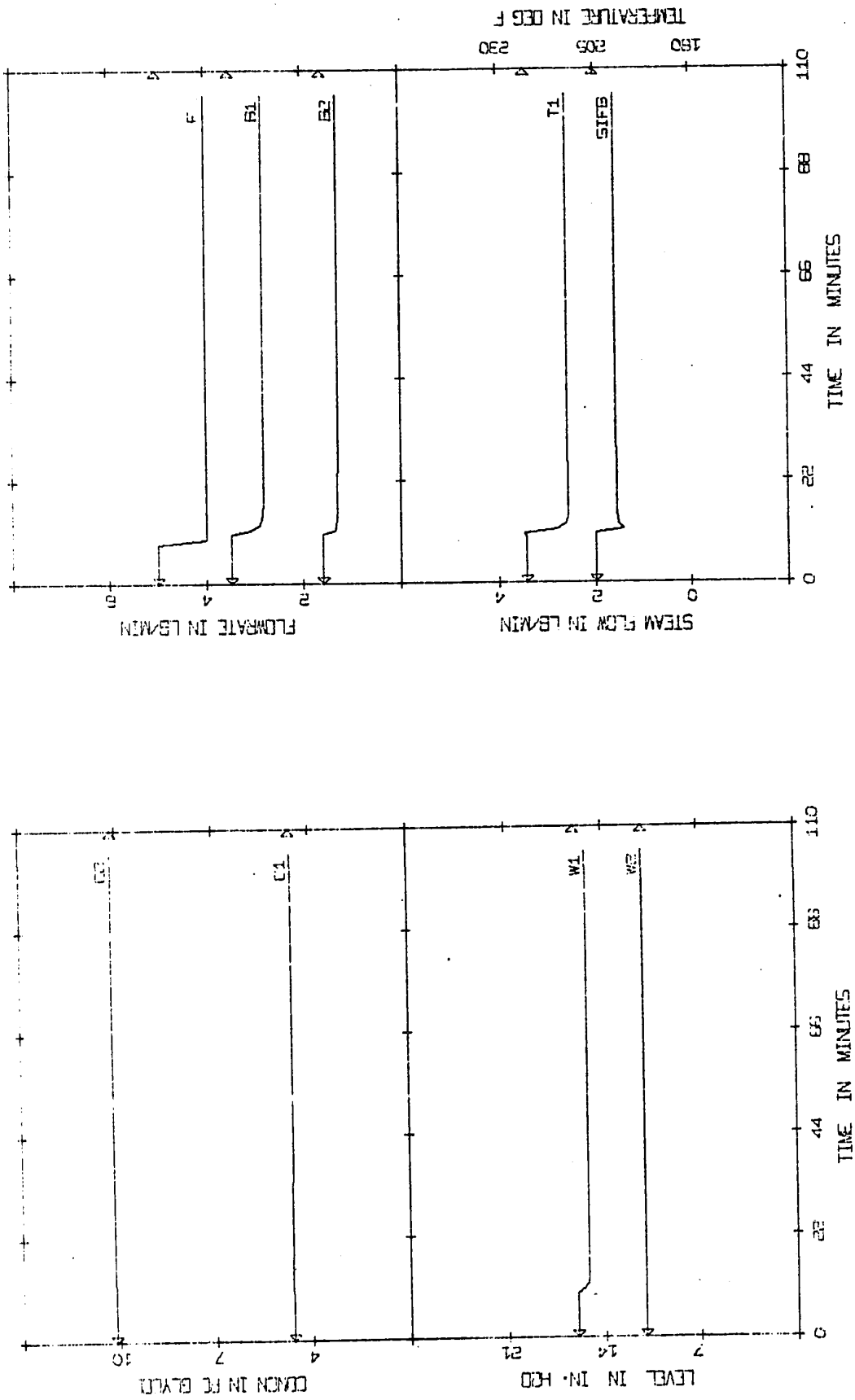

FIGURE 3.12 (SIM/-20%F/FB) —— deterministic response

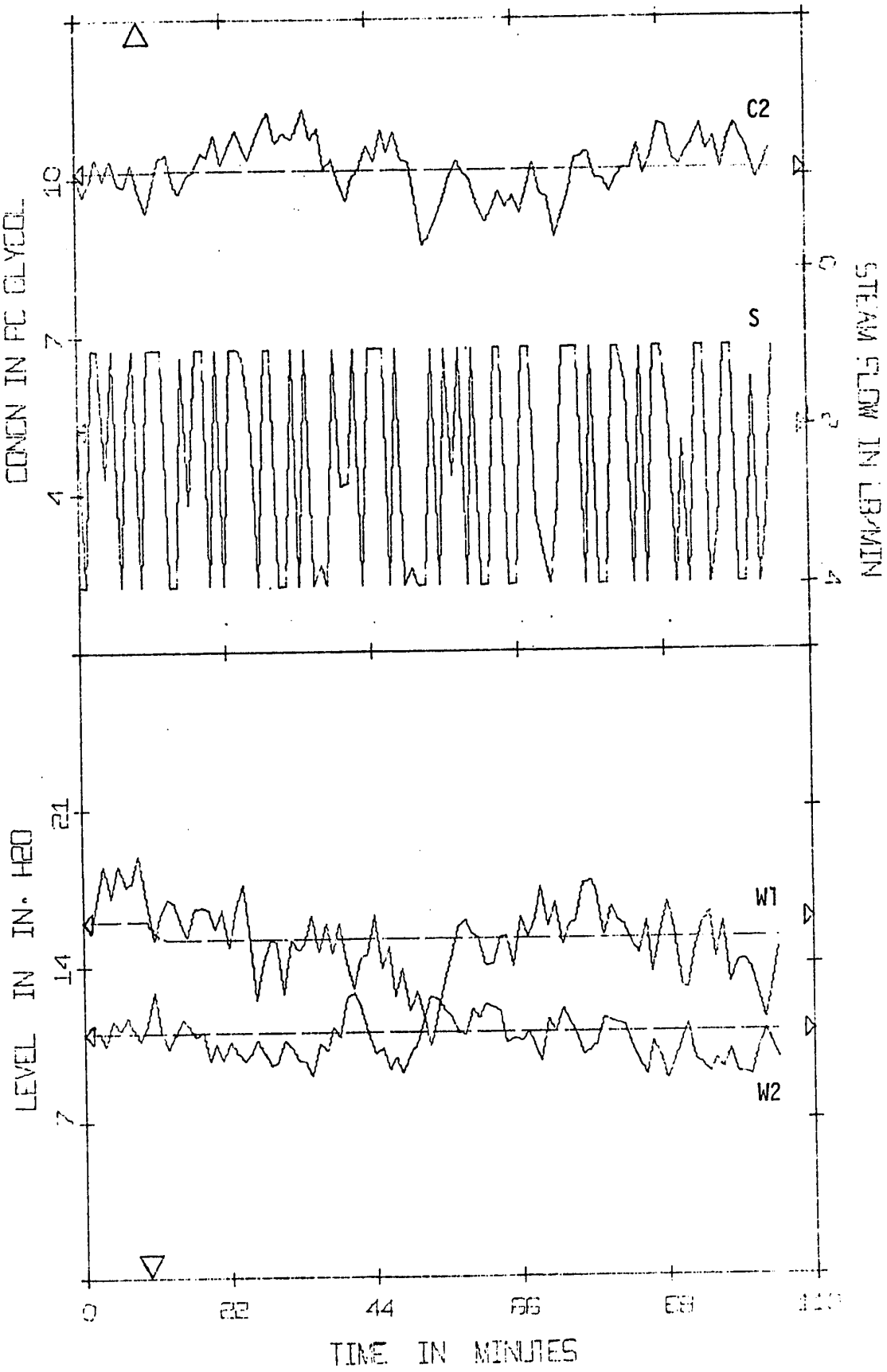

FIGURE 3.13 (SIM/-20%F/FB) --- deterministic, —— unfiltered

trend of the controlled variables is good, the states are very noisy and the control action required is excessive. Figure 3.14 shows the improved control that results when Kalman filter 1A (where the filter is aware of the disturbance) is used. It is doubtful if these controlled states could be made much closer to the deterministic case since these curves must always reflect a certain level of process noise and therefore some fluctuation is to be expected. The manipulated variables still fluctuate to a certain extent but this is greatly reduced compared to the unfiltered case.

3.5.1 Effect of the Weighting Matrices and Unmeasured Step Disturbances

The effect of an unmeasured disturbance is illustrated in Figure 3.15 where Kalman filter 1B was used. Since the estimates of the states did not respond quickly enough to reflect the disturbance in feed flow, the control action was not able to prevent a considerable drop in the first effect level (W1) and a smaller drop in the separator level (W2). Product concentration, C2, was controlled reasonably well but the draining of W1 to less than half the original value is an undesirable result.

In Figures 3.16 and 3.17 the run of Figure 3.14 was repeated with Kalman filters 5A and 5B, respectively, where an R:Q ratio of 100:1 was used in computing the gain matrix. Filter 5A gave very good results for the controlled states and it is notable that the manipulated variables are very smooth. The success of this run is due to the accuracy of the model and the fact that the disturbance was measured. In Figure 3.17 Kalman filter 5B was not aware of the disturbance and the effect of weighting the model so heavily proved to be disastrous: the first effect level drained out completely, the

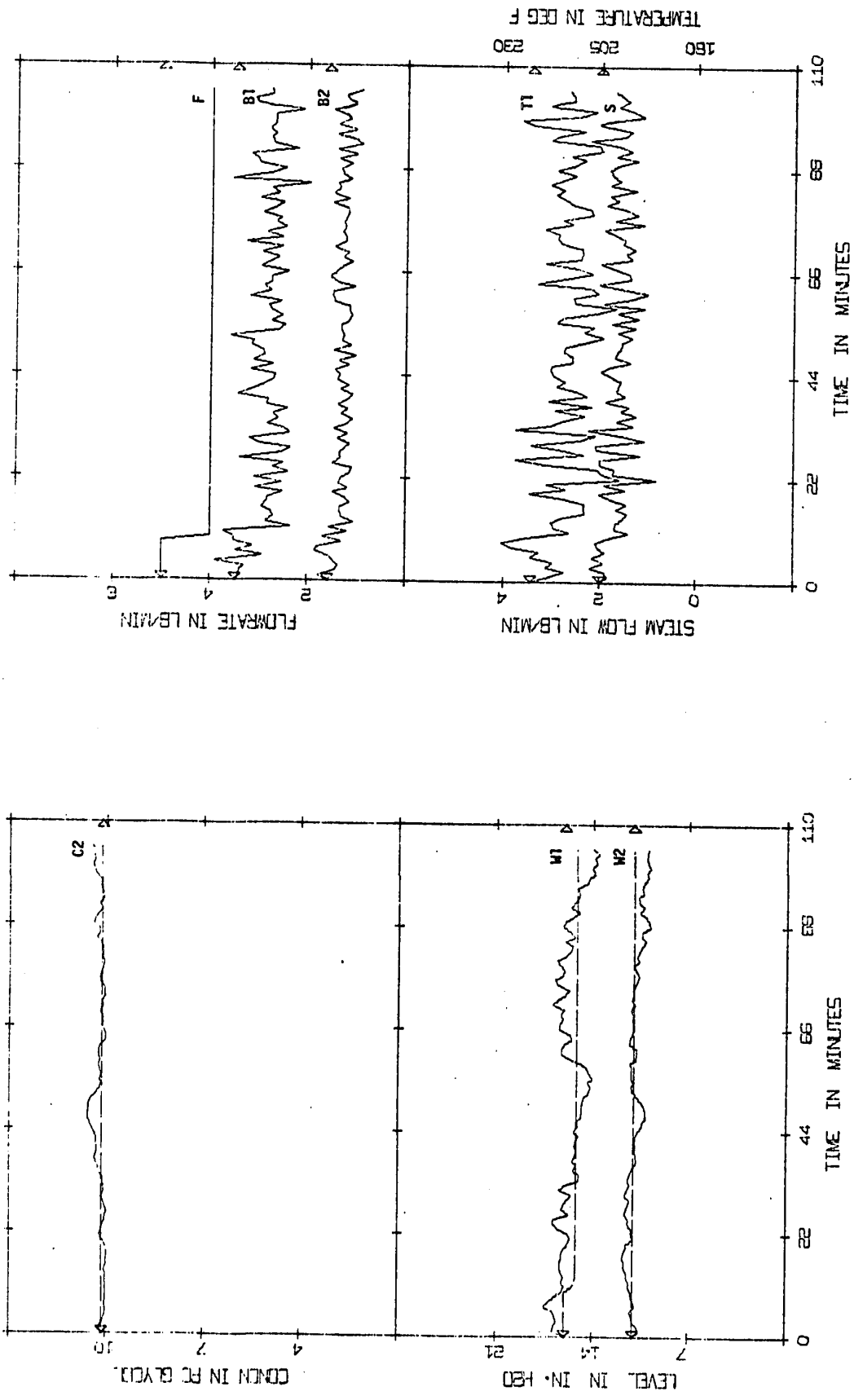

FIGURE 3.14 (SIM/-20%F/FB) --- deterministic, —— Kalman filter 1A

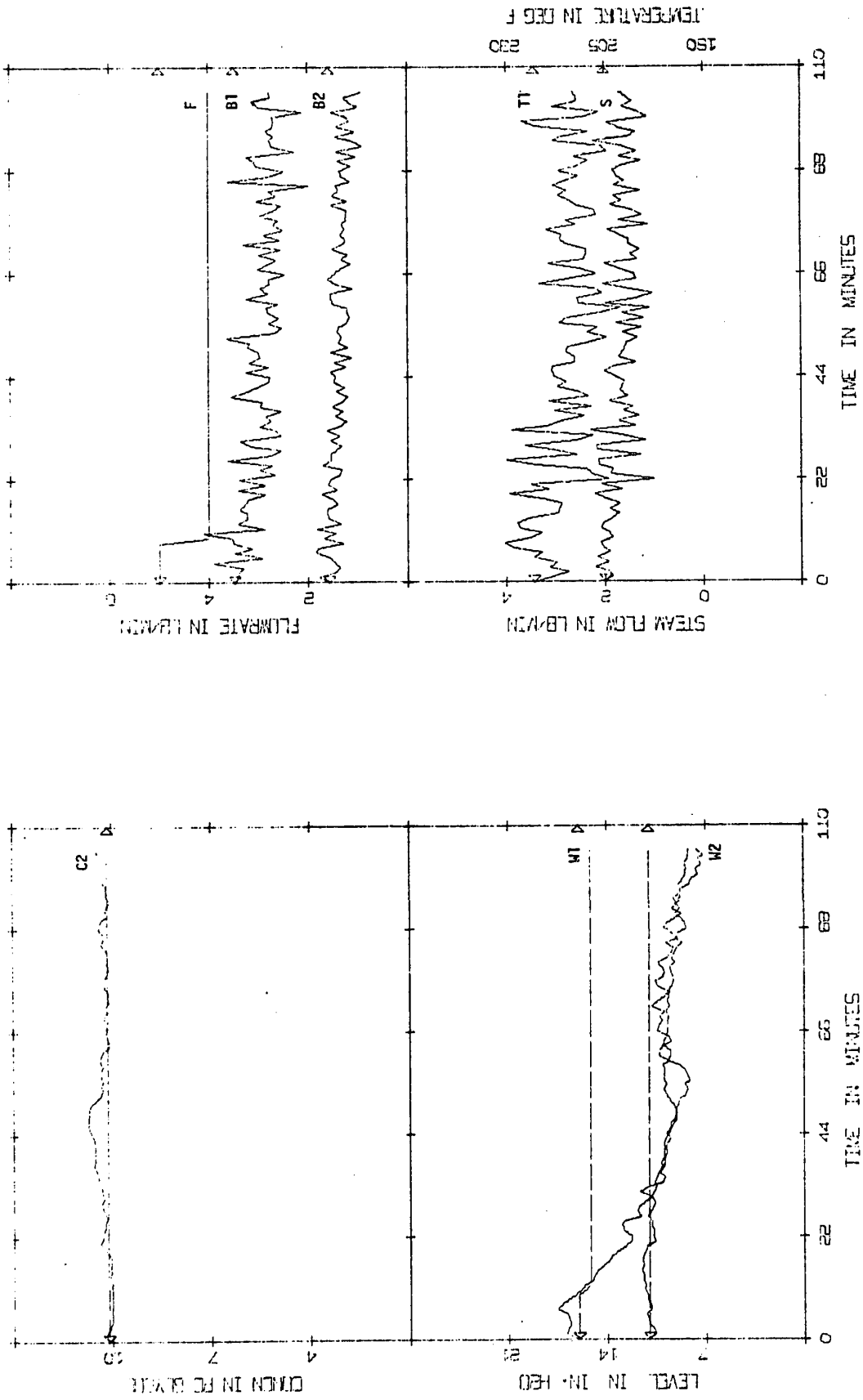

FIGURE 3.15 (SIM/-20%F/FB) --- deterministic, —— Kalman filter 1B

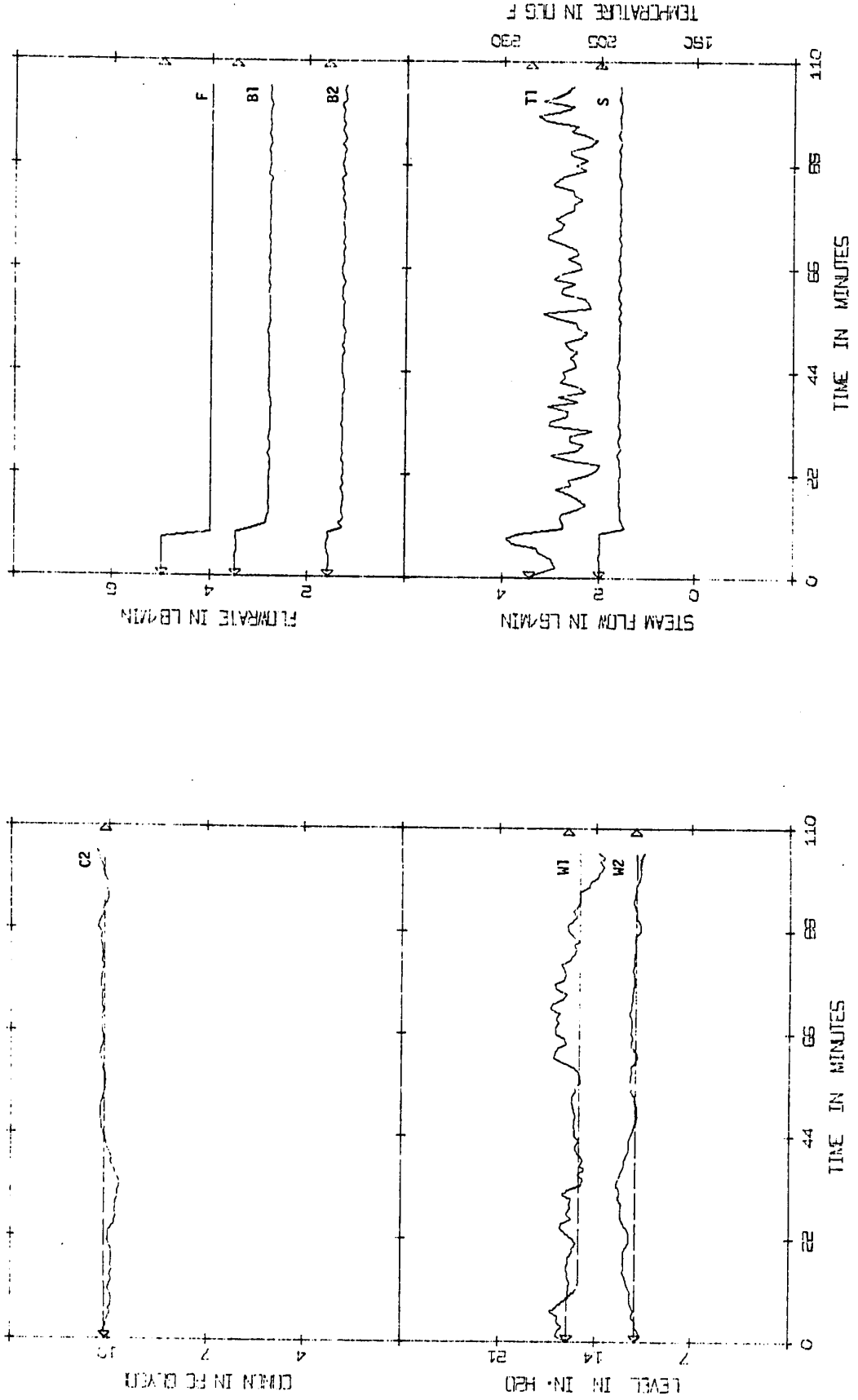

FIGURE 3.16 (SIM/-20%F/FB) --- deterministic, —— Kalman filter 5A

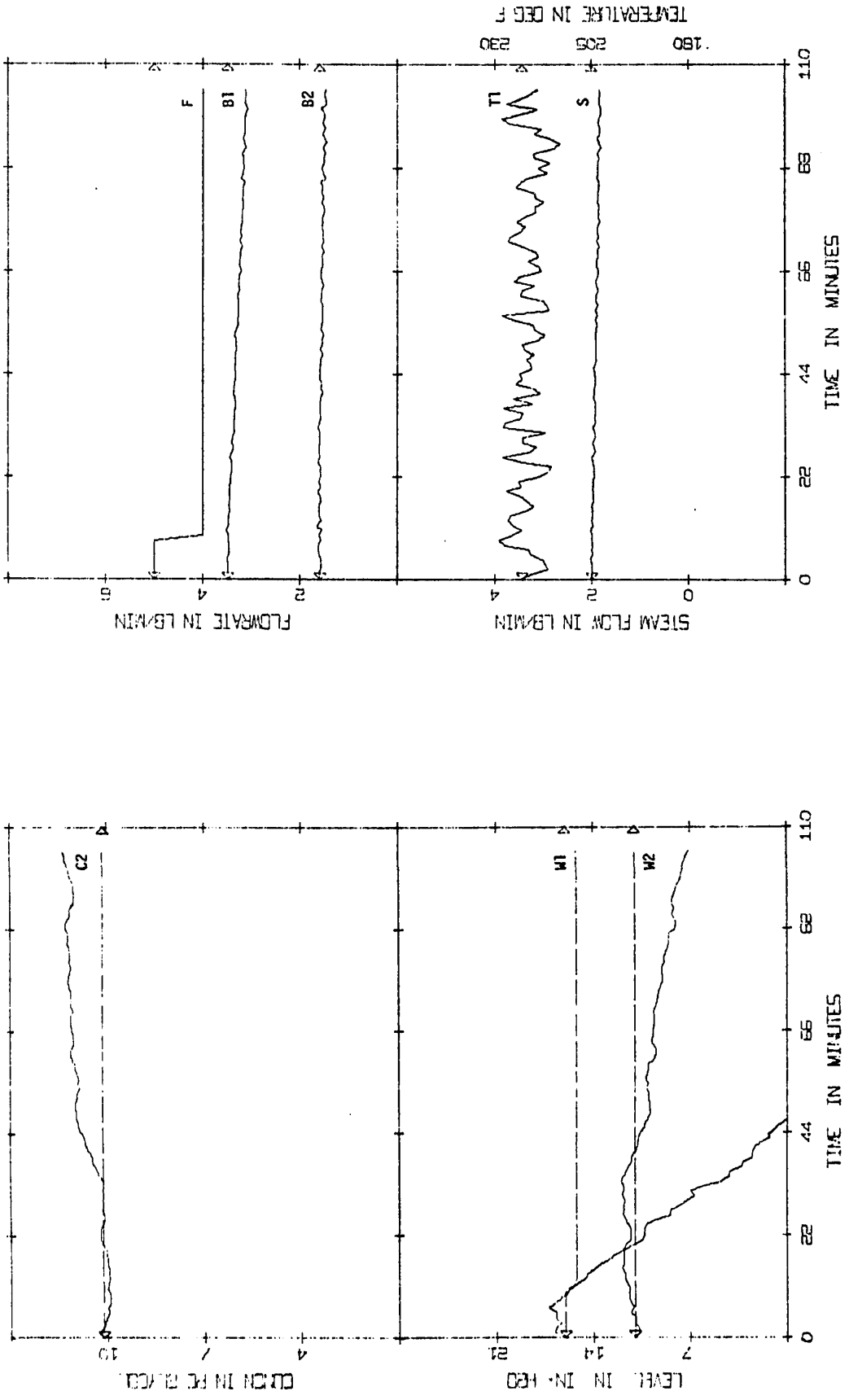

FIGURE 3.17 (SIM/-20%F/FB) --- deterministic, —— Kalman filter 5B

second effect level began to fall and the product concentration drifted upwards. It can be seen by examining the manipulated variables that very little control action has been taken. In fact the manipulated variables respond only slightly due to the extremely small weighting on the measurements which do reflect the disturbance to the process.

At the opposite extreme, Figure 3.18 shows the results when an R:Q ratio of 1:100 was used in computing the gain matrix. With such a high weighting on the measurements the results tended towards the case with no filtering and there was little or no difference if the step disturbance was not measured.

3.5.2 Comparison With a Sub-Optimal Filter

Figure 3.19 illustrates the results obtained by using sub-optimal filter 2. Again the curves are quite noisy since the measurements are weighted strongly and there are rapid fluctuations in the manipulated variables (not shown). In this case there was also very little difference in the performance of the filter if the disturbance was not observed and included in the model calculations.

3.5.3 Comparison With the Exponential Filter

In the closed loop simulations four different exponential filters were investigated. Knowledge of a step disturbance here only affects the value of C1 (which is obtained from a model calculation), since the other four state estimates are merely "smoothed" measurements. Since only small changes in the estimate of C1 resulted (for measured disturbances), in Figures 3.20 - 3.23 the filter did not include a knowledge of the disturbance.

Figures 3.20 - 3.23 show the results for exponential filters with α = 0.7, 0.5, 0.3 and 0.1 respectively. With large values of α

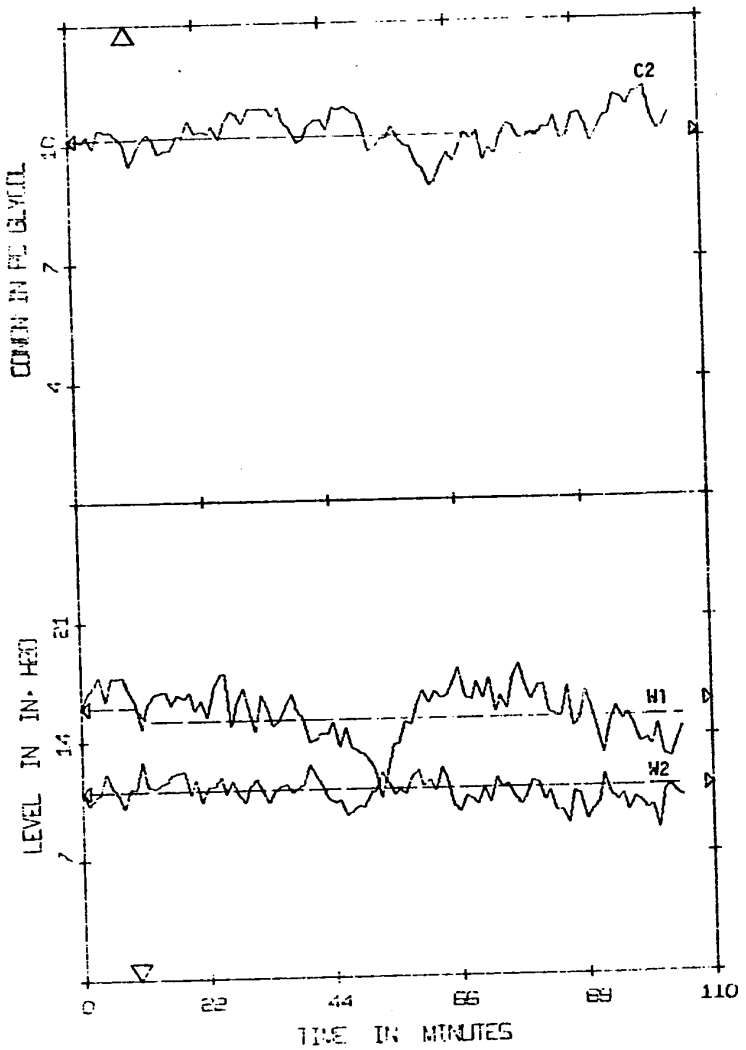

FIGURE 3.18 (SIM/-20%F/FB) --- deterministic, —— Kalman filter 2A

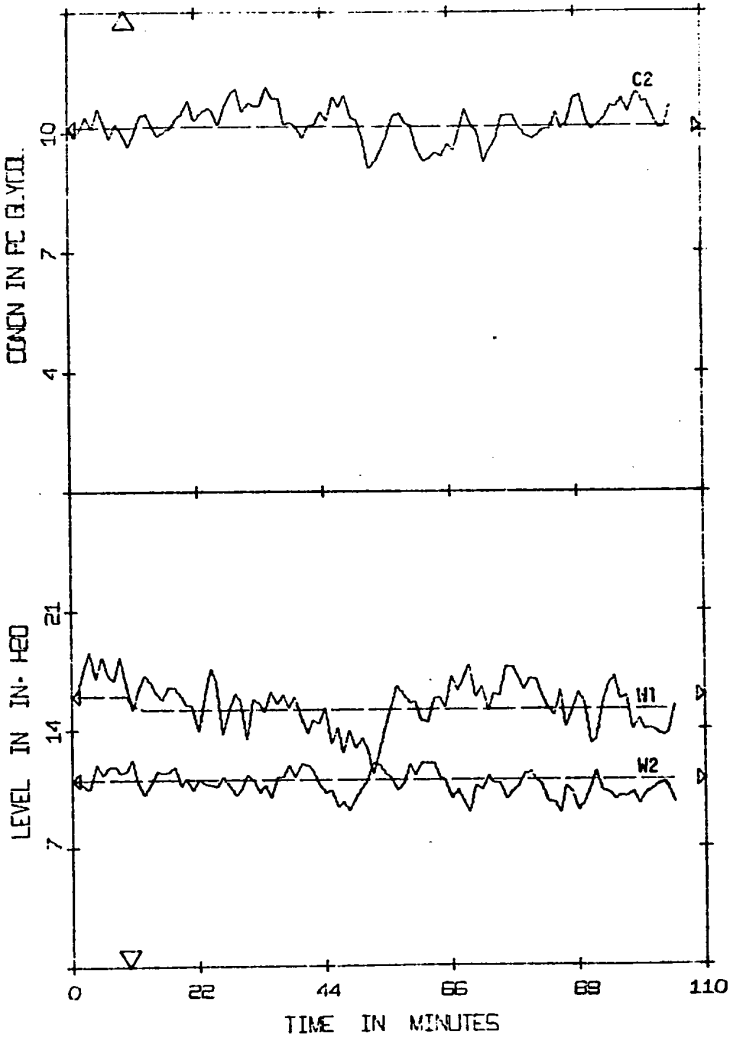

FIGURE 3.19 (SIM/-20%F/FB) --- deterministic, —— sub-optimal filter 2

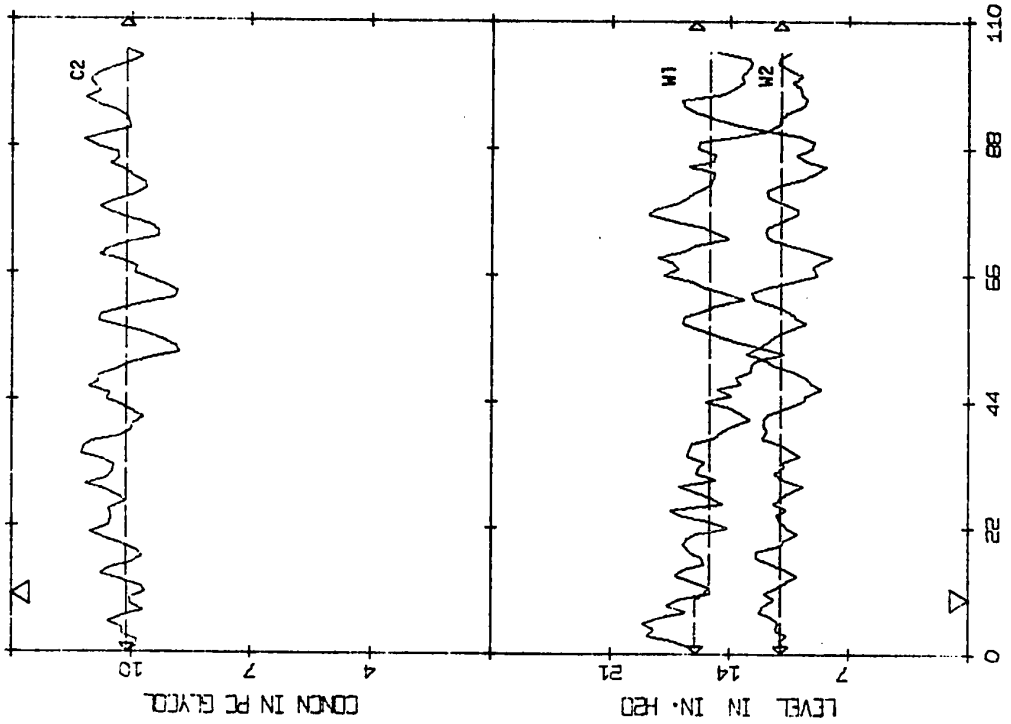

FIGURE 3.21 (SIM/-20%F/FB) --- deterministic, —— exponential filter 2

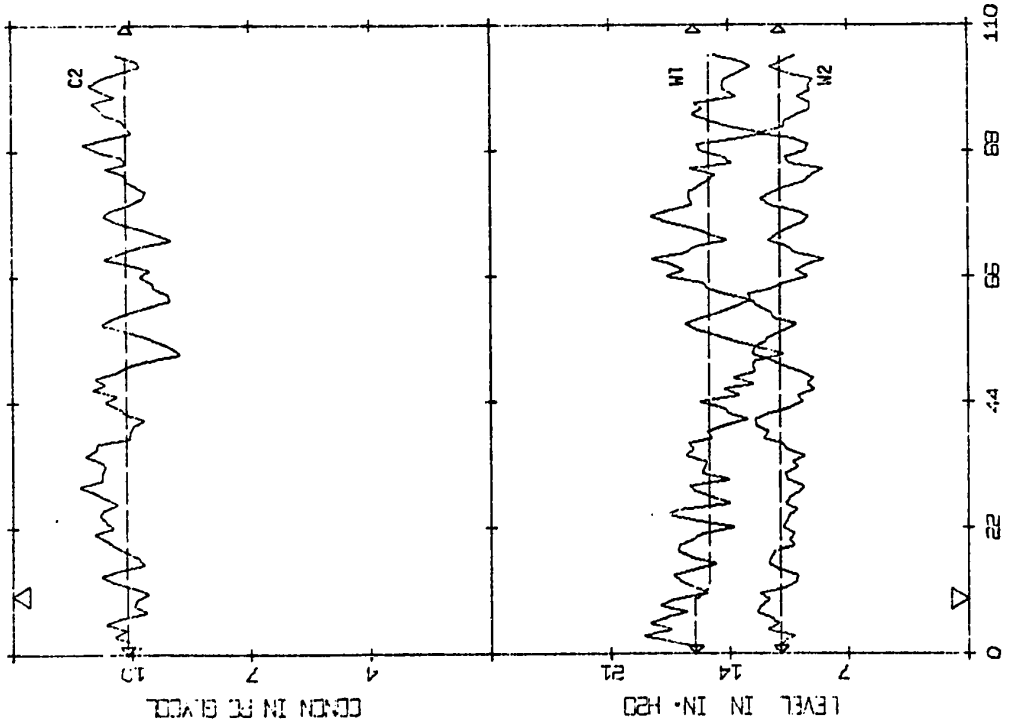

FIGURE 3.20 (SIM/-20%F/FB) --- deterministic, —— exponential filter 1

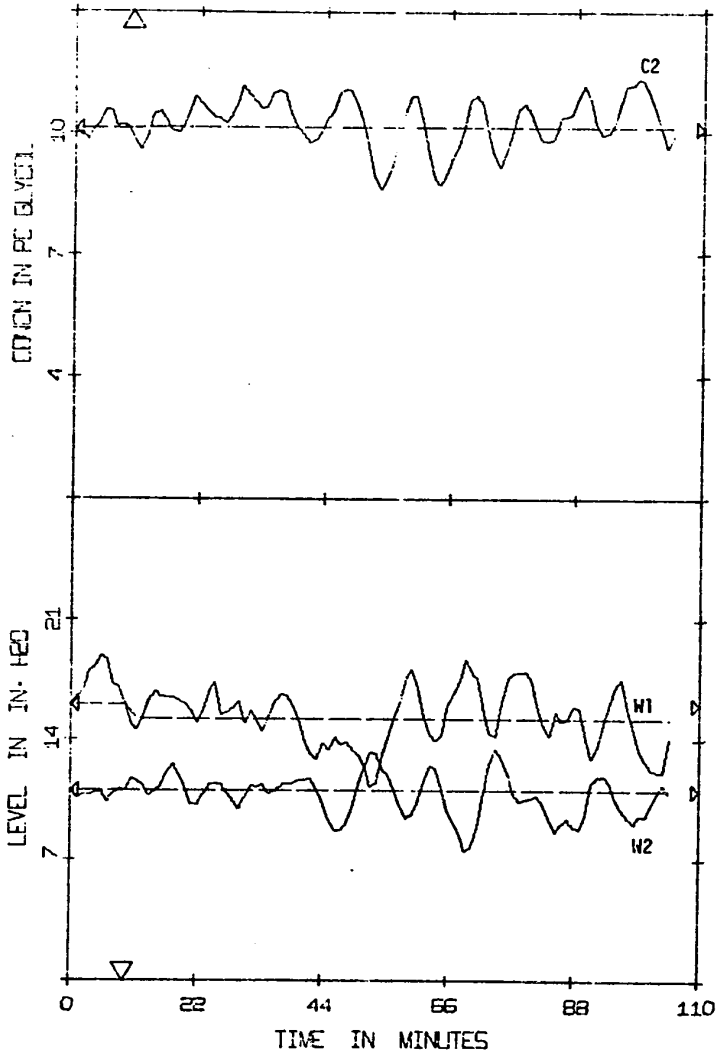

FIGURE 3.22 (SIM/-20%F/FB) --- deterministic, —— exponential filter 3

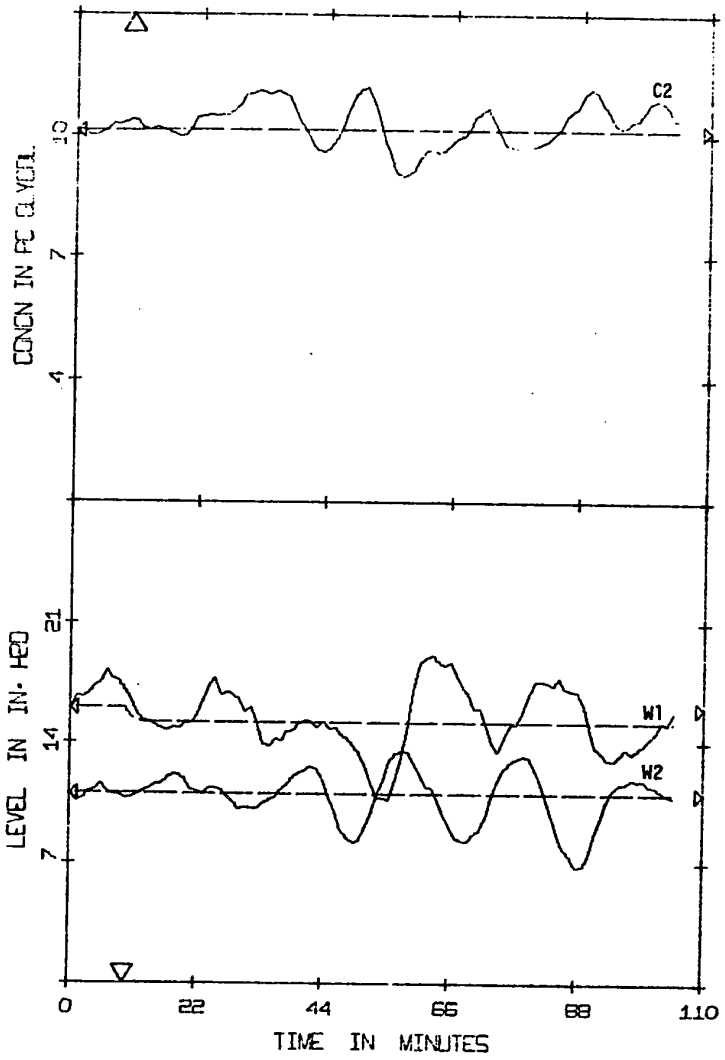

FIGURE 3.23 (SIM/-20%F/FB) --- deterministic, —— exponential filter 4

there is clearly very little difference from the unfiltered run in Figure 3.13. As α is decreased the high frequency noise is smoothed out but a larger time lag is introduced and this results in a more oscillatory response (see Figure 3.23). It would appear from these results that control of the process cannot be improved by using an exponential filter with the present control scheme. It should be pointed out however that significant improvements could probably be achieved with a small value of α if the time delay introduced was accounted for in designing the deterministic controller.

3.6 EXPERIMENTAL PROCEDURE

To experimentally verify the previous simulation results, a similar set of runs were performed using the actual double effect evaporator.

A statistical analysis of experimental data was initially made in order to estimate actual measurement and process noise levels at the normal steady state. These estimates were found to be very much less than the 10% levels used in the simulation study. The measurement noise levels were found to range from 0.1% to 2% and the process noise levels from 0.1% to 5%; only three of the ten noise elements were greater than 1% (W1 = 2%, B1 = 5%, B2 = 4%). As a result it was decided to artificially add measurement noise to the measured states before filtering and before performing the control calculations. This was done with the same random number generator that was used in the simulation program.

In all the runs the measurements were obtained from the standard DDC loops which contain simple single variable filters such as exponential or D.C. Union filters. This was done so that reasonably

smooth, accurate data could be used to represent the state of the process before adding the measurement noise. Obviously this means that a small time lag is introduced immediately due to these DDC filters but since the scan rate of the DDC loops is very fast (about 60 times faster than the data collection) this time lag is negligible. 10% noise was added to each of the four measurements and since the data had been filtered earlier by the DDC loops, it was assumed that each element had the same noise level (i.e. 0.1 standard deviation).

No attempt was made to achieve 10% process noise levels as this would have been a difficult problem physically, requiring noise generators to drive the process. Thus most of the elements in the process noise vector were insignificant and herein lies a difference from the simulation study.

Only one open loop experimental run was made with the measurements recorded and stored before any noise was added. This data was then used as the basis for several computer runs which evaluated various filters as in the simulation study. This procedure was very convenient in that a computer run was much faster and more easily accomplished than the corresponding experimental run.

For the closed loop runs, both the measurements before noise was added and the estimates of the states were recorded and stored so that either could be displayed at a later date. As indicated earlier, the former set of data was assumed to give a fairly precise indication of the true state of the process. Consequently, these states were of more interest in the closed loop runs since they provided the means of evaluating the combined estimation and control algorithm and hence the effectiveness of the filter.

3.7 COMPUTER PROGRAMS FOR THE EXPERIMENTAL STUDY

The program (EPECS) used for the off-line processing of the open loop experimental data was, in fact, a modified form of the simulation program (SPECS), the main difference being the source of the data.

The computer programs used in the closed loop experimental work were basically those developed by Newell [3]. Only two modifications were required, with both made in the main control coreload, RBN31.

The first change was to add artificial measurement noise immediately prior to the filter calculations. Since an option for using the Kalman filter equation had already been included in the programs, this alteration was sufficient for all the Kalman filter and sub-optimal filter runs. When using the exponential filter, however, it was also necessary to change the coding for the filter equation. Both changes were easily implemented and the user's manual for these programs [3] is still appropriate.

3.8 OPEN LOOP EXPERIMENTAL STUDY

The open loop experimental run for a 30% step down in feed concentration was used to evaluate the Kalman filter with two different R:Q ratios, a sub-optimal filter, and the exponential filter with three different values of α. The details of Figures 3.24 - 3.32 are given in Table 3.4.

In Figure 3.24 the "noise-free" run is shown together with the data after noise was added but not filtered. This shows the actual process states and the noisy measurements which are to be filtered in order to obtain good state estimates. In all of the succeeding figures

TABLE 3.4

DETAILS OF FIGURES 3.24 - 3.32: OPEN LOOP EXPERIMENTAL

Figures 3.24 - 3.32 show the open loop evaporator response to a 30% step down in feed concentration before measurement noise is added, in addition to the estimates (after noise is added) as tabulated below (see appendix for the elements of $\underline{\underline{Q}}$, $\underline{\underline{R}}$ and $\underline{\underline{C}}$).

A - denotes a filter which has knowledge of a step disturbance

B - denotes a filter which is unaware of a step disturbance

Figure	Filter Used	$\underline{\underline{Q}}$	$\underline{\underline{R}}$	$\underline{\underline{C}}$	α
3.24	Unfiltered	-	-	-	-
3.25	Kalman 6A	$\underline{\underline{Q4}}$	$\underline{\underline{R1}}$	-	-
3.26	Kalman 6B	$\underline{\underline{Q4}}$	$\underline{\underline{R1}}$	-	-
3.27	Kalman 1A	$\underline{\underline{Q1}}$	$\underline{\underline{R1}}$	-	-
3.28	Kalman 1B	$\underline{\underline{Q1}}$	$\underline{\underline{R1}}$	-	-
3.29	Sub-optimal 2	-	-	$\underline{\underline{C2}}$	-
3.30	Exponential 1	-	-	-	$\alpha 1 = 0.7$
3.31	Exponential 3	-	-	-	$\alpha 3 = 0.3$
3.32	Exponential 4	-	-	-	$\alpha 4 = 0.1$

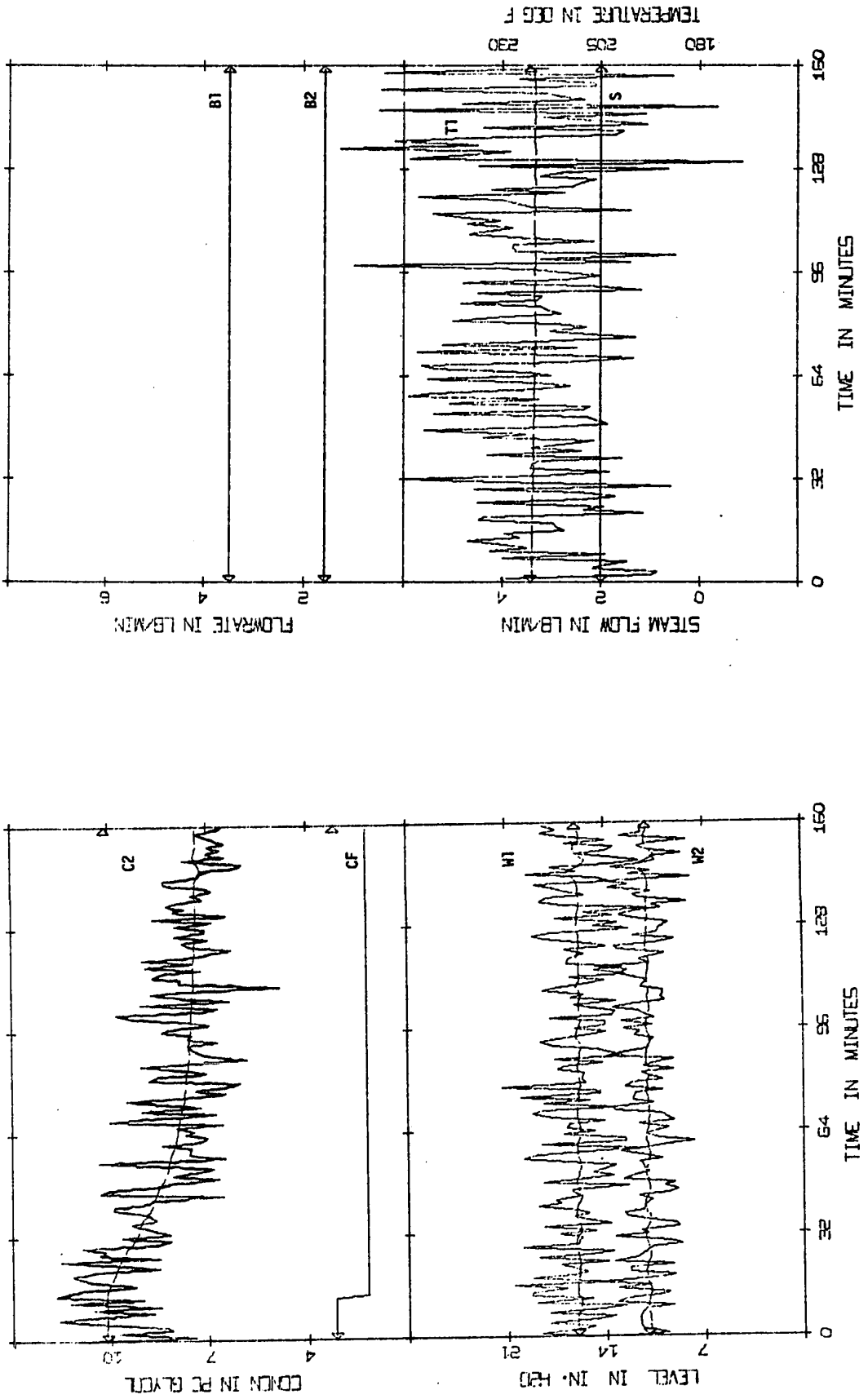

FIGURE 3.24 (EXP/OL) --- actual states, —— unfiltered

in this section, the actual states and the estimated states have been plotted together in order to readily evaluate the performance of the filter. Plots for the actual values of C1 could not be included since C1 was not measured.

Figure 3.25 shows the estimates given by Kalman filter 6A which uses a R:Q ratio of 25:1 and includes knowledge of the step disturbance in the model calculations. The estimated states are accurate because the model (which is favoured strongly here) is a good one and the step disturbance is measured.

It can be seen from Figure 3.25 and the other figures that there is a small "blip" at t = 140 minutes in the actual C2, W1 and W2 curves. The reason for this is not fully understood although this problem has been investigated by several previous workers. The source of the "blip" appears to be the sight glass which is used to measure the first effect level. Various explanations of this phenomenon have been proposed and tests are currently being carried out in order to solve this problem.

In contrast to Figure 3.25, the C2 estimate in Figure 3.26, where the filter was not aware of the step disturbance, is very inaccurate. With an R:Q ratio of 1:1, Kalman filters 1A and 1B were used to obtain the curves in Figures 3.27 and 3.28 respectively. In Figure 3.27 the model was aware of the disturbance and the estimates, though a little noisy, are in very good agreement with the actual states. The noise is still filtered out reasonably well in Figure 3.28, but again, because the disturbance was not included in the model calculations, there is some discrepancy between the actual and estimated

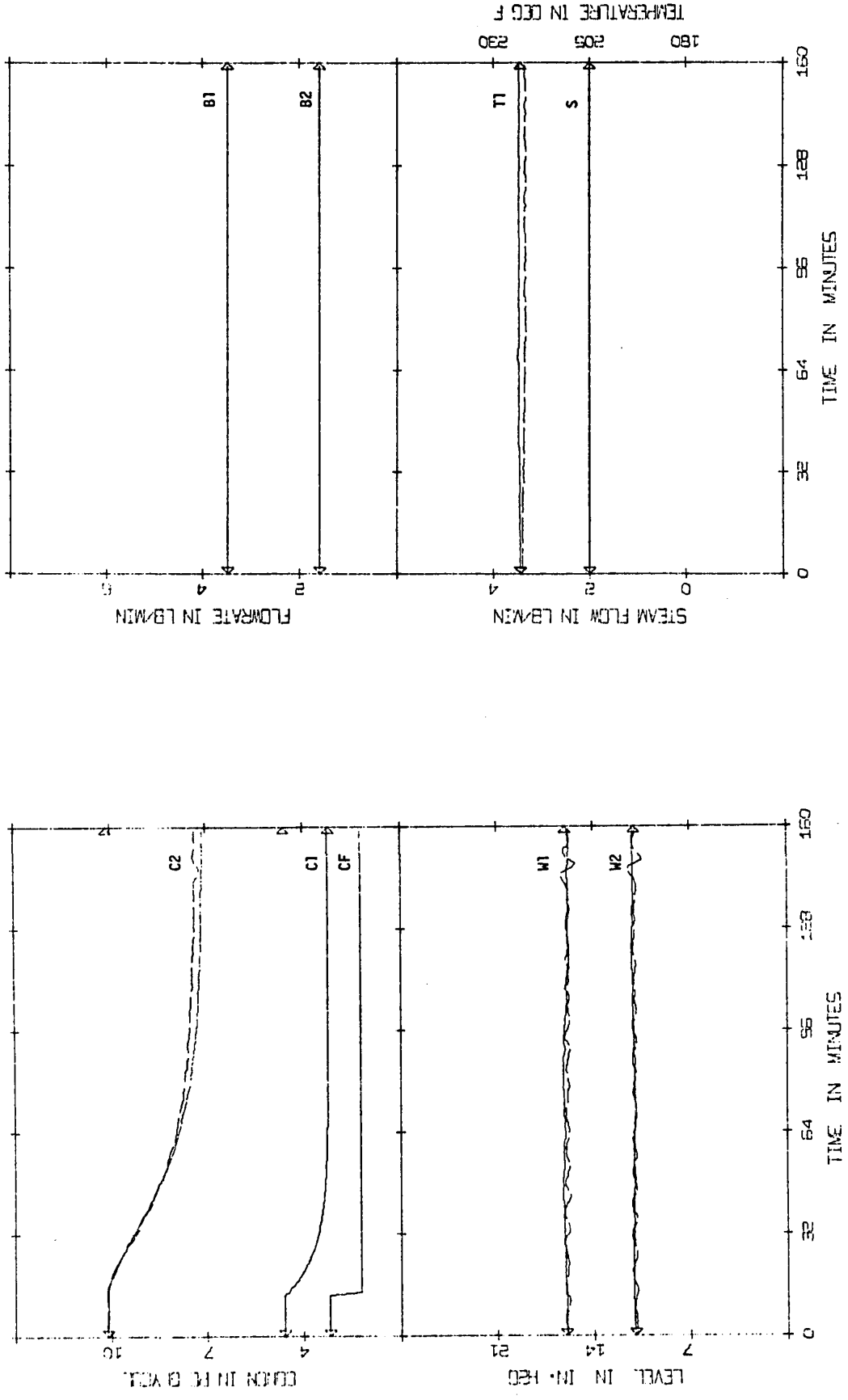

FIGURE 3.25 (EXP/OL) --- actual states, —— Kalman filter 6A

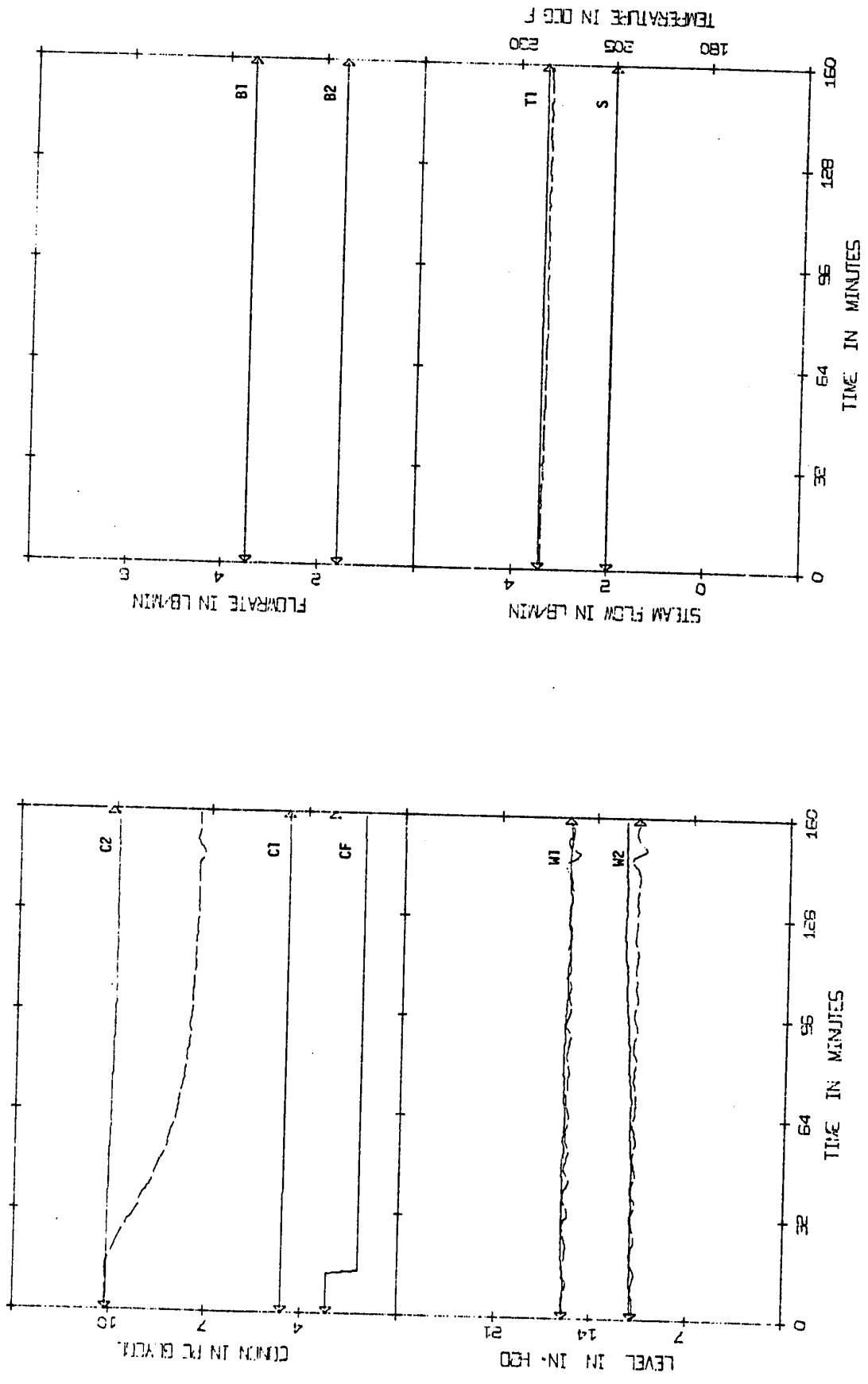

FIGURE 3.26 (EXP/OL) --- actual states, —— Kalman filter 6B

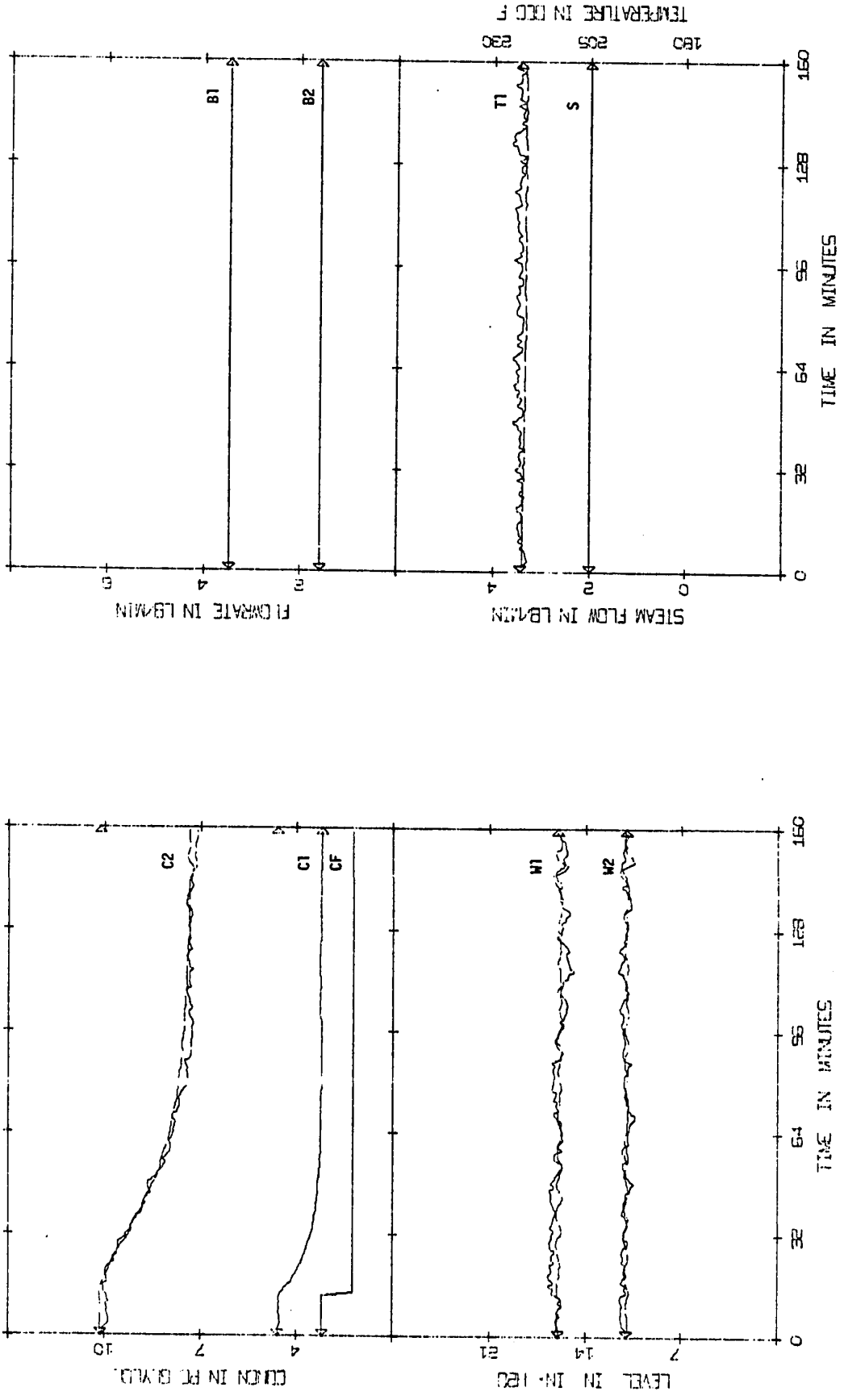

FIGURE 3.27 (EXP/OL) --- actual states, —— Kalman filter 1A

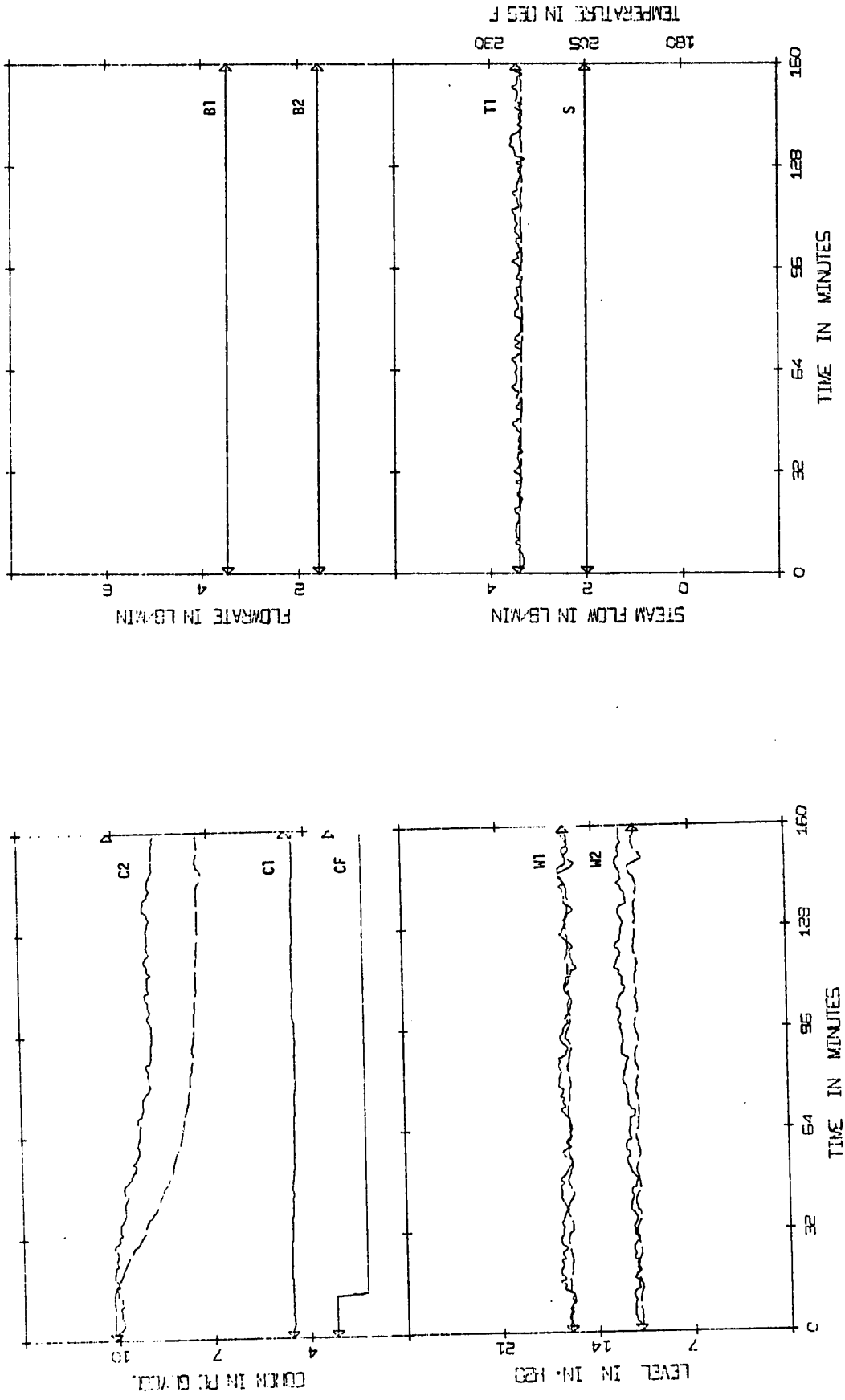

FIGURE 3.28 (EXP/OL) --- actual states, —— Kalman filter 1B

values of C2. However, the effect of an "unseen" disturbance is not nearly as great as it was in Figure 3.26 due to the lower R:Q ratio and, consequently, greater reliance on process measurements.

Sub-optimal filter 2 was used in Figure 3.29 resulting in estimates which were only a slight improvement over the unfiltered states. In the curves shown here, knowledge of the disturbance was included in the model calculations, but with such a low degree of filtering this factor has little significance. Figures 3.30, 3.31 and 3.32 show the performance of an exponential filter for increasing values of α. In each of these plots four of the states were estimated by the exponential filter while the fifth state, C1, was calculated from the deterministic model which included a knowledge of the disturbance.

In Figure 3.30, where a value of $\alpha = 0.7$ was used, the estimated states are almost identical to the unfiltered states as was the case in the simulation studies. With $\alpha = 0.3$, Figure 3.31 shows a marked improvement in reducing noise and still gives accurate estimates of the states. In Figure 3.32 the curves were further smoothed by using an α of 0.1 but there is a slight indication of the estimate lagging the actual curve for the case of C2.

3.9 CLOSED LOOP EXPERIMENTAL STUDY

A total of ten closed loop experimental runs were also made on the evaporator and each run was plotted separately for clarity. The manipulated variables plotted are the actual measured flows and not the calculated values.

The base case is shown in Figure 3.33 where a "noise-free"

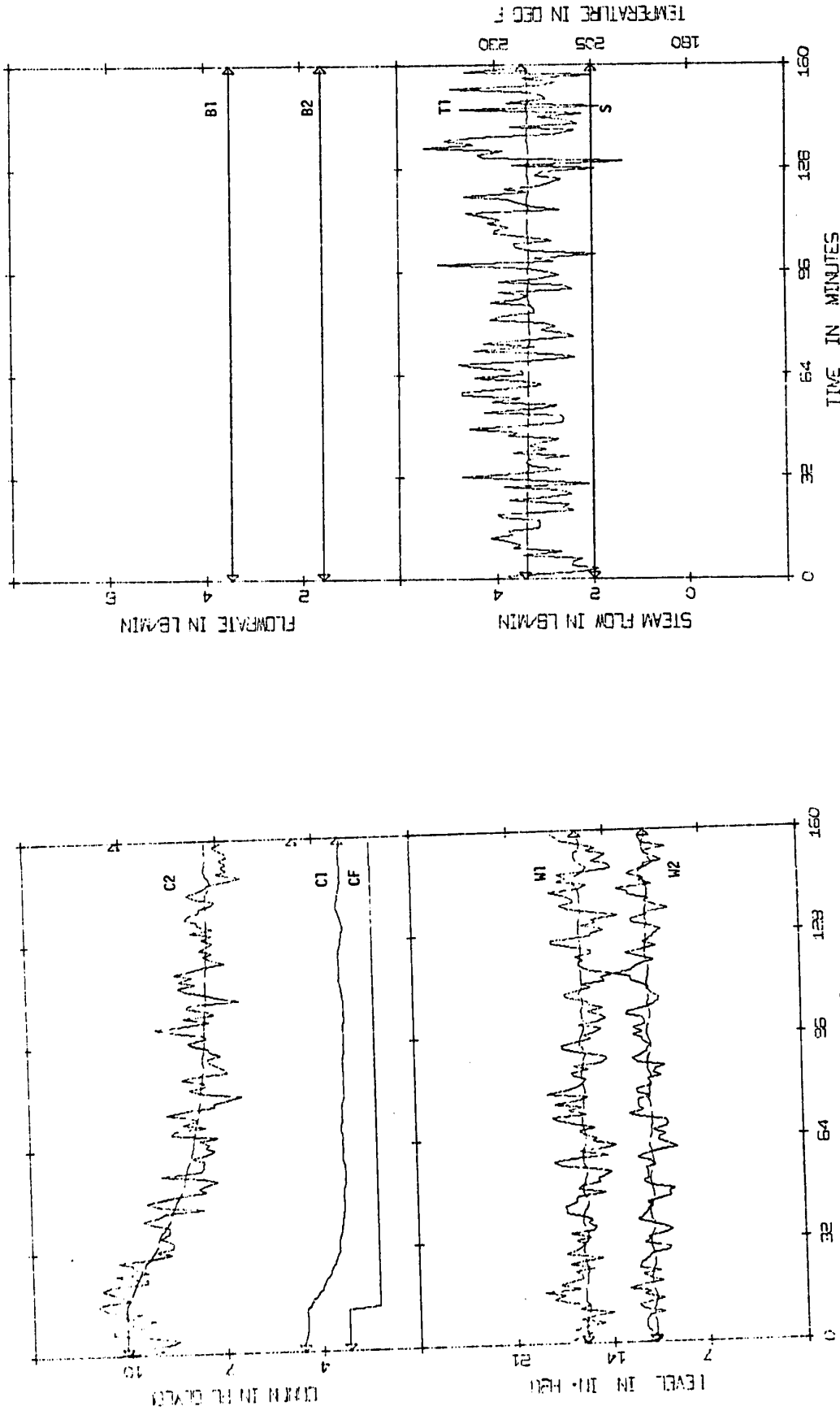

FIGURE 3.29 (EXP/OL) --- actual states, —— sub-optimal filter 2

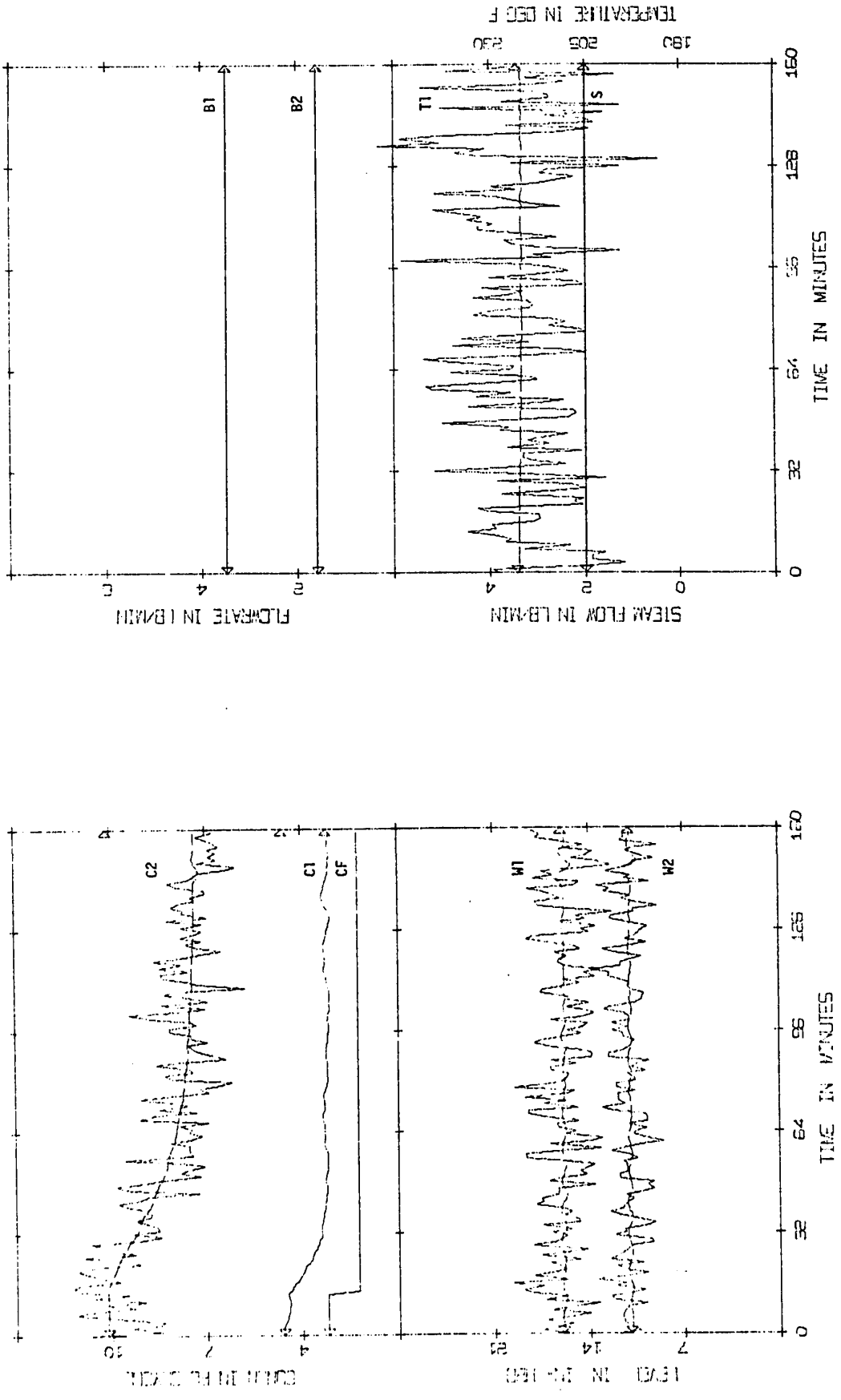

FIGURE 3.30 (EXP/OL) --- actual states, —— exponential filter 1

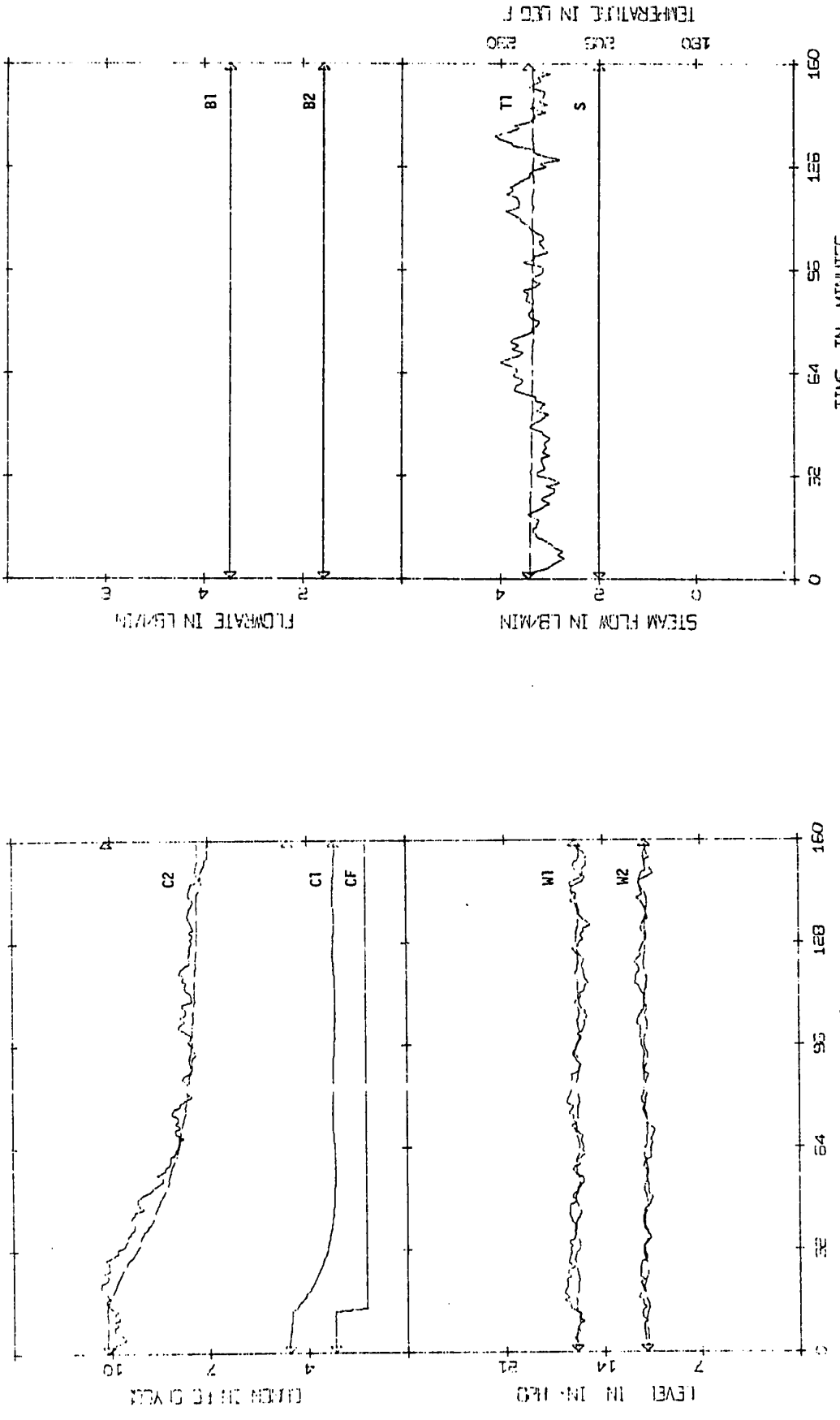

FIGURE 3.31 (EXP/OL) --- actual states, —— exponential filter 3

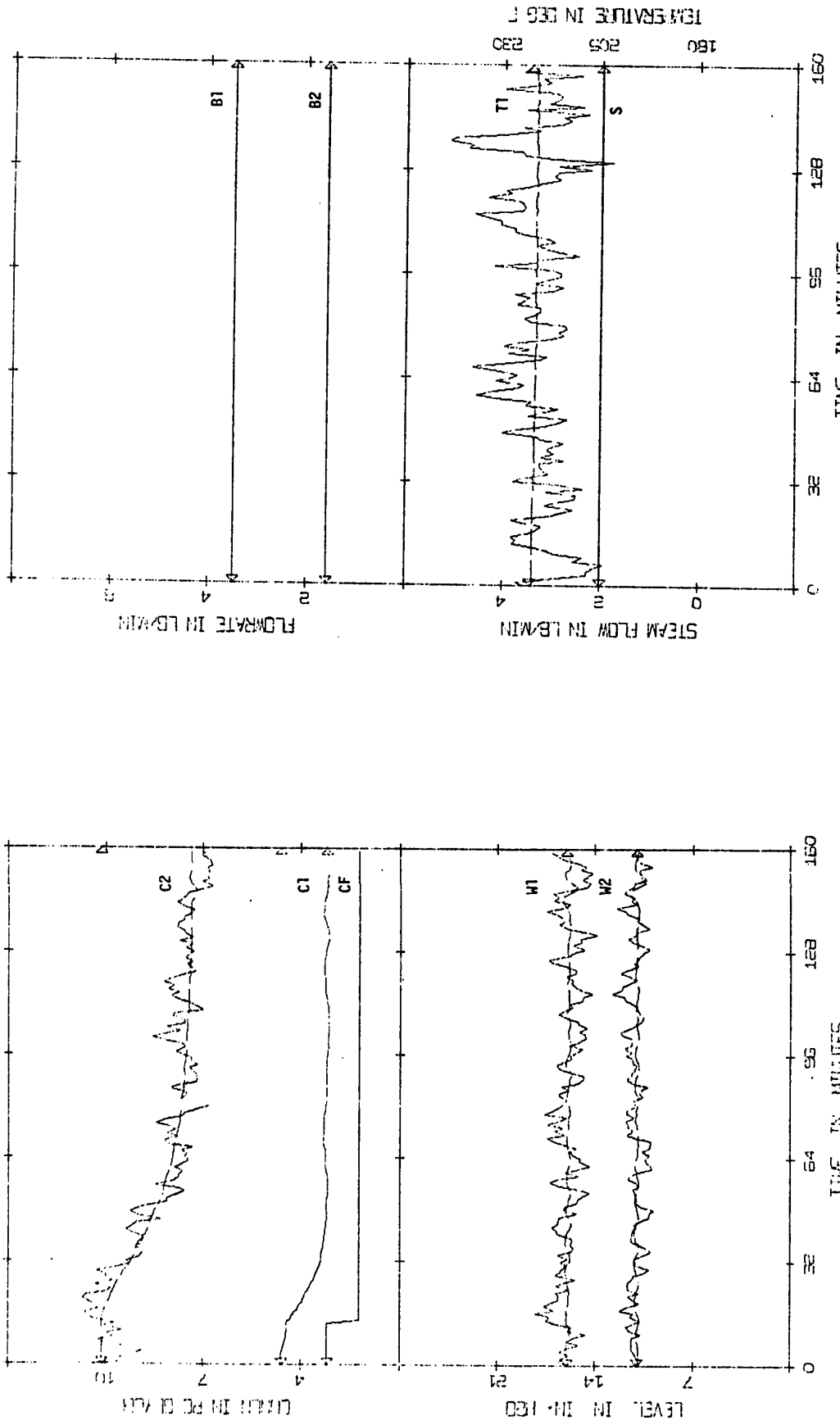

FIGURE 3.32 (EXP/OL) --- actual states, —— exponential filter 4

run was made, using the four state measurements and a value of C1 calculated from the deterministic model as estimates of the states for control purposes. The disturbance applied was a 20% step down in feed flow followed by a 20% step up, approximately 30 minutes later. The process was controlled very successfully and little movement of the primary controlled variable, C2, was detected. The details for Figures 3.33 - 3.42 are given in Table 3.5.

This run was repeated with noise added to the measurements and with the control calculations based on the noisy measurements and the model value for C1. The results in Figure 3.34 show the actual states, C2, W1 and W2. C1 is not shown since the actual value could not be determined and the T1 curve which normally appears on the second page plot had to be omitted since the wild fluctuations of the manipulated variables rendered this page incomprehensible. Due to the noisy measurements the manipulated variables fluctuate rapidly and the states, though controlled reasonably well trendwise, are quite oscillatory.

Figures 3.35 and 3.36 illustrate the results obtained by using a Kalman filter based on a R;Q ratio of 25:1 and as expected the curves are very smooth. In Figure 3.35 the disturbance was "seen" and consequently the trend of the process was controlled reasonably well. Figure 3.36 confirms the results obtained in the simulation studies where a filter, which favours the model quite strongly, is not aware of a disturbance. Since the estimates did not reflect the disturbances in the feed flow, the first effect drained out on the step down and then recovered on the step back up. By comparing the manipulated variables in Figures 3.35 and 3.36 these results are readily

TABLE 3.5

DETAILS OF FIGURES 3.33 - 3.42: CLOSED LOOP EXPERIMENTAL

Figures 3.33 - 3.42 show the closed loop response of the evaporator to a 20% step down in feed flow followed by a 20% step back up. The estimates used in the control algorithm are tabulated below (see appendix for the elements of $\underline{\underline{Q}}$ and $\underline{\underline{R}}$).

A - denotes a filter which has knowledge of a step disturbance

B - denotes a filter which is unaware of a step disturbance

Figure	States Displayed	Filter Used	$\underline{\underline{Q}}$	$\underline{\underline{R}}$	α	Remarks
3.33	Actual	No filter (noise-free)	-	-	-	model value of C1 used in control calculations
3.34	Actual	No filter (noisy)	-	-	-	
3.35	Actual	Kalman 6A	$\underline{\underline{Q4}}$	$\underline{\underline{R1}}$	-	
3.36	Actual	Kalman 6B	$\underline{\underline{Q4}}$	$\underline{\underline{R1}}$	-	
3.37	Actual	Kalman 1A	$\underline{\underline{Q1}}$	$\underline{\underline{R1}}$	-	
3.38	Actual	Kalman 1B	$\underline{\underline{Q1}}$	$\underline{\underline{R1}}$	-	
3.39	Actual	Kalman 4A	$\underline{\underline{Q3}}$	$\underline{\underline{R1}}$	-	
3.40	Actual	Kalman 4B	$\underline{\underline{Q3}}$	$\underline{\underline{R1}}$	-	
3.41	Actual	Exponential 3	-	-	$\alpha 3=0.3$	model value of C1 used in control calculations
3.42	Actual	Exponential 4	-	-	$\alpha 4=0.1$	

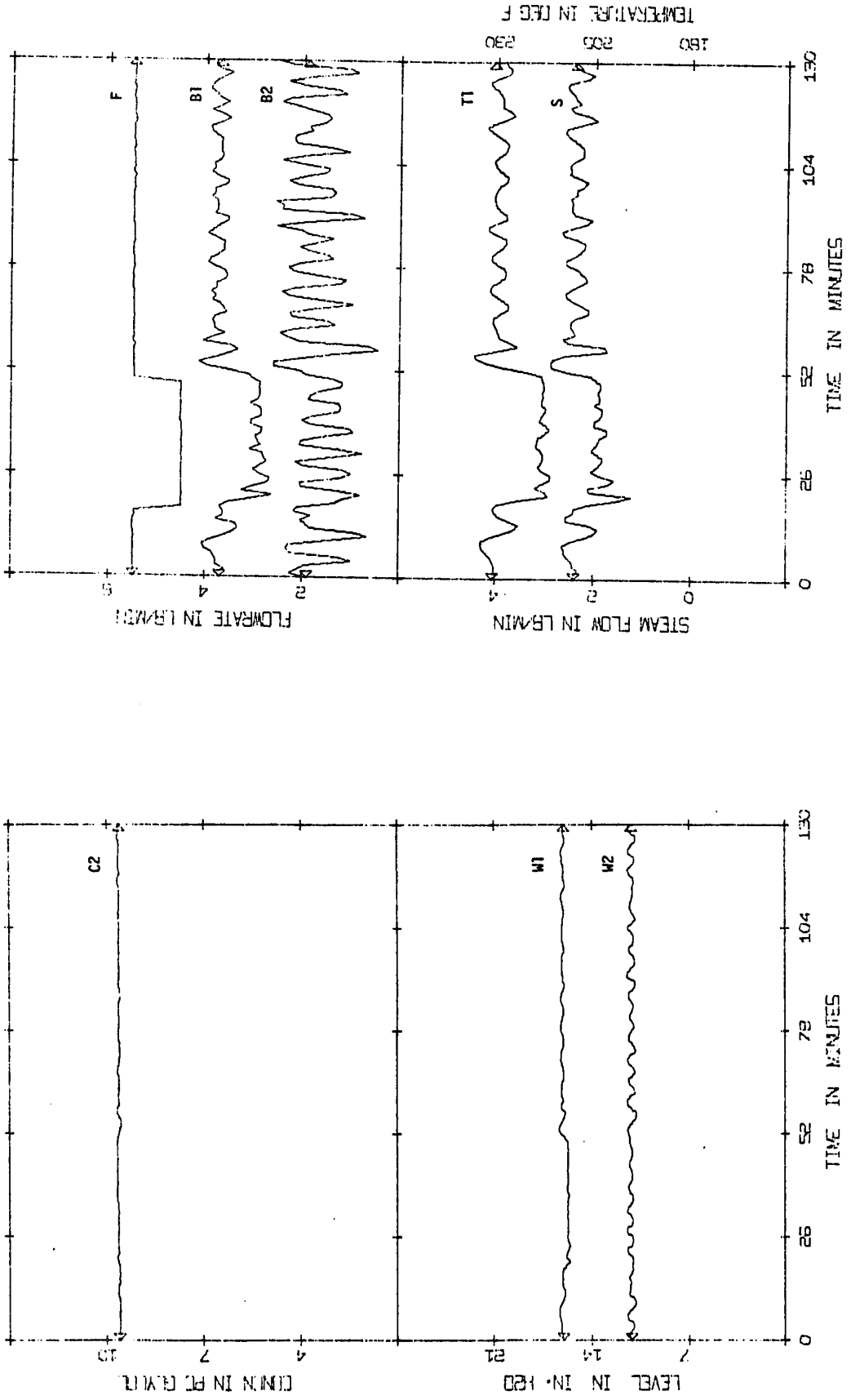

FIGURE 3.33 (EXP/-20%F,+20%F/FB) noise-free process

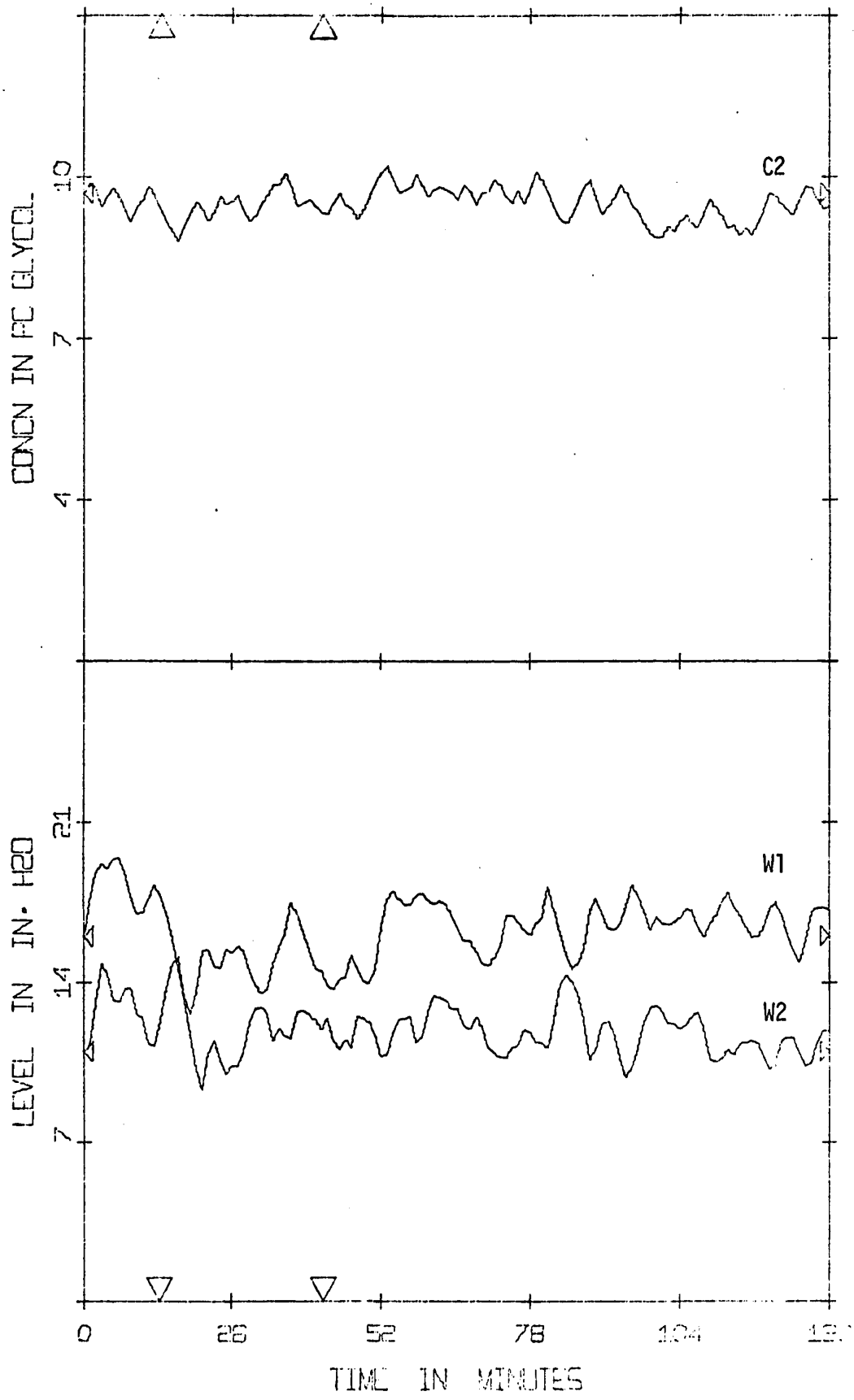

FIGURE 3.34 (EXP/-20%F,+20%F/FB) actual states, control based on unfiltered measurements

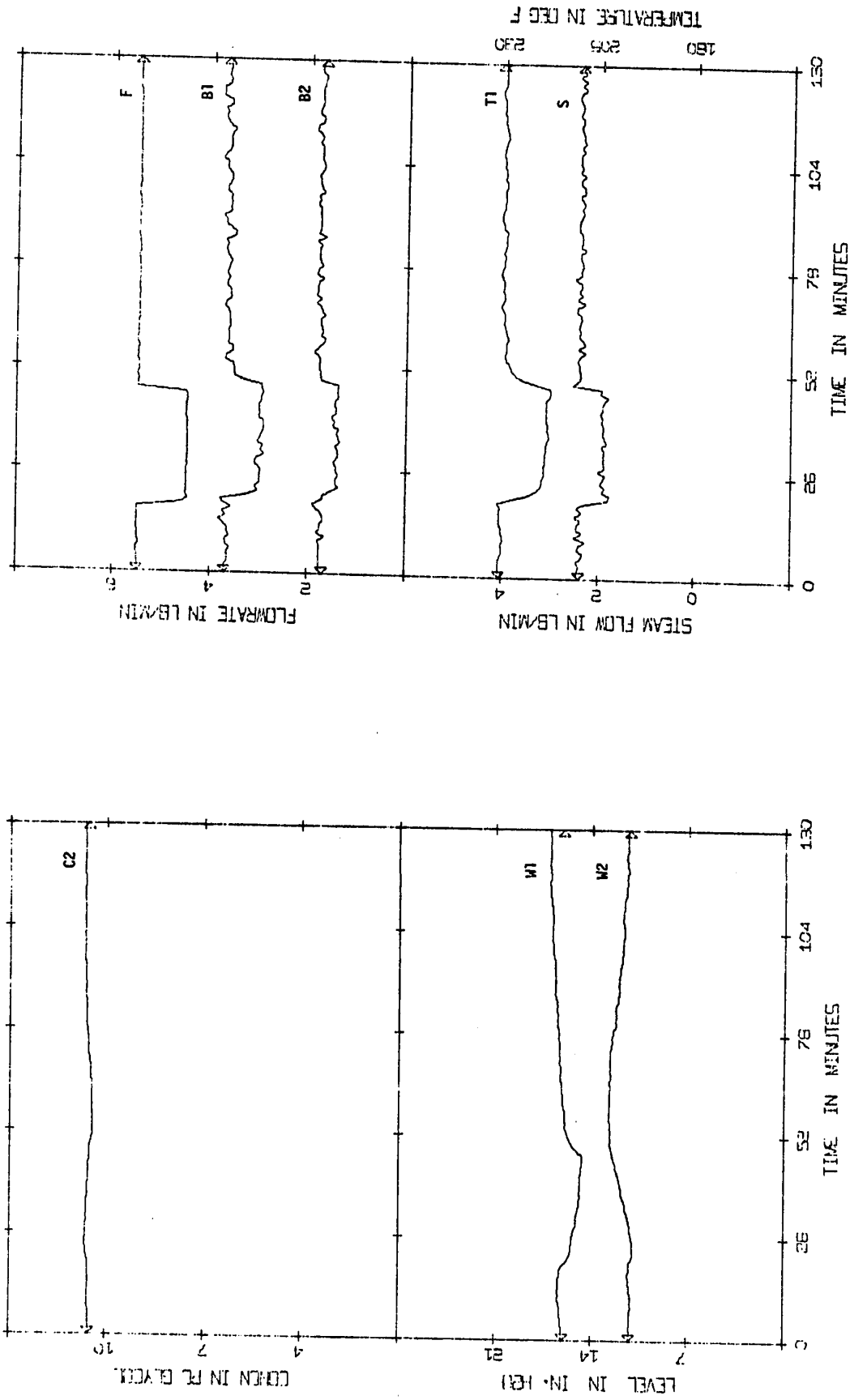

FIGURE 3.35 (EXP/-20%F,+20%F/FB) actual states, control based on Kalman filter 6A estimates

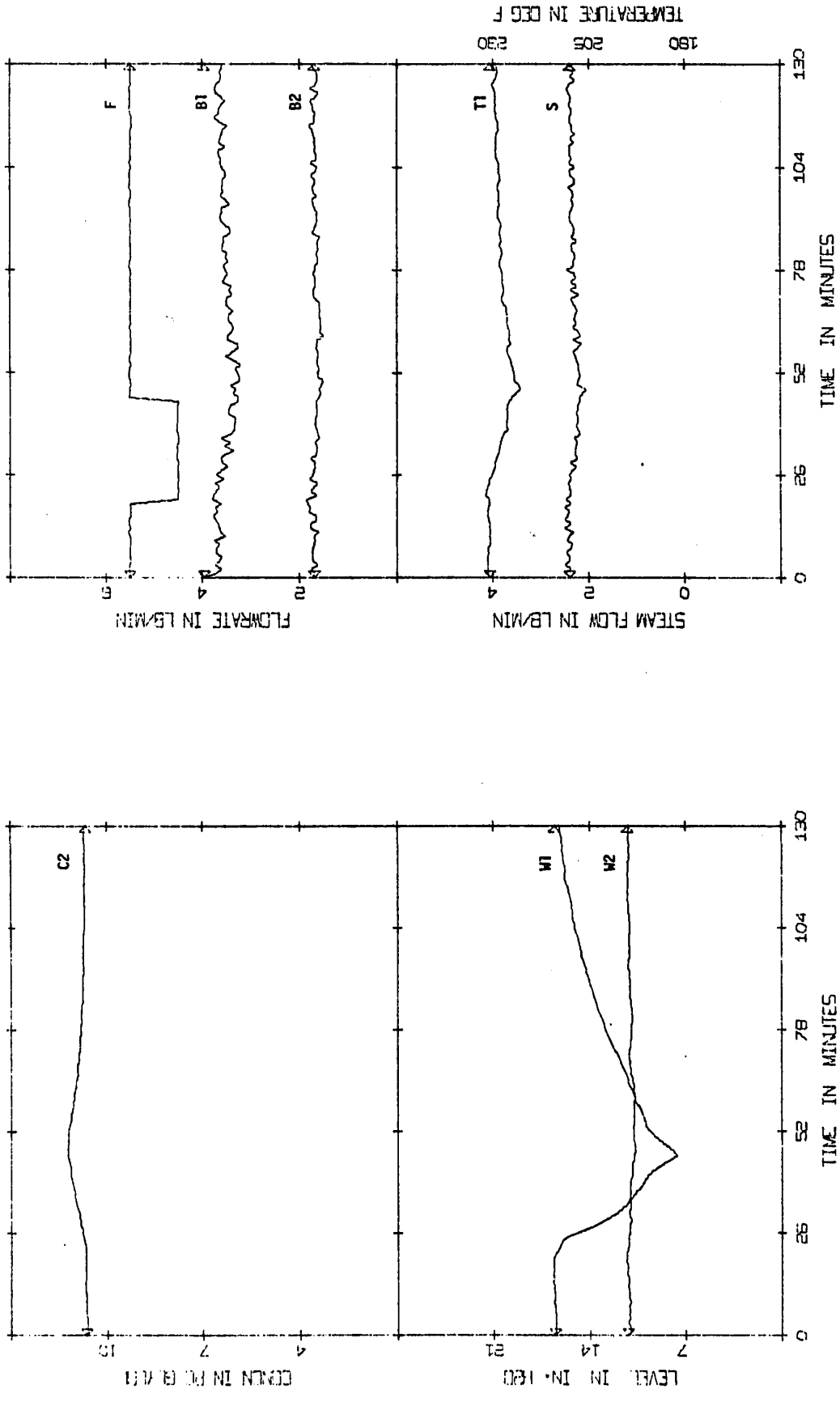

FIGURE 3.36 (EXP/-20%F,+20%F/FB) actual states, control based on Kalman filter 6B estimates

understood. In the latter case the control action is almost nil since the estimates did not indicate any deviation from the steady state and hence the process was virtually uncontrolled. Had the second step in feed flow not been applied, the first effect would have drained out completely.

The runs shown in Figures 3.35 and 3.36 were repeated using Kalman filter 1 (Figures 3.37 and 3.38) and Kalman filter 4 (Figures 3.39 and 3.40). For each of these two filters, the first figure mentioned shows the results obtained with knowledge of the disturbances, and the second, those obtained without this knowledge.

The curves in Figures 3.37 again show good control but, since Kalman filter 1A has a 1:1 ratio for R:Q, the state estimates are more noisy and the controlled variables fluctuate more than with Kalman filter 6A. However C2 is still controlled very well. In Figure 3.38 the first effect level did begin to drain out on the step down in feed flow but not to the same extent as with Kalman filter 6B. This is to be expected since the measurements were weighted more heavily for this run. The control of C2 is not quite as good as in Figure 3.37 but is still acceptable. There is very little difference between Figures 3.39 and 3.40 since Kalman filter 4 has an R:Q ratio of 1:4, and consequently knowledge of the disturbance is less significant. Therefore, a small R:Q ratio offers the advantage that the control is less likely to suffer due to "unseen" disturbances. However, the general control of the levels and, to a lesser extent the second effect concentration was not so good since by weighting the measurements more heavily, the estimates and hence the manipulated variables are noisier. This in turn leads to the actual states being noisier. The control of the process is still,

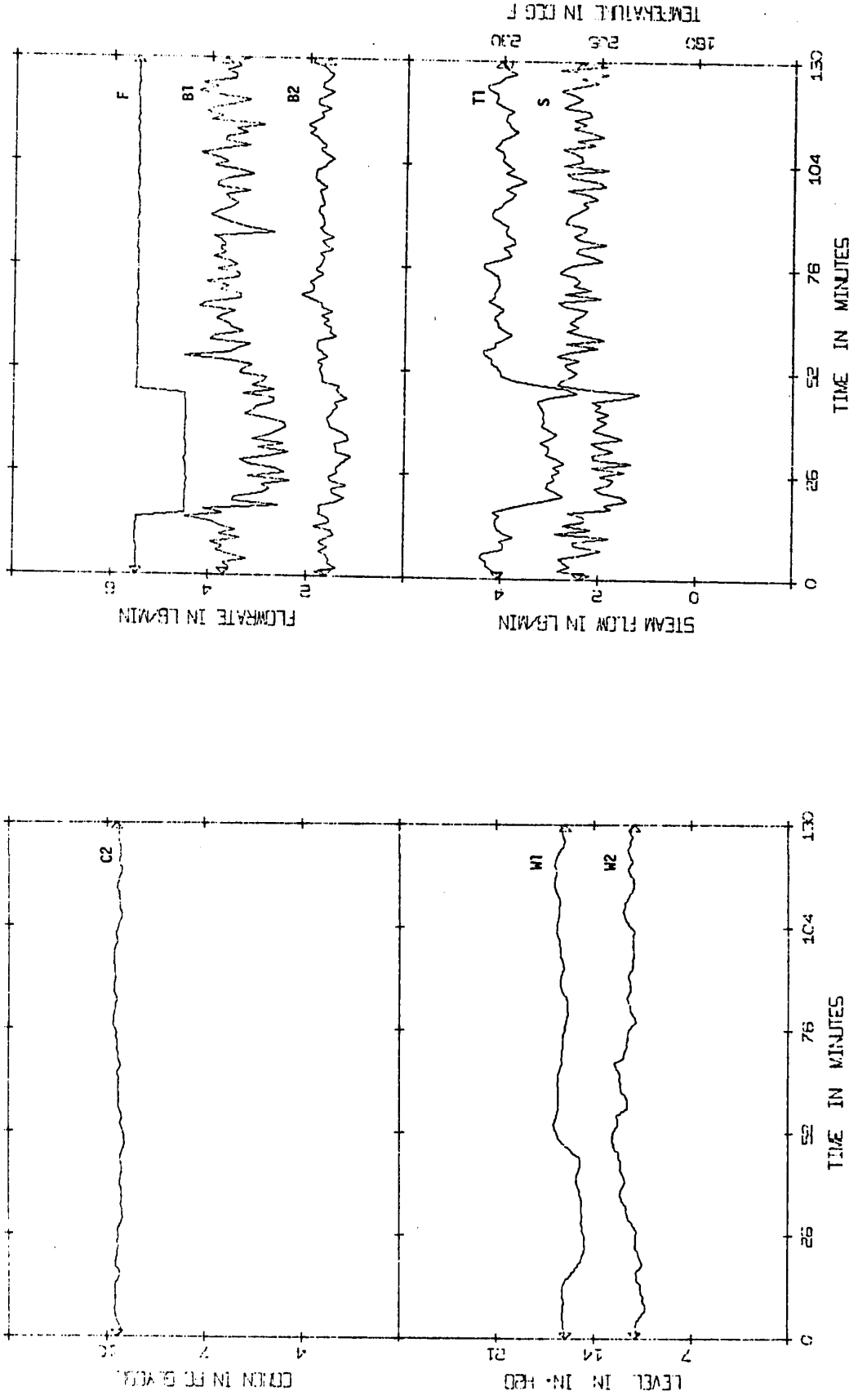

FIGURE 3.37 (EXP/-20%F,+20%F/FB) actual states, control based on Kalman filter 1A estimates

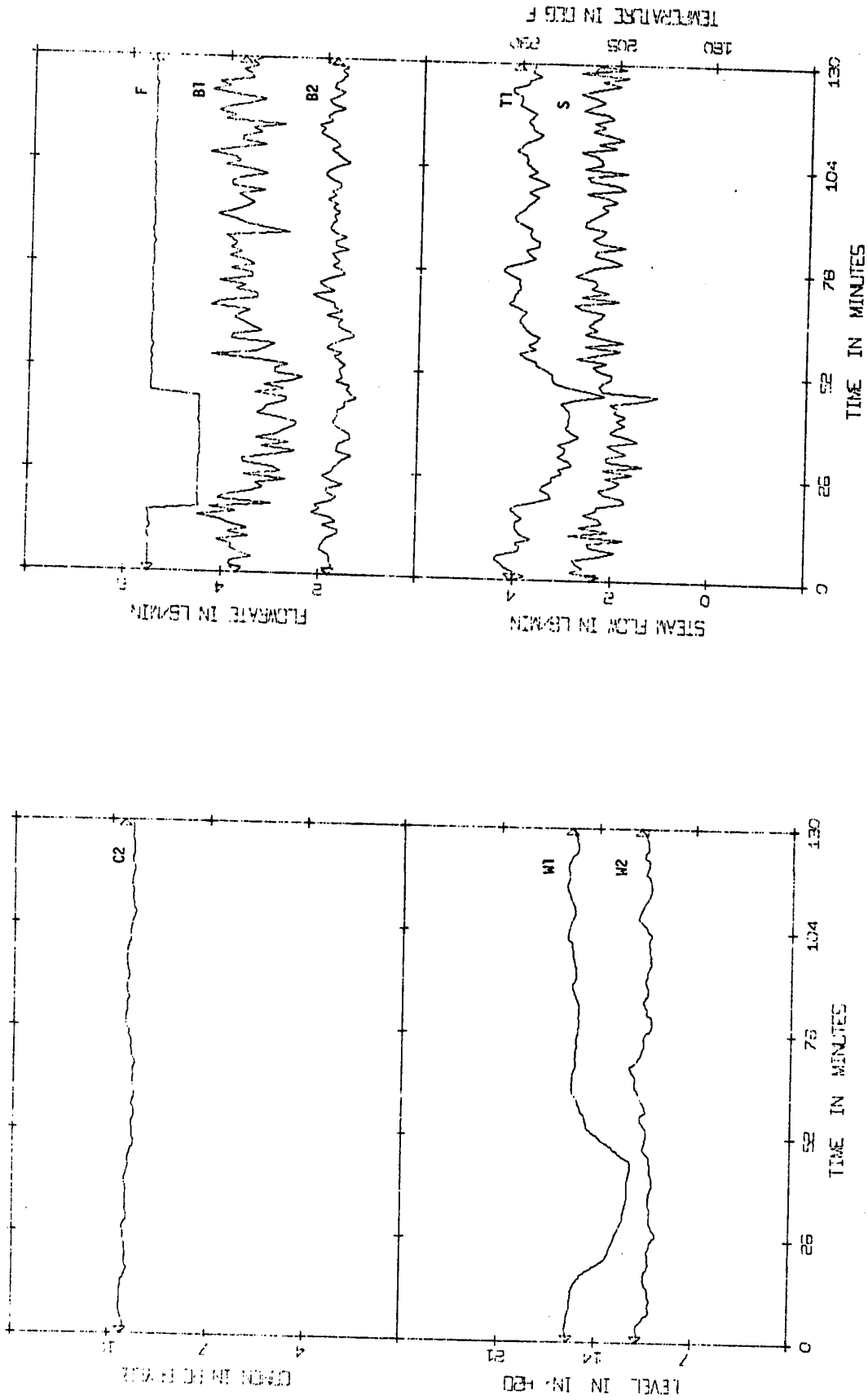

FIGURE 3.38 (EXP/-20%F,+20%F/FB) actual states, control based on Kalman filter 1B estimates

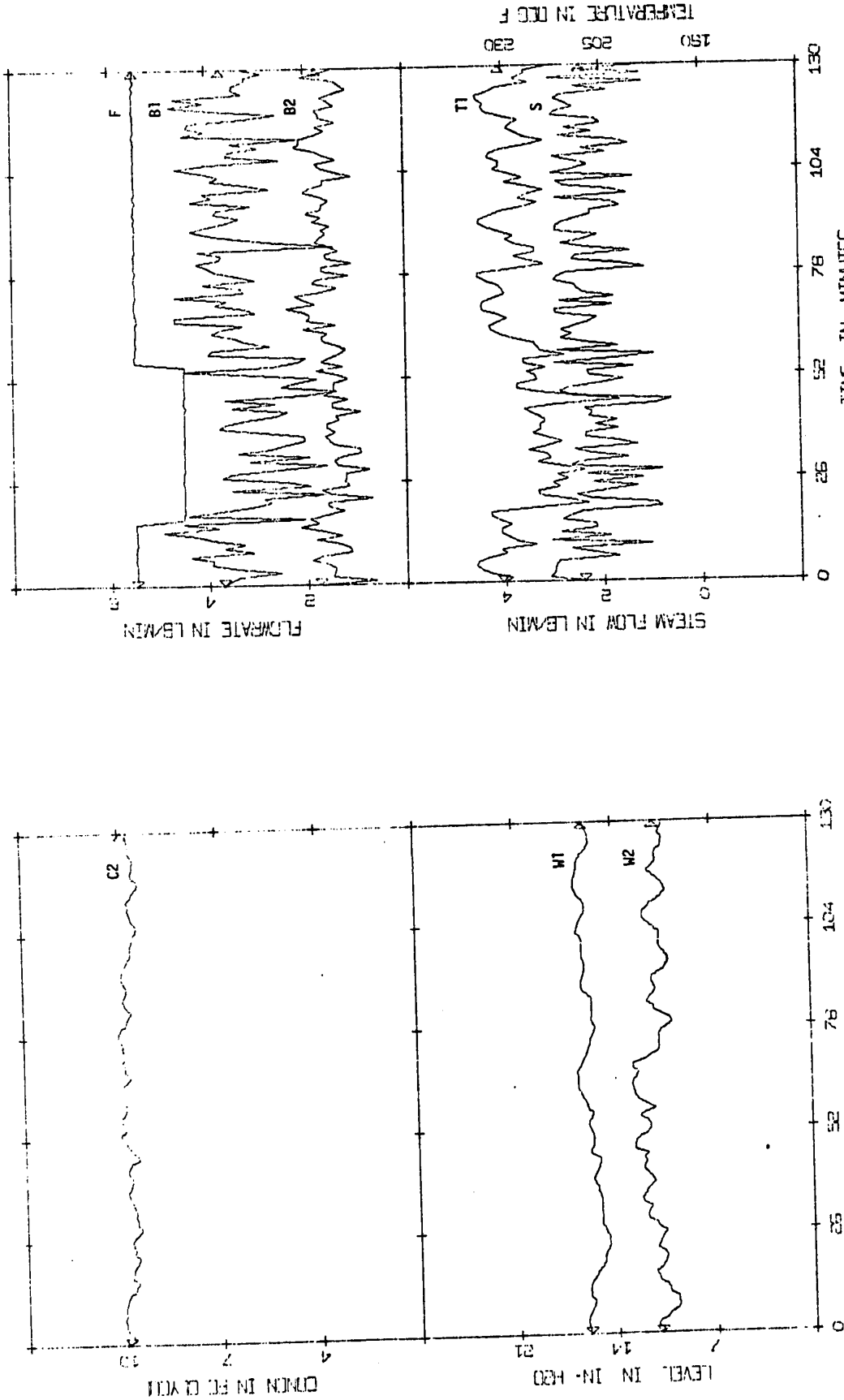

FIGURE 3.39 (EXP/-20%F,+20%F/FB) actual states, control based on Kalman filter 4A estimates

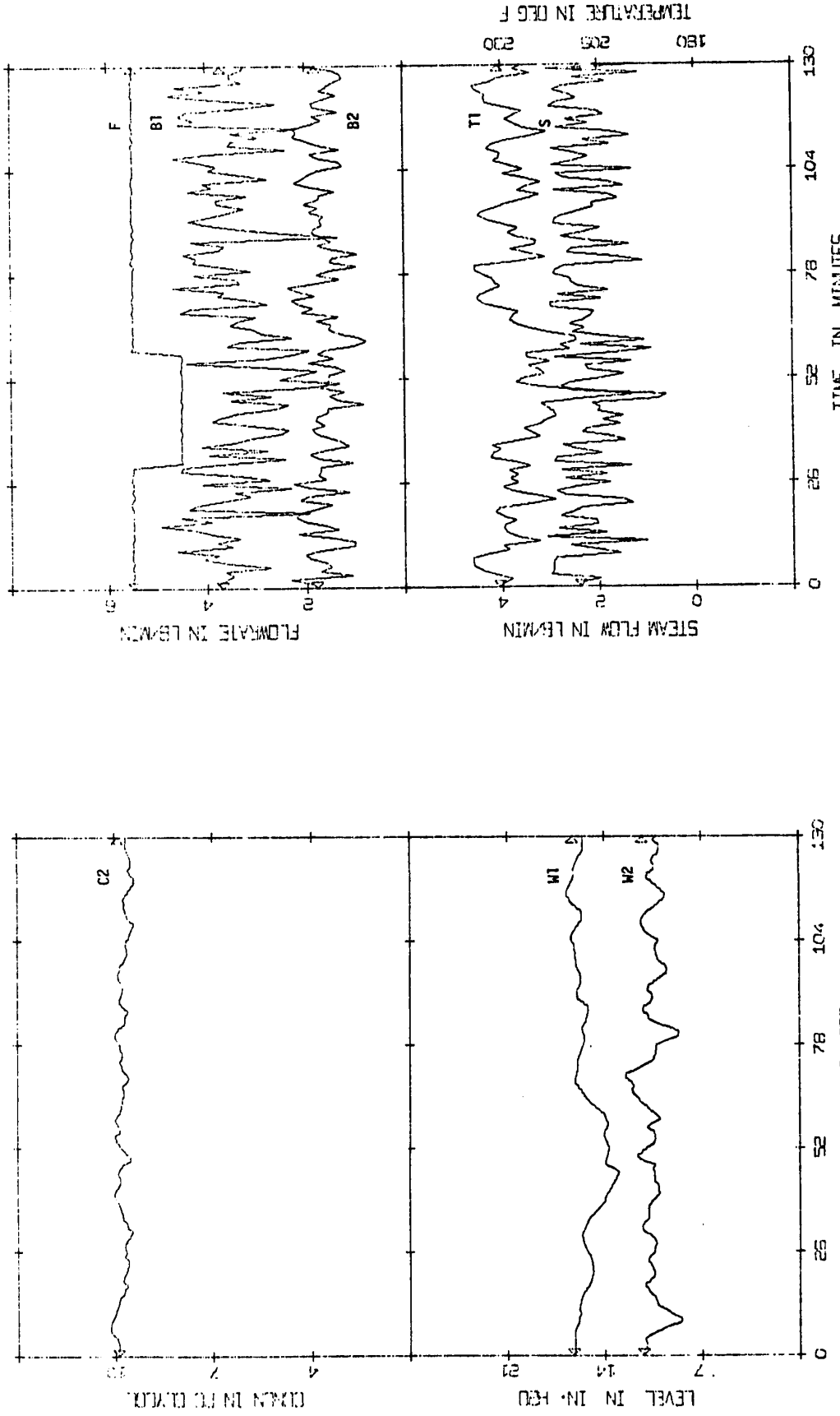

FIGURE 3.40 (EXP/-20%F,+20%F/FB) actual states, control based on Kalman filter 4B estimates

nevertheless, a considerable improvement over the case of unfiltered measurements (c.f. Figure 3.34).

Figures 3.41 and 3.42 illustrate the detrimental effect of the lag introduced by low values of α in the exponential filter. Since the simulation studies and open loop experimental studies indicated that only small values of α would produce any significant differences from the unfiltered case, only $\alpha = 0.3$ and $\alpha = 0.1$ were used in the closed loop experimental runs.

In Figure 3.41, with $\alpha = 0.3$, the curves were smoothed considerably but the time lag due to the filter resulted in oscillations of greater amplitude than the original noisy fluctuations. The flattened parts of the separator level oscillations indicate that on three occasions this level dropped below the physical limit of the measuring device (sight glass). Another detrimental effect was that since the process was controlled so poorly with this filter, the first effect pressure oscillated from very high to very low values quite rapidly. This resulted in solution overflowing from the separator to the condenser periodically, whenever the first effect pressure became high.

With $\alpha = 0.1$ the situation became more extreme as shown in Figure 3.42. Here, although the oscillations were still smoother their amplitude increased and the frequency decreased. The same problems were again encountered but to a greater extent. The separator level was controlled so badly in fact that, at approximately the 60 minute mark, a bad input was read by the computer; consequently this control loop was put on manual operation by the DDC program with a low output value such that the separator level rose and did not return to its

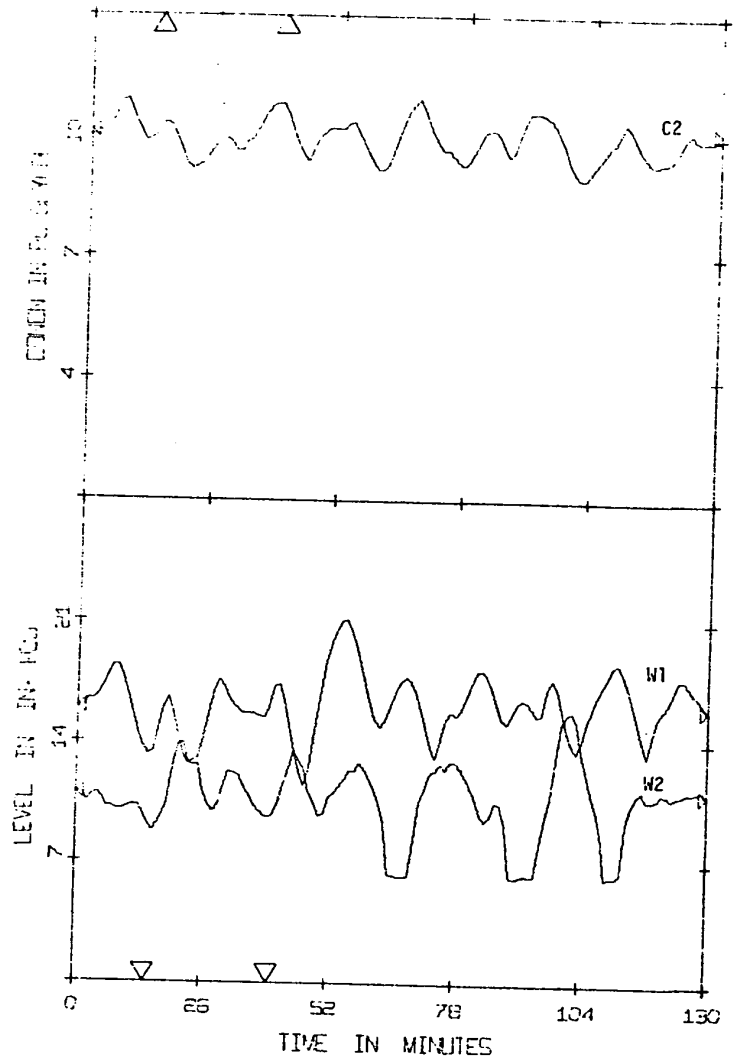

FIGURE 3.41 (EXP/-20%F,+20%F/FB) actual states, control based on exponential filter 3 estimates

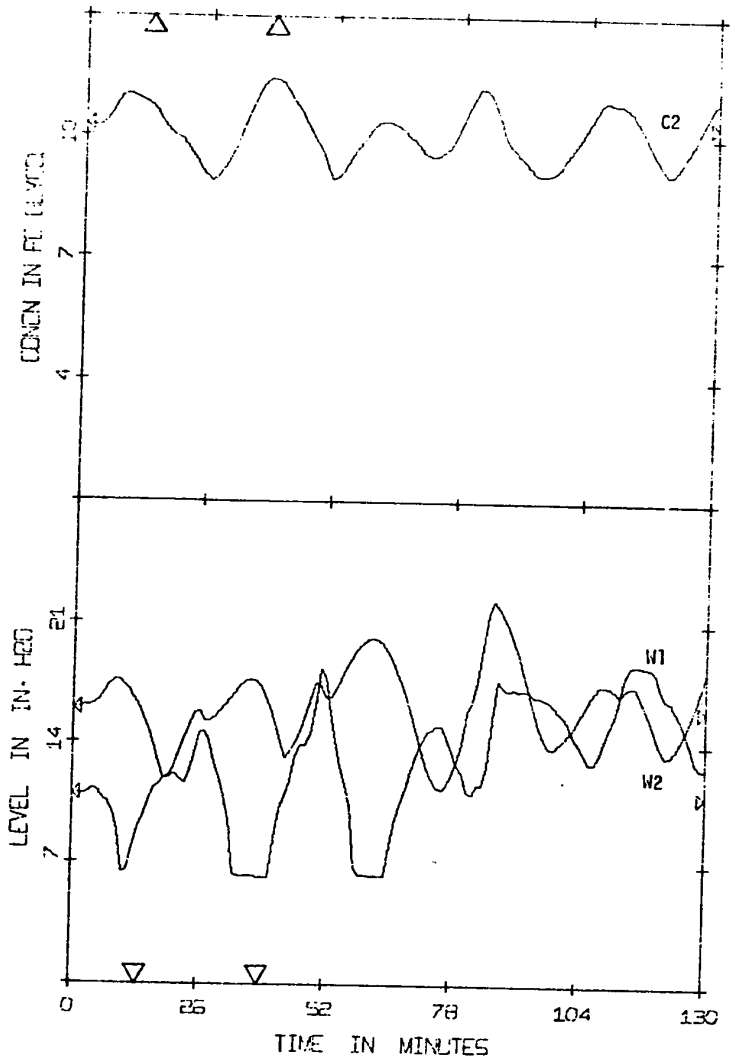

FIGURE 3.42 (EXP/-20%F,+20%F/FB) actual states, control based on exponential filter 4 estimates

normal steady state. From a control point of view this run was a disaster and the previous one in Figure 3.41 was not much better. These runs confirm the conclusion of the simulation study that using the present control algorithm, which does not account for any time lag in estimation, an exponential filter could not improve upon the unfiltered control run.

3.10 CONCLUSIONS

Both simulation and experimental studies demonstrated that the Kalman filter could successfully be used to estimate the states of a stochastic process. Further, it has been shown that these estimates can be very effectively used in an optimal multivariable control system giving a marked improvement over the situation where noisy measurements are not filtered.

A sub-optimal filter of the same form as the Kalman filter but having an arbitrary gain matrix was also briefly studied. The elements of the gain matrices used were found to be too high so that the filtering of the noisy measurements was inadequate. Although it might be possible to improve the estimates of the sub-optimal filter by trial and error changes in the elements of the gain matrix, the systematic selection of this matrix by the Kalman filter is a distinct advantage.

A conventional exponential filter was considered in some detail but it was found that very small values of α were required to reduce the noise level in the open loop state estimates. Due to the time lag inherent in this technique, it was observed that values of α small enough to reduce the noise produced oscillations in the closed loop system. These oscillations increased in amplitude as α was

decreased. It should be possible to improve upon this situation if the time lag was accounted for in the control system, but for the present control algorithm, the exponential filter was not able to improve upon the situation with no filter.

The success of the Kalman filter depended very strongly on two factors:

1) the choice of the weighting matrices $\underline{\underline{R}}$ and $\underline{\underline{Q}}$, and
2) knowledge of the step disturbance in the model calculations.

If the model of the process under consideration is reasonably accurate and it is possible for the filter to "see" any input disturbances, "best" closed loop results can be achieved by using a high R:Q ratio as shown in Figure 3.16 (simulation) and Figure 3.35 (experimental). However, by weighting the model so heavily (i.e. large R:Q ratio) the control will be disastrous if the filter is not aware of sustained disturbances (Figures 3.17 and 3.36).

For the case where it is not possible to measure the input disturbances, the estimation and hence the control cannot be as good. Here the measurements have to be weighted more heavily in order to compensate for unmeasured disturbances; hence the R:Q ratio must be relatively small (see Figures 3.18 and 3.40). Even a 1:1 ratio was found to give reasonable results in a closed loop experimental run (Figure 3.38) but this filter may not have been so successful had the second step in feed flow not been applied. A similar situation arises if the model does not represent the process very accurately. In this case the measurements have to be weighted more heavily and again a small R:Q ratio is required.

The studies here dealt with a stochastic process with relatively high noise levels. Although the conclusions indicate general trends for any such process, it should be noted that for less noisy systems the measurements could be weighted more heavily while still achieving good results.

In general it is advantageous to weight the measurements as highly as possible (while eliminating the noise as much as possible) so that the problems of having an inaccurate model or "unseen" disturbances are minimized.

CHAPTER FOUR

LITERATURE SURVEY AND BASIC EQUATIONS FOR THE LUENBERGER OBSERVER

4.1 INTRODUCTION

In 1964 Luenberger [1] formally demonstrated that the state vector of a linear, time-invariant, deterministic system could be reconstructed from observations of the system inputs and outputs. It was shown that the Luenberger observer is itself a linear system whose complexity decreases as the number of output quantities available increases.

In most control situations the entire state vector is not available for measurement and the minimal order Luenberger observer has been shown to be a most useful tool in reconstructing these states. Luenberger demonstrated that the design of the observer is relatively simple and proved that the order of the observer need only be equal to the number of unmeasured states, i.e. a "minimal-order observer".

4.2 LITERATURE SURVEY

The theory was originally developed by Luenberger [1,2] and since then many modifications and extensions have been proposed as described by Luenberger in his recent review of observer theory [3]. A few of these extensions will be briefly discussed below.

For the continuous-time case, several authors [4,5,6] have extended the theory to include time-varying systems and noise [7]. Aoki and Huddle [8] derived the discrete form of the observer for a deterministic system and also developed an estimator for a stochastic, discrete-time, linear, time-invariant system. The authors illustrated

by a simple example that the performance of the observer could be comparable to that of the optimal filter. The design of this stochastic observer is considerably more complex than for the deterministic case but the form of the final equations is identical in both cases. The authors call the observer a "constrained estimator" since a constraint is imposed in the design in order to achieve a minimal-order observer. It is interesting to note that if this constraint were not imposed, the stationary Kalman filter is obtained. The time-varying discrete case has also been investigated [9,10].

Newmann [11] developed a reduced-order filter for a linear, stochastic, continuous system analogous to the work in [8] for the discrete case.

There have been several papers published (and some confusion in the literature) regarding the effect of an observer on control system performance, as indicated by a quadratic cost functional. Sarma and Deekshatulu [12] used the Luenberger observer in an optimal linear regulator and demonstrated the improved performance over the optimal regulator with incomplete state feedback. However, the authors stated that, even with a correct initial state estimate and a deterministic system, there is a small loss in performance due to the inclusion of the observer in the closed-loop system. Porter and Woodhead [13], and Newmann [14] quickly corrected this misconception and showed that the loss in performance, under these conditions, was due entirely to numerical inaccuracy. Bongiorno and Youla [15,16] presented a comprehensive mathematical treatment of this problem, proving that in general, there is an increase in cost when an observer is used in a control system due to inevitable inaccuracy in the initial state estimates. It

should also be noted that in practical applications there are model inaccuracies and noise which contribute to a further increase in cost. The authors also demonstrated mathematically that this increase in cost cannot be made arbitrarily small by choosing observer eigenvalues with highly negative real parts. This is a somewhat surprising result since the estimation errors are reduced more quickly with large negative eigenvalues. (The corresponding result for the discrete case applies to small positive observer eigenvalues.) The possibility that a feedback law, other than the optimal one, could be better, when the observer is employed in regulators, was also investigated. The authors concluded that, with no prior statistical information about the initial states, no feedback control law could reduce the additional cost (for all initial plant states) below the value obtained with the optimal deterministic controller. These conclusions were all obtained for the infinite-time optimal feedback control problem. Sarma and Jayaraj [17] presented the corresponding results for the finite-time problem.

Newmann [18] derived an expression for the increase in cost in terms of the initial conditions of the observer and also showed that the increase was an implicit function of the design parameters of the observer. He investigated the situation where statistical information about the initial state estimates is available and optimized the design of the observer by choosing the design parameters to minimize the increase in cost. This procedure was extended to optimize the feedback control matrix but it was thought that the increased computations may not be justified. Yuksel and Bongiorno [19] also presented an algorithm for the design of "asymptotic state estimators" (or observers). It was shown that this estimator can be employed in optimally designed regulators

provided an increase in cost from the optimal cost can be tolerated. The dangers of having estimator eigenvalues with large negative (continuous case) real parts was again pointed out (i.e. cost $\rightarrow \infty$ as $\lambda_i \rightarrow -\infty$).

Other authors [20,21] have proposed alternative design procedures for the observer which obviate some of the mathematical difficulties involved with the original technique while still fulfilling the basic requirements.

There have been several reports of observers being used in feedback control systems [22-26] but these studies are all of a theoretical nature. Bona [26] investigated the application of an observer to an inertial navigation system and compared the results with those obtained using the Kalman filter. Both techniques were found to give comparable results but the observer was much easier to implement. The author also confirmed that very small eigenvalues (discrete case) can give bad results when noise (or modelling errors) are present.

Most of the literature on this topic is concerned with theoretical aspects of observers. There have been a few numerical and simulation examples reported with reference to guidance and tracking systems. This survey has not revealed any reports of observers being used in the field of process control.

4.3 THEORY

The observer theory is presented for a discrete-time system since this is appropriate for digital computer control systems. The basic derivation is given along with two alternative design procedures.

The dynamics of any errors in the estimates obtained from the observer is analyzed and an expression for the steady state error between the actual and estimated states for unseen disturbances is derived.

4.3.1 Basic Theory

The basic theory involved in designing a minimal-order Luenberger observer for a discrete linear time-invariant system is presented here. The nomenclature is (where appropriate) consistent with the equations for the Kalman filter study.

The discrete state space model is given in Equation (4.1):

$$\underline{x}(k+1) = \underline{\underline{\phi}}\ \underline{x}(k) + \underline{\underline{\Delta}}\ \underline{u}(k) + \underline{\underline{\theta}}\ \underline{d}(k) \quad , k = 0,1,2... \qquad (4.1)$$

with output equation:

$$\underline{y}(k) = \underline{\underline{H}}\ \underline{x}(k) \qquad (4.2)$$

The optimal feedback control law whose derivation was discussed in Chapter 2 has the following form:

$$\underline{u}(k) = \underline{\underline{K}}_{FB}\ \underline{x}(k) \qquad (4.3)$$

The object of the observer design is to reconstruct the state variables, $\underline{x}$, from observations of the process inputs, $\underline{u}$ and $\underline{d}$, and outputs, $\underline{y}$, so that the optimal feedback control law (Equation (4.3)) can be used.

Since the rigorous mathematical design of the Luenberger observer has been presented in the literature many times [1-3,8], various results will be summarized below without proof.

If the order of the process (i.e. the dimension of the state vector) is n and the number of outputs is m, where m<n, then the $(n-m)^{th}$ order observer has the following form:

$$\underline{z}(k+1) = \underline{\underline{E}}\,\underline{z}(k) + \underline{\underline{C}}\,\underline{y}(k) + \underline{\underline{F}}\,\underline{d}(k) + \underline{\underline{G}}\,\underline{u}(k) \tag{4.4}$$

where the observer is driven by both the inputs and outputs of the process (see Equation (4.1)). The (n-m)-dimensional vector, $\underline{z}$, is the observer state vector. In Equation (4.4) there are four matrices to be specified ($\underline{\underline{E}}$, $\underline{\underline{C}}$, $\underline{\underline{F}}$ and $\underline{\underline{G}}$). These matrices must satisfy the following relations such that a transformation matrix, $\underline{\underline{T}}$, exists:

$$\underline{\underline{T}}\,\underline{\underline{\phi}} - \underline{\underline{E}}\,\underline{\underline{T}} = \underline{\underline{C}}\,\underline{\underline{H}} \tag{4.5}$$

$$\underline{\underline{F}} = \underline{\underline{T}}\,\underline{\underline{\theta}} \tag{4.6}$$

$$\underline{\underline{G}} = \underline{\underline{T}}\,\underline{\underline{\Delta}} \tag{4.7}$$

Then the relationship between, $\underline{z}$ and $\underline{x}$, is given by:

$$\underline{z}(k) = \underline{\underline{T}}\,\underline{x}(k) \tag{4.8}$$

provided that

$$\underline{z}(0) = \underline{\underline{T}}\,\underline{x}(0) \tag{4.9}$$

The transformation matrix, $\underline{\underline{T}}$, is an mxn matrix.

If Equation (4.9) is not satisfied, Luenberger [1] reasoned that since the eigenvalues of the dynamic matrix, $\underline{\underline{E}}$, could be selected to be arbitrarily small, the error in the observed states tends to zero as time tends to infinity (see Section 4.3.3 for a treatment of the dynamic error equation). As was noted in the literature survey, however, there is a trade-off between the speed of response to errors and the increase in cost for closed loop systems so that there is an optimum range of eigenvalues which will satisfy both goals within reasonable

limits.

Two equations are now available for reconstructing the entire state vector:

$$\underline{y}(k) = \underline{\underline{H}}\,\underline{x}(k) \tag{4.2}$$

$$\underline{z}(k) = \underline{\underline{T}}\,\underline{x}(k) \tag{4.8}$$

Combining these gives

$$\begin{bmatrix} \underline{z}(k) \\ \cdots \\ \underline{y}(k) \end{bmatrix} = \begin{bmatrix} \underline{\underline{T}} \\ \cdots \\ \underline{\underline{H}} \end{bmatrix} \underline{x}(k) \tag{4.10}$$

or solving for $\underline{x}(k)$ gives

$$\underline{x}(k) = \begin{bmatrix} \underline{\underline{T}} \\ \cdots \\ \underline{\underline{H}} \end{bmatrix}^{-1} \begin{bmatrix} \underline{z}(k) \\ \cdots \\ \underline{y}(k) \end{bmatrix}$$

or

$$\underline{x}(k) = \underline{\underline{L}} \begin{bmatrix} \underline{z}(k) \\ \cdots \\ \underline{y}(k) \end{bmatrix} \tag{4.11}$$

where $\underline{\underline{L}}$ is termed the reconstruction matrix and is defined by:

$$\underline{\underline{L}} = \begin{bmatrix} \underline{\underline{T}} \\ \cdots \\ \underline{\underline{H}} \end{bmatrix}^{-1} \tag{4.12}$$

Thus, if the observer is driven by the inputs and outputs of the process then the entire state vector can be reconstructed from the outputs of the process together with observer states according to

Equation (4.11).

Some auxiliary relations are derived for use in the second design technique. The reconstruction matrix, $\underline{\underline{L}}$, may be partitioned so that Equation (4.11) becomes:

$$\underline{x}(k) = [\underline{\underline{L}}_1 \vdots \underline{\underline{L}}_2] \begin{bmatrix} \underline{z}(k) \\ \cdots \\ \underline{y}(k) \end{bmatrix}$$

$$\underline{x}(k) = \underline{\underline{L}}_1 \underline{z}(k) + \underline{\underline{L}}_2 \underline{y}(k) \tag{4.13}$$

It is immediately obvious from the definition of $\underline{\underline{L}}$ that:

$$[\underline{\underline{L}}_1 \vdots \underline{\underline{L}}_2] \begin{bmatrix} \underline{\underline{T}} \\ \cdots \\ \underline{\underline{H}} \end{bmatrix} = \underline{\underline{I}}$$

or

$$\underline{\underline{L}}_1 \underline{\underline{T}} + \underline{\underline{L}}_2 \underline{\underline{H}} = \underline{\underline{I}} \tag{4.14}$$

It can then be easily shown that the relations:

$$\underline{\underline{E}} = \underline{\underline{T}} \underline{\underline{\Phi}} \underline{\underline{L}}_1 \tag{4.15}$$

$$\underline{\underline{C}} = \underline{\underline{T}} \underline{\underline{\Phi}} \underline{\underline{L}}_2 \tag{4.16}$$

are necessary and sufficient conditions for Equation (4.5) to be satisfied.

These are the basic relations for the Luenberger observer; the design methods are considered in the next section.

4.3.2 Design Techniques

Two design techniques are considered. The first is the original method presented by Luenberger [1] and the second is an

alternative approach developed by Newmann [21]. These methods will be referred to in this study by the names of the respective authors.

(a) Luenberger's Method

Referring back to Equation (4.4) there are four design matrices to be specified ($\underline{\underline{E}}$, $\underline{\underline{C}}$, $\underline{\underline{F}}$ and $\underline{\underline{G}}$) with the constraints:

$$\underline{\underline{T}}\,\underline{\underline{\phi}} - \underline{\underline{E}}\,\underline{\underline{T}} = \underline{\underline{C}}\,\underline{\underline{H}} \tag{4.5}$$

$$\underline{\underline{F}} = \underline{\underline{T}}\,\underline{\underline{\theta}} \tag{4.6}$$

$$\underline{\underline{G}} = \underline{\underline{T}}\,\underline{\underline{\Delta}} \tag{4.7}$$

By specifying $\underline{\underline{E}}$ and $\underline{\underline{C}}$ the transformation matrix, $\underline{\underline{T}}$, is fixed. Equations (4.6) and (4.7) then fix matrices $\underline{\underline{F}}$ and $\underline{\underline{G}}$, respectively, so that the problem reduces to one of selecting $\underline{\underline{E}}$ and $\underline{\underline{C}}$ such that $\underline{\underline{T}}$ exists and the reconstruction matrix, $\underline{\underline{L}}$, is invertible. Luenberger [1] showed that if $\underline{\underline{\phi}}$ and $\underline{\underline{E}}$ have no common eigenvalues and the system is observable, then $\underline{\underline{T}}$ exists and $\underline{\underline{L}}$ will be nonsingular. Here $\underline{\underline{C}}$ may be arbitrarily specified. The observer can then be designed in the following steps:

(1) Specify $\underline{\underline{E}}$ (eigenvalues distinct and distinct from those of $\underline{\underline{\phi}}$) and $\underline{\underline{C}}$.

(2) Evaluate $\underline{\underline{T}}$ from Equation (4.5).

(3) Calculate $\underline{\underline{F}}$ and $\underline{\underline{G}}$ from Equations (4.6) and (4.7).

(4) Calculate $\underline{\underline{L}}$ from Equation (4.12).

The state variables can then be reconstructed from a combination of the process outputs and the observer states.

Step (2) is the most difficult and Luenberger [27] has published a paper which may be helpful in solving Equation (4.5). The problem can also be solved by the application of Kronecker matrix products [28,29].

The advantage of this design method is that the designer has direct control of the matrix $\underline{\underline{E}}$ and hence control of the eigenvalues of $\underline{\underline{E}}$. From the foregoing discussion this is obviously a desirable feature. The disadvantage is in the difficulty of step (2) and possible ill-conditioning of matrix, $\underline{\underline{L}}$.

(b) Newmann's Method

Newmann's approach relies on the arbitrary choice of the transformation matrix subject to the condition that the resulting reconstruction matrix is nonsingular.

Utilizing Equations (4.15) and (4.16), his design reduces to choosing one matrix, $\underline{\underline{T}}$.

The procedure is as follows:

(1) Choose any $\underline{\underline{T}}$ so that $\underline{\underline{L}}$ exists (this involves calculating $\underline{\underline{L}}$ from Equation (4.12) as a check).

(2) Obtain $\underline{\underline{L}}_1$ and $\underline{\underline{L}}_2$ by partitioning $\underline{\underline{L}}$.

(3) Calculate $\underline{\underline{E}}$, $\underline{\underline{C}}$, $\underline{\underline{F}}$ and $\underline{\underline{G}}$ from Equations (4.15), (4.16), (4.6) and (4.7) respectively.

The states can then be reconstructed as before.

The advantages of this method are:

(1) Only one design matrix need be specified.

(2) Inversion is guaranteed without any restrictions on the eigenvalues of $\underline{\underline{E}}$ and it is no longer necessary that the plant be completely observable.

The one disadvantage is that there is no direct control over the eigenvalues of $\underline{\underline{E}}$ and hence no control over the speed of response to errors.

4.3.3 Error Dynamics of the Observer Estimates *

The estimated state variables, $\hat{\underline{x}}$, which are reconstructed by the Luenberger observer, can be related to the actual states, $\underline{x}$, by the following equation:

$$\hat{\underline{x}}(k) = \underline{x}(k) + \underline{\Delta x}(k) \tag{4.17}$$

which defines the error vector, $\underline{\Delta x}$.

Multiplying throughout by $\underline{\underline{T}}$ gives:

$$\underline{\underline{T}}\,\hat{\underline{x}}(k) = \underline{\underline{T}}\,\underline{x}(k) + \underline{\underline{T}}\,\underline{\Delta x}(k)$$

or

$$\hat{\underline{z}}(k) = \underline{z}(k) + \underline{\Delta z}(k) \tag{4.18}$$

Thus, recognizing the possibility of errors in the estimated states, the observer equation becomes:

$$\hat{\underline{z}}(k+1) = \underline{\underline{E}}\,\hat{\underline{z}}(k) + \underline{\underline{C}}\,\underline{y}(k) + \underline{\underline{F}}\,\underline{d}(k) + \underline{\underline{G}}\,\underline{u}(k) \tag{4.19}$$

Now

$$\underline{\Delta z}(k+1) = \hat{\underline{z}}(k+1) - \underline{z}(k+1)$$

or from Equation (4.8):

$$\underline{\Delta z}(k+1) = \hat{\underline{z}}(k+1) - \underline{\underline{T}}\,\underline{x}(k+1)$$

Substituting for $\hat{\underline{z}}$ from Equation (4.19) gives:

$$\underline{\Delta z}(k+1) = \underline{\underline{E}}\,\hat{\underline{z}}(k) + \underline{\underline{C}}\,\underline{y}(k) + \underline{\underline{F}}\,\underline{d}(k) + \underline{\underline{G}}\,\underline{u}(k) - \underline{\underline{T}}\,\underline{x}(k+1)$$

or

$$\underline{\Delta z}(k+1) = \underline{\underline{E}}\,\hat{\underline{z}}(k) + \underline{\underline{C}}\,\underline{y}(k) + \underline{\underline{F}}\,\underline{d}(k) + \underline{\underline{G}}\,\underline{u}(k) - \underline{\underline{T\phi}}\,\underline{x}(k) - \underline{\underline{T\Theta}}\,\underline{d}(k) - \underline{\underline{T\Delta}}\,\underline{u}(k)$$

* For the Luenberger observer study in Chapters 4 and 5, "estimates" refers to the values of the state variables calculated by the observer, and is not used in the statistical sense.

Rearranging gives:

$$\underline{\Delta z}(k+1) = \underline{\underline{E}}\ \underline{\hat{z}}(k) + (\underline{\underline{CH}} - \underline{\underline{T\phi}})\ x(k) + (\underline{\underline{F}} - \underline{\underline{T\theta}})\ d(k) + (\underline{\underline{G}} - \underline{\underline{T\Delta}})\ u(k) \quad (4.20)$$

Substituting Equations (4.5), (4.6) and (4.7) gives:

$$\underline{\Delta z}(k+1) = \underline{\underline{E}}\ \underline{\hat{z}}(k) - \underline{\underline{E}}\ \underline{\underline{T}}\ \underline{x}(k)$$

or

$$\underline{\Delta z}(k+1) = \underline{\underline{E}}(\underline{z}(k) + \underline{\Delta z}(k) - \underline{\underline{T}}\ \underline{x}(k))$$

or

$$\underline{\Delta z}(k+1) = \underline{\underline{E}}\ \underline{\Delta z}(k)$$

Thus we have the dynamic error equation for the observer states:

$$\underline{\Delta z}(k+1) = \underline{\underline{E}}\ \underline{\Delta z}(k) \quad (4.21)$$

which shows that if the eigenvalues of $\underline{\underline{E}}$ are small then the error in the observation will quickly tend to zero with time.

Since it was of interest to investigate the performance of the observer with unmeasured step disturbances to the process it was decided to derive an expression for the steady state gain of the dynamic error equation for the process state variables.

The analysis proceeds as before except that the observer is not driven by the disturbance vector, $\underline{d}$. Equation (4.19) then becomes:

$$\underline{\hat{z}}(k+1) = \underline{\underline{E}}\ \underline{\hat{z}}(k) + \underline{\underline{C}}\ \underline{y}(k) + \underline{\underline{G}}\ \underline{u}(k) \quad (4.22)$$

Carrying this through the analysis, Equation (4.21) has an additional term due to the unmeasured disturbance vector, $\underline{d}$:

$$\underline{\Delta z}(k+1) = \underline{\underline{E}}\ \underline{\Delta z}(k) - \underline{\underline{T}}\ \underline{\underline{\theta}}\ \underline{d}(k) \tag{4.23}$$

After a step disturbance to the process $\underline{\Delta z}(k+1)$ will eventually equal $\underline{\Delta z}(k)$ at the new steady state, i.e. Equation (4.23) becomes

$$\underline{\Delta z}_{ss} = \underline{\underline{E}}\ \underline{\Delta z}_{ss} - \underline{\underline{T}}\ \underline{\underline{\theta}}\ \underline{d}_{ss} \tag{4.24}$$

where ss denotes the steady state.

Rearranging Equation (4.24) gives:

$$\underline{\Delta z}_{ss} = (\underline{\underline{E}} - \underline{\underline{I}})^{-1}\ \underline{\underline{T}}\ \underline{\underline{\theta}}\ \underline{d}_{ss} \tag{4.25}$$

Going back to Equation (4.13) gives:

$$\underline{x}(k) = \underline{\underline{L}}_1\ \underline{z}(k) + \underline{\underline{L}}_2\ \underline{y}(k) \tag{4.13}$$

and

$$\hat{\underline{x}}(k) = \underline{\underline{L}}_1\ \hat{\underline{z}}(k) + \underline{\underline{L}}_2\ \underline{y}(k) \tag{4.26}$$

Recalling Equation (4.17):

$$\underline{\Delta x}(k) = \hat{\underline{x}}(k) - \underline{x}(k) \tag{4.17}$$

gives

$$\underline{\Delta x}_{ss} = \hat{\underline{x}}_{ss} - \underline{x}_{ss} \tag{4.27}$$

$$\underline{\Delta x}_{ss} = \underline{\underline{L}}_1\ \hat{\underline{z}}_{ss} + \underline{\underline{L}}_2\ \underline{y}_{ss} - \underline{\underline{L}}_1\ \underline{z}_{ss} - \underline{\underline{L}}_2\ \underline{y}_{ss} \tag{4.28}$$

$$\underline{\Delta x}_{ss} = \underline{\underline{L}}_1(\hat{\underline{z}}_{ss} - \underline{z}_{ss})$$

$$\underline{\Delta x}_{ss} = \underline{\underline{L}}_1\ \underline{\Delta z}_{ss} \tag{4.29}$$

Substituting Equation (4.25) into Equation (4.29) gives the steady state gain equation for the error in the reconstructed states due to an unmeasured disturbance:

$$\underline{\Delta x}_{ss} = \underline{\underline{L}}_1 (\underline{\underline{E}} - \underline{\underline{I}})^{-1} \underline{\underline{T}} \underline{\underline{\theta}} \underline{d}_{ss} \tag{4.30}$$

Obviously, for no disturbances, $\underline{d}_{ss} = \underline{0}$ and consequently the steady state error in the reconstructed states is zero. In general, the vector $\underline{\Delta x}_{ss}$ will have zeros corresponding to the measured states and nonzero elements for the unmeasured states. It can be seen from Equation (4.30) that the steady state offset is not a simple function of the observer design parameters and it is impossible to design an observer which will minimize the offsets for all states for all disturbances.

CHAPTER FIVE

EVALUATION OF THE LUENBERGER OBSERVER

5.1 INTRODUCTION

The results of the simulation and experimental evaluations of the Luenberger observer are presented in this chapter. First a simple numerical example, chosen from a report by Munro [1], was investigated for both continuous-time and discrete-time models (the results for the discrete case are presented in detail). The computer programs used in the double effect evaporator simulation and experimental studies are briefly described followed by presentation of the results.

Using the evaporator model, three simulation studies were performed with different assumptions concerning which state variables are measured in each case. The first study considers the situation where the first effect enthalpy and the first effect concentration are not measured so that a second order observer is required. Another second order observer was investigated for the second case where the first and second effect concentrations are not measured, and finally the product (second effect) concentration only was assumed to be inaccessible, yielding a first order observer. The first and third of these studies were also investigated experimentally. A description of the double effect evaporator is given in Chapter 3.

5.2 NUMERICAL EXAMPLE OF MUNRO [1]

A numerical example was chosen from a report by Munro [1]. The original problem comprised a fourth-order, continuous, state space model with two inputs, $\underline{d}$, and two outputs, $\underline{y}$:

$$\dot{\underline{x}}(t) = \begin{bmatrix} -2 & 1 & 0 & 0 \\ 0 & -2 & 1 & 0 \\ 0 & 0 & -1 & 1 \\ -1 & 0 & 0 & 0 \end{bmatrix} \underline{x}(t) + \begin{bmatrix} 0 & 0 \\ 0 & 0 \\ 0 & 1 \\ 1 & 0 \end{bmatrix} \underline{d}(t) \qquad (5.1)$$

$$\underline{y}(t) = \begin{bmatrix} 1 & 0 & 0 & 0 \\ 0 & 0 & 1 & 0 \end{bmatrix} \underline{x}(t) \qquad (5.2)$$

The eigenvalues for this system consist of two complex conjugate pairs:

$$\lambda_{1,2} = -0.307 \pm 0.318\, j$$

$$\lambda_{3,4} = -2.192 \pm 0.547\, j$$

Munro extended Luenberger's original design procedure to include a systematic selection of the coefficient matrix $\underline{\underline{C}}$ (in the dynamic observer equation) after having specified $\underline{\underline{E}}$. The final observer design for this example was presented in his report but no attempt was made to evaluate the effectiveness of the observer.

The $\underline{\underline{E}}$ and $\underline{\underline{C}}$ matrices used by Munro were:

$$\underline{\underline{E}} = \begin{bmatrix} -3 & 0 \\ 0 & -3 \end{bmatrix} \qquad (5.3)$$

$$\underline{\underline{C}} = \begin{bmatrix} -1 & -1 \\ -1 & -6 \end{bmatrix} \qquad (5.4)$$

In the present work, this observer design was verified using

the original design method and the input matrices ($\underline{\underline{E}}$ and $\underline{\underline{C}}$) specified by Munro. This observer was then simulated using IBM's Continuous Systems Modelling Program (CSMP) on an IBM 1800 digital computer. Since the simulation results for the continuous observer correspond very closely to the results for the discrete case (see below), they will not be considered in detail.

The system equations and the dynamic observer equation were then discretized to obtain the corresponding discrete system. Using this design as a base case, two other observers were designed with faster dynamics by simply reducing the eigenvalues of the $\underline{\underline{E}}$ matrix. These three observers were evaluated to discover the effect of unmeasured disturbances and incorrect initial estimates; the results are presented in the following section.

5.2.1 Evaluation of the Observer for the Discrete System

The continuous model was discretized for a time interval of 0.13 using the GEMSCOPE program [2]. The resulting discrete model is given by:

$$\underline{x}(k+1) = \begin{bmatrix} 0.7687 & 0.1011 & 0.0069 & 0.0003 \\ -0.003 & 0.7687 & 0.1081 & 0.0076 \\ -0.0076 & -0.0003 & 0.8767 & 0.1232 \\ -0.1756 & -0.0073 & -0.0003 & 1.0000 \end{bmatrix} \underline{x}(k)$$

$$+ \begin{bmatrix} 0.0000 & 0.0003 \\ 0.0003 & 0.0076 \\ 0.0083 & 0.1232 \\ 0.1315 & 0.0000 \end{bmatrix} \underline{d}(k) \qquad (5.5)$$

$$\underline{y}(k) = \begin{bmatrix} 1 & 0 & 0 & 0 \\ 0 & 0 & 1 & 0 \end{bmatrix} \underline{x}(k) \tag{5.6}$$

The observer design is identical to that for the continuous case except the discrete form of the observer is now used:

$$\underline{z}(k+1) = \begin{bmatrix} 0.6771 & 0 \\ 0 & 6.771 \end{bmatrix} \underline{z}(k) + \begin{bmatrix} -0.1077 & 0.1077 \\ -0.1077 & -0.6460 \end{bmatrix} \underline{y}(k)$$

$$+ \begin{bmatrix} 0.0014 & -0.0048 \\ 0.1334 & -0.3926 \end{bmatrix} \underline{d}(k) \tag{5.7}$$

where

$$\underline{z}(k) = \begin{bmatrix} -1.1625 & 1.2839 & -0.1150 & 0.0167 \\ 0.0942 & -0.0176 & -3.1858 & 1.2158 \end{bmatrix} \underline{x}(k) \tag{5.8}$$

and the reconstruction matrix is:

$$\underline{\underline{L}} = \begin{bmatrix} 0 & 0 & 1 & 0 \\ 0.7788 & -0.0094 & 0.9062 & 0.0595 \\ 0 & 0 & 0 & 1 \\ 0.0112 & 0.8223 & -0.0644 & 2.6211 \end{bmatrix} \tag{5.9}$$

The other designs differed only in that the eigenvalues of $\underline{\underline{E}}$ were made more negative (see Table 5.1 for these values).

All the observer designs successfully reconstructed the state variables when the initial state estimates were exact and the observer was aware of all disturbances.

The effects of incorrect initial state estimates and unseen disturbances in each of the inputs (d1 or d2) were investigated. In each investigation, the actual response and the response of the observer were generated using the digital simulation program SPES and plotted by the program LPLOT. The results are summarized in Table 5.1.

Figure 5.1 shows the actual model response to a nonzero initial value for x1. Figures 5.2 - 5.4 illustrate the response of the observer to bad initial estimates for x2 and x4. In each of these three figures, only estimates of x2 and x4 are plotted since the remaining two state variables (x1 and x3) are reconstructed exactly. This follows since x1 and x3 are also output variables (cf. equation (5.6)). These figures show that the errors in the state estimates decrease more rapidly when observers with smaller eigenvalues are used.

In Figure 5.5 the model response to a step change in d1 is plotted, while Figures 5.6 - 5.8 show the reconstructed states $\hat{x}2$ and $\hat{x}4$ for the case where the observer was not driven by the step disturbance. State variable x2 is reconstructed exactly but $\hat{x}4$ deviates somewhat from x4. By comparing Figures 5.6 - 5.8, it can be seen that smaller eigenvalues reduce this discrepancy.

An unmeasured step change in d2 again gave an excellent estimate of x2, but a significant error in the estimate of x4 resulted. Figure 5.9 shows the actual response of the model and the reconstructed states $\hat{x}2$ and $\hat{x}4$ are illustrated in Figures 5.10 - 5.12. In this case the smaller eigenvalues change the shape of the $\hat{x}4$ curve but do not appear to reduce the final offset.

TABLE 5.1

DETAILS OF FIGURES 5.1 - 5.12: MUNRO'S EXAMPLE

Figure	Observer Eigenvalues	Initial States	Initial State Estimates	Disturbances	Disturbance is Measured?
5.1	Actual response	$x1(0) = 1.0$	-	None	-
5.2	0.6771	$x1(0) = 1.0$	$\hat{x}2 = 1.0$ $\hat{x}4 = 1.0$	None	-
5.3	0.0202	$x1(0) = 1.0$	$\hat{x}2 = 1.0$ $\hat{x}4 = 1.0$	None	-
5.4	2.26×10^{-6}	$x1(0) = 1.0$	$\hat{x}2 = 1.0$ $\hat{x}4 = 1.0$	None	-
5.5	Actual response	Zero	-	$d1 = 1.0$	-
5.6	0.6771	Zero	Correct	$d1 = 1.0$	No
5.7	0.0202	Zero	Correct	$d1 = 1.0$	No
5.8	2.26×10^{-6}	Zero	Correct	$d1 = 1.0$	No
5.9	Actual response	Zero	-	$d2 = 1.0$	-
5.10	0.6771	Zero	Correct	$d2 = 1.0$	No
5.11	0.0202	Zero	Correct	$d2 = 1.0$	No
5.12	2.26×10^{-6}	Zero	Correct	$d2 = 1.0$	No

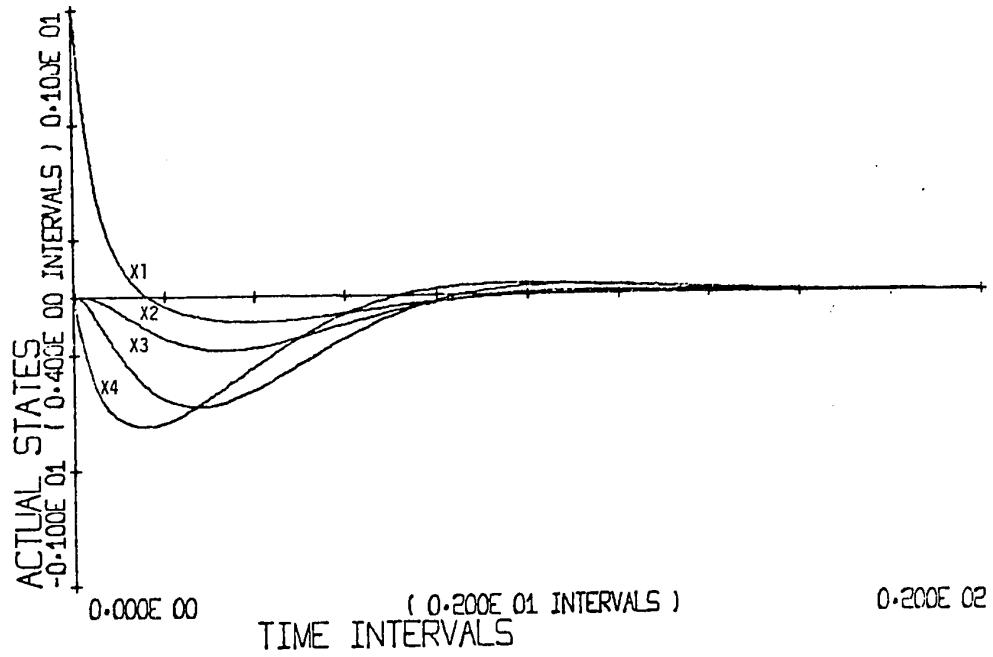

FIGURE 5.1 Actual Response for X1(0) = 1.0

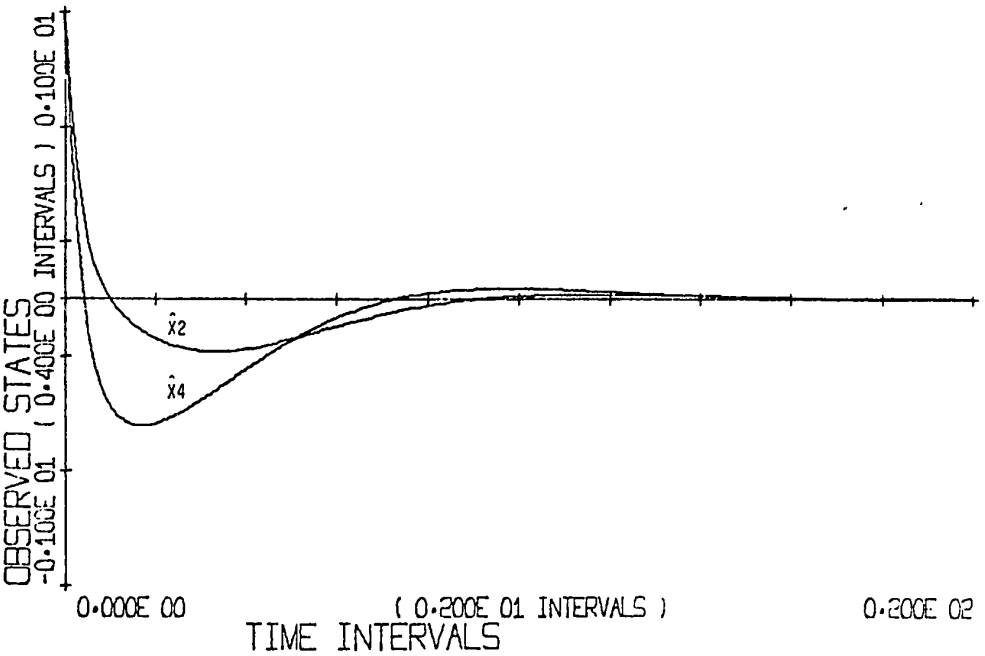

FIGURE 5.2 Observer Response for X1(0) = 1.0 With Incorrect Initial State Estimates (Observer Eigenvalues = 0.6771)

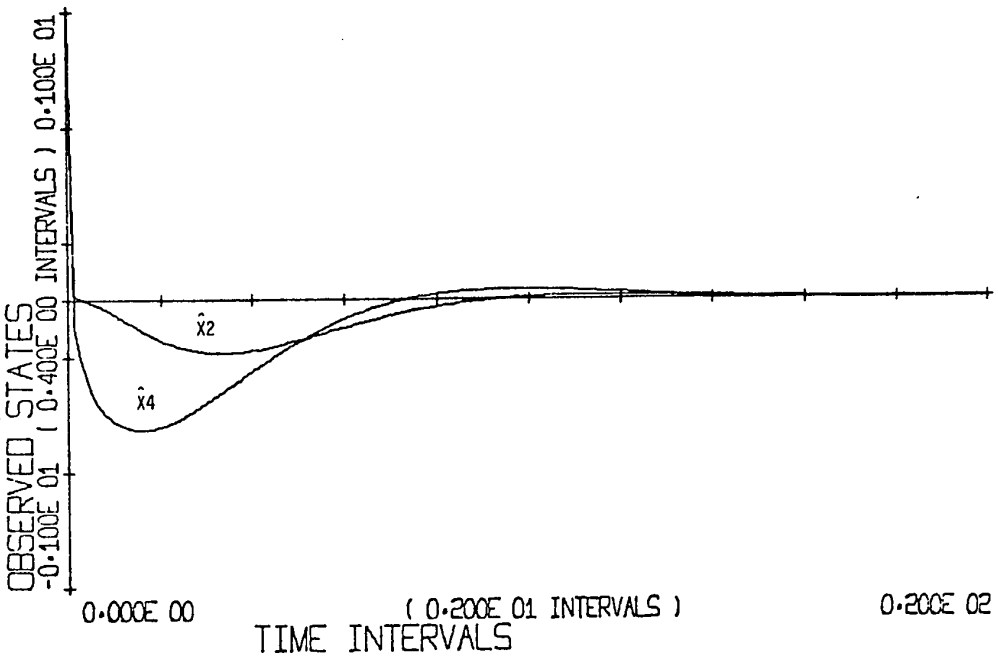

FIGURE 5.3 Observer Response for X1(0) = 1.0 With Incorrect Initial State Estimates (Observer Eigenvalues = 0.0202)

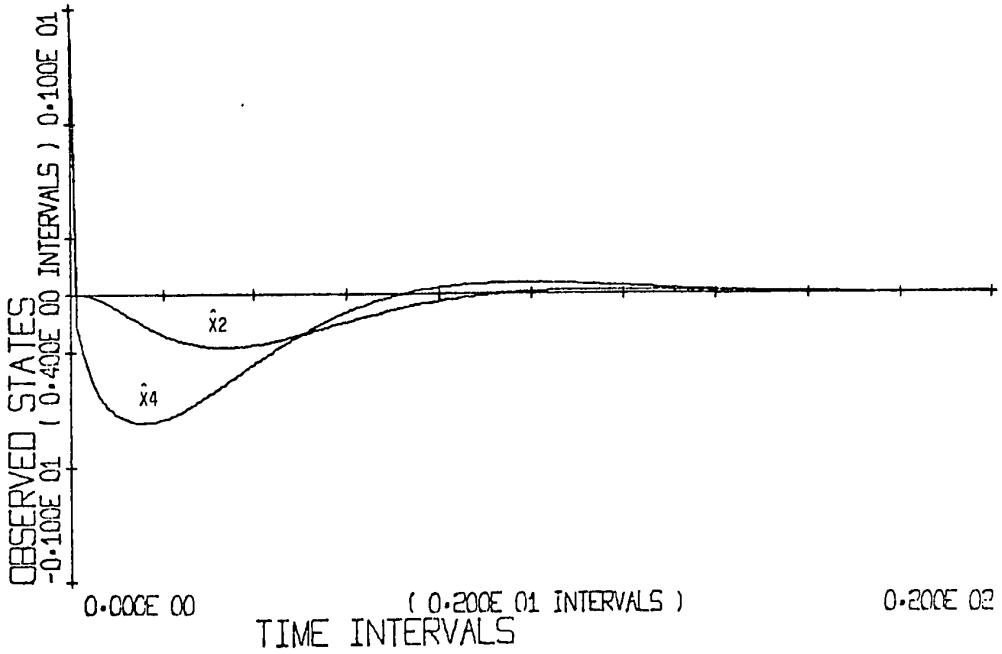

FIGURE 5.4 Observer Response for X1(0) = 1.0 With Incorrect Initial State Estimates (Observer Eigenvalues = $2.26X10^{-}$)

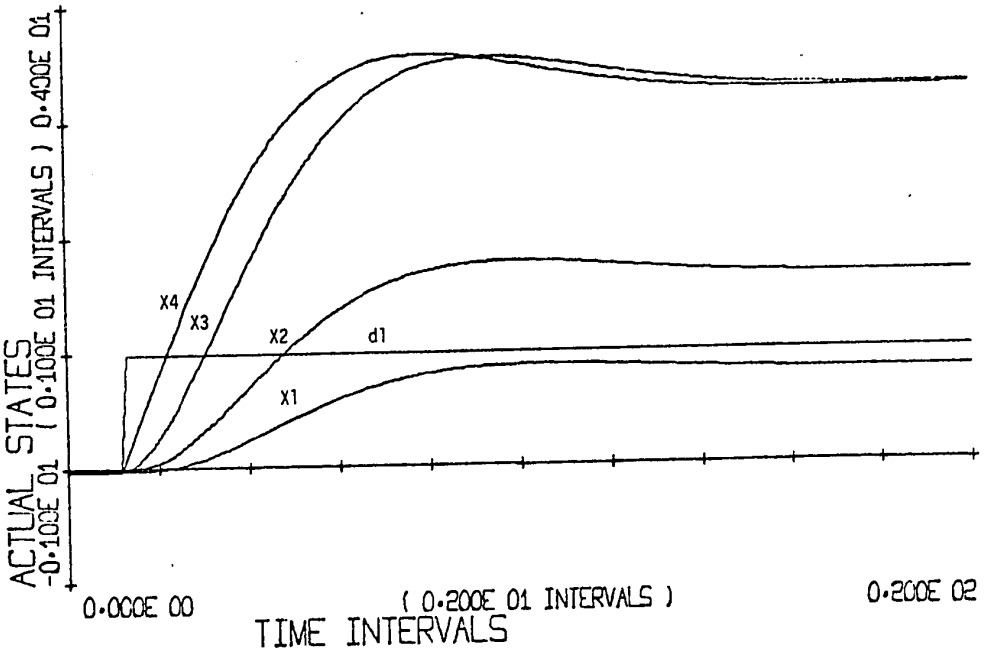

FIGURE 5.5 Actual Response for a Step Change in d1

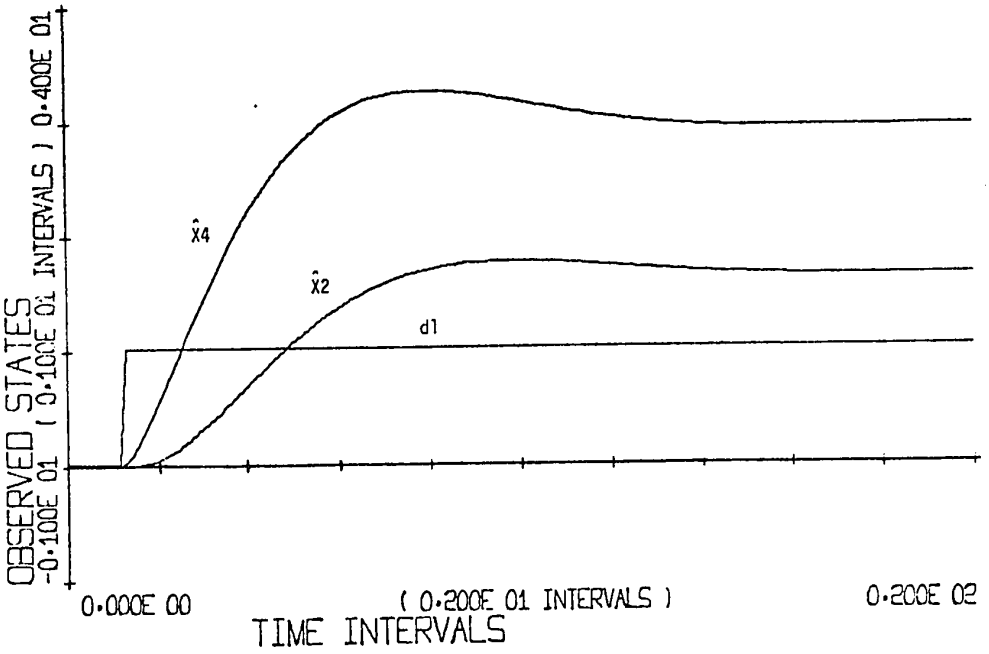

FIGURE 5.6 Observer Response for an Unmeasured Step Change in d1
(Observer Eigenvalues = 0.6771)

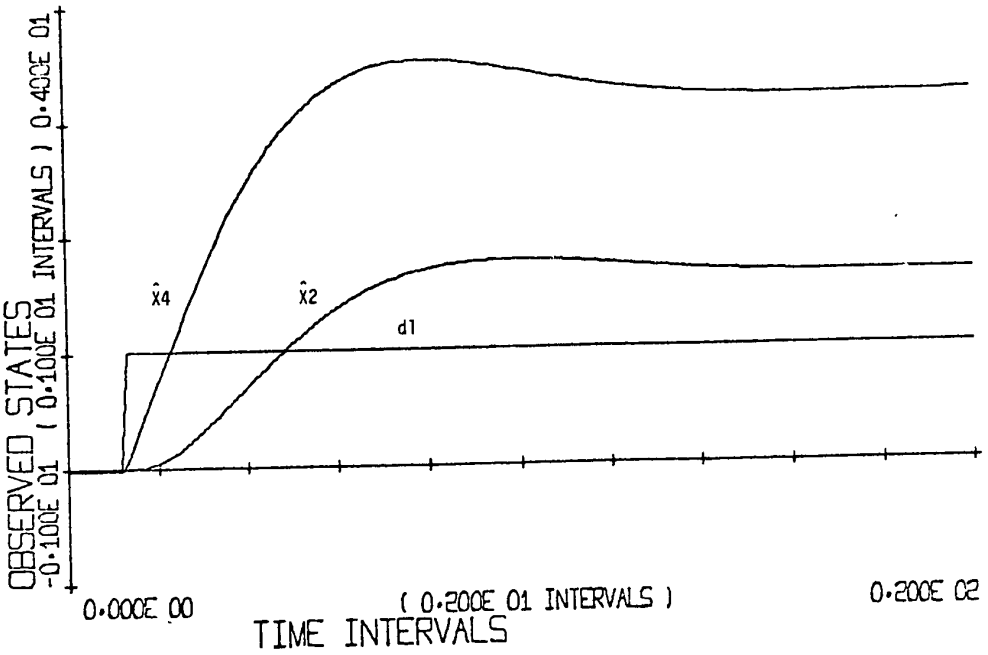

FIGURE 5.7 Observer Response for an Unmeasured Step Change in d1
(Observer Eigenvalues = 0.0202)

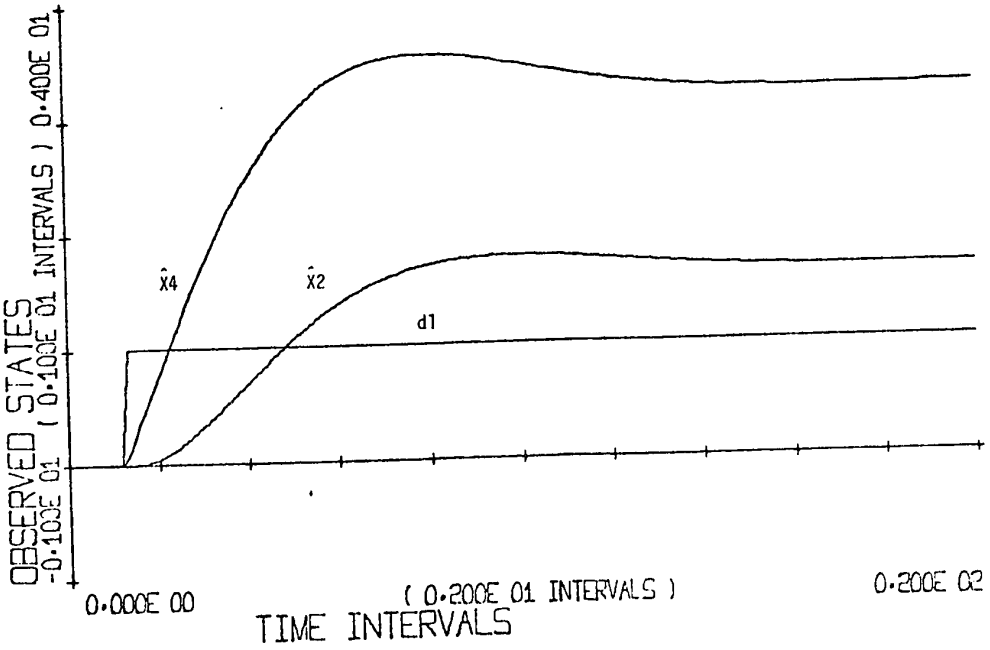

FIGURE 5.8 Observer Response for an Unmeasured Step Change in d1
(Observer Eigenvalues = $2.26X10^{-11}$)

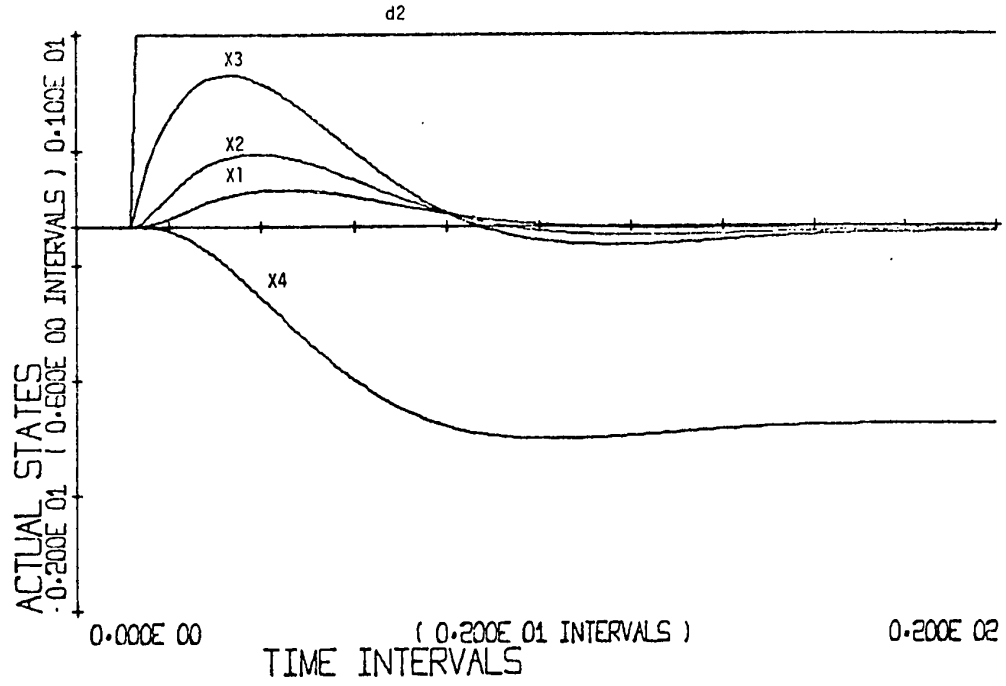

FIGURE 5.9 Actual Response for a Step Change in d2

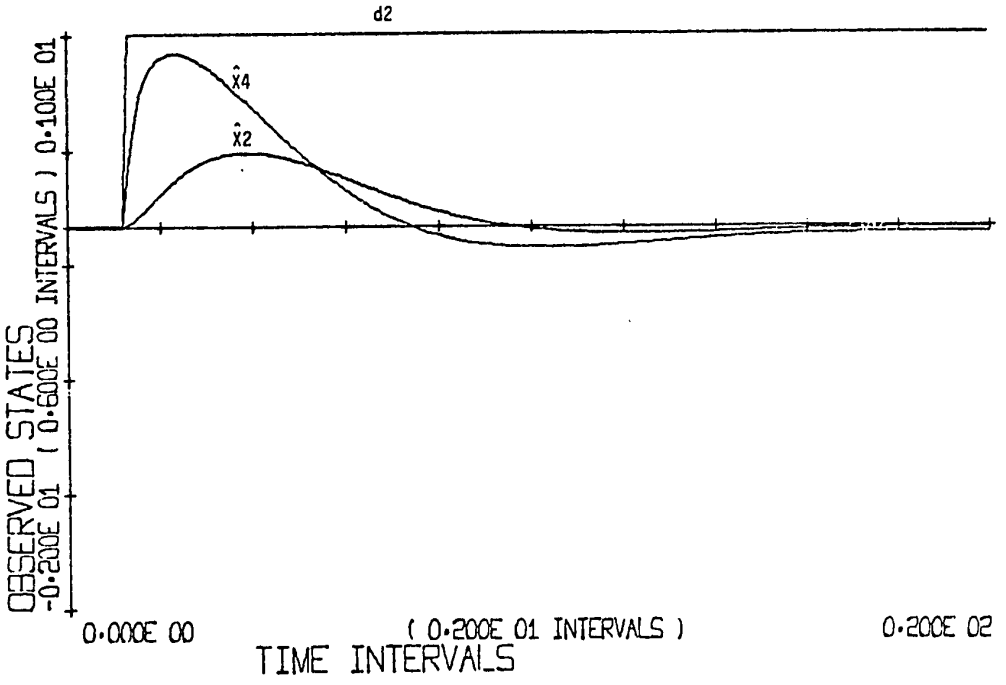

FIGURE 5.10 Observer Response for an Unmeasured Step Change in d2
(Observer Eigenvalues = 0.6771)

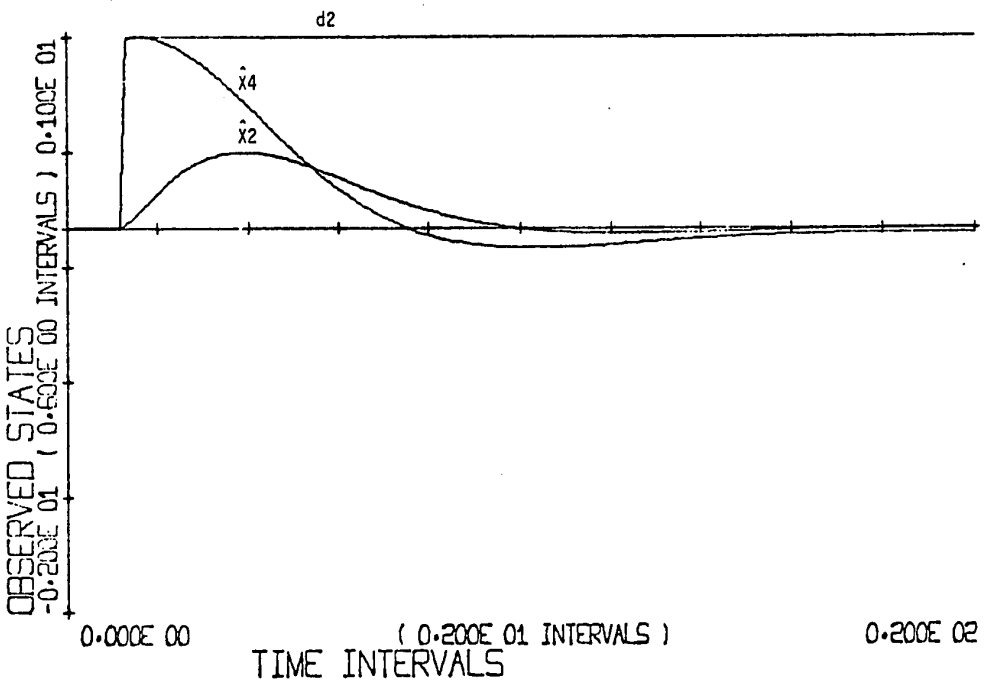

FIGURE 5.11 Observer Response for an Unmeasured Step Change in d2
(Observer Eigenvalues = 0.0202)

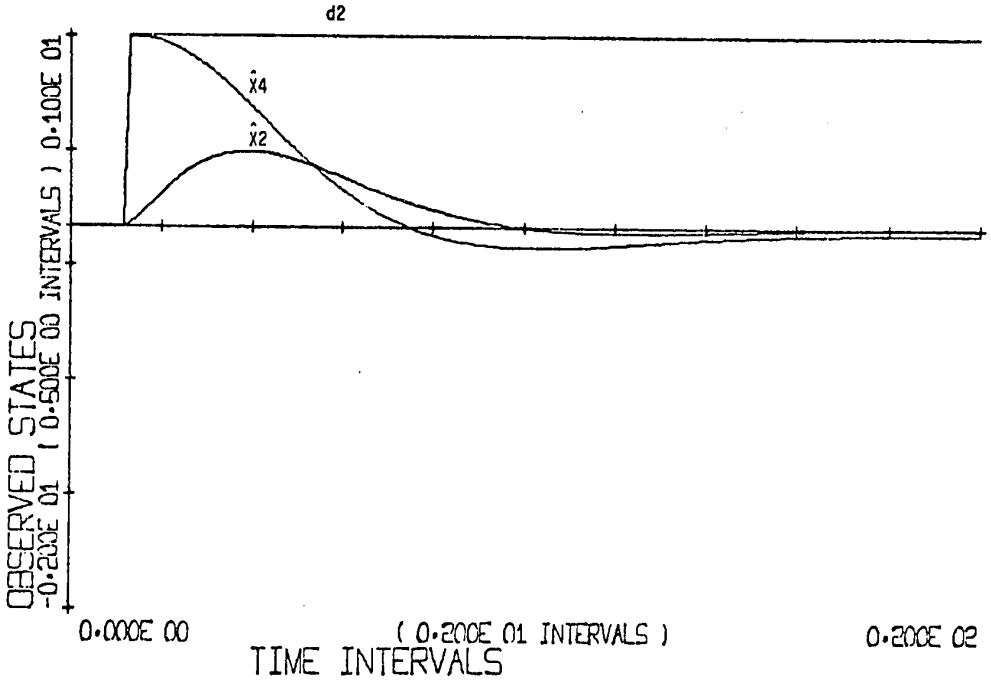

FIGURE 5.12 Observer Response for an Unmeasured Step Change in d2
(Observer Eigenvalues = 2.26×10^{-6})

The results obtained with incorrect initial state estimates are as expected. However, the theory does not predict either the effect of unmeasured disturbances or the best eigenvalues (large or small) which should be used when such step changes occur. The results here indicate that the effect of these unmeasured disturbances depends on the specific disturbance and that changes in the eigenvalues may improve one situation but not the other. Exactly the same conclusions were drawn from the corresponding study of the continuous system.

5.3 COMPUTER PROGRAMS FOR THE SIMULATION AND EXPERIMENTAL STUDIES

The computer programs used were basically those described in Chapter 3 for the Kalman filter studies. The simulation program, SPECS, was modified to include the Luenberger observer for state estimation. Process and measurement noise were optional for the observer but otherwise the program remained unchanged. An additional program, LUEN, was written to perform the observer design calculations off-line. The experimental programs were simply adapted to include the Luenberger observer option, and the plotting routines were used as before to present the results.

5.4 EVAPORATOR SIMULATION STUDY 1: W1, W2, C2 MEASURED

In the first simulation study for the double effect evaporator, three states (W1, W2 and C2) were measured and a second order observer was used to reconstruct the entire state vector, $\underline{x}$, (i.e. the remaining states, C1 and H1).

Several observer designs for a range of observer eigenvalues successfully reconstructed the states in both open and closed loop runs where there was no noise present, no unmeasured disturbances and

no incorrect initial conditions. Referring back to the theoretical analysis in Chapter Four, it is obvious that the state reconstruction should be exact for these conditions. The results presented here illustrate the performance of the observer when these ideal conditions no longer hold; the details of the figures are presented in Table 5.2.

5.4.1 Effect of Incorrect Initial Estimates

Small observer eigenvalues were successfully employed in open-loop (see Figure 5.16) and closed-loop (Figure 5.17) runs with incorrect initial state estimates. When larger eigenvalues were used, the observer was still effective but the response to the initial error was slower. With small observer eigenvalues in the closed-loop control scheme, the response time could be reduced and oscillations were only introduced when the eigenvalues became as small as 10^{-5} (see Figure 5.13).

The results here were as expected with an eventual breakdown in the observer estimates which was attributed to numerical difficulties due to the very small eigenvalues. With even smaller eigenvalues than those used in Figure 5.13 the oscillations became very bad and the general trend of the state variables was not controlled.

5.4.2 Effect of Unmeasured Feed Flow Disturbances

Figure 5.14 shows the response of an observer with large eigenvalues to an open loop run which included a nonzero initial value for C2 and two unmeasured disturbances in feed flow. As expected, the three measured states are reconstructed exactly. The C1 curve is estimated quite accurately but $\hat{H}1$ (i.e. $\hat{T}1$) deviates from the true value (the actual curves are also plotted for comparison). A closed loop run subject to the same initial conditions and disturbances was also made

TABLE 5.2

DETAILS OF FIGURES 5.13 - 5.20: SIMULATION STUDY 1

For the open loop runs the actual response is plotted for a comparison with the observer response. The "ideal" closed-loop curves with exact estimates of the states are also plotted for the runs with optimal feedback control. Further details are tabulated below and the numerical values of the elements of the $\underline{\underline{E}}$ and $\underline{\underline{C}}$ matrices can be found in the appendix.

A - denotes an observer which has knowledge of a step disturbance.

B - denotes an observer which is unaware of a step disturbance.

Figure	Control	States Displayed in Figures	Observer Used	$\underline{\underline{E}}$	$\underline{\underline{C}}$	Initial State	Initial State Estimate	Noise	Step Disturbance
5.13	FB	Actual	Observer 1A	$\underline{E16}$	$\underline{C1}$	C2 = -30%	$\hat{C}1$ = -30% $\hat{H}1$ = -30%	-	± 20% F
5.14	OL	Estimated	Observer 2B	$\underline{E11}$	$\underline{C1}$	C2 = -30%	Correct	-	± 20% F
5.15	FB	Actual	Observer 2B	$\underline{E11}$	$\underline{C1}$	C2 = -30%	Correct	-	± 20% F
5.16	OL	Estimated	Observer 3B	$\underline{E2}$	$\underline{C1}$	C2 = -30%	$\hat{C}1$ = -30%	-	± 20% F
5.17	FB	Actual	Observer 3B	$\underline{E2}$	$\underline{C1}$	C2 = -30%	$\hat{C}1$ = -30% $\hat{H}1$ = -30%	-	± 20% F
5.18	OL	Estimated	Observer 2B Observer 3B	$\underline{E11}$ $\underline{E2}$	$\underline{C1}$ $\underline{C1}$	Zero	Correct	-	-30% CF
5.19	FB	Actual	Observer 2A	$\underline{E11}$	$\underline{C1}$	C2 = -30%	$\hat{C}1$ = -30%	yes	± 20% F
5.20	FB	Actual	Observer 3A	$\underline{E2}$	$\underline{C1}$	C2 = -30%	$\hat{C}1$ = -30%	yes	± 20% F

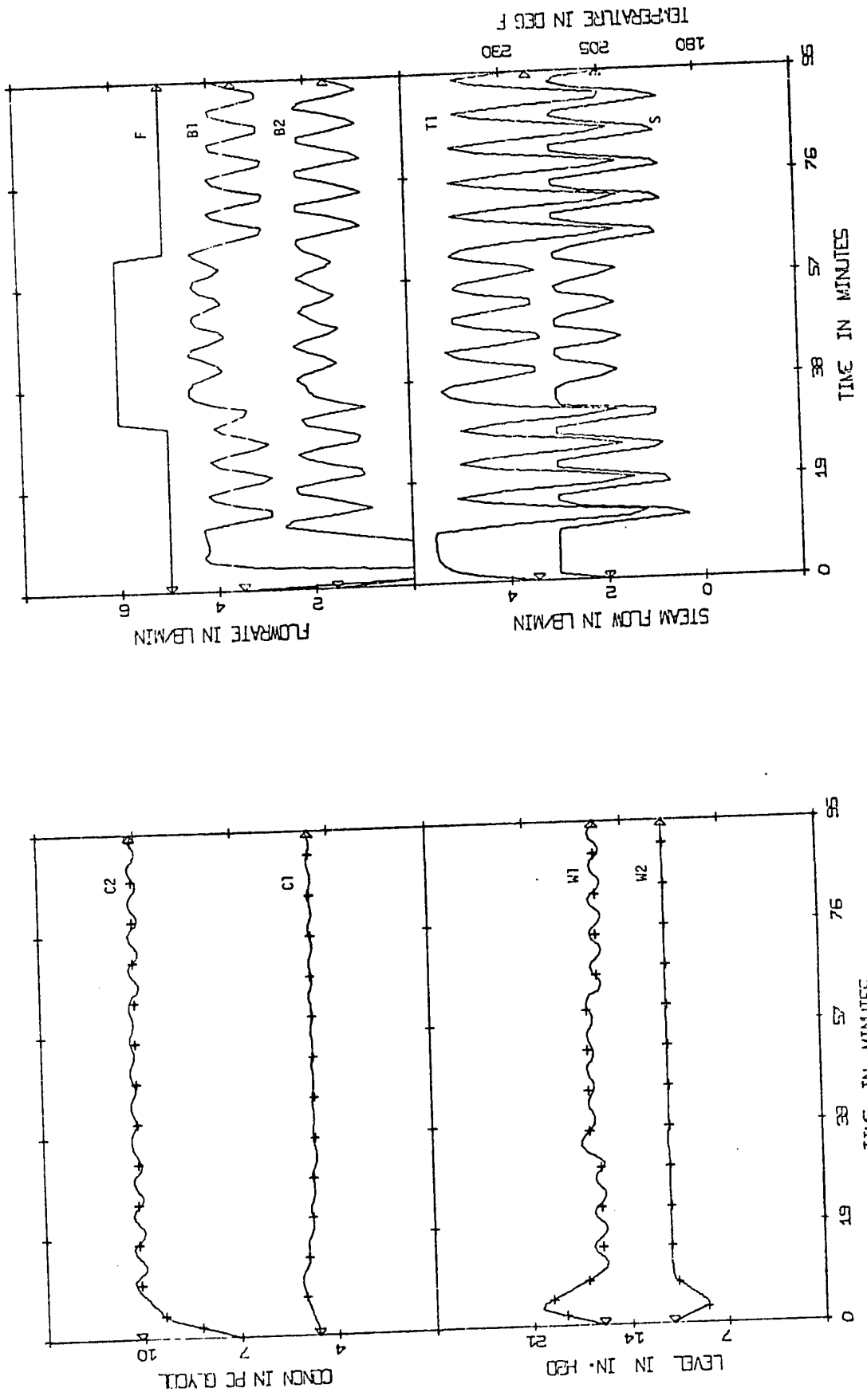

FIGURE 5.13 (SIM/±20%F/FB) +++ Ideal Case, —— Control Based on Observer 1A Estimates

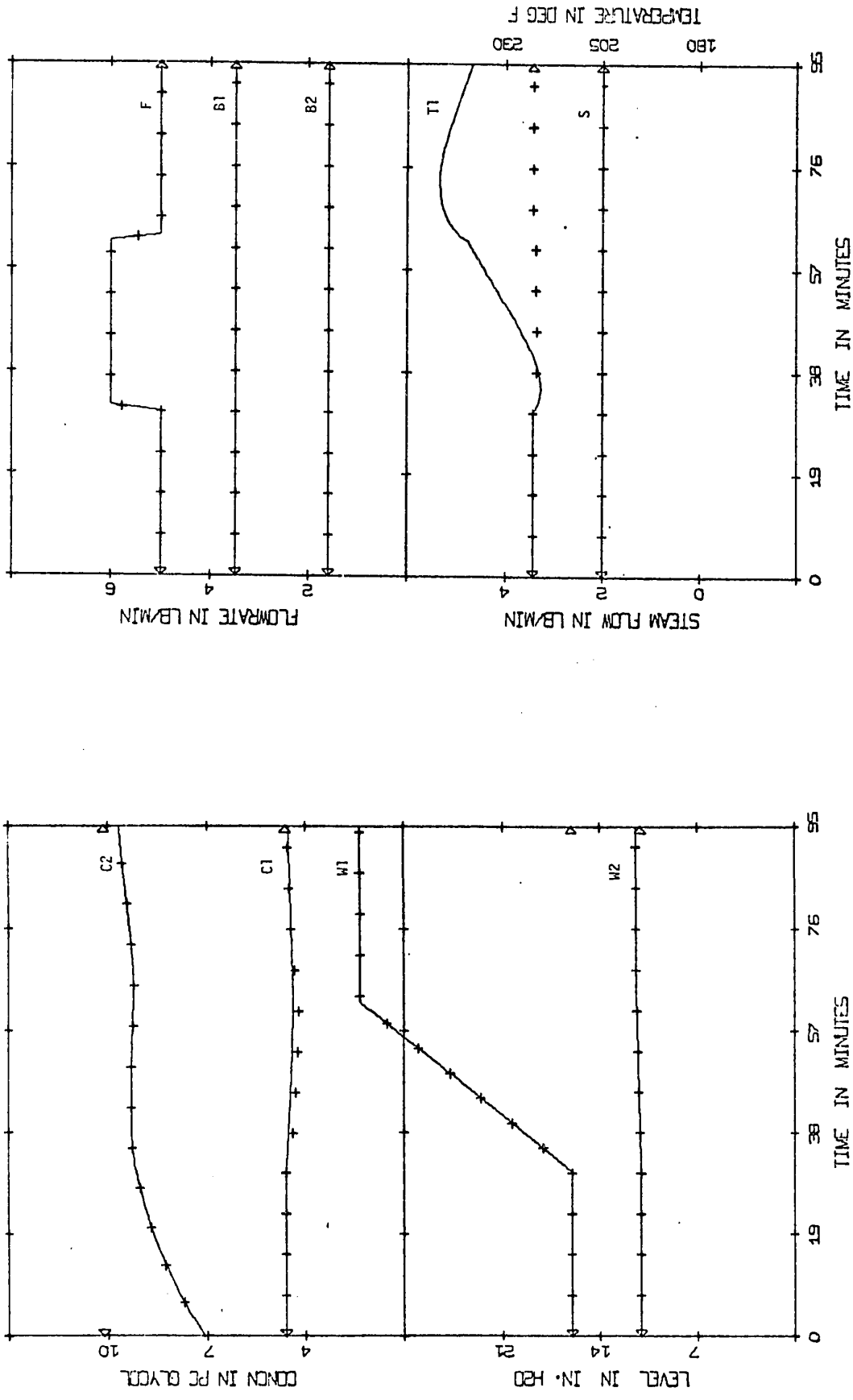

FIGURE 5.14 (SIM/±20%F/OL) +++ Actual States, —— Estimates from Observer 2B

(Figure 5.15) using optimal feedback control based on the observer estimates ($\underline{K}_{FB}$ is given in the Appendix). The same observer was used for the closed loop run and the actual controlled states are illustrated together with the ideal curves (i.e. deterministic system with exact states estimates) in Figure 5.15. The results show that the system responds to the initial offset quite quickly and the "unseen" feed flow disturbances do not upset the process unduly.

The runs in Figures 5.14 and 5.15 were then repeated using faster (i.e. smaller) observer eigenvalues. In the open loop run (Figure 5.16), the C1 and H1 curves show spikes due to the "unseen" disturbances and in the case of the C1 estimate there is a considerable offset between the step changes. It is noteworthy that for this run there was also a bad initial estimate for C1 but the fast eigenvalues deal with the situation very quickly and effectively, as can be seen in the C1 and H1 curves. The results of the closed loop run are shown in Figure 5.17. The offset due to the observer in the open loop run obviously has a bad effect on the control of W1 and C2, particularly.

It would appear then that for "unseen" disturbances in feed flow, the larger (slower) eigenvalues are better. Again it should be noted that the run shown in Figure 5.17 includes bad initial estimates for both C1 and H1 but since the observer responds so quickly this has a negligible effect on the closed loop response.

5.4.3 Effect of Unmeasured Feed Concentration Disturbances

Figure 5.18 shows the actual open loop response of the model to a 30% step down in feed concentration. Also plotted are the reconstructed states using two observer designs - one with fast eigenvalues (Observer 3B) and one with slow eigenvalues (Observer 2B). The

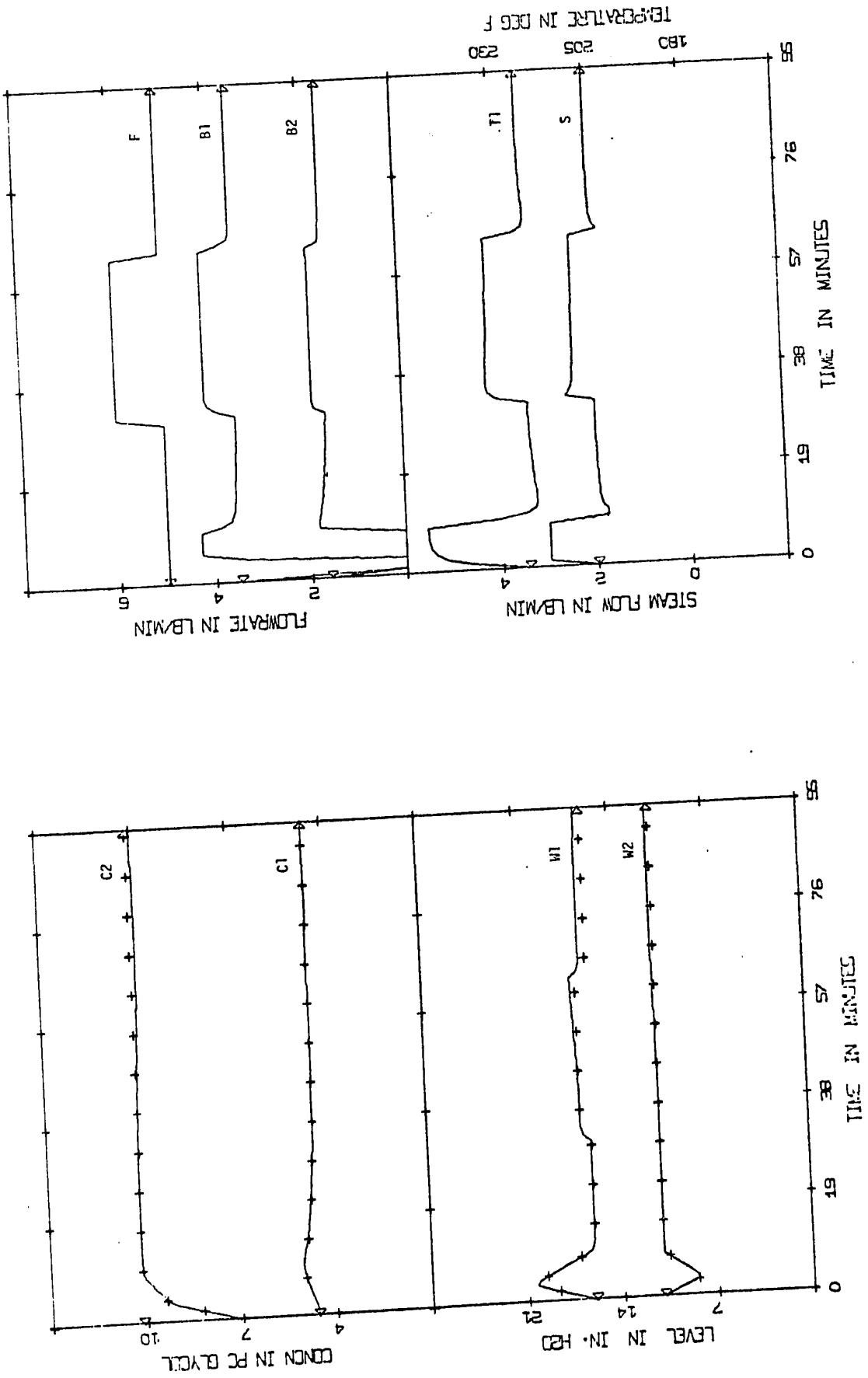

FIGURE 5.15 (SIM /±20%F/FB) +++ Ideal Case —— Control Based on Observer 2B Estimates

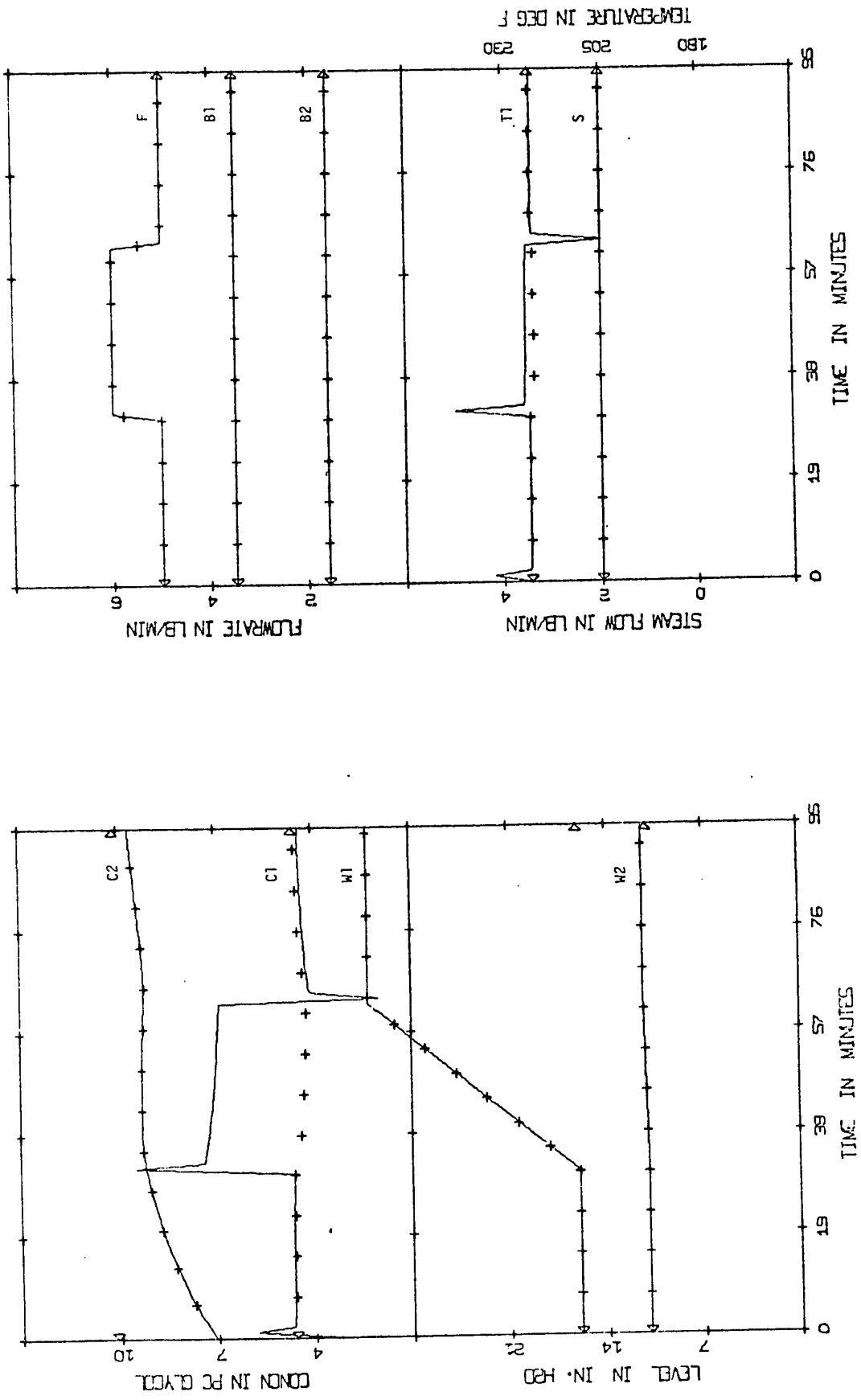

FIGURE 5.16 (SIM/±20%F/OL) +++ Actual States, —— Estimates from Observer 3B

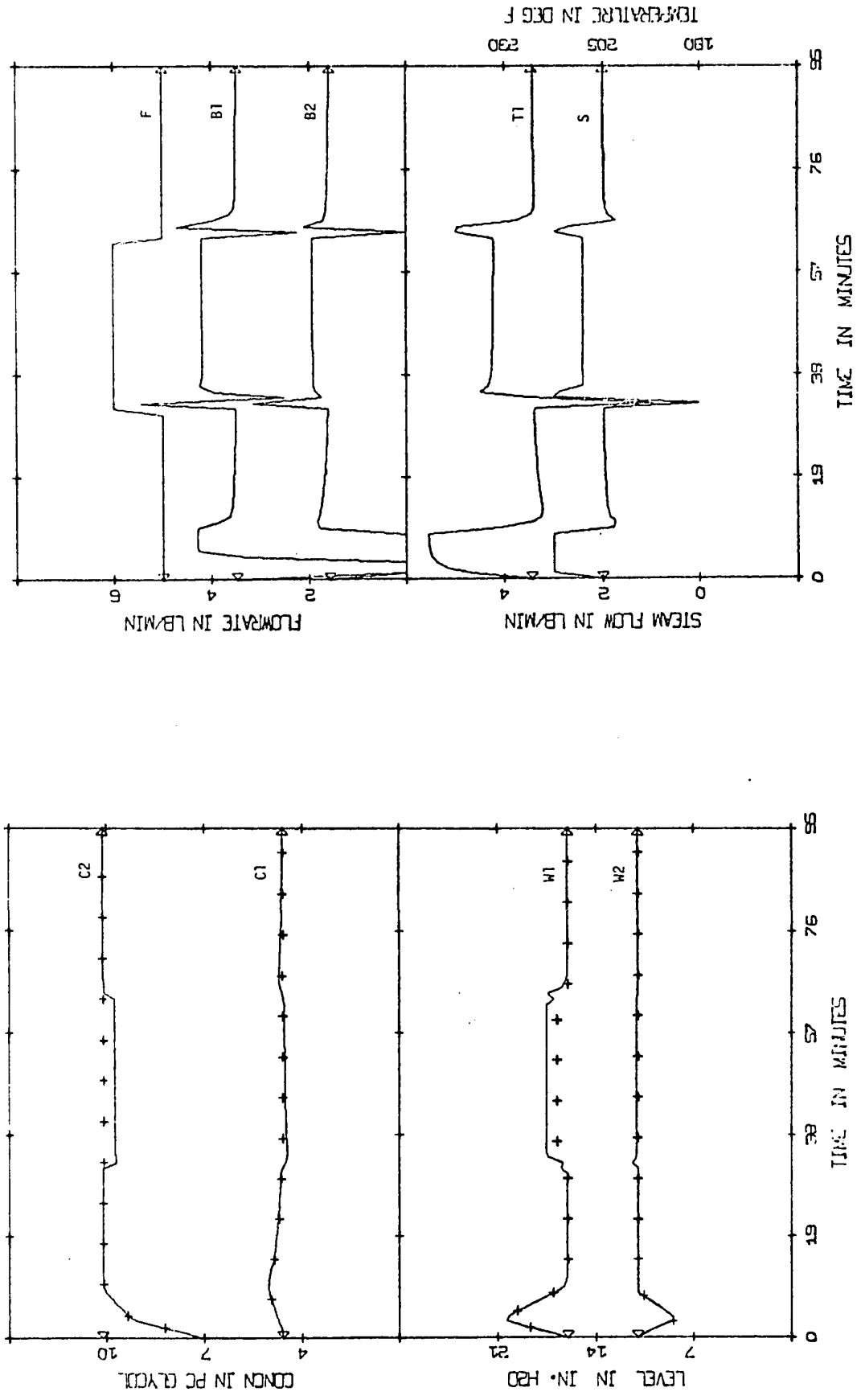

FIGURE 5.17 (SIM/±20%F/FB) +++ Ideal Case, —— Control Based on Observer 3B Estimates

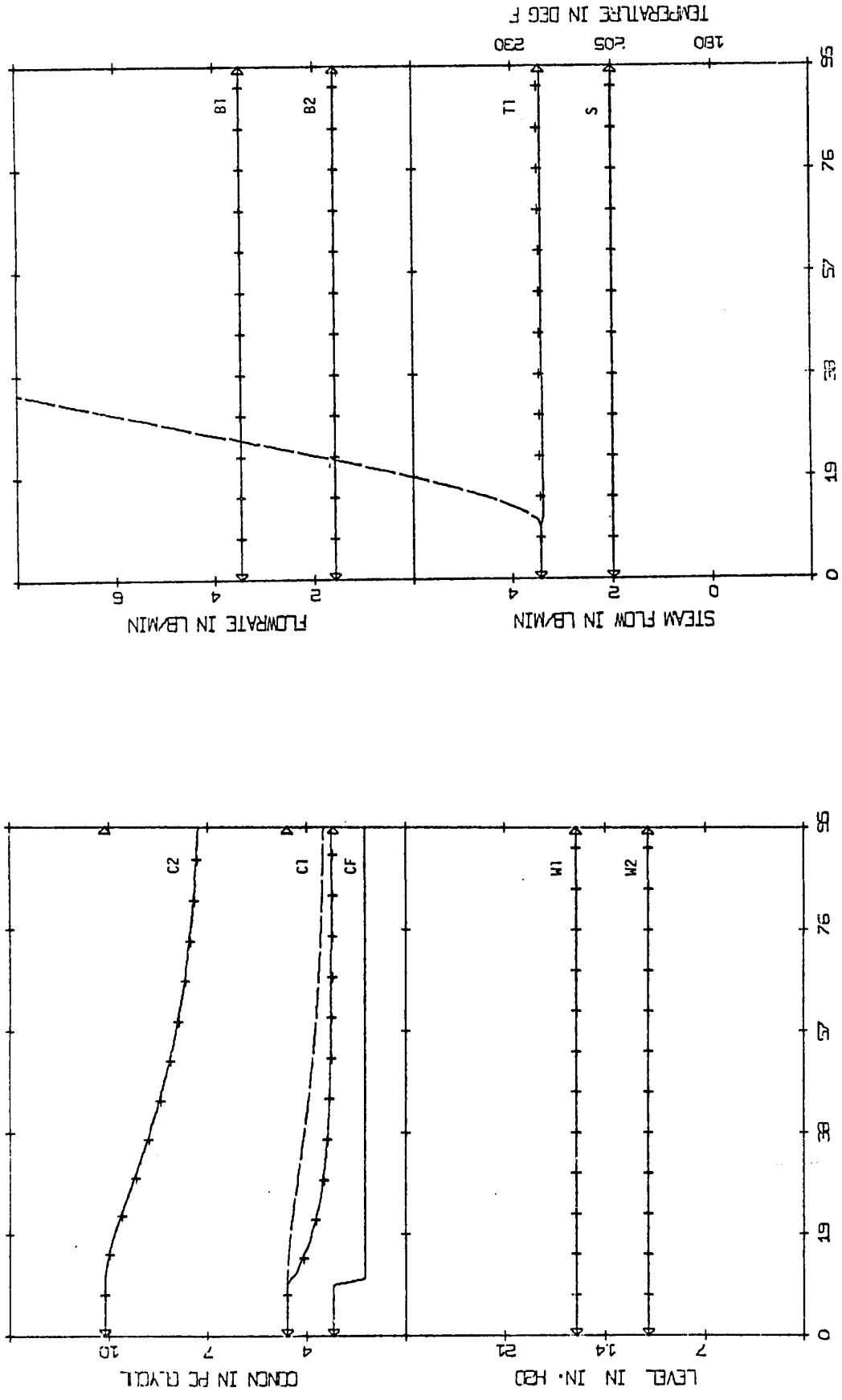

FIGURE 5.18 (SIM/-30%CF/OL) +++ Actual States, --- Estimates from Observer 2B, ——Estimates from Observer 3B

observer with slow eigenvalues does not respond very well to the unmeasured disturbance. The C1 curve is not very good and the H1 curve is very poor resulting in a final estimate of about 1.6 times the actual steady state value. The fast eigenvalues allow the observer to reconstruct the states almost exactly. This implies that fast eigenvalues are better for a feed composition disturbance which is contrary to the conclusions reached in the previous section for feed flow disturbances.

5.4.4 Observer Design Considerations

In practical situations there are liable to be incorrect initial estimates and "unseen" disturbances so that it is desirable to design an observer which is satisfactory for all these situations. As was seen in the previous sections, there is no observer which is best for all conditions; consequently some sort of compromise in the design is necessary. In view of this problem, an investigation of the steady state errors in the observer estimates was carried out in an attempt to find a satisfactory design. This design should give small observer errors for all types of unmeasured disturbances and should also respond quickly to incorrect initial state estimates.

Referring to the theory in section 4.3.3, it can be seen that the steady state error in observing the states can be calculated for any observer design and for each of the three types of disturbances (F, CF and HF). A computer program was written to perform this task and the steady state errors for three typical "unseen" disturbances were tabulated as a function of the observer eigenvalues. A study was also made to determine if different $\underline{\underline{C}}$ matrices (coefficient matrix of the model outputs in the dynamic observer equation) would affect the observer errors for "unseen" disturbances.

The disturbances considered were:

(a) a +20% step change in feed flowrate,

(b) a -30% step change in feed concentration, and

(c) a +20% step change in feed enthalpy.

The results of this study are presented in Table 5.3. The $\underline{\underline{C}}$ matrix used in this study was $\underline{\underline{C1}}$:

$$\underline{\underline{C1}} = \begin{bmatrix} 1 & 1 & 1 \\ 1 & 1 & 1 \end{bmatrix}$$

Referring to Table 5.3 it is difficult to choose the 'best' set of observer eigenvalues. Faster eigenvalues are more satisfactory for disturbances (b) and (c) whereas the slowest eigenvalues are best for disturbance (a). The best compromise seems to be the eigenvalue set: 0.7, 0.8. This design gives reasonably small errors for disturbances (b) and (c) and although the estimate of C1 for disturbance (a) is not very good, it is desirable that the observer eigenvalues should not be too large in order to achieve a quick response to incorrect initial state estimates. Another reason for not using the largest eigenvalues is that, for the evaporator, disturbance (b) is the one which is most difficult to detect and is therefore the most likely "unseen" disturbance.

Using the largest set of eigenvalues in Table 5.3, the elements of the $\underline{\underline{C}}$ matrix were varied to discover the effect of this matrix on the steady state estimation error for "unseen" disturbances.

As in the previous study, regarding the observer eigenvalues, it is very difficult to see, a priori, how (or if) changes in the

TABLE 5.3

DEPENDENCE OF STEADY STATE ESTIMATION ERRORS ON THE $\underline{\underline{E}}$ MATRIX OF THE LUENBERGER OBSERVER

Eigenvalues of the $\underline{\underline{E}}$ Matrix	Unmeasured Step Disturbance					
	(a) +20% feed flow		(b) -30% feed concentration		(c) +20% feed enthalpy	
	steady state error (%)		steady state error (%)		steady state error (%)	
	$\hat{C}1$	$\hat{H}1$	$\hat{C}1$	$\hat{H}1$	$\hat{C}1$	$\hat{H}1$
0.945, 0.940	2	21	4	168	7	-62
0.7, 0.8	29	8	14	-4	-4	-3
0.5, 0.6	46	0.4	5	-0.1	-6	-2
0.3, 0.4	54	0.1	2	-0.02	-7	-2
0.1, 0.2	59	0.6	0.1	-0.2	-8	-2
0.001, 0.002	62	1	-0.8	-0.4	-8	-2

Note: the steady state error vector is defined as: $\underline{\Delta x}_{ss} = \underline{\hat{x}}_{xx} - \underline{x}_{ss}$

TABLE 5.4

DEPENDENCE OF STEADY STATE ESTIMATION ERRORS ON THE $\underline{\underline{C}}$ MATRIX OF THE LUENBERGER OBSERVER

$\underline{\underline{C}}$ matrix	Unmeasured Step Disturbance					
	(a) +20% feed flow		(b) -30% feed concentration		(c) +20% feed enthalpy	
	steady state error (%)		steady state error (%)		steady state error (%)	
	$\hat{C}1$	$\hat{H}1$	$\hat{C}1$	$\hat{H}1$	$\hat{C}1$	$\hat{H}1$
C1	2	21	4	168	6	-62
C11	-88	-620	56	293	0.5	-21
C12	6	15	78	369	3	-4
C13	-2	55	-2	154	10	-67
C14	-0.9	56	1	161	8	-65
C15	2	21	0.9	161	8	-65
C16	13664	36189	-5951	-15801	-1796	-4771
C3	2	21	4	168	6	-62
C17	-49	263	43	-15	0.08	-31
C18	-41	206	40	13	-0.1	-34

Note: the steady state error vector is defined as: $\underline{\Delta x}_{ss} = \underline{\hat{x}}_{ss} - \underline{x}_{ss}$

elements of the $\underline{\underline{C}}$ matrix will affect the observer estimates. It was therefore decided to investigate the situation systematically by changing the weighting of various columns of $\underline{\underline{C}}$ and also by increasing all the elements of the $\underline{\underline{C}}$ matrix. The weighting on two specific elements was also increased, in turn, to see if this would produce any improvements.

The results are presented in Table 5.4. It appears that, although changes in the $\underline{\underline{C}}$ matrix do affect the steady state estimation errors quite significantly, there is no $\underline{\underline{C}}$ matrix which will give better results, for all situations, than $\underline{\underline{C1}}$. Simulation studies (not presented) indicated that changes in the $\underline{\underline{C}}$ matrix had very little effect on the dynamic response of the observer. The numerical values of the elements of the $\underline{\underline{C}}$ matrices used can be found in the appendix.

5.4.5 Effect of Process and Measurement Noise

The Luenberger observer was not originally designed for stochastic processes [3] but it was of interest in this study to see how process and measurement noise would affect the performance of the observer. Several runs with noise were made using the observer for both open and closed loop simulations. In general the observer did not respond well to noise and only the observers with large eigenvalues provided a satisfactory estimate.

Figures 5.19 and 5.20 compare the performance of the observer with 10% noise levels (process and measurement noise) with the ideal case of perfect, noise-free state estimates. The runs began with C2 initially 30% below the normal steady state value and with an incorrect initial estimate for C1. The observer estimates were used in the optimal controller and the curves show the actual controlled state

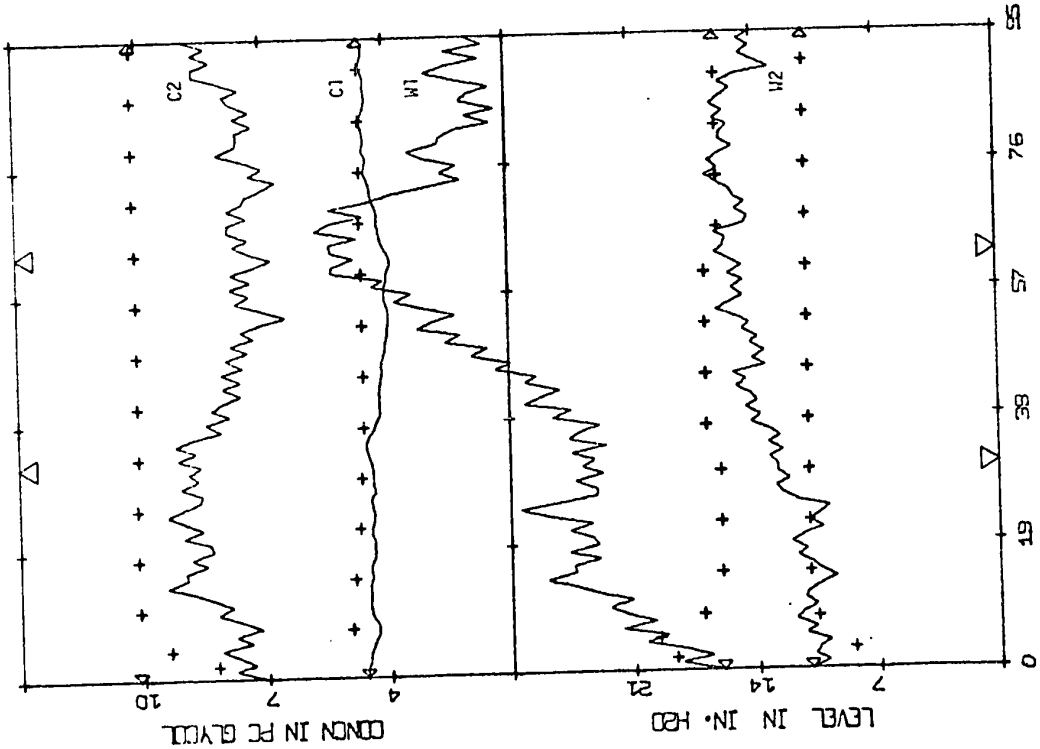

FIGURE 5.20 (SIM/±20%F/FB) +++ Ideal Case, —— Control Based on Observer 3A Estimates

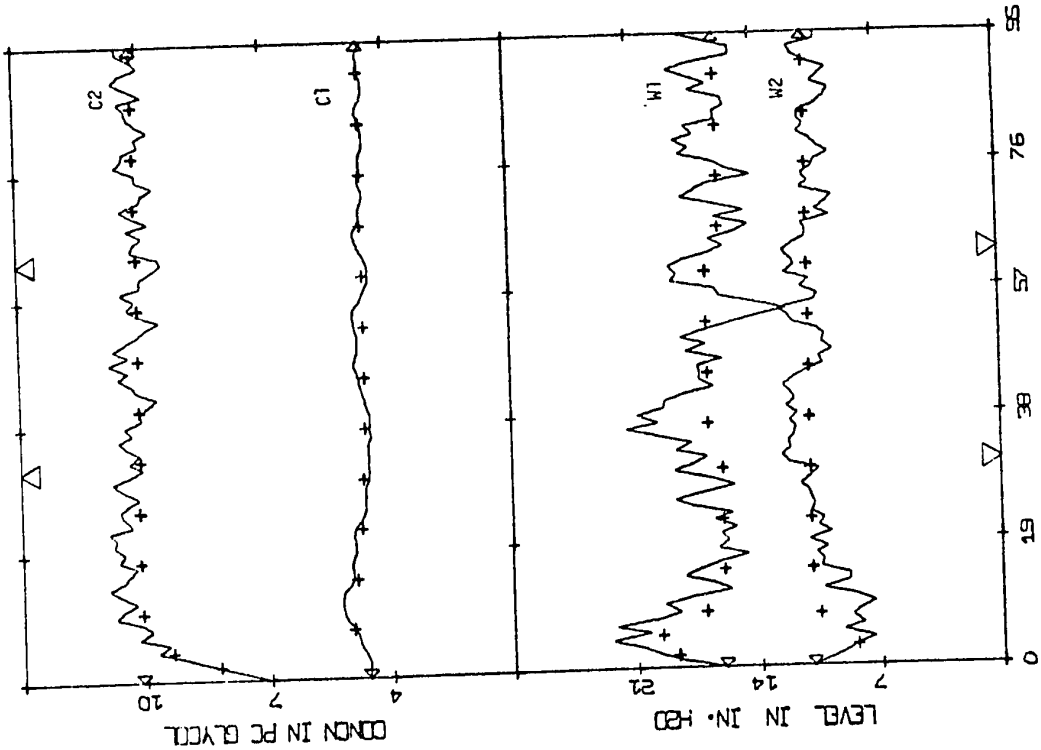

FIGURE 5.19 (SIM/±20%F/FB) +++ Ideal Case, —— Control Based on Observer 2A Estimates

variables before measurement noise was added. Two step disturbances in feed flow were applied. The observer eigenvalues used in Figure 5.19 were large and although the curves are very noisy the general trend seems to be controlled. However, in Figure 5.20 where smaller eigenvalues were used, the control is very poor and quite unacceptable.

It can be concluded that, as expected, the deterministic Luenberger observer is not a very satisfactory method of state estimation for stochastic systems, but where noise is encountered better results can be achieved with larger rather than smaller observer eigenvalues. In this case, a better approach would be to use either the estimator proposed by Aoki and Huddle [4], which is an extension of the observer for stochastic systems, or the Kalman filter used in the first part of this thesis.

5.5 EVAPORATOR SIMULATION STUDY 2: W1, H1, W2 MEASURED

For the second simulation study it was assumed that state variables C1 and C2 could not be measured so that the observer was again second order and was driven by the outputs W1, H1 and W2. Many problems were encountered with this system and although the reasons are not fully understood, it is believed that these difficulties are due to the system being "marginally" observable.

Before discussing this point further, the results for this system are briefly summarized.

The first problem was that even for perfect conditions (i.e. correct initial state estimates, no noise and no unmeasured disturbances) an oscillatory closed loop response was observed with an observer design using eigenvalues of 0.1, 0.2. These eigenvalues are not very small and it is surprising that the control is so poor. Strange results

were also encountered when the effect of incorrect initial estimates was investigated. For bad initial estimates of C2 the observer behaved normally with smaller eigenvalues giving a faster response. However, for bad initial estimates of C1 only very large eigenvalues would give stable observations and hence the response was slow. Runs with "unseen" disturbances were all unsatisfactory due to very sharp peaks in the observed curves.

In Luenberger's original paper [3] it was stated that further study would be required for "marginally" observable systems. The observability of the system was checked by applying a standard test [5, p. 401]. This meant constructing the matrix $\underline{\underline{S}}$:

$$\underline{\underline{S}} = [\underline{\underline{H}}^T \vdots \underline{\underline{\phi}}^T \underline{\underline{H}}^T \vdots \underline{\underline{\phi}}^{T^2} \underline{\underline{H}}^T \vdots \underline{\underline{\phi}}^{T^3} \underline{\underline{H}}^T \vdots \underline{\underline{\phi}}^{T^4} \underline{\underline{H}}^T] \qquad (5.10)$$

The system is completely observable if and only if the 5 x 15 matrix is of rank 5. If there is a nonzero 5 x 5 determinant then the rank of $\underline{\underline{S}}$ is 5. However, if these determinants are all very small the system, though theoretically observable, is very close to being unobservable and a case can be made for stating that it is "marginally" observable. Now in Luenberger's design method it is necessary for the system to be observable so that the $\underline{\underline{L}}$ matrix is non-singular. If the system is "marginally" observable then the $\underline{\underline{L}}$ matrix will be close to being singular and numerical difficulties can be expected with the matrix inversion procedure required to generate $\underline{\underline{L}}$.

By checking the observability of system 2 it was found that the determinants were very small and also much smaller than those for system 1 (by an order of 10^4).

A more physical interpretation of observability is given by Ogata [5, p. 372] -- "Essentially, a system is completely observable if every transition of the system's state eventually affects the system's

output". By examining the transition matrix, $\underline{\underline{\phi}}$, (see appendix) it can be seen that a change in C2 affects only C2, and to a very small extent, W2. Furthermore a change in W2 affects only W2. Although a change in C1 affects all five state variables, the measurement states (W1, H1, W2) are affected much less than the unmeasured ones. Thus from a physical viewpoint it also follows that this system is "marginally" observable. Intuitively, we would also expect some difficulty in estimating two concentrations based on measurements of only holdups and the first effect enthalpy. By contrast for system 1 changes in C1 and H1 (especially) affect the measured states to a much larger degree so that we would expect system 1 to behave more satisfactorily than system 2.

5.6 EVAPORATOR SIMULATION STUDY 3: W1, H1, W2, C2 MEASURED

An investigation similar to Simulation Study 1 (in section 5.4) was carried out for the case where state variables W1, H1, W2 and C2 are measured and C1 is estimated by the first order observer. This is the current physical situation for the pilot plant evaporator since the first effect concentration is not measured on-line. A direct comparison was also made here with the sub-optimal filter used by Newell [6] for this system to see if the Luenberger observer could improve upon previous results. The sub-optimal filter used was identical to that for the Kalman filter study and the gain matrix had the following form:

$$\begin{bmatrix} 0.9 & 0 & 0 & 0 \\ 0 & 0 & 0 & 0 \\ 0 & 0.9 & 0 & 0 \\ 0 & 0 & 0.9 & 0 \\ 0 & 0 & 0 & 0.9 \end{bmatrix}$$

TABLE 5.5

DEPENDENCE OF STEADY STATE ESTIMATION ERRORS ON THE SCALAR, E, OF THE LUENBERGER OBSERVER

	Unmeasured Step Disturbance		
	(a) +20% feed flow	(b) -30% feed concentration	(c) +20% feed enthalpy
Value of E	steady state error in Cl(%)	steady state error in Cl (%)	steady state error in Cl(%)
0.9	16	23	-5
0.8	35	11	-15
0.7	43	7	-31
0.6	49	5	-61
0.5	53	4	-134
0.4	64	3	-588
0.3	56	2	420
0.2	51	2	184
0.1	53	2	128
0.01	55	1	105

Note: the steady state error vector is defined as: $\underline{\Delta x}_{ss} = \underline{\hat{x}}_{ss} - \underline{x}_{ss}$

A study was made of the steady state estimation errors due to "unseen" disturbances for several observer designs in order to find the "best" design. This was similar to the analysis carried out for system 1 in section 5.4.4.

Again, the disturbances considered were as before:

(a) a +20% step change in feed flowrate,

(b) a -30% step change in feed concentration, and

(c) a +20% step change in feed enthalpy.

The $\underline{\underline{C}}$ matrix was arbitrarily chosen to be:

$$\underline{\underline{C}} = [1 \quad 1 \quad 1 \quad 1]$$

and several values of the scalar, E, were tried in order to find the "best" design for all unmeasured disturbances.

From Table 5.5 it can be seen that large eigenvalues are better for disturbances (a) and (c) whereas small eigenvalues give smaller errors for disturbance (b). Using the largest eigenvalues, the errors appear to be tolerable for all types of unmeasured disturbance whereas a small decrease gives a rather large error for "unseen" disturbances in feed flow. It was therefore thought desirable to choose E = 0.9 as the "best" observer design for all possible situations.

It is of interest to compare the steady state estimation errors obtained with the Luenberger observer to those for the stationary Kalman filter (for the case of unmeasured disturbances). Therefore, a similar error analysis was carried out for the Kalman filter (see appendix for Chapter 5 for the derivation of the steady state error equation). It can be seen from Table 5.6 that offsets

TABLE 5.6

DEPENDENCE OF KALMAN FILTER STEADY STATE ESTIMATION ERRORS ON THE R:Q RATIO

Filter	R:Q Ratio	Steady State Error (%) in: $\hat{W}1$	$\hat{C}1$	$\hat{H}1$	$\hat{W}2$	$\hat{C}2$	Type of Unmeasured Disturbance
Kalman 1	1:1	-30	4	0	-10	-1	+20% feed flow
Kalman 2	1:100	0	-23	0	0	0	
Kalman 5	100:1	-248	9	0	-388	11	
Kalman 1	1:1	2	26	0	6	16	-30% feed concentration
Kalman 2	1:100	0	5	0	0	0	
Kalman 5	100:1	0	30	0	8	30	
Kalman 1	1:1	5	-1	-2	4	-3	+20% feed enthalpy
Kalman 2	1:100	0	0	0	0	0	
Kalman 5	100:1	35	-4	-2	1826	-12	

also occur for the Kalman filter when unmeasured step disturbances are applied to the process. However, these errors are not restricted to the estimates of the unmeasured variable, Cl. Due to the multivariable nature of the Kalman filter, all the estimates are affected by an incorrect model (one which is unaware of step disturbances). Three filters were analyzed: Kalman filter 1 has an R:Q ratio of 1:1, Kalman filter 2 a ratio of 1:100 and Kalman filter 5 a ratio of 100:1. Thus filter 1 weights the model and measurements equally whereas filter 2 favours the measurements strongly and filter 5 favours the model. The results show that the steady state estimation errors increase as the weighting tends towards the model, as would be expected. It is interesting to note that for Kalman filter 2, where the measurements are favoured, the only steady state error is in $\hat{Cl}$ which is not measured.

Using the "best" observer design, comparisons were made between the Luenberger observer and the sub-optimal filter for two types of "unseen" disturbance and for incorrect initial estimates of Cl. The details for the subsequent figures in this study are presented in Table 5.7.

5.6.1 Comparison of the Luenberger Observer and Suboptimal Filter for an Incorrect Initial Estimate of Cl

Two open loop runs were performed where the initial estimate of Cl was 30% below the actual steady state value. Although the unforced process remained at the initial steady state, the estimated curves show an initial transient due to the bad initial state estimates. Figure 5.21 shows the actual states and the response of both the Luenberger observer and the sub-optimal filter. A smaller value of

TABLE 5.7

DETAILS OF FIGURES 5.21 - 5.25: SIMULATION STUDY 3

For the open loop runs, the actual response is plotted for a comparison with the estimates. Observer 4 was designed with an eigenvalue of 0.9 and a coefficient matrix, $\underline{\underline{C}} = [1 \quad 1 \quad 1 \quad 1]$. Details of the figures are tabulated below.

B - denotes an observer which is unaware of a step disturbance

Figure	Control	States Displayed in the Figures	Estimator Used	Initial States	Initial State Estimates	Step Disturbance
5.21	OL	Estimated	Observer 4 Sub-optimal Filter	Zero	$\hat{C}1$ = -30%	-
5.22	OL	Estimated	Observer 4B Sub-optimal Filter	Zero	Correct	± 20% F
5.23	FB	Actual	Observer 4B Sub-optimal Filter	Zero	Correct	± 20% F
5.24	OL	Estimated	Observer 4B Sub-optimal Filter	Zero	Correct	- 30% CF
5.25	FB	Actual	Observer 4B Sub-optimal Filter	Zero	Correct	- 30% CF

E would speed up the rate of response of the Luenberger observer but this would cause problems for some of the later runs with "unseen" disturbances.

5.6.2 Comparison of the Luenberger Observer and Suboptimal Filter for an Unseen Disturbance in Feed Flowrate

Here, the system was subjected to a 20% step up in feed flow after 30 mins. and a step back down after 60 mins. Both open and closed loop runs were made for the sub-optimal filter and the Luenberger observer.

For the open loop system, Figure 5.22 shows the actual states and the response of both the observer and the sub-optimal filter to the unmeasured disturbances. It is apparent from these curves that the sub-optimal filter is slightly better than the Luenberger observer. However, for the closed loop runs the difference in the curves cannot be detected (Figure 5.23) and both methods give a satisfactory closed loop performance which is very close to the ideal case. The closed loop runs exhibit excellent control because slight inaccuracies in the C1 estimate have little effect on the control action since the optimal controller design included little weighting of the C1 response (i.e. deviations of C1 are not considered to be as critical as those in C2, W1 and W2).

5.6.3 Comparison of the Luenberger Observer and Suboptimal Filter for an Unseen Disturbance in Feed Concentration

The base case for this comparison was a 30% step down in feed concentration at the 10 minute mark and again both open and closed loop runs were made with the Luenberger observer and the sub-optimal filter. Neither open loop run gave a very accurate estimate of C1 but the

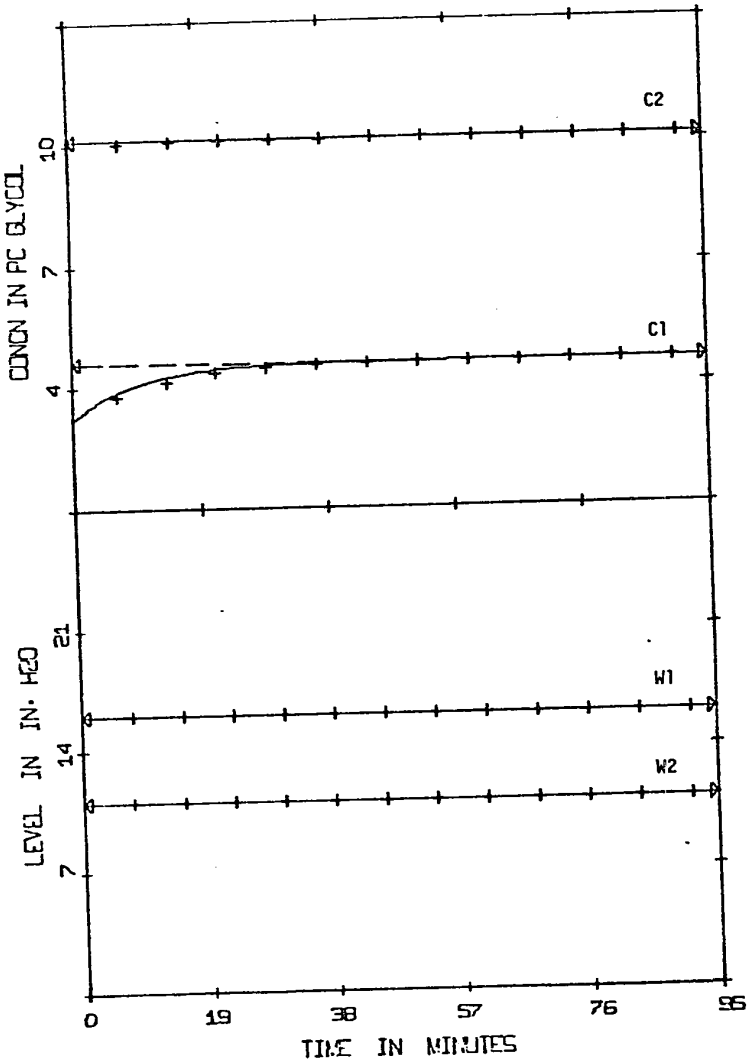

FIGURE 5.21 (SIM/OL) --- Actual States, —— Estimates from Observer 4, +++ Estimates from Sub-Optimal Filter

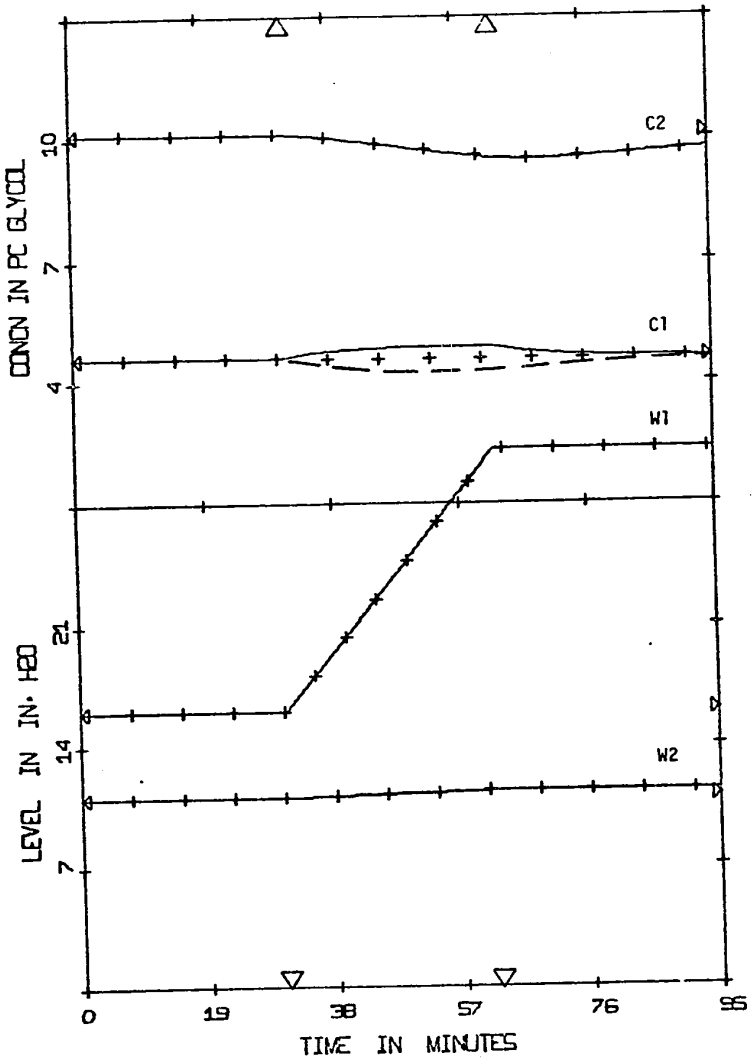

FIGURE 5.22 (SIM/±20%F/OL) --- Actual States, —— Estimates from Observer 4B, +++ Estimates from Sub-Optimal Filter

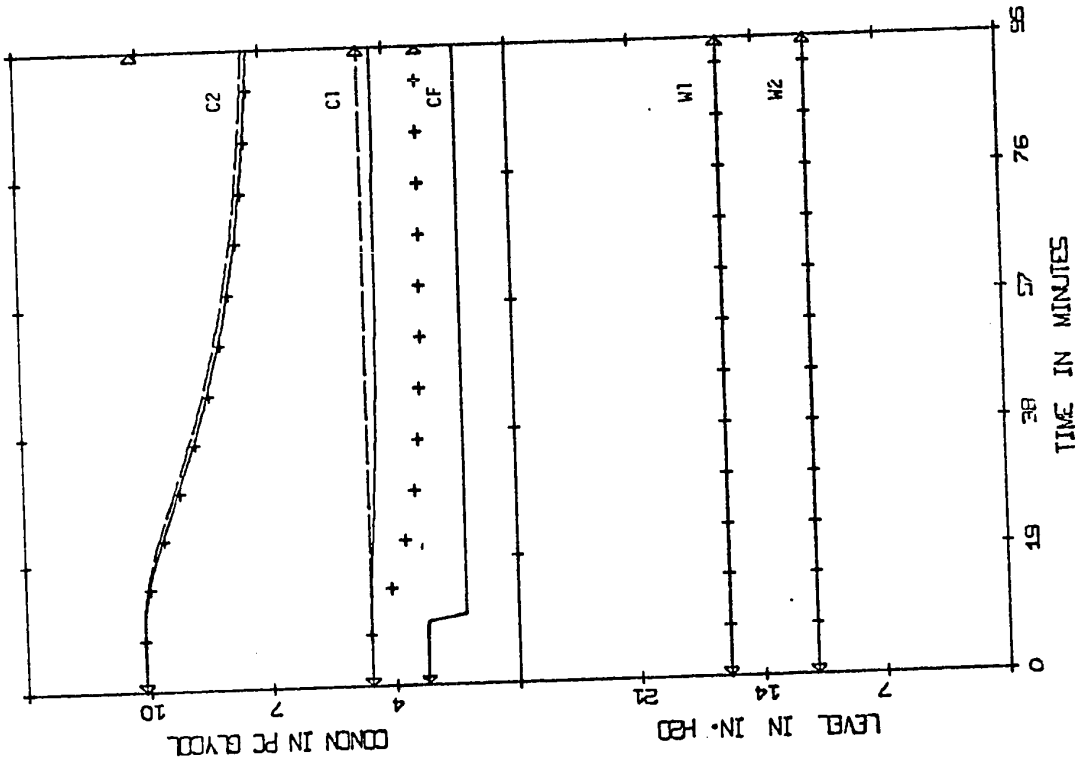

FIGURE 5.24 (SIM/-30%CF/OL) +++ Actual States, —— Estimates from Observer 4B, --- Estimates from Sub-Optimal Filter

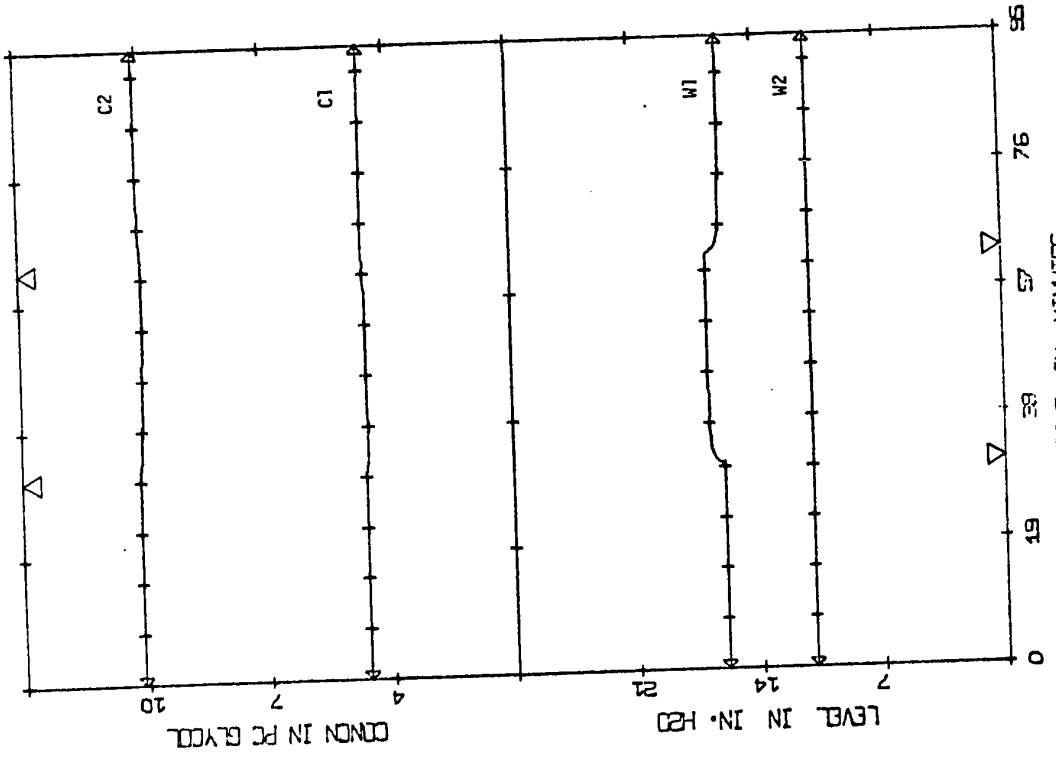

FIGURE 5.23 (SIM/±20%F/FB) —— Control Based on Observer 4B Estimates, +++ Control Based on Sub-Optimal Filter Estimates

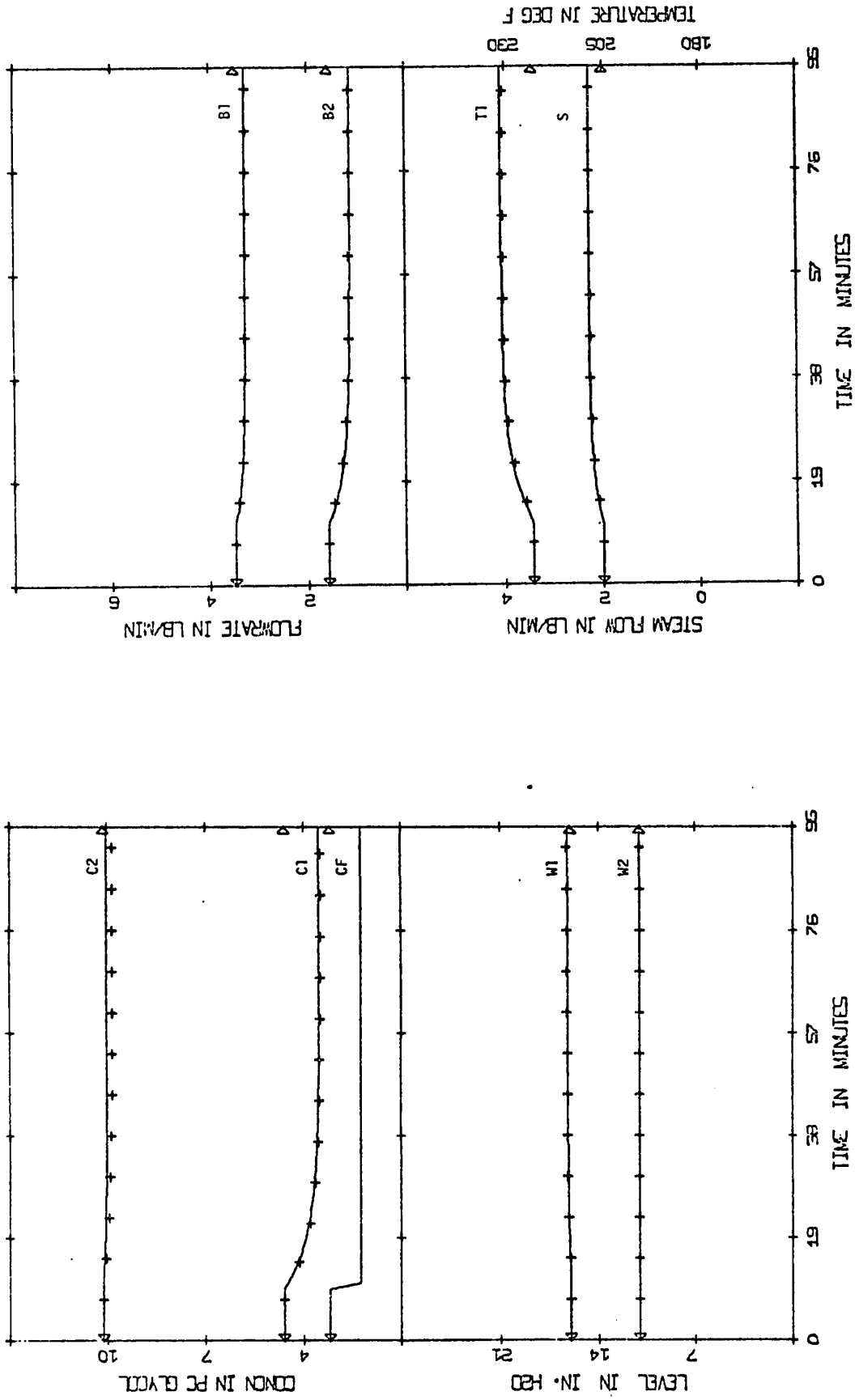

FIGURE 5.25 (SIM/-30%CF/FB) —— Control Based on Observer 4B Estimates, +++ Control Based on Sub-Optimal Filter Estimates

observer is slightly better than the sub-optimal filter (see Figure 5.24). The closed loop runs in Figure 5.25 were both very good in that the primary controlled variable (C2) and the two levels were all controlled very well. The observer is only slightly better than the sub-optimal filter and in both cases the control was very close to the ideal case.

It can be concluded that the observer is only very slightly superior (if at all) to the sub-optimal filter used by Newell [6] but it remains to be seen whether experimental runs (with a small degree of process and measurement noise and slight model inaccuracies) will confirm this result.

5.7 EVAPORATOR EXPERIMENTAL STUDY 1: W1, W2, C2 MEASURED

Both open and closed loop runs were made on the evaporator using the second order observer to estimate the entire state vector. The details of the experimental runs in this study are given in Table 5.8.

The base case for the open loop runs was the same response to a -30% step change in feed concentration that was used in the Kalman filter study in section 3.8. The open loop data taken from the evaporator included the four state measurements, W1, H1, W2 and C2, although the off-line analysis of this data using the second order observer required only three of these measurements: W1, W2 and C2. In the figures, for the open loop runs, the four measured variables are plotted for comparison with the observer estimates. The actual C1 response is not shown since this variable was not measured. Figure 5.26 compares the estimated responses of observers 5A and 5B with the actual response. Observer 5A reconstructed the states reasonably well but amplified the noisy data so that the estimated T1 (i.e. H1) curve fluctuates more

TABLE 5.8

DETAILS OF FIGURES 5.26 - 5.31: EXPERIMENTAL OBSERVER RUNS

The open loop runs compare the actual and estimated responses for different observers and a -30% step change in feed concentration. In the closed loop runs, the observer estimates were used in the control algorithm but the actual states are shown in the figures. For all the runs the process was initially at steady state and the initial state estimates were correct.

A - denotes a filter which has knowledge of a step disturbance.
B - denotes a filter which is unaware of a step disturbance.

Figure	Control	States Displayed	States Used in Control	$\underline{\underline{E}}$	$\underline{\underline{C}}$	Disturbance
5.26	OL	Observer 5A Observer 5B	-	$\underline{\underline{E22}}$	$\underline{\underline{C1}}$	-30% CF
5.27	OL	Observer 3B	-	$\underline{\underline{E1}}$	$\underline{\underline{C1}}$	-30% CF
5.28	FB	Actual	Observer 5A	$\underline{\underline{E22}}$	$\underline{\underline{C1}}$	±20% F
5.29	FB	Actual	Observer 5B	$\underline{\underline{E22}}$	$\underline{\underline{C1}}$	-20% F
5.30	FB	Actual	Observer 5B	$\underline{\underline{E22}}$	$\underline{\underline{C1}}$	-30% CF
5.31	FB*	Actual	Observer 5A	$\underline{\underline{E22}}$	$\underline{\underline{C1}}$	±20% F

* A $\underline{\underline{K}}_{FB}$ with smaller elements (i.e. gains) was used for this run (see text).

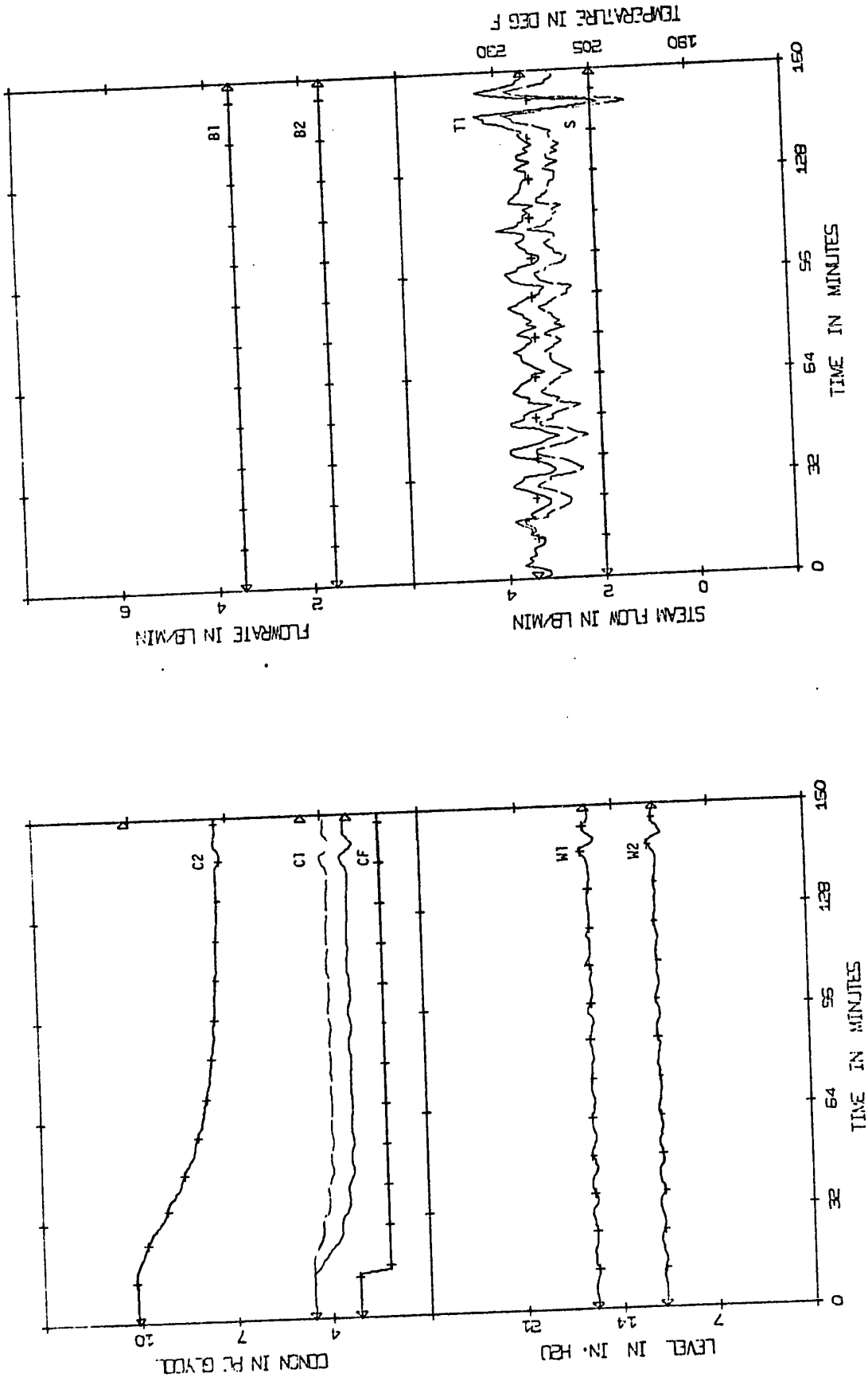

FIGURE 5.26 (EXP/-30%CF/OL) +++ Actual States, —— Estimates from Observer 5A, --- Estimates from Observer 5B

than the original data. Since W1, W2 and C2 are measured, the estimates of these states (from the observer) are simply the actual experimental values. Observer 5B gave a similar response except that the unmeasured disturbance resulted in offsets for both the unmeasured states, C1 and H1. It is interesting to note the response of the observer to the unanticipated disturbance in the experimental data towards the end of the run ($t \simeq 140$ min.).

Observer 3B was used in Figure 5.27 and again the results are in good agreement with the simulation study (see Figure 5.18). The C1 and H1 (especially) curves are not accurately reconstructed due to the "unseen" disturbance in feed concentration.

For the closed loop runs, three of the four measurements were again used to drive the second order observer and the reconstructed state vector was then used in the optimal feedback control law. The standard $\underline{K}_{FB}$ (see appendix) was used in all the runs except the one illustrated in Figure 5.31. The four measured state variables are plotted to evaluate the performance of the observer-controller combination.

Figure 5.28 shows the closed loop performance of the system where observer 5A was used to reconstruct the entire state vector. In this run there was a 20% step down and a 20% step up in feed flowrate and the observer was aware of these disturbances. The control is reasonably good although there is some oscillation following the first step in feed flow. The response to the second step was much better and this may be an indication of system nonlinearities.

In Figure 5.29 the curves show the closed loop response to an unmeasured 20% step down in feed flowrate. Observer 5B was used and it

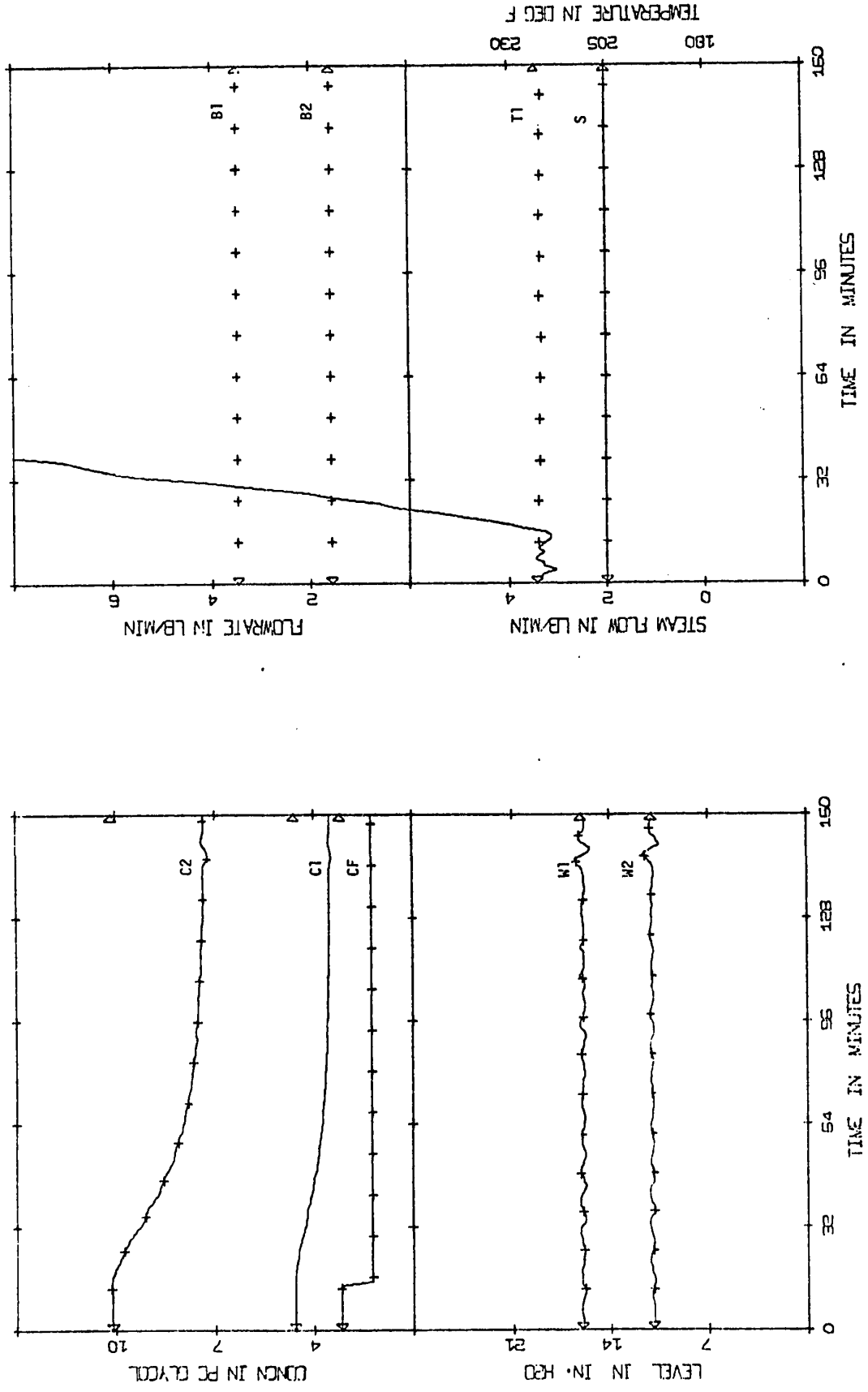

FIGURE 5.27 (EXP/-30%CF/OL) +++ Actual States, —— Estimates from Observer 3B

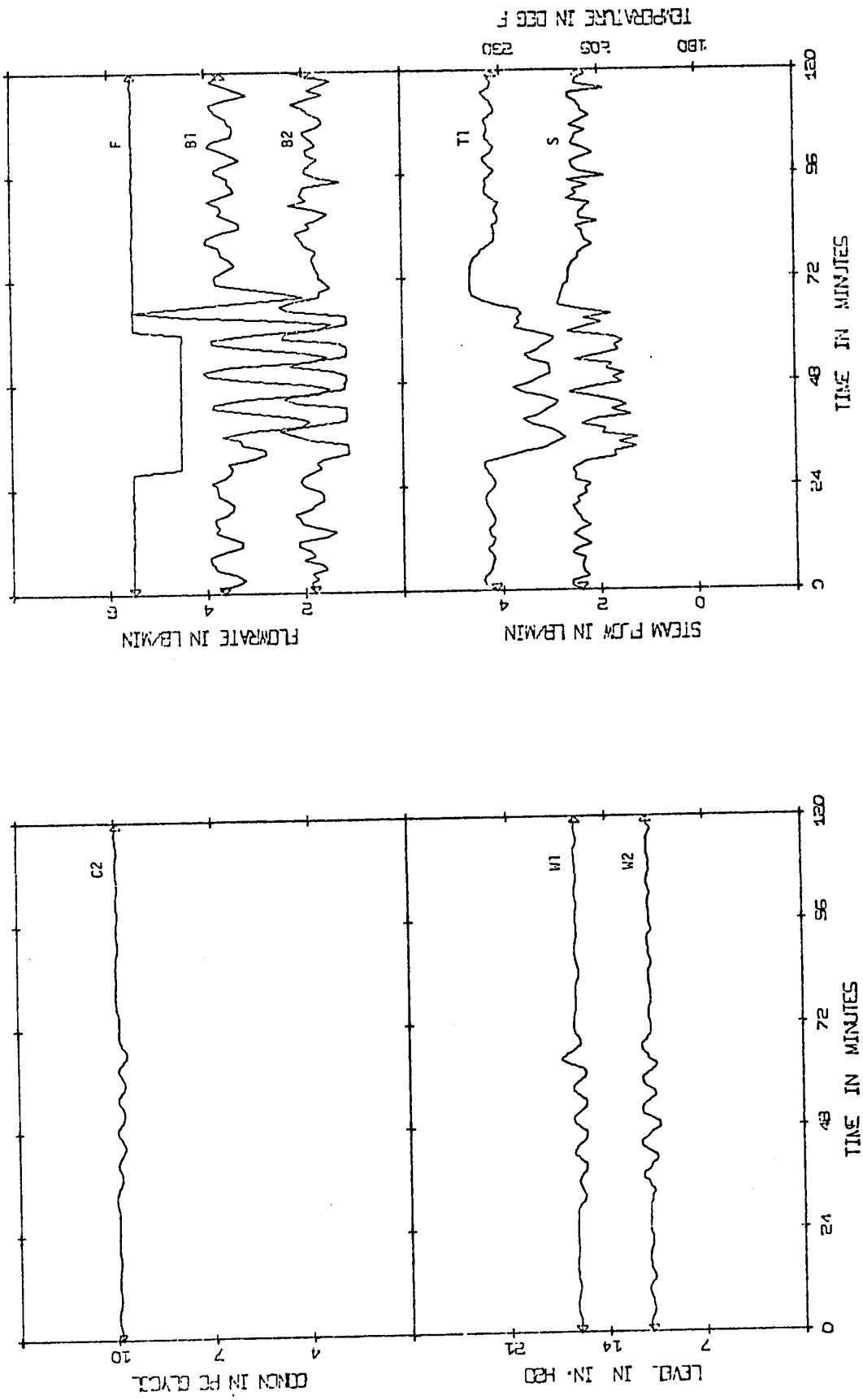

FIGURE 5.28 (EXP/±20%F/FB) Actual States, Control Based on Observer 5A Estimates

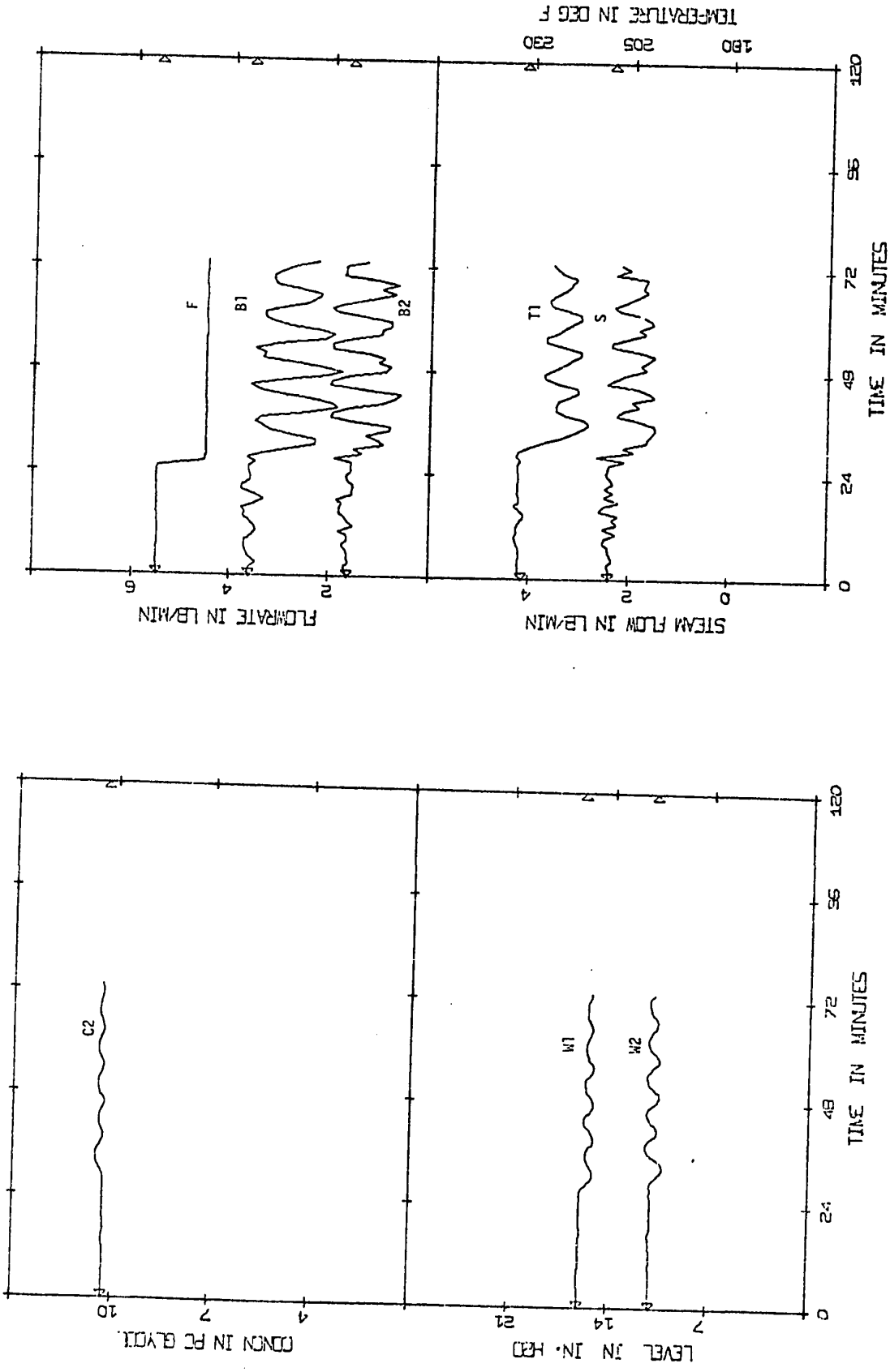

FIGURE 5.29 (EXP/-20%F/FB) Actual States, Control Based on Observer 5B Estimates

can be seen that the control is comparable with that obtained by using observer 5A in Figure 5.28.

Figure 5.30 shows the effect of an "unseen" -30% step disturbance in feed concentration on the closed loop system. Again observer 5B was used and the controlled variables are very smooth. However, the C2 curve tends to drift down slightly while the W1 curve moves upwards.

In an attempt to reduce the oscillations between step changes observed in Figure 5.28, this run was repeated using a feedback control matrix with lower gains. This control matrix was derived by weighting the controls in the discrete quadratic performance index (see section 2.3). The standard control matrix was derived with a zero weighting on the controls and a state weighting matrix:

$$\underline{\underline{Q}}_1 = \text{diag. } [10, 1, 1, 10, 100]$$

The control matrix for the run in Figure 5.31 had the same state weighting but also had a control weighting matrix:

$$\underline{\underline{R}}_1 = \text{diag. } [0.05, 0.05, 0.05]$$

This had the effect of restricting the expenditure of control "energy" and hence resulted in a feedback control matrix with lower gains:

$$\underline{\underline{K}}_{FB} = \begin{bmatrix} 6.5 & -1.2 & -3.2 & -0.1 & -13.1 \\ 3.8 & 0.4 & 0.7 & 1.4 & 9.7 \\ 3.1 & 1.1 & 0.0 & 9.8 & 11.6 \end{bmatrix}$$

Figure 5.31 shows the results obtained using this control matrix together with observer 5A. The oscillations in both state

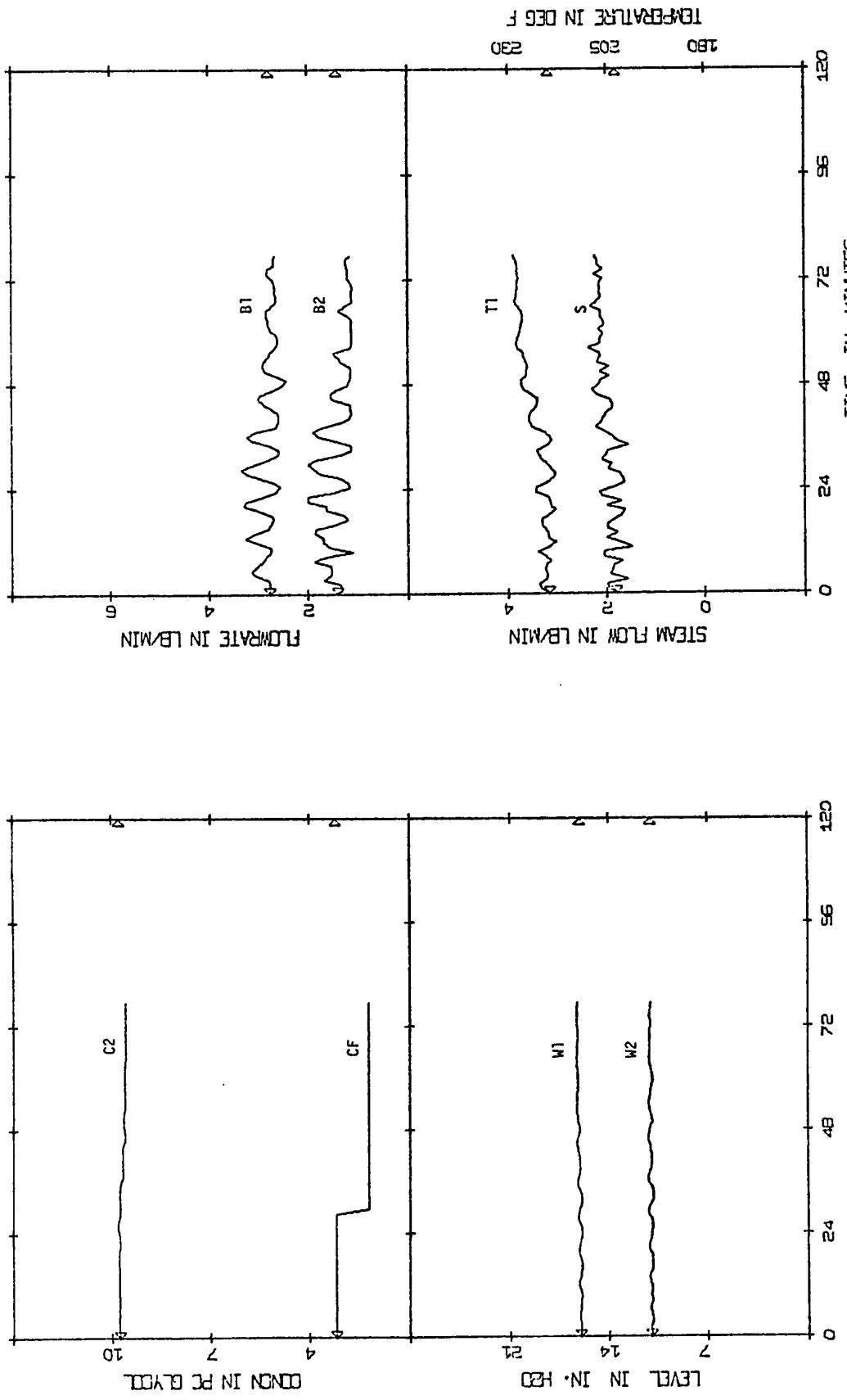

FIGURE 5.30 (EXP/-30%CF/FB) Actual States, Control Based on Observer 5B Estimates

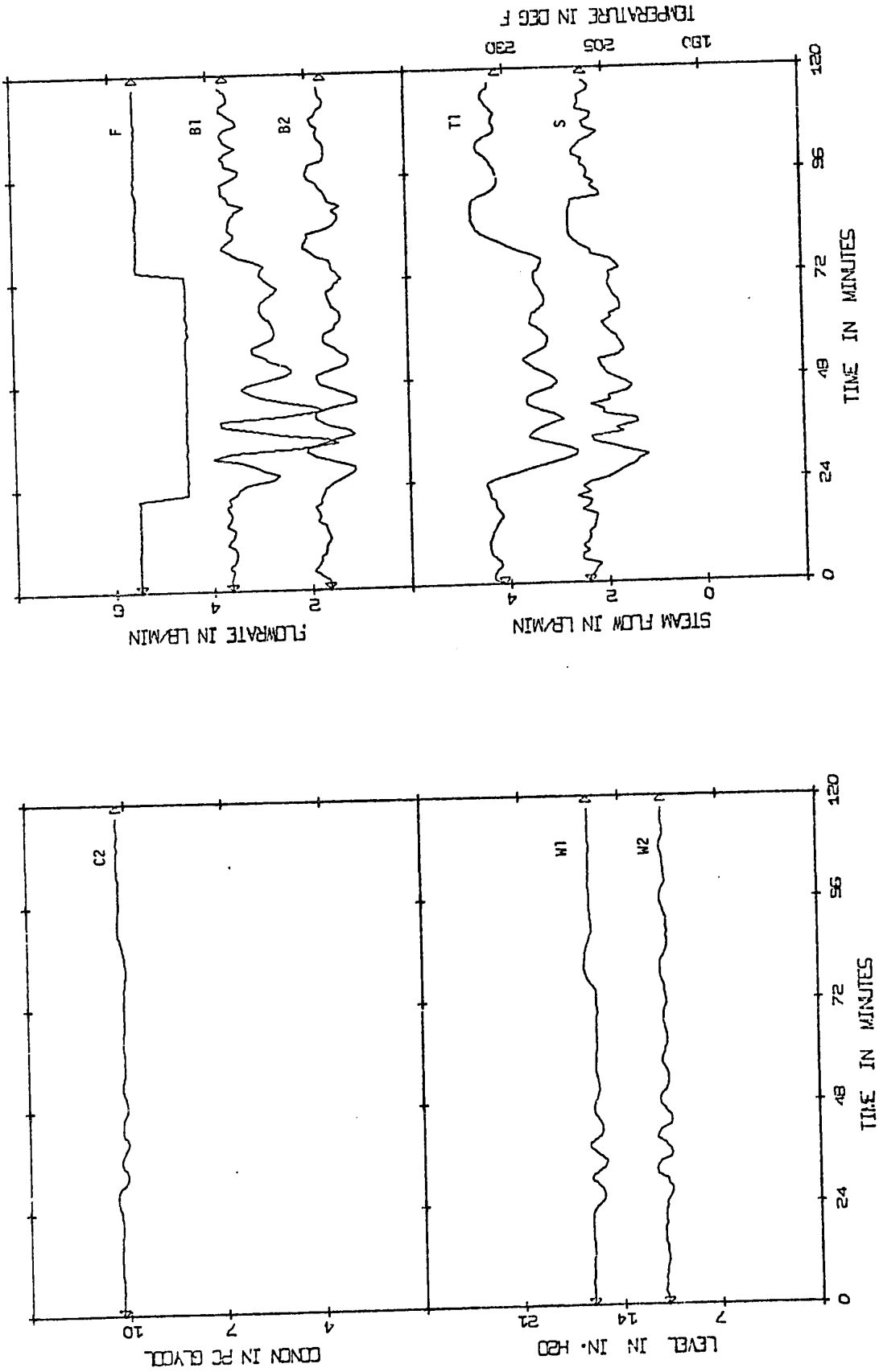

FIGURE 5.31 (EXP/±20%F/FB) Actual States, Control Based on Observer 5A Estimates (Lower Gains Used in Feedback Control Matrix)

variables and control variables are reduced considerably giving some improvement over the run in Figure 5.28. Again a better response was observed for the second step disturbance.

5.8 EVAPORATOR EXPERIMENTAL STUDY 2: W1, H1, W2, C2 MEASURED

In this study C1 is the only state variable which is not measured and consequently a first order observer was used to reconstruct the entire state vector. Both open and closed loop runs were made. For the latter case a comparison was made between the performance of the observer and a sub-optimal filter. The details of the runs in this study are given in Table 5.9.

In the open loop runs the base case was again the response to a 30% step down in feed concentration. In Figure 5.32, the actual measurements are plotted together with the states reconstructed by observer 4B which was not aware of the step disturbance. As expected, all the measured states were reconstructed exactly. The actual C1 curve is not known but by comparing the estimate with the corresponding model response it would appear that $\hat{C1}$ remained higher than the true value.

The closed loop run shown in Figure 5.33 illustrates the control obtained by using observer 4A to estimate the state vector. The disturbance applied was a 20% step down followed by a 20% step up in feed flow. The standard $\underline{\underline{K}}_{FB}$ (see appendix) was used.

The control is good and compares favourably with the corresponding run (Figure 5.34) where the sub-optimal filter of section 5.6 was used to estimate the states.

In Figure 5.35 observer 4B was again used and an unmeasured 20% step down in feed flowrate was applied to the process. As can be

TABLE 5.9

DETAILS OF FIGURES 5.32 - 5.37: EXPERIMENTAL OBSERVER RUNS

The open loop run compares the actual response and the estimated response of observer 4B to a 30% step down in feed concentration. In the closed loop runs either the observer estimates or the sub-optimal filter estimates were used in the control calculations but the actual states are shown in the figures. For all the runs the process was initially at steady state and the initial state estimates were correct. Observer 4 was designed with an eigenvalue of 0.9 and a coefficient matrix, $\underline{\underline{C}} = [1 \quad 1 \quad 1 \quad 1]$.

A - denotes a filter which has knowledge of a step disturbance.

B - denotes a filter which is unaware of a step disturbance.

Figure	Control	States Displayed	States used in Control	Disturbance
5.32	OL	Observer 4B	-	-30% CF
5.33	FB	Actual	Observer 4A	±20% F
5.34	FB	Actual	Sub-optimal Filter A	±20% F
5.35	FB	Actual	Observer 4B	-20% F
5.36	FB	Actual	Sub-optimal Filter B	-20% F
5.37	FB	Actual	Observer 4B	-30% CF

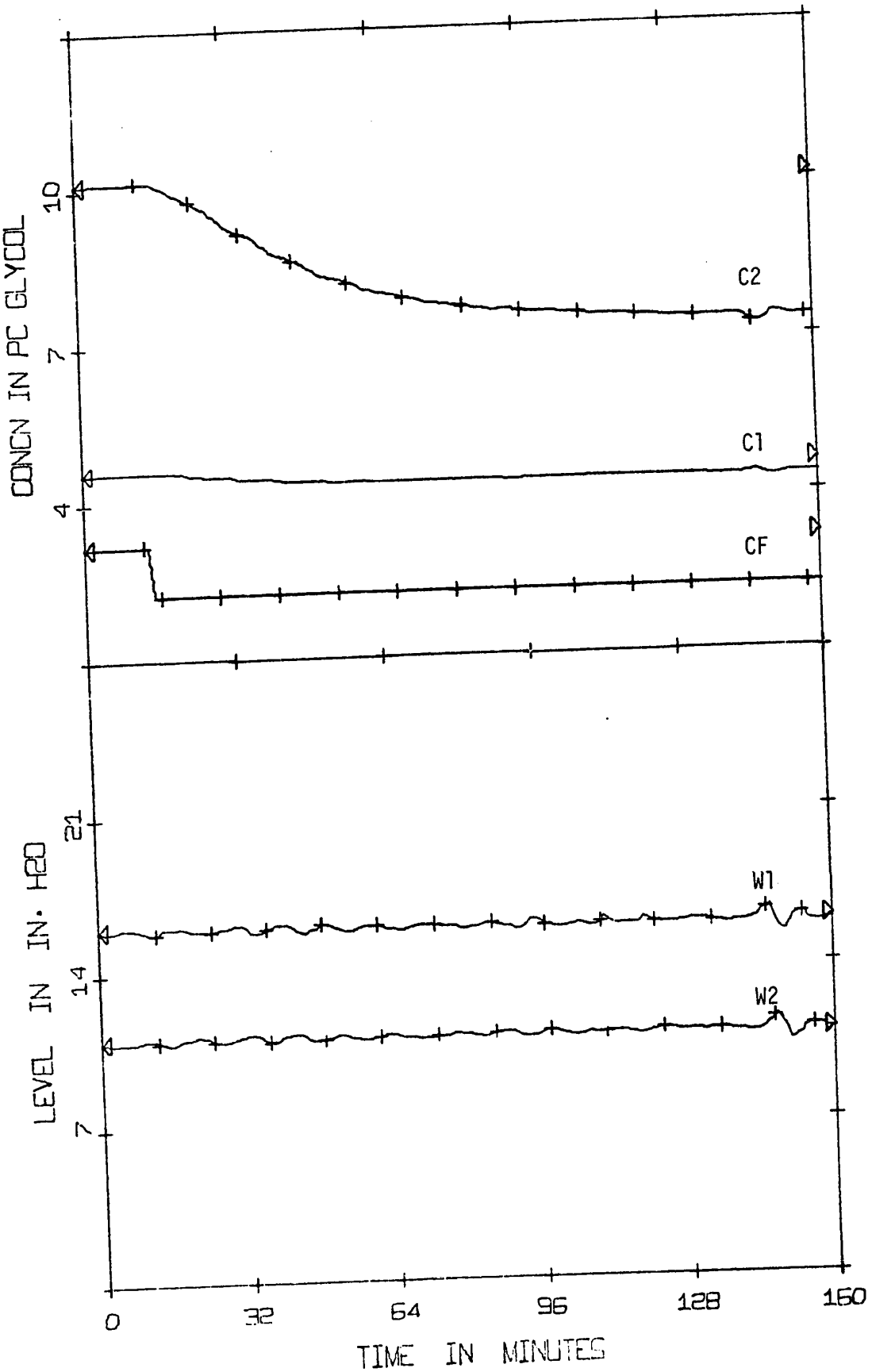

FIGURE 5.32 (EXP/-30%CF/OL) +++ Actual States, —— Estimates from Observer 4B

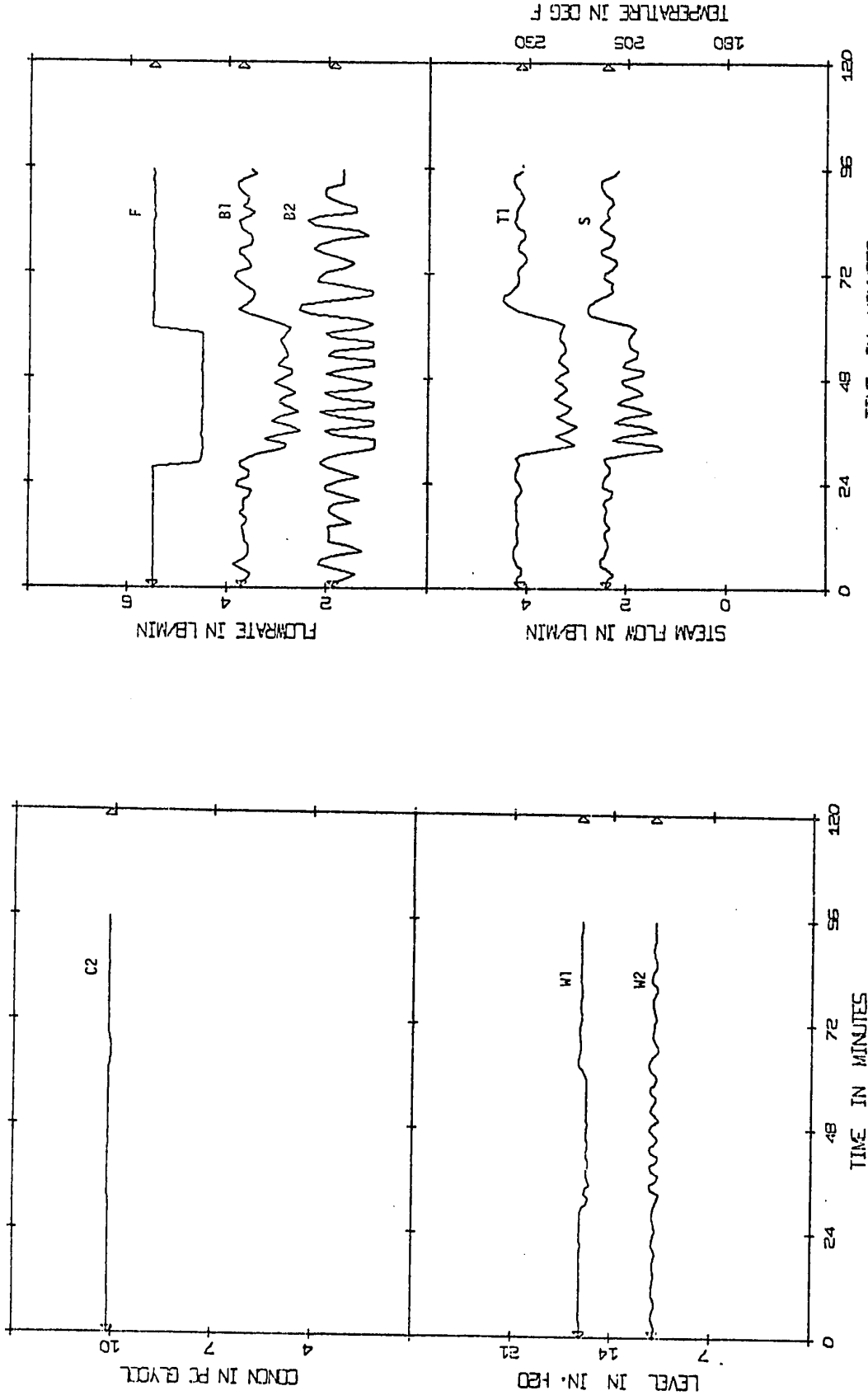

FIGURE 5.33 (EXP/±20%/FB) Actual States, Control Based on Observer 4A Estimates

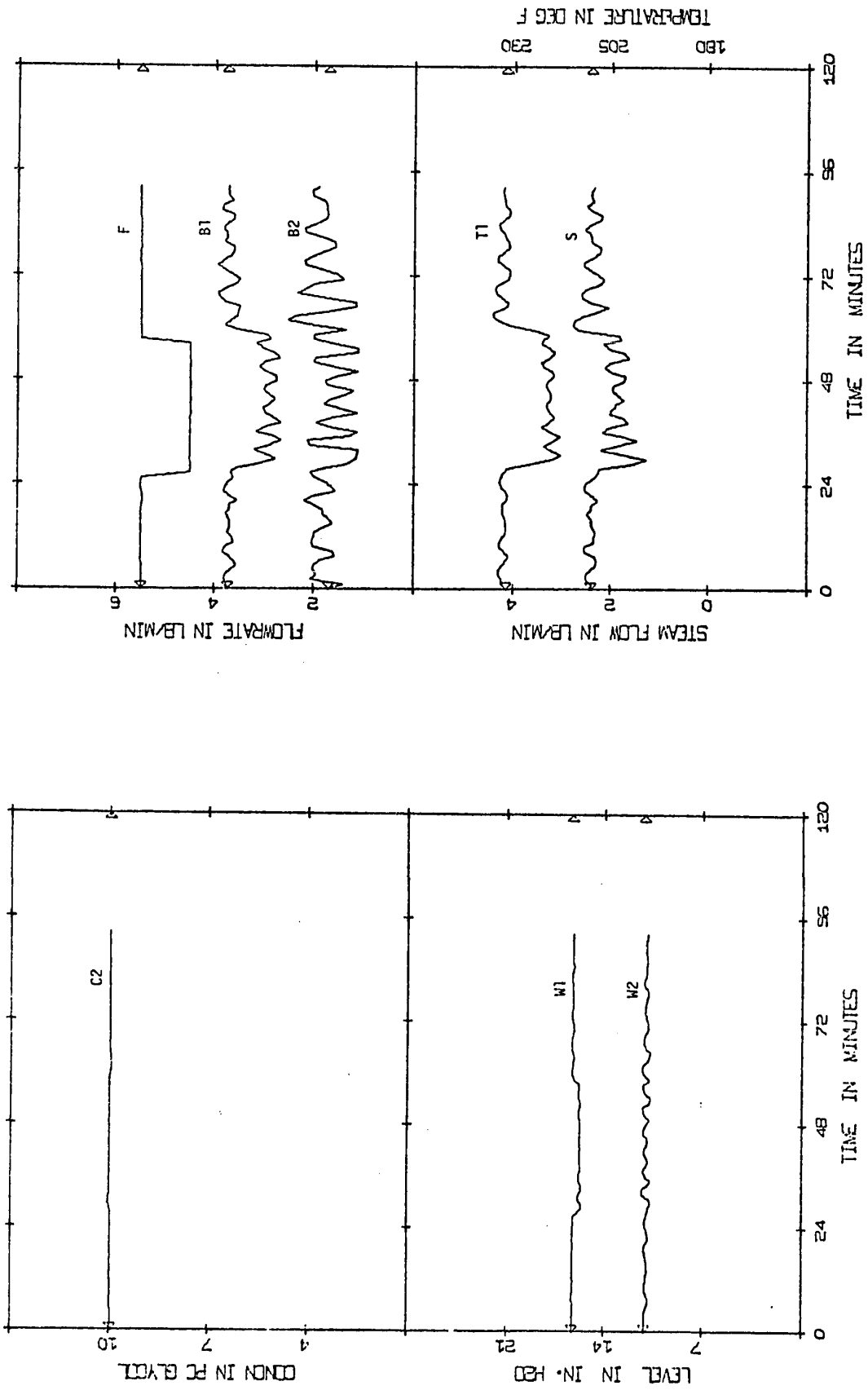

FIGURE 5.34 (EXP/±20%F/FB) Actual States, Control Based on Sub-Optimal Filter A Estimates

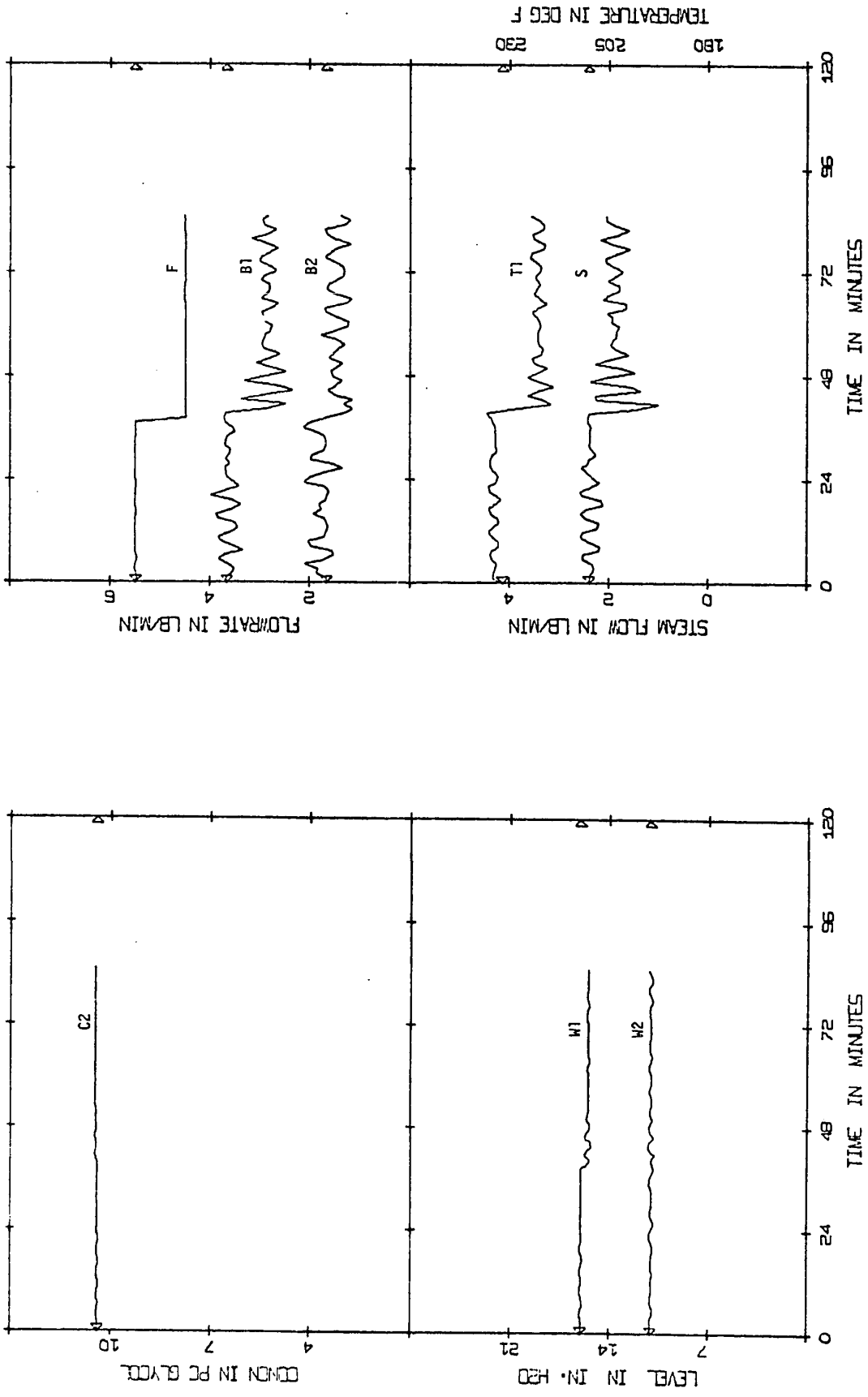

FIGURE 5.35 (EXP/-20%F/FB) Actual States, Control Based on Observer 4B Estimates

seen from the curves, the response in comparable to that for the first step distrubance shown in Figure 5.33 where the distrubances were measured. When this run was repeated using the sub-optimal filter, the control was also good and virtually identical to the previous run (see Figure 5.36). The sub-optimal filter was not aware of the disturbance in this case.

Finally, Figure 5.37 illustrates the effect of an unmeasured 30% step down in feed concentration with observer 4B used to reconstruct the states. The control here is good but the C2 curve drifts down slightly and W1 drifts up just as they did in the corresponding case for the second order observer.

5.9 CONCLUSIONS

The simulation and experimental studies for the double effect evaporator illustrated that the Luenberger observer could be successfully implemented in a multivariable control system. A satisfactory design was achieved for both a first order and a second order observer and the control based on these observer estimates was comparable to the ideal case where all the states are measured.

It was shown that the observer responds quickly to incorrect initial state estimates even when large observer eigenvalues are used. As predicted from the theory, the observer response time is decreased as the eigenvalues are made smaller. Varying the elements of the $\underline{\underline{C}}$ matrix in the design of the observer had little effect on the dynamic response.

In the experimental runs, the observer was found to be quite sensitive to process and measurement noise; this is not a surprising

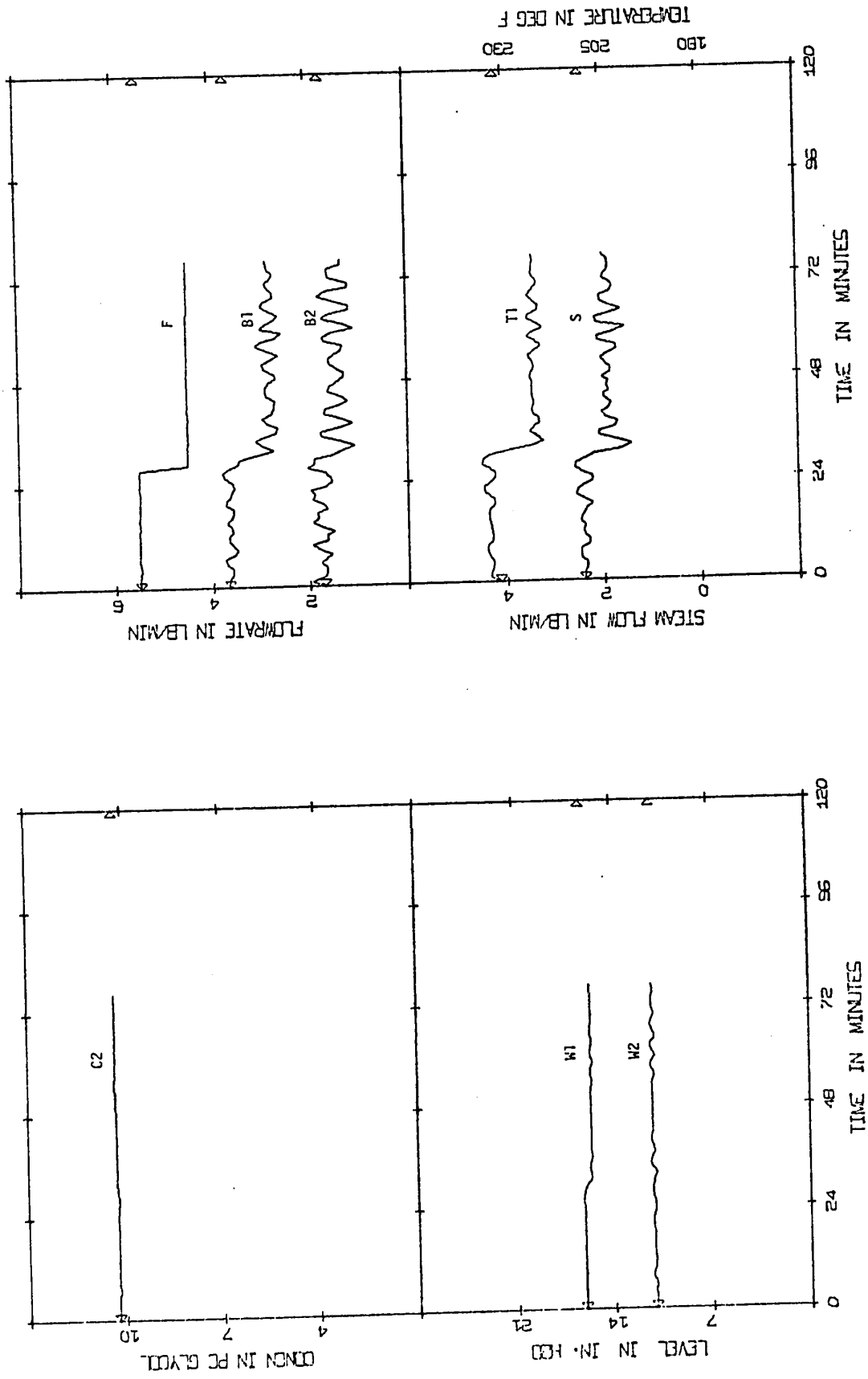

FIGURE 5.36 (EXP/-20%F/FB) Actual States, Control Based on Sub-Optimal Filter B Estimates

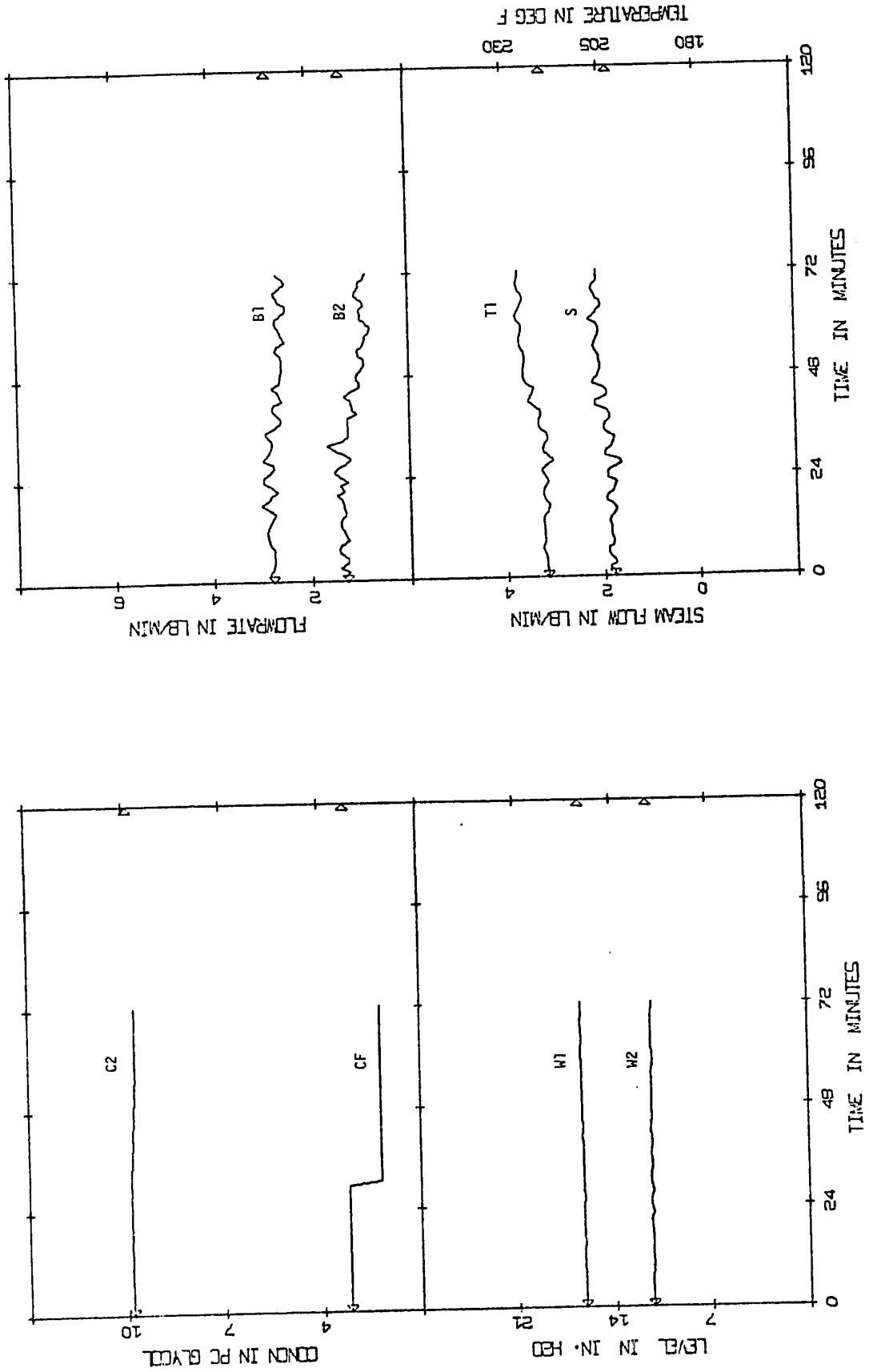

FIGURE 5.37 (EXP/-30%CF/FB) Actual States, Control Based on Observer 4B Estimates

result since the Luenberger observer was initially proposed for only deterministic systems. It is recommended, however, that large eigenvalues be used whenever noise is a significant factor since the estimates can become quite oscillatory under these conditions with small observer eigenvalues.

The response of the observer to unmeasured step disturbances is difficult to predict and the observer errors depend on both the observer design and the type of disturbance applied to the process. A satisfactory observer design which gives acceptable offsets in the estimates for all disturbances can only be found by off-line analysis of these errors for several different designs. Even though the design matrices can be chosen somewhat arbitrarily, it is obvious that in order to obtain the "best" design the choice of these matrices must be strongly influenced by:

(1) speed of response desired,

(2) behaviour of the observer for unmeasured disturbances,

(3) process and measurement noise levels.

An important conclusion of this study is that considerable difficulty in designing a satisfactory observer can be encountered for systems which are "marginally" observable. The second evaporator simulation study (section 5.5) considered a system which was theoretically observable but only "marginally" so. For this situation a satisfactory design was not found even under ideal conditions (i.e. correct initial state estimates, all disturbances measured and no noise). The difficulties are due to the matrix inversion procedure required to generate the reconstruction matrix, $\underline{\underline{L}}$; for "marginally" observable systems this matrix is close to being singular so that numerical problems arise and the gains tend to be very large.

A comparison of the first order observer with the sub-optimal filter used in all the previous control studies on the evaporator illustrated that there was very little difference in the performance of the two estimators. In view of this fact and the effort required in designing the observer, it is recommended that the much simpler sub-optimal filter be used for this application.

CHAPTER SIX

OVERALL CONCLUSIONS FROM THE KALMAN FILTER AND LUENBERGER OBSERVER STUDIES

Both the Kalman filter and the Luenberger observer were successfully implemented in a multivariable control system for a pilot scale, double effect evaporator.

Simulation and experimental studies demonstrated that the stationary form of the discrete Kalman filter could provide satisfactory estimates of the states of a stochastic process. The success of the Kalman filter was found to depend on the accuracy of the mathematical process model and the choice of the weighting matrices in the design of the filter. Theoretically, the weighting matrices should be made equal to the noise covariance matrices. However in practice, these matrices are not known exactly and process models are imperfect so that estimates of the matrices are used. In particular unmeasured disturbances necessitate weighting the measurements more heavily in designing the filter (i.e. assume large elements for the process noise covariance matrix). Fortunately, the Kalman filter is quite insensitive to these design matrices and satisfactory results can be obtained with weighting matrices which are considerably different from the ideal values. Generally, it is desirable to weight the measurements as highly as possible to eliminate problems associated with inaccurate process models or unmeasured disturbances. However, if the measurements are weighted too heavily, little filtering occurs, and the resulting state estimates are too noisy.

A satisfactory Luenberger observer for the evaporator was designed but in general, there were more problems with this technique

than would be expected from the theory. The standard observer is quite sensitive to noise and unmeasured disturbances and is not recommended for a stochastic process. A comparison of the observer with a simple sub-optimal filter indicated that the performance of both estimators was almost identical and in view of this, it is difficult to justify the effort required to obtain a satisfactory design.

For the evaporator application it is recommended that the current method of state estimation (i.e. the sub-optimal filter) be retained. The Luenberger observer does not give any improvement over this filter. The Kalman filter could be used to systematically select a gain matrix which may give slight improvements over the sub-optimal filter. However, since the current filter gives such satisfactory results it hardly seems likely that any improvement would be significant.

6.1 FUTURE WORK

The future work in this area would involve more studies with the Kalman filter. Firstly a brief study could be conducted using the Kalman filter without the addition of artificial noise, and applications where more than one state variable is not measured could be considered. A more detailed study would involve the application of the extended Kalman filter in order to estimate the "drift" in the product concentration measurement. This is a continual problem and at the present time it is necessary to clean and recalibrate the refractometer daily. An accurate estimate of this "drift" would be a great asset to the continuous operation of the evaporator.

NOMENCLATURE FOR CHAPTER TWO

(a) Alphabetic

$\underline{\underline{A}}$	State coefficient matrix for the continuous model
$\underline{\underline{B}}$	Control coefficient matrix for the continuous model
$\underline{\underline{C}}$	Gain matrix for the sub-optimal filter
$\underline{d}$	Disturbance vector
$\underline{\underline{D}}$	Disturbance coefficient matrix for the continuous model
E	Expected value
$\underline{\underline{H}}$	Output coefficient matrix
$\underline{\underline{I}}$	Identify matrix
j	Time increment counter
J	Performance index
k	Time increment counter
$\underline{\underline{K}}$	Gain matrix for the Kalman filter
$\underline{\underline{K}}_{FB}$	Feedback control matrix
m	Dimension of control vector
$\underline{\underline{M}}$	A priori variance matrix
n	Dimension of state vector
N	Final time
p	Dimension of disturbance vector
$\underline{\underline{P}}$	A posteriori variance matrix
q	Dimension of output vector
$\underline{\underline{Q}}$	Weighting matrix for the process noise
$\underline{\underline{Q}}_1$	State weighting matrix
r	Dimension of process noise vector
$\underline{\underline{R}}$	Weighting matrix for the measurement noise

NOMENCLATURE FOR CHAPTER TWO (continued)

$\underline{\underline{R}}_1$	Control weighting matrix
$\underline{\underline{S}}$	Final state weighting matrix
t	Time
T	Sampling period
$\underline{u}$	Control vector
$\underline{v}$	Measurement noise vector
$\underline{w}$	Process noise vector
$\underline{x}$	State vector
$\underline{y}$	Output vector

(b) Greek

α	Coefficient scalar in exponential filter equation
$\underline{\underline{\Gamma}}$	Process noise coefficient matrix for the discrete model
δ	Kronecker delta function
$\underline{\underline{\Delta}}$	Control coefficient matrix for the discrete model
$\underline{\underline{\theta}}$	Disturbance coefficient matrix for the discrete model
$\underline{\underline{\Phi}}$	Transition matrix

(c) Subscripts

i	i^{th} element of the output vector
-	Vector
=	Matrix

(d) Superscripts

.	Time derivative
T	Matrix transpose
-1	Matrix inverse

*	Optimum value of the variable
^	Estimated value
-	Model value

(e) Abbreviations

cov	Covariance

NOMENCLATURE FOR CHAPTER THREE

		Steady State
(a)	Process Variables	
$\underline{x}$	Five element state vector:	
W1	Holdup in the first effect	46 lb. (16.0 in)
C1	Concentration in the first effect	4.59% glycol
H1	First effect solution enthalpy	1.90 BTU/lb.
W2	Holdup in the second effect	42 lb. (11.0 in)
C2	Concentration in the second effect	10.11% glycol
$\underline{u}$	Three element control vector:	
S	Steam flowrate to the first effect	2.00 lb./min.
B1	First effect bottoms flowrate	3.49 lb./min.
B2	Second effect bottoms flowrate	1.58 lb./min.
$\underline{d}$	Three element disturbance vector:	
F	Feed flowrate	5.0 lb./min.
CF	Feed concentration	3.2% glycol
HF	Feed enthalpy	162 BTU/lb.
	Other Process Variables	
O1	Overheads from first effect	
O2	Overheads from second effect	
P1	Pressure in first effect	
P2	Pressure in second effect	
TF	Temperature of feed	
T1	Temperature in first effect	
T2	Temperature in second effect	

(b) Alphabetic

$\underline{\underline{C}}$ Gain matrix for the sub-optimal filter

NOMENCLATURE FOR CHAPTER THREE (continued)

$\underline{\underline{K}}$ Gain matrix for the Kalman filter

$\underline{\underline{K}}_{FB}$ Feedback control matrix

$\underline{\underline{Q}}$ Weighting matrix for the process noise

$\underline{\underline{R}}$ Weighting matrix for the measurement noise

(c) Greek

α Filter constant for the exponential filter

$\underline{\underline{\Gamma}}$ Coefficient matrix for the process noise

$\underline{\underline{\Delta}}$ Control coefficient matrix

$\underline{\underline{\theta}}$ Disturbance coefficient matrix

$\underline{\underline{\phi}}$ Transition matrix

(d) Subscripts

- Vector

$\underline{\underline{\ }}$ Matrix

(e) Abbreviations

CC Concentration controller

CR Concentration recorder

DDC Direct Digital Control

FC Flow controller

FR Flow recorder

LC Level controller

PC Pressure controller

(f) Code for Computer Graphs

Δ, ∇ Denote time of step disturbance

$\triangleleft, \triangleright$ Denote initial steady state

Type of run:

SIM Simulated

EXP Experimental

Disturbance (±/X%/XX):

+,- Positive or negative step

X% Step size as percentage of steady state

XX Process variable disturbed

Control mode:

OL Open loop

FB Optimal multivariable feedback

NOMENCLATURE FOR CHAPTER FOUR

(a) Alphabetic

$\underline{\underline{C}}$	Observer coefficient matrix for the outputs
$\underline{d}$	Disturbance vector
$\underline{\underline{E}}$	Observer transition matrix
$\underline{\underline{F}}$	Observer coefficient matrix for the disturbances
$\underline{\underline{G}}$	Observer coefficient matrix for the controls
$\underline{\underline{H}}$	Output coefficient matrix
$\underline{\underline{I}}$	Identity matrix
k	Time increment counter
$\underline{\underline{K}}_{FB}$	Feedback control matrix
$\underline{\underline{L}}$	State reconstruction matrix
$\underline{\underline{L}}_1, \underline{\underline{L}}_2$	Partitions of the state reconstruction matrix
m	Dimension of output vector
n	Dimension of state vector
$\underline{\underline{T}}$	Transformation matrix
$\underline{u}$	Control vector
$\underline{x}$	Model state vector
$\underline{\Delta x}$	Difference between actual and estimated model state vectors
$\underline{y}$	Output vector
$\underline{z}$	Observer state vector
$\underline{\Delta z}$	Difference between actual and estimated observer state vectors

(b) Greek

$\underline{\underline{\Delta}}$	Control coefficient matrix
$\underline{\underline{\theta}}$	Disturbance coefficient matrix
$\underline{\underline{\phi}}$	Transition matrix

(c) Subscripts

-	Vector
=	Matrix
ss	Steady state value

(d) Superscripts

-1	Matrix inverse
^	Estimated value

NOMENCLATURE FOR CHAPTER FIVE

		Steady State
(a)	Evaporator Process Variables	
$\underline{x}$	Five element state vector:	
W1	Holdup in the first effect	46 lb. (16.0 in)
C1	Concentration in the first effect	4.59% glycol
H1	First effect solution enthalpy	1.90 BTU/lb.
W2	Holdup in the second effect	42 lb. (11.0 in)
C2	Concentration in the second effect	10.11% glycol
$\underline{u}$	Three element control vector:	
S	Steam flowrate to the first effect	2.00 lb./min.
B1	First effect bottoms flowrate	3.49 lb./min.
B2	Second effect bottoms flowrate	1.58 lb./min.
$\underline{d}$	Three element disturbance vector:	
F	Feed flowrate	5.0 lb./min.
CF	Feed concentration	3.2% glycol
HF	Feed enthalpy	162 BTU/lb.
T1	Temperature in first effect	

(b) Alphabetic

$\underline{\underline{C}}$	Observer coefficient matrix for the outputs
$\underline{d}$	Disturbance vector
d1, d2	Elements of disturbance vector for numerical example
$\underline{\underline{E}}$	Observer transition matrix
k	Time increment counter
$\underline{\underline{L}}$	State reconstruction matrix
t	Time

$\underline{\underline{T}}$ Transformation matrix

$\underline{u}$ Control vector

$\underline{x}$ State vector

x1,x2,x3,x4 Elements of state vector for numerical example

$\underline{\Delta x}$ Difference between actual and estimated model state vectors

$\underline{y}$ Output vector

$\underline{z}$ Observer state vector

(c) Greek

$\underline{\underline{\Delta}}$ Control coefficient matrix

$\underline{\underline{\theta}}$ Disturbance coefficient matrix

$\underline{\underline{\phi}}$ Transition matrix

λ Eigenvalue

(d) Subscripts

- Vector

= Matrix

ss Steady state value

(e) Superscripts

$\hat{}$ Estimated value

- Model value

(f) Code for Computer Graphs

Δ,∇ Denote time of step disturbance

$\triangleleft,\triangleright$ Denote initial steady state

Type of run:

SIM	Simulated
EXP	Experimental

Disturbance (±/x%/xx):

+,-	Positive or negative step
x%	Step size as percentage of steady state
xx	Process variable disturbed

Control mode:

OL	Open loop
FB	Optimal multivariable feedback

REFERENCES FOR CHAPTER ONE

1. Kalman, R.E., "A New Approach to Linear Filtering and Prediction Problems", Trans. of the ASME, J. of Basic Eng., 82, 35 (1960).

2. Kalman, R.E. and Bucy, R.S., "New Results in Linear Filtering and Prediction Theory", Trans. of the ASME, J. of Basic Eng., 83, 95 (1961).

3. Cox, H., "On the Estimation of State Variables and Parameters for Noisy Dynamic Systems", I.E.E.E. Trans. Autom. Control, AC-9, No. 1, 5 (1964).

4. Sorenson, H.W., "Kalman Filtering Techniques", in "Advances in Control Systems", edited by C.T. Leondes, 3, Academic Press, New York and London (1966).

5. Seinfeld, J.H., "Nonlinear Estimation Theory", Ind. Engng. Chem., 62, No. 1, 32 (1970).

6. Luenberger, D.G., "Observing the State of a Linear System", I.E.E.E. Trans. Military Electronics, MIL-8, No. 2, 74 (1964).

7. Aoki, M. and Huddle, J.R., "Estimation of the State Vector of a Linear Stochastic System with a Constrained Estimator", JACC, Seattle, p. 694 (1966), published in I.E.E.E. Trans. Autom. Control, AC-11, No. 4, 432 (1967).

8. Wolovich, W.A., "On State Estimation of Observable Systems", 1968 JACC Preprints, 210.

9. Newell, R.B., "Multivariable Computer Control of an Evaporator", Ph.D. Thesis, Department of Chemical and Petroleum Engineering, University of Alberta (1970).

REFERENCES FOR CHAPTER TWO

1. Kalman, R.E., "A New Approach to Linear Filtering and Prediction Problems", Trans. of the ASME, J. of Basic Eng., 82, 35 (1960).

2. Kalman, R.E. and Bucy, R.S., "New Results in Linear Filtering and Prediction Theory", Trans. of the ASME, J. of Basic Eng., 83, 95 (1961).

3. Cox, H., "On the Estimation of State Variables and Parameters for Noisy Dynamic Systems", I.E.E.E. Trans. Autom. Control, AC-9, No. 1, 5 (1964).

4. Sorenson, H.W., "Kalman Filtering Techniques", in Advances in Control Systems, edited by C.T. Leondes, 3, Academic Press, New York and London (1966).

5. Bucy, R.S., "Linear and Nonlinear Filtering", Proc. I.E.E.E., 58, No. 6, 854 (1970).

6. Gura, I.A. and Bierman, A.B., "On Computational Efficiency of Linear Filtering Algorithms", Automatica, 7, No. 3, 299 (1971).

7. Astrom, K.J., "Introduction to Stochastic Control Theory", Academic Press, New York and London (1970).

8. Sage, A.P., "Optimum Systems Control", Prentice Hall, Englewood Cliffs, N.J. (1968).

9. Bryson, A.E., Jr. and Ho, Y.C., "Applied Optimal Control", Blaisdell Publishing Company, Waltham, Mass. (1969).

10. Sage, A.P. and Melsa, J.L., "Estimation Theory with Applications to Communications and Control", McGraw-Hill, N.Y. (1971).

11. Aoki, M. and Huddle, J.R., "Estimation of the State Vector of a Linear Stochastic System with a Constrained Estimator", JACC, Seattle, p. 694 (1966), published in I.E.E.E. Trans. Autom. Control, AC-12, No. 4, 432 (1967).

12. Newmann, M.M., "A Continuous-Time Reduced Order Filter for Estimating the State Vector of a Linear Stochastic System", Int. J. Control, 11, No. 2, 229 (1970).

13. Wells, C.H., "An Approximation of the Kalman Filter Equations", I.E.E.E. Trans. Autom. Control, AC-13, No. 4, 445 (1968).

14. Friedland, B., "Treatment of Bias in Recursive Filtering", I.E.E.E. Trans. Autom. Control, AC-14, No. 4, 359 (1969).

15. Seinfeld, J.H., "Nonlinear Estimation Theory", Ind. Engng. Chem., 62, No. 1, 32 (1970).

REFERENCES FOR CHAPTER TWO (continued)

16. Coggan, G.C. and Noton, A.R.M., "Discrete-Time Sequential State and Parameter Estimation in Chemical Engineering", Trans. Instn. Chem. Engr., 48, T255 (1970).

17. Singer, R.A. and Frost, P.A., "On the Relative Performance of the Kalman and Wiener Filters", I.E.E.E. Trans. Autom. Control, AC-14, No. 4, 390 (1969).

18. Bucy, R.S. and Joseph, P.D., "Filtering for Stochastic Processes with Application to Guidance", Interscience, New York (1968).

19. Wells, C.H. and Larson, R.E., "Application of Combined Optimum Control and Estimation Theory to DDC", Proc. I.E.E.E. 58, No. 1, 16 (1970).

20. Detchmendy, D.M. and Sridhar, R., "Sequential Estimation of States and Parameters in Noisy Dynamical Systems", 1965 JACC Preprints, Troy, New York, p. 56 (1965).

21. Seinfeld, J.H., "Optimal Stochastic Control of Nonlinear Systems", AIChE J., 16, No. 6, 1016 (1970).

22. Gavalas, G.R. and Seinfeld, J.H., "Sequential Estimation of States and Kinetic Parameters in Tubular Reactors with Catalyst Decay", Chem. Engng. Sci., 24, No. 4, 625 (1969).

23. Wells, C.H., "Application of Modern Estimation and Identification Techniques to Chemical Processes", 1969 JACC Preprints, Boulder, Colorado, p. 473 (1969). Published in AIChE J., 17, No. 4, 966 (1971).

24. Wells, C.H., "Optimum Estimation of Carbon and Temperature in a Simulated BOF", 1970 JACC Preprints, Atlanta, Georgia, p. 7 (1970).

25. Sastry, V.A. and Wood, R.K., "Adaptive Kalman Filtering with Unknown Parameters", 4th Asilomar Conf. on Systems and Circuit Theory (1970).

26. Goldmann, S.F. and Sargent, R.W.H., "Applications of Linear Estimation Theory to Chemical Processes: A Feasibility Study", Chem. Eng. Sci., 26, 1535 (1971).

27. Sastry, V.A., Vetter, W.J. and Caston, R., "The Application of Identification Methods to an Industrial Process", 1969 JACC Preprints, Boulder, Colorado, p. 787 (1969).

28. Sastry, V.A. and Vetter, W.J., "A Papermaking Wet-end Dynamics Model and Parameter Identification by Iterative Filtering", Proc. 1969 Nat. Conf. Autom. Control, Edmonton, Alberta (1969).

REFERENCES FOR CHAPTER TWO (continued)

29. Noton, A.R.M. and Choquette, P., "The Application of Modern Control Theory to the Operation of an Industrial Process", Proc. IFAC/IFIP Symp. (Toronto, Ontario), June 1968.

30. Choquette, P., Noton, A.R.M. and Watson, C.A.G., "Remote Computer Control of an Industrial Process", Proc. I.E.E.E., 58, No. 1, 10 (1970).

31. Ogata, K., "State Space Analysis of Control Systems, Prentice-Hall, Englewood Cliffs, N.J. (1967).

32. Newell, R.B., "Multivariable Computer Control of an Evaporator", Ph.D. Thesis, Department of Chemical and Petroleum Engineering, University of Alberta (1970).

33. Oliver, W.K., "Model Reference Adaptive Control: Hybrid Simulation and Experimental Verification", M.Sc. Thesis, Department of Chemical and Petroleum Engineering, University of Alberta (1972).

34. Koppel, L.B., "Introduction to Control Theory", Prentice-Hall, Englewood Cliffs, N.J. (1968).

REFERENCES FOR CHAPTER THREE

1. Newell, R.B., "Multivariable Computer Control of an Evaporator", Ph.D. Thesis, Department of Chemical and Petroleum Engineering, University of Alberta (1971).

2. Newell, R.B. and Fisher, D.G., "Plotting Evaporator Data", Research Report 701203, Department of Chemical and Petroleum Engineering, University of Alberta (1970).

3. Newell, R.B. and Fisher, D.G., "User's Manual for Multivariable Control Programs", Research Report 701201, Department of Chemical and Petroleum Engineering, University of Alberta (1970).

REFERENCES FOR CHAPTER FOUR

1. Luenberger, D.G., "Observing the State of a Linear System", IEEE Trans. on Mil. Electronics, MIL-8, No. 2, 74 (1964).

2. Luenberger, D.G., "Observers for Multivariable Systems", IEEE Trans. on AC, AC-11, No. 2, 190 (1966).

3. Luenberger, D.G., "An Introduction to Observers", IEEE Trans. Autom. Control, AC-16, No. 6, 596 (1971).

4. Wolovich, W.A., "On State Estimation of Observable Systems", 1968 JACC Preprints, 210.

5. Dellon, F. and Sarachik, P.E., "Optimal Control of Unstable Linear Plants with Inaccessible States", IEEE Trans. Autom. Control, AC-13, 491 (1968).

6. Johnson, G.W., "A Deterministic Theory of Estimation and Control", 1969 JACC Preprint, 155; also IEEE Trans. Autom. Control, (Short Papers), AC-14, 380 (1969).

7. Ash, R.H. and Lee, I., "State Estimation in Linear Systems - A Unified Theory of Minimum Order Observers", Proc. 3rd Hawaii Int. Conf. on System Sciences, 107 (1970).

8. Aoki, M. and Huddle, J.R., "Estimation of the State Vector of a Linear Stochastic System with a Constrained Estimator", 1966 JACC Preprints, 694, published in IEEE Trans. Autom. Control, AC-12, No. 4, 432 (1967).

9. Tse, E. and Athans, M., "Optimal Minimal-Order Observer-Estimators for Discrete Linear Time-Varying Systems", IEEE Trans. Autom. Control, AC-15, No. 4, 416 (1970).

10. Bona, B.E., "Designing Observers for Time-Varying State Systems", in Rec. 4th Asilomar Conf. Circuits and Systems, (1970).

11. Newmann, M.M., "A Continuous-Time Reduced-Order Filter for Estimating the State Vector of a Linear Stochastic System", Int. J. Control, 11, No. 2, 229 (1970).

12. Sarma, V.V.S. and Deekshatulu, B.L., "Optimal Control When Some of the State Variables are not Measurable", Int. J. Control, 7, No. 3, 251 (1968).

13. Porter, B. and Woodhead, M.A., "Performance of Optimal Control Systems When Some of the State Variables are not Measurable", Int. J. Control, 8, No. 2, 191 (1968).

14. Newmann, M.M., "Optimal and Sub-Optimal Control Using an Observer When Some of the State Variables are not Measurable", Int. J. Control, 9, No. 3, 281 (1969).

REFERENCES FOR CHAPTER FOUR (continued)

15. Bongiorno, Jr., J.J. and Youla, D.C., "On Observers in Multi-Variable Control Systems", Int. J. Control, 8, No. 3, 221 (1968).

16. Bongiorno, Jr., J.J. and Youla, D.C., "Discussion of 'On Observers In Multi-Variable Control Systems'", Int. J. Control, 12, No. 1, 183 (1970).

17. Sarma, I.G. and Jayaraj, C., "On the Use of Observers in Finite-Time Optimal Regulator Problems", Int. J. Control, 11, No. 3, 489 (1970).

18. Newmann, M.M., "Specific Optimal Control of the Linear Regulator Using a Dynamical Controller Based on the Minimal-Order Luenberger Observer", Int. J. Control, 12, No. 1, 33 (1970).

19. Yuksel, Y.O. and Bongiorno, Jr., J.J., "Observers for Linear Multi-variable Systems with Applications", IEEE Trans. on Autom. Control, AC-16, No. 6, 603 (1971).

20. Cumming, S.D.G., "Design of Observers of Reduced Dynamics", Electronic Letters, 5, No. 10, 213 (1969).

21. Newmann, M.M., "Design of Algorithms for Minimal-Order Luenberger Observers", Electronic Letters, 5, No. 17, 391 (1969).

22. Chen, R.T.N., "On the Construction of State Observers in Multi-variable Control Systems", Proceedings of the Nat. Electron. Conf., 25, 62 (1969).

23. Simon, J.D. and Mitter, S.I.L., "A Theory of Modal Control", Inform. Contr., 13, 316 (1968).

24. Nadezhdin, P.V., "The Optimal Control Law in Problems with Arbitrary Initial Conditions", Eng. Cybern., (USSR), 170 (1968).

25. Mayne, D.Q. and Murdock, P., "Modal Control of Linear Time-Invariant Systems", Int. J. Control, 11, No. 2, 223 (1970).

26. Bona, B.E., "Application of Observers and Optimum Filters to Inertial Systems", presented at the IFAC Symp. Multivariable Control Systems, Dusseldorf, Germany (1968).

27. Luenberger, D.G., "Invertible Solutions to the Operator Equation TA-BT=C", in Proc. Am. Math. Soc., 16, No. 6, 1226 (1965).

28. Davison, E.J. and Mann, F.T., "The Numerical Solution of $A^TQ+QA=-C$", IEEE Trans. Autom. Control, AC-13, No. 4, 448 (1968).

29. Neudecker, H., "A Note on Kronecker Matrix Products and Matrix Equation Systems", SIAM J. Appl. Math., 17, No. 3, 603 (1969).

REFERENCES FOR CHAPTER FIVE

1. Munro, N., "A Systematic Design Procedure for Reduced-Order Observers", Control Systems Centre Report No: 178, Institute of Science and Technology, University of Manchester (1971).

2. Fisher, D.G., Wilson, R.G., and Agostinis, W., "Digital Computer Programs for the Design and Simulation of DDC Systems", Preprints of IFAC Symposium on Digital Simulation of Continuous Processes, Gyor, Hungary, Paper F5 (1971). (To be published in Automatica.)

3. Luenberger, D.G., "Observing the State of a Linear System", I.E.E.E., Trans. Military Electronics, MIL-8, No. 2, 74 (1964).

4. Aoki, M. and Huddle, J.R., "Estimation of the State Vector of a Linear Stochastic System with a Constrained Estimator", 1966 JACC Preprints, 694, published in I.E.E.E. Trans. Autom. Control, AC-12, No. 4, 432 (1967).

5. Ogata, K., "State Space Analysis of Control Systems", Prentice Hall, Englewood Cliffs, N.J. (1967).

6. Newell, R.B., "Multivariable Computer Control of an Evaporator", Ph.D. Thesis, Department of Chemical and Petroleum Engineering, University of Alberta (1971).

APPENDIX FOR CHAPTER THREE

(a) Weighting matrices for the process noise

Code	Diagonal Elements
$\underline{\underline{Q1}}$	10^{-2}
$\underline{\underline{Q2}}$	10^{-4}
$\underline{\underline{Q3}}$	4×10^{-2}
$\underline{\underline{Q4}}$	4×10^{-4}

(b) Weighting matrices for the measurement noise

Code	Diagonal Elements
$\underline{\underline{R1}}$	10^{-2}
$\underline{\underline{R2}}$	10^{-4}
$\underline{\underline{R3}}$	4×10^{-2}

(c) Gain matrices for the sub-optimal filter

$$\underline{\underline{C1}} = \begin{bmatrix} 0.9 & 0 & 0 & 0 \\ 0 & 0 & 0 & 0 \\ 0 & 0.9 & 0 & 0 \\ 0 & 0 & 0.9 & 0 \\ 0 & 0 & 0 & 0.9 \end{bmatrix}$$

$$\underline{\underline{C2}} = \begin{bmatrix} 0.5 & 0 & 0 & 0 \\ 0 & 0 & 0 & 0 \\ 0 & 0.5 & 0 & 0 \\ 0 & 0 & 0.5 & 0 \\ 0 & 0 & 0 & 0.5 \end{bmatrix}$$

(d) Values of α for the exponential filter

$\alpha 1 = 0.7$

$\alpha 2 = 0.5$

$\alpha 3 = 0.3$

$\alpha 4 = 0.1$

(e) Matrices for the discrete evaporator model (T = 64 seconds)

$$\underline{\underline{\phi}} = \begin{bmatrix} 1.0 & -0.0008 & -0.0912 & 0 & 0 \\ 0 & 0.9223 & 0.0871 & 0 & 0 \\ 0 & -0.0042 & 0.4377 & 0 & 0 \\ 0 & -0.0009 & -0.1052 & 0 & 0.0001 \\ 0 & 0.0391 & 0.1048 & 1.0 & 0.9603 \end{bmatrix}$$

$$\underline{\underline{\Delta}} = \begin{bmatrix} -0.0119 & -0.0817 & 0 \\ 0.0116 & 0 & 0 \\ 0.1569 & 0 & 0 \\ -0.0137 & 0.0847 & -0.0406 \\ 0.0137 & -0.0432 & 0 \end{bmatrix}$$

$$\underline{\underline{\theta}} = \begin{bmatrix} 0.1182 & 0 & -0.0050 \\ -0.0351 & 0.0785 & 0.0049 \\ -0.0135 & -0.0002 & 0.0662 \\ 0.0012 & 0 & -0.0058 \\ -0.0019 & 0.0016 & 0.0058 \end{bmatrix}$$

$$\underline{\underline{H}} = \begin{bmatrix} 1 & 0 & 0 & 0 & 0 \\ 0 & 0 & 1 & 0 & 0 \\ 0 & 0 & 0 & 1 & 0 \\ 0 & 0 & 0 & 0 & 1 \end{bmatrix}$$

$$\underline{\underline{K}}_{FB} = \begin{bmatrix} 10.78 & -1.61 & -4.82 & 0 & -19.57 \\ 5.35 & 0.36 & 0.55 & 0 & 12.49 \\ 7.52 & 1.27 & 0.18 & 24.61 & 32.69 \end{bmatrix}$$

APPENDIX FOR CHAPTER FIVE

(a) Steady state error in the Kalman filter estimates for unmeasured step disturbances

The steady state error in the Kalman filter estimate for unmeasured deterministic disturbances can be derived from the following three equations:

Filter equation:

$$\hat{\underline{x}}(k) = \bar{\underline{x}}(k) + \underline{\underline{K}}[\underline{y}(k) - \underline{\underline{H}}\,\bar{\underline{x}}(k)] \tag{a-1}$$

Model equation:

$$\bar{\underline{x}}(k) = \underline{\underline{\phi}}\,\hat{\underline{x}}(k-1) + \underline{\underline{\Delta}}\,\underline{u}(k-1) + \underline{\underline{\theta}}\,\underline{d}(k-1) \tag{a-2}$$

Deterministic process:

$$\underline{x}(k) = \underline{\underline{\phi}}\,\underline{x}(k-1) + \underline{\underline{\Delta}}\,\underline{u}(k-1) + \underline{\underline{\theta}}\,\underline{d}(k-1) \tag{a-3}$$

For a deterministic process the output equation is:

$$\underline{y}(k) = \underline{\underline{H}}\,\underline{x}(k) \tag{a-4}$$

It should be noted that $\bar{\underline{x}}(k) \neq \underline{x}(k)$ if there are model inaccuracies (eg. unseen disturbances) or incorrect initial state estimates.

To proceed with the analysis it is necessary to define the following error equations:

$$\hat{\underline{x}}(k) = \underline{x}(k) + \underline{\Delta x}(k) \tag{a-5}$$

and

$$\bar{\underline{x}}(k) = \underline{x}(k) + \underline{\Delta \bar{x}}(k) \tag{a-6}$$

Now suppose there are unmeasured step disturbances applied to the process; Equation (a-2) then becomes

$$\bar{\underline{x}}(k) = \underline{\underline{\phi}}\, \hat{\underline{x}}(k-1) + \underline{\underline{\Delta}}\, \underline{u}(k-1) \tag{a-7}$$

and

$$\underline{\Delta\bar{x}}(k) = \underline{\underline{\phi}}\, [\hat{\underline{x}}(k-1) - \underline{x}(k-1)] - \underline{\underline{\theta}}\, \underline{d}(k-1)$$

$$\underline{\Delta\bar{x}}(k) = \underline{\underline{\phi}}\, \underline{\Delta x}(k-1) - \underline{\underline{\theta}}\, \underline{d}(k-1) \tag{a-8}$$

At steady state Equation (a-8) becomes:

$$\underline{\Delta\bar{x}}_{ss} = \underline{\underline{\phi}}\, \underline{\Delta x}_{ss} - \underline{\underline{\theta}}\, \underline{d}_{ss} \tag{a-9}$$

Now substituting Equation (a-6) into Equation (a-1) gives:

$$\hat{\underline{x}}(k) = \bar{\underline{x}}(k) - \underline{\underline{K}}\, \underline{\underline{H}}\, \underline{\Delta\bar{x}}(k) \tag{a-10}$$

and subtracting $\underline{x}(k)$ from both sides yields:

$$\underline{\Delta x}(k) = \underline{\Delta\bar{x}}(k) - \underline{\underline{K}}\, \underline{\underline{H}}\, \underline{\Delta\bar{x}}(k)$$

$$\underline{\Delta x}(k) = (\underline{\underline{I}} - \underline{\underline{K}}\, \underline{\underline{H}})\, \underline{\Delta\bar{x}}(k) \tag{a-11}$$

Again, at steady state Equation (a-11) becomes:

$$\underline{\Delta x}_{ss} = (\underline{\underline{I}} - \underline{\underline{K}}\, \underline{\underline{H}})\, \underline{\Delta\bar{x}}_{ss} \tag{a-12}$$

and substituting Equation (a-9) into Equation (a-12) gives:

$$\underline{\Delta x}_{ss} = (\underline{\underline{I}} - \underline{\underline{K}}\, \underline{\underline{H}})\, \underline{\underline{\phi}}\, \underline{\Delta x}_{ss} - (\underline{\underline{I}} - \underline{\underline{K}}\, \underline{\underline{H}})\, \underline{\underline{\theta}}\, \underline{d}_{ss}$$

or

$$\underline{\Delta x}_{ss} = (\underline{\underline{I}} - \underline{\underline{\phi}} + \underline{\underline{K}}\, \underline{\underline{H}}\, \underline{\underline{\phi}})^{-1}\, (\underline{\underline{K}}\, \underline{\underline{H}} - \underline{\underline{I}})\, \underline{\underline{\theta}}\, \underline{d}_{ss} \tag{a-13}$$

Equation (a-13) expresses the steady state estimation error as a function of the unmeasured step disturbances. Obviously for no disturbances (or for measured disturbances) $\underline{\Delta x}_{ss} = \underline{0}$. The errors incurred for unmeasured disturbances can be evaluated by solving Equation (a-13) on the computer.

(b) Design matrices for the 2nd order Luenberger observer

Observer	Design matrices
Observer 1	E16 and C1
Observer 2	E11 and C1
Observer 3	E2 and C1
Observer 5	E22 and C1

$\underline{E2}$ = diag. [0.001, 0.002]

$\underline{E11}$ = diag. [0.945, 0.940]

$\underline{E16}$ = diag. [0.00001, 0.00002]

$\underline{E22}$ = diag. [0.7, 0.8]

$$\underline{C1} = \begin{bmatrix} 1 & 1 & 1 \\ 1 & 1 & 1 \end{bmatrix}$$

$$\underline{C3} = \begin{bmatrix} 100 & 100 & 100 \\ 100 & 100 & 100 \end{bmatrix}$$

$$\underline{C11} = \begin{bmatrix} 10 & 1 & 1 \\ 10 & 1 & 1 \end{bmatrix}$$

$$\underline{C12} = \begin{bmatrix} 1 & 10 & 1 \\ 1 & 10 & 1 \end{bmatrix}$$

$$\underline{C13} = \begin{bmatrix} 1 & 1 & 10 \\ 1 & 1 & 10 \end{bmatrix}$$

$$\underline{C14} = \begin{bmatrix} 0.1 & 1 & 1 \\ 0.1 & 1 & 1 \end{bmatrix}$$

$$\underline{C15} = \begin{bmatrix} 1 & 0.1 & 1 \\ 1 & 0.1 & 1 \end{bmatrix}$$

$$\underline{C16} = \begin{bmatrix} 1 & 1 & 0.1 \\ 1 & 1 & 0.1 \end{bmatrix}$$

$$\underline{C17} = \begin{bmatrix} 10 & 1 & 1 \\ 1 & 1 & 1 \end{bmatrix}$$

$$\underline{C18} = \begin{bmatrix} 1 & 1 & 1 \\ 10 & 1 & 1 \end{bmatrix}$$

(c) Matrices for the discrete evaporator model

$$\underline{\underline{\Phi}} = \begin{bmatrix} 1.0 & -0.008 & -0.0912 & 0 & 0 \\ 0 & 0.9223 & 0.0871 & 0 & 0 \\ 0 & -0.0042 & 0.4377 & 0 & 0 \\ 0 & -0.0009 & -0.1052 & 0 & 0.0001 \\ 0 & 0.0391 & 0.1048 & 1.0 & 0.9603 \end{bmatrix}$$

$$\underline{\underline{\Delta}} = \begin{bmatrix} -0.0119 & -0.0817 & 0 \\ 0.0116 & 0 & 0 \\ 0.1569 & 0 & 0 \\ -0.0137 & 0.0847 & -0.0406 \\ 0.0137 & -0.0432 & 0 \end{bmatrix}$$

$$\underline{\underline{\theta}} = \begin{bmatrix} 0.1182 & 0 & -0.0050 \\ -0.0351 & 0.0785 & 0.0049 \\ -0.0135 & -0.0002 & 0.0662 \\ 0.0012 & 0 & -0.0058 \\ -0.0019 & 0.0016 & 0.0058 \end{bmatrix}$$

$$\underline{\underline{H}} = \begin{bmatrix} 1 & 0 & 0 & 0 & 0 \\ 0 & 0 & 1 & 0 & 0 \\ 0 & 0 & 0 & 1 & 0 \\ 0 & 0 & 0 & 0 & 1 \end{bmatrix}$$

$$\underline{\underline{K}}_{FB} = \begin{bmatrix} 10.78 & -1.61 & -4.82 & 0 & -19.57 \\ 5.35 & 0.36 & 0.55 & 0 & 12.49 \\ 7.52 & 1.27 & 0.18 & 24.61 & 32.69 \end{bmatrix}$$

(d) Eigenvalues for the discrete evaporator model

$$\{\lambda_i\} = 1.0,\ 1.0,\ 0.9606,\ 0.9220,\ 0.4407$$